



TECHNISCHE UNIVERSITÄT MÜNCHEN

Wissenschaftszentrum weihenstephan entwicklungsbiologie der pflanzen

**Analysis of STRUBBELIG signaling pathway in the control of tissue morphogenesis in
*Arabidopsis thaliana***

STRUBBELIG regulates cell wall signaling in *Arabidopsis thaliana*

Ajeet Chaudhary

Vollständiger Abdruck der von der Fakultät Wissenschaftszentrum Weihenstephan für Ernährung, Landnutzung und Umwelt der Technischen Universität München zur Erlangung des akademischen Grades eines

Doktors der Naturwissenschaften (Dr. rer. Nat.)
genehmigten Dissertation.

Vorsitzender:

Prof. Dr. Erwin Grill

Prüfer der Dissertation:

1. Prof. Dr. Kay Heinrich Schneitz
2. Prof. Dr. Ralph Hückelhoven

Die Dissertation wurde am 27.09.2019 bei der Technischen Universität München eingereicht und durch die Fakultät Wissenschaftszentrum Weihenstephan für Ernährung, Landnutzung und Umwelt am 21.11.2019 angenommen

Table of Contents

I. Tables of contents	i
II. Lists of figures.....	v
III. Lists of tables.....	vii
V. Summary.....	viii
VI.Zusammenfassung.....	x
1. Introduction	1
1.1 The plant cell wall	1
1.2 The role of cell wall signaling in plant morphogenesis	5
1.3 CWI sensor proteins in plant.....	10
1.3.1 Catharanthus roseus RLK1-like kinases	10
1.3.2 Wall-associated kinases (WAKs)	12
1.3.3 Proline-rich Extensin-like Receptor Kinases (PERKs).....	13
1.3.4 Leucine-Rich Repeat Receptor Kinases (LRR-RKs).....	13
1.3.5 Leguminous L-Type Lectin RLKs (LecRKs).....	14
1.3.6 Histidine Kinases (HKs)	14
1.3.7 Mechanosensitive Receptors and Ion Channels.....	15
1.3.8 Other candidate proteins involved in cell wall signaling.....	15
1.4 Downstream signaling processes involved in the response to CWD.....	16
1.4.1 Ca ²⁺ and ROS	16
1.4.2 CBI induced cell wall damage and response	17
1.5 The STRUBBELIG signaling pathway and its role in plant morphogenesis.....	18
1.5.1 STRUBBELIG is atypical RK.....	18
1.5.2 SUB regulates tissue morphogenesis in Arabidopsis.....	19
1.5.3 Novel components in the SUB signaling pathway	21
1.5.4 SUB:EGFP is enriched at plasmodesmata and interacts with QKY at PD.....	21
1.5.5 SUB signaling affects cell wall biochemistry	23
1.6 Objectives.....	24
2 Materials and Methods	25
2.1 Plant work, plant genetics, and plant transformation	25
2.2 Recombinant DNA work.....	27
2.3 Arabidopsis genomic DNA extraction and genotyping PCR.....	30
2.4 RNA extraction from the plant material and cDNA synthesis.....	31
2.5 Generation of various reporter constructs	31

2.5.1	Construction of Y2H vectors	31
2.5.2	Generation of root hair patterning construct pGL2::GUS:EGFP pGGZ001	32
2.5.3	Generation of <i>KIN7.4</i> promoter reporter construct pKIN7.4::NLS-GUS:EGFP:tKIN7.4.....	33
2.5.4	pKIN7.4::EGFP:gKIN7.4:tKIN7.4 pCambia3300	33
2.6	Yeast-two-hybrid (Y2H) assay.....	33
2.7	Scanning electron microscopy (SEM).....	34
2.8	Confocal laser scanning microscopy (CLSM)	34
2.9	Three-dimensional ovule imaging using CLSM and MorphoGraphX.....	35
2.10	Phenotyping flower organ	35
2.11	Drug treatments	36
2.12	Immunoprecipitation and western blot analysis.....	36
2.13	Growth media, growth conditions and frequently used buffers	36
2.14	Bioinformatics	38
2.15	Cellulose quantification.....	38
2.16	ROS, lignin, and callose staining	38
2.17	Hypocotyl and root measurements.....	39
2.18	Statistics	39
2.19	Microscopy and artwork.....	40
3	Results	41
3.1	The receptor kinase STRUBBELIG promotes the response to cellulose deficiency in <i>Arabidopsis thaliana</i>	41
3.1.1	<i>SUB</i> does not affect cellulose production	41
3.1.2	<i>SUB</i> promotes the isoxaben-induced CWD response	42
3.1.3	The <i>SUB</i> -mediated CBI response is sensitive to sorbitol	47
3.1.4	<i>SUB</i> attenuates isoxaben-induced cell swelling and promotes root growth recovery	49
3.1.5	<i>SUB</i> attenuates root growth in <i>prc1-1</i>	51
3.1.6	<i>SUB</i> and <i>THE1</i> share partially overlapping functions	52
3.2	Morphogenesis in <i>Arabidopsis</i> during cellulose deficient condition is regulated by the activity of <i>SUB</i>	55
3.2.1	Isoxaben treatment reduces <i>SUB</i> transcriptionally and post-translationally	55
3.2.2	Exposing plants to sub-lethal doses of isoxaben induces <i>sub</i> -like root hair patterning defects.....	57

3.2.3	Exposing plants to sub-lethal doses of isoxaben induces <i>sub</i> -like floral defects ...	60
3.2.4	Ectopic expression of <i>SUB</i> attenuates several detrimental effects of isoxaben.....	62
3.3	Additional candidate genes involved in the <i>SUB</i> signaling pathway.....	65
3.3.1	Validation of interaction of promising candidate gene in Y2H.....	71
3.4	<i>SUB</i> signaling regulates microtubule organization.....	73
3.5	Characterization of KINESIN 7.4 (KIN7.4) in Arabidopsis.....	76
3.5.1	In silico structure-function analysis of KIN7.4.....	76
3.5.2	Phylogenetic analysis of KIN7.4.....	77
3.5.3	Expression analysis of <i>KIN7.4</i>	77
3.5.4	Analysis of <i>KIN 7.4</i> promoter activity.....	79
	80
3.5.5	Phenotypic characterization of <i>kin7.4</i> and <i>kin7.2</i> mutant alleles.....	80
3.5.6	Complementation of <i>kin7.4</i> mutant phenotype.....	88
3.5.7	Subcellular distribution of EGFP:gKIN7.4 fusion protein.....	89
3.5.8	EGFP:gKIN7.4 is colocalizing with gSUB:mCherry in the root epidermis.....	91
3.5.9	KIN7.4 interacts with SUB in yeast two-hybrid and in vitro.....	92
3.5.10	Mapping of protein domains involved in the SUB-ICD and KIN7.4 interaction... ..	94
4	Discussion	96
4.1	<i>SUB</i> participates in the response to changes cell wall.....	96
4.1.1	<i>SUB</i> is required for tissue morphogenesis in cellulose deficient condition.....	98
4.1.2	The relation of <i>SUB</i> to <i>THE1</i> and <i>MIK2</i>	98
4.2	Isoxaben treatment results in <i>SUB</i> downregulation.....	99
4.3	Novel Candidate factors of the <i>SUB</i> signaling pathway.....	99
4.4	<i>SUB</i> signaling regulates microtubule organization.....	100
4.5	Characterization of KINESIN 7.4.....	101
4.5.1	In silico analysis of KIN7.4 and KIN7.2.....	101
4.5.2	Expression analysis of <i>KIN7.4</i> and <i>KIN7.2</i>	102
4.5.3	Analysis of floral organ morphology of <i>kin7.4</i> and <i>kin7.2</i> mutant alleles.....	103
4.5.4	Role of <i>KIN7.4</i> and <i>KIN7.2</i> for root hair cell patterning (RHP).....	103
4.5.5	Genetic complementation of <i>kin7.4</i> mutant phenotype.....	104
4.5.6	Subcellular distribution of EGFP: KIN7.4 fusion protein.....	104
4.5.7	EGFP:gKIN7.4 is colocalizing with gSUB:mCherry in the root epidermis.....	105

4.5.8	KIN7.4 interacts with SUB in yeast two-hybrid and in vitro	105
4.5.9	Mapping of protein domain involved in SUB-KIN7.4 interaction	106
4.6	Working model of SUB signaling pathway	106
5	Conclusion	108
6	References	109
7	Supplementary Data	133
8	Acknowledgements	145

List of figure

Figure 1 Schematic diagram of cell wall from plants..	2
Figure 2 Model of the plant cell wall integrity maintenance system	6
Figure 3 Overview of selected potential cell wall-related signaling receptors and signals.	9
Figure 4 Overview of the domain architecture of SUB.	18
Figure 5 Phenotype comparison of the overall above-ground morphology of <i>Ler</i> and <i>sub-1</i>	19
Figure 6 Sub-cellular phenotype comparison of the <i>Ler</i> and <i>sub-1</i>	20
Figure 7 Interaction between SUB and QKY..	22
Figure 8 SUB signaling affects cell wall chemistry.....	23
Figure 9 Effects of <i>SUB</i> on cellulose content in seven-day-old seedlings.....	41
Figure 10 SUB affect on isoxaben-induced ROS production.	43
Figure 11 SUB affects isoxaben-induced ectopic lignification.....	45
Figure 12 SUB affects isoxaben-induced callose accumulation..	46
Figure 13 SUB effects on isoxaben-induced marker gene expression accumulation..	44
Figure 14 The effects of sorbitol on lignin and callose accumulation upon isoxaben expo	48
Figure 15 Root epidermal cell shape changes upon isoxaben treatment.....	49
Figure 16 SUB effect on root growth inhibition in <i>prc1-1</i>	52
Figure 17 Influence of THE1 on etiolated hypocotyl length of <i>prc1-1</i> and isoxaben-induced ROS accumulation in root tips.....	53
Figure 18 Effect of isoxaben treatment on SUB.	56
Figure 19 The consequence of reduced CBI on the GL2::EGFP expression pattern.....	58
Figure 20 Influence of isoxaben treatment on floral and ovule morphogenesis.	61
Figure 21 Twisted petiole organization of <i>tor</i> is attenuated in <i>tor sub</i> double mutant.....	69
Figure 22 Yeast two-hybrid interaction of SUB with WAK2, TOR1, and KIN7.4.....	71
Figure 23 Cortical microtubule patterning in different zones of the arabidopsis root.	74
Figure 24 Organization of cortical microtubule in the elongation zone epidermal cell.....	75
Figure 25 Schematic depiction of KIN7.4 domain structure.	76
Figure 26 qRT analysis of KIN7.4 expression.....	79
Figure 27 Promoter activity of KIN7.4 in 7-day-old root.....	80
Figure 28 Gene structure of KIN7.4 and KIN7.2 including T-DNA insertion sites.....	81
Figure 29 Phenotype comparison between <i>Col-0</i> , <i>sub-9</i> , <i>kin7.4-1</i> , <i>kin7.4-2</i> and <i>sub-9 kin7.4-1</i>	82
Figure 30 Phenotype comparison between <i>Col-0</i> , <i>sub-9</i> , <i>kin7.2-1</i> , <i>kin7.2-2</i> and <i>sub-9 kin7.2-1</i>	84
Figure 31 Phenotype comparison between <i>Col-0</i> , <i>kin7.4-1</i> , <i>kin7.2-1</i> , and <i>kin7.4-1 kin7.2-1</i>	85

Figure 32 Expression pattern of pGL2::GUS:EGFP in Col wild-type, <i>sub-9</i> , <i>kin7.4-1</i> , <i>kin7.4-2</i> , <i>kin7.4-1</i> ^{+/-} <i>kin7.4-1</i> ^{+/-} <i>sub-9</i> ^{+/-} , <i>sub-9 kin7.4-1</i> and <i>sub-9 kin7.4-2</i> mutants.....	87
Figure 33 Expression pattern of pGL2::GUS:EGFP in wild-type, <i>kin7.1-1</i> , and <i>kin7.2-2</i> mutants.....	88
Figure 34 Complementation of <i>kin7.4</i> pGL2::GUS:EGFP with pKIN7.4::EGFP:gKIN7.4.....	89
Figure 35 Sub-cellular distribution of EGFP:gKIN7.4 fusion protein in root..	90
Figure 36 Co-localization of EGFP:gKIN7.4 with RFP-TUB6 in root epidermis cell.....	91
Figure 37 Co-localization of EGFP:gKIN7.4 with mCherry:gSUB in root epidermis cells.....	92
Figure 38 Yeast two-hybrid and in vitro pull-down assay.....	93
Figure 39 Mapping of interaction domain involved in SUB-ICD and KIN7.4 interaction.....	95
Figure 40 A schematic representation of SUB signaling pathway in development and cell wall stress	107

List of table

Table 1 List of candidate genes screened with tDNA line no.....	25
Table 2 PCR reaction mix and cycler program.....	28
Table 3 Plasmid vectors used in this work.....	29
Table 4 Reaction mix and steps involved in cDNA synthesis.....	31
Table 5 Root growth recovery after isoxaben treatment.....	51
Table 6 Position-dependent pattern of GL2::EGFP reporter expression in root epidermal cells upon a 48 hour exposure to isoxaben.....	58
Table 7 Distribution of root hair and nonhair cells in the root epidermis.....	60
Table 8 Number of periclinal cell divisions in L2 layer of stage 3 floral meristems of plants exposed to different concentrations of isoxaben.....	63
Table 9 Comparison of integument defects between Col, <i>sub-9</i> , <i>sub-21</i> , and Col plants exposed to different concentrations of isoxaben.....	63
Table 10 List of putative SUB signaling candidate gene.....	66
Table 11 Number of periclinal cell divisions in the L2 layer of stage 3 floral meristems.....	83
Table 12 Comparison of integument defects between Col, <i>sub-9</i> , <i>kin7.4-1</i> , <i>kin7.4-2</i> and <i>sub-9 kin7.4-1</i> mutants.....	83
Table 13 List of primers.....	129

Summary

Plant tissue morphogenesis requires the cell to cell communication during many processes like growth, development, and cellular responses to biotic and abiotic stress. The cell wall constitutes the principal element of the underlying mechanism in plants and it undergoes remodeling to accommodate tissue morphogenesis and counteract pathogen attack. The cell wall remodeling suggests a necessity for a mechanism that would sense any physico-chemical alterations occurred in the cell wall, and elicit a corresponding cellular response. The essential cell wall surveillance mechanisms remain poorly understood in plants. In Arabidopsis, the cell surface leucine-rich repeat receptor kinase STRUBBELIG (SUB) is involved in tissue morphogenesis of many organs. In previous work, SUB and its signaling components QUIRKY (QKY) and ZERZAUST (ZET) have been linked to cell wall biology. The whole-genome transcriptomic analysis revealed that many genes responsive to SUB-mediated signal transduction relate to cell wall remodeling (Fulton *et al.*, 2009). Additionally, the *sub*, *qky*, and *zet* mutants share overlapping defects in cell wall biochemistry (Vaddepalli *et al.*, 2017). To understand the molecular mechanism underlying SUB regulated cell wall biochemistry, the role of SUB in cell wall signalling is analysed.

Cellulose is a load-bearing element in the cell wall and synthesized by cellulose synthase (CESA) complex at the plasma membrane. In recent past years, impairing cellulose biosynthesis has become a popular method to study cell wall integrity signaling in Arabidopsis. Plant cells respond to alteration in cellulose content of the cell wall, for example, genetically or pharmacologically inhibition of cellulose biosynthesis results in ectopic lignification, callose accumulation and transcriptional upregulation of defense marker genes. The herbicide isoxaben is a well-characterized cellulose biosynthesis inhibitor and has been frequently used to create cell wall damage (CWD) in the plant cell. The data presented here indicate that *SUB* promotes cellular responses like reactive oxygen species (ROS) production, stress marker gene induction, ectopic lignin, and callose accumulation upon isoxaben treatment. Additionally, my data also suggest that *SUB* signaling is required for the recovery of the root growth after transient exposure to isoxaben. Furthermore, genetic data indicate that *SUB* promotes the isoxaben-induced cell wall stress response independently from other known receptor kinase genes mediating this response, such as *THESEUS1* or *MIK2*. In this study, I also report that cellulose biosynthesis inhibition (CBI) upon isoxaben treatment results in the *sub* like root and floral organ phenotypic defect in wild type plant. Further analysis revealed that CBI induced CWD eventually attenuate *SUB* activity by a post-transcriptional mechanism. Ectopic expression of *SUB* in

wild type plant ameliorates the detrimental effect of isoxaben on floral organ morphology and root hair cell patterning. The combined data reveal a novel role for SUB signaling in the response to cell wall damage induced by CBI. Thus, I propose *SUB* to function in at least two distinct biological processes: the control of tissue morphogenesis and the cell wall stress response.

Cortical microtubule regulates the architecture of the cell wall by directing the deposition patterns of cell wall material at the plasma membrane. In light of *SUB*'s role in regulating cell wall biochemistry, I also explored microtubule dynamics in *sub* mutants. My analysis revealed that *sub* mutants exhibit a defect in microtubule orientation in root epidermis cell. In my third task to identify additional factors of the SUB signaling pathway, I have found several interesting candidate genes like *KINESIN 7.4* (*KIN7.4*), *TORTIFOLIA 1* (*TOR1*), *Wall associated kinase 2* (*WAK2*), and *Clathrin heavy chain 2* (*CHC2*). In this study, *KIN7.4* has been characterized. *KIN7.4* is a microtubule-binding motor protein. It belongs to kinesin family 7 in Arabidopsis and member of this family have been shown to be involved in establishing cell polarity during plant development. The functional analysis revealed that *KIN7.4* is a positive regulator of root hair cell patterning in Arabidopsis. However, its closest homolog *KIN7.2* does not participate in SUB mediated floral organ morphogenesis or root hair cell patterning. The Gene expression analysis suggests that *KIN7.4* is expressed broadly and has an overlapping expression pattern as *SUB*. Protein localization experiments indicate that EGFP:*KIN7.4* is associated with cortical microtubule and also colocalize with SUB:mCherry at the plasma membrane. Genetic and yeast-two-hybrid data indicate that SUB and *KIN7.4* can interact directly. Thus, my data suggest that *KIN7.4* is involved in SUB mediated tissue morphogenesis in a tissue-dependent manner.

Zusammenfassung

Gewebemorphogenese in Pflanzen setzt Zell-Zell-Kommunikation für viele Prozesse, wie Wachstum, Entwicklung und zelluläre Reaktionen auf biotischen und abiotischen Stress, voraus. Die Zellwand stellt in Pflanzen das Grundelement des zu Grunde liegenden Mechanismus dar und durchläuft Umstrukturierung, um die Gewebemorphogenese zu ermöglichen und Pathogenangriffen entgegenzuwirken. Die Umstrukturierung der Zellwand legt die Notwendigkeit eines Mechanismus nahe, der physicochemische Veränderungen der Zellwand bemerkt, und eine entsprechende zelluläre Antwort auslöst. Der zentrale Zellwand-Überwachungsmechanismus in Pflanzen bleibt wenig verstanden. In Arabidopsis ist die atypische Retzeptorkinase STRUBBELIG (*SUB*) an der Gewebemorphogenese vieler Organe beteiligt. In vorherigen Arbeiten wurden *SUB* und seine Signalkomponenten QUIRKY (*QKY*) und ZERZAUST (*ZET*) mit der Zellwandbiologie in Verbindung gebracht. Die whole-genome Transkriptionsanalyse zeigte, dass viele Gene, die auf *SUB*-vermittelte Signaltransduktion reagieren, die Zellwandumstrukturierung betreffen (Fulton et al., 2009). Zusätzlich teilen die *sub*, *qky* und *zet* Mutanten überlappende Defekte der Zellwandbiochemie (Vaddepalli et al., 2017). Um die molekularen Mechanismen hinter der *SUB*-regulierten Zellwandbiochemie zu verstehen, wird die Rolle von *SUB* im Zellwand-signalling analysiert.

Zellulose ist ein Fracht-tragendes Element der Zellwand und wird durch den Zellulose-Synthase (*CESA*) Komplex an der Plasmamembran synthetisiert. In den letzten Jahren, wurde die Beeinträchtigung der Zellulose Biosynthese eine beliebte Methode, um das Zellwandintegritätssignalling in Arabidopsis zu untersuchen. Pflanzenzellen reagieren auf Veränderungen im Celluloseanteil der Zellwand. Beispielsweise bewirkt genetische oder pharmakologische Hemmung der Zellulose Biosynthese eine ektoische Lignifizierung, Callose Akkumulation und transkriptionelle Hochregulierung von Abwehr Markergenen. Das Herbizid Isoxaben ist ein gut charakterisierter Zellulose Biosynthesehemmer und wurde häufig genutzt um Zellwandbeschädigungen (*CWD*) hervorzurufen. Die hier präsentierten Daten deuten darauf hin, dass *SUB* nach Isoxaben-Behandlung eine zelluläre Antwort, wie Reactive oxygen species (*ROS*) Produktion, Stressmarkergen-Induktion, ektoisches Lignin und Callose Akkumulation, fördert. Zusätzlich deuten meine Daten auch darauf hin, dass *SUB*-signalling für die Erholung des Wurzelwachstums nach vorübergehender Isoxabenbehandlung notwendig ist. Zudem lassen genetische Daten darauf schließen, dass *SUB* die durch Isoxaben ausgelöste Zellwandstressantwort unabhängig von anderen Rezeptorkinasen, die gleiche Antwort steuern, fördert. Beispiele hierfür sind *THESEUS1* oder *MIK2*. In dieser Studie berichte ich auch, dass Zellulose Biosynthesehemmung (*CBI*) nach Isoxabenbehandlung in einem *sub*-

ähnlichen phenotypischen Defekt der Wurzeln und Blüten in Wildtyp-Pflanzen hervorruft. Weitere Untersuchungen zeigten, dass CBI-induzierte CWD eventuell die Aktivität von *SUB* durch posttranskriptionelle Mechanismen schwächt. Ektopische Expression von *SUB* in Wildtyp-Pflanzen verbessert die schädlichen Effekte von Isoxaben der Blütenorganmorphogenese und Wurzelhaar-Zellanordnung. Die kombinierten Daten zeigen eine neue Rolle des SUB-signalling in der Antwort auf CBI-induzierte Zellwandschädigungen. Demnach schlage ich vor, dass *SUB* in mindestens zwei unterschiedlichen biologischen Prozessen fungiert: Der Kontrolle der Gewebemorphogenese und der Zellwand Stressantwort.

Kortikale Mikrotubuli regulieren die Architektur der Zellwand, indem sie die Depositionsmuster von Zellwandmaterial an der Plasmamembran dirigieren. Im Licht der Rolle von *SUB*^{rs} in der Zellwandbiochemieregulierung, habe ich auch die Dynamiken der Mikrotubuli in *sub*-Mutanten untersucht. Meine Analysen zeigen, dass *sub*-Mutanten einen Defekt in der Orientierung der Mikrotubuli in Zellen der Wurzelepisdermis aufweisen. In meiner dritten Aufgabe weitere Faktoren des SUB-Signaltransduktionsweges, habe ich einige interessante Kandidaten wie *KINESIN 7.4* (*KIN7.4*), *TORTIFOLIA 1* (*TOR1*), *Wall associated kinase 2* (*WAK2*), und *Clathrin heavy chain 2* (*CHC2*) gefunden. In dieser Arbeit wurde *KIN7.4* charakterisiert. *KIN7.4* ist ein Mikrotubuli-bindendes Motorprotein. Es gehört zur Kinesin-Familie 7 in Arabidopsis, von deren Mitgliedern gezeigt wurde, dass sie an der Etablierung der Zellpolarität während der Pflanzenmorphogenese beteiligt sind. Die funktionelle Analyse zeigte, dass *KIN7.4* ein positiver Regulator des Wurzelhaar Zellmusters in Arabidopsis ist. Dennoch ist sein nächstes Homolog *KIN7.2* nicht an der SUB-vermittelten Blütenmorphogenese oder des Wurzelhaar Zellmusters beteiligt. Die Genexpressionsanalyse lässt vermuten, dass *KIN7.4* weit exprimiert wird und ein mit *SUB* überlappendes Expressionsmuster besitzt. Proteinlokalisierungsexperimente deuten darauf hin, dass EGFP:*KIN7.4* mit kortikalen Mikrotubuli assoziiert und auch mit *SUB*:mCherry an der Plasmamembran kolokalisiert. Genetische und yeast-two-hybrid Daten deuten darauf hin, dass *SUB* und *KIN7.4* direkt miteinander interagieren können. Somit deuten meine Daten darauf hin, dass *KIN7.4* gewebeabhängig an der SUB-vermittelten Gewebemorphogenese beteiligt ist.

1. Introduction

Plants being sessile organism are continuously challenged to various biotic and abiotic stresses during the whole life span. To equilibrate for their lack of mobility, plants require a permanent and efficient adjustment to ever-changing environmental conditions and flexibly adapt their postembryonic developmental program. In plants, the extracellular cell wall constitutes a central element of the underlying molecular mechanism. The plant cell wall is mainly composed of carbohydrates, such as cellulose, hemicellulose, and pectin, and phenolic compounds, including lignin. The growth and development of plants rely on the ability of the cell wall to regenerate and remodeled without losing its integrity. In this regard, plants can detect the perturbation of their cell wall and activate respective modifications in cell wall polymer interaction. These considerations imply a necessity for plant cells to monitor cell wall integrity (CWI). Such a mechanism would sense any physio-chemical alterations that occurred in the cell wall, and elicit a corresponding compensatory and protective cellular response (Voxeur and Höfte, 2016; Wolf, 2017a; Franck *et al.*, 2018)

1.1 The plant cell wall

The plant cell wall is a highly complex and heterogeneous network of cellulose microfibrils, which are cross-linked to a matrix consisting of hemicellulose and pectin, structural proteins and lignin (Humphrey *et al.*, 2007). The cell wall between two neighboring cells comprises three layers: the middle lamella, the primary cell wall and the secondary cell wall (Albersheim *et al.*, 2010). During cytokinesis, middle lamella is formed and is surrounded by two layers of the primary cell wall of two adjacent cells. In typical growing cells first, the primary cell wall is made. It is typically a thin, flexible layer (0.1–1 μm) that consists primarily of complex polysaccharides and a small number of structural proteins (Cosgrove, 2005). Once cells reach their mature size, some cells lay down a thick secondary cell wall beneath the primary wall that provides plants with the mechanical properties (Cosgrove, 2005; Keegstra, 2010).

The primary cell wall of most of the land plants mainly consists of three main components: cellulose, hemicelluloses, and pectins although their relative proportion differs across different plant species (Reddy and Yang, 2005; Humphrey *et al.*, 2007). Cellulose is the main load-bearing element of the cell wall and is synthesized by hexameric cellulose synthase (CESA) complexes traveling in the plasma membrane (Desprez *et al.*, 2007). The cellulose microfibrils are 3–5 nm wide and are organized in parallel through non-covalent hydrogen bonds (Somerville, 2006; Cosgrove, 2014). Arabidopsis

contains 10 *CESA* genes and *CESA* proteins show more than 60% sequence identity among themselves (Holland *et al.*, 2000). The cellulose production during primary cell wall formation requires *CESA* rosette complex consists of *CESA*1, *CESA*3, and *CESA*6 proteins whereas cellulose production during secondary cell wall synthesis requires *CESA* 4, 7 & 8 (Somerville, 2006). Although *CESA*3 and *CESA*6 were thought to have a redundant function and compensate for the loss of one another, however, both are needed for the formation of a functional rosette complex during primary cell wall formation (Desprez *et al.*, 2002). *CESA* complexes are thought to be directionally guided by interactions with microtubules. They propel themselves through the plasma membrane by the excretion of glucan chains which coalesce to form cellulose microfibrils (Somerville, 2006; Keegstra, 2010). The orientation of cellulose microfibril deposition creates mechanical anisotropy in the wall and thus decides the growth direction of the cell (Somerville, 2006; Cosgrove and J., 2014). They are embedded in a matrix of complex polysaccharides, which are divided into two classes – hemicelluloses and pectins.

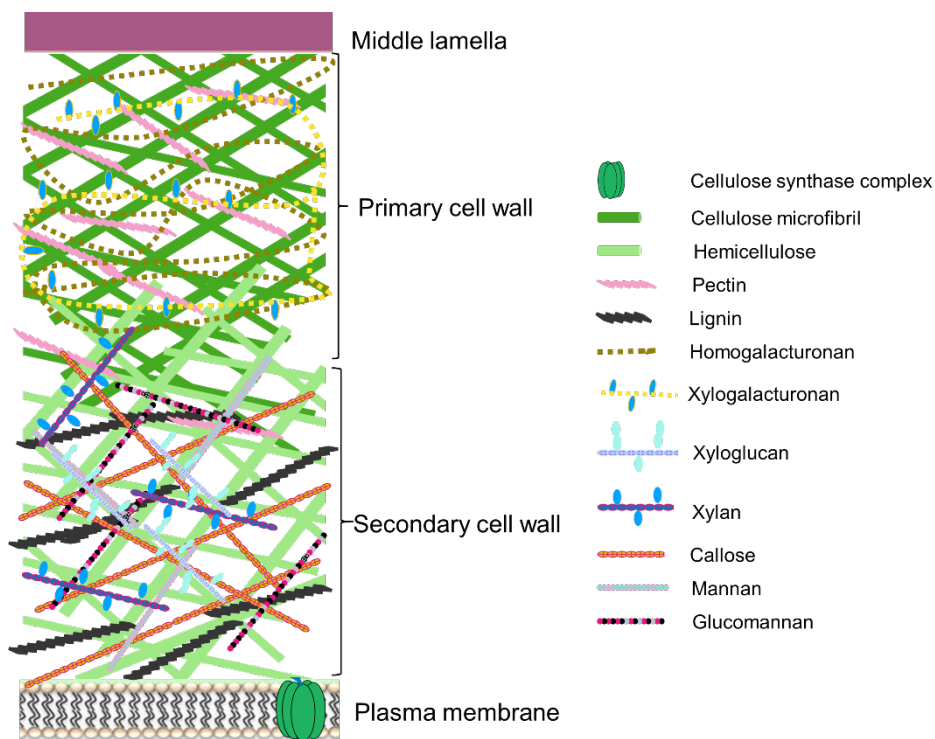


Figure 1. Schematic diagram of the plant cell wall. The plant cell consists of cellulose, pectin polysaccharides (homogalacturonan, rhamnogalacturonan I and rhamnogalacturonan II) and two major hemicelluloses, xyloglucan and xylan, together with minor fractions of mannan and glucomannan. In some plant tissues, cells also generate a secondary cell wall that is largely composed of cellulose, hemicelluloses (mostly xylans) and lignin.

Hemicelluloses are β -(1,3; 1,4)-linked glucans chains and grouped into xyloglucans, xylans, mannans and glucomannans (Scheller and Ulvskov, 2010). Xyloglucans are most abundant hemicellulose with a linear β -1,4-linked glucan chain as backbone similar to cellulose but it is decorated with xylose branches on three out of four glucose residues. It can also contain galactose and fucose residues. Arabinoxylan consists of a (1,4)-linked β -D-xylan backbone decorated with arabinose branches (Cosgrove, 2005; Scheller and Ulvskov, 2010; Burton *et al.*, 2010). Other residues, such as glucuronic acid and ferulic acid esters, also exist in arabinoxylans that are particularly abundant in cereal grasses. Mannans are also found in primary cell walls and most likely function in the same way as xyloglucan and arabinoxylan.

Pectin is considered as one of the most complex macromolecules in nature and comprises an elaborated and heterogeneous group of covalently linked polysaccharides (Ridley *et al.*, 2001). Pectin is the main component of the gel-like matrix of the cell wall, especially in dicots. It includes homogalacturonan (HG), rhamnogalacturonan I (RG-I), and to a lesser extent rhamnogalacturonan II (RG-II), xylogalacturonan (XGA), arabinan and arabinogalactan I (Cosgrove, 2005; Mohnen, 2008; Burton *et al.*, 2010). Most pectin polysaccharides are a linear homopolymer of α -1,4-covalently linked galacturonic acid (GalA) (Figure 1). It is also known as Homogalacturonan (HG) and it makes up to 65% of pectin (Mohnen, 2008; Sénéchal *et al.*, 2014). HG has been shown to undergo polymerization in the range of 81-117 GalA residues (Yapo *et al.*, 2007), and they are methylated at the C-6 carboxyl and O-acetylated at O-2 or O-3 (O'Neill *et al.*, 1990). The mechanical property of the cell wall is greatly influenced by the degree of methyl esterification (DM) of HG. The DM of HG is regulated by cell wall-localized pectin methyltransferase enzyme (PMEs, E.C. 3.1.1.11). The activity of PMEs is controlled by endogenous PME inhibitors (PMEIs) (Pelloux *et al.*, 2007; Wolf *et al.*, 2009). PMEs catalyzes the removal of the methyl groups from the HG leading to release of free carboxyl groups, methanol, and protons (Wolf *et al.*, 2009). PMEIs regulate PME activity by making a stoichiometric 1:1 complex and thereby inhibiting PME activity in the cell wall in a pH and ion concentration-dependent (Matteo *et al.*, 2005). The de-methyl esterified form of HG makes an egg-box structure by crosslinking with Ca^{2+} . The egg-box structure provides adhesion between two cells (Willats *et al.*, 2001) and cell wall strength. The modulation of HG methyl esterification has a dramatic influence on cell growth and has been shown to be the direct consequence of pectin-degrading enzymes such as polygalacturonases, pectate lyases, and pectate lyases-like (Liners *et al.*, 1992; Bouton *et al.*, 2002; Wolf *et al.*, 2009; Sénéchal *et al.*, 2014; Higaki *et al.*, 2015). Moreover, methyl esterification state of HG plays a vital role in various developmental processes such as phyllotaxis, lateral organ initiation in

shoot apical meristem (SAM), hypocotyl development, pollen maturation and fruit ripening (Wakabayashi *et al.*, 2003; Francis *et al.*, 2006; Derbyshire *et al.*, 2007; Peaucelle *et al.*, 2008, 2011; Pelletier *et al.*, 2010; Braybrook and Peaucelle, 2013; Paniagua *et al.*, 2014).

The plant cell wall is also a great source of signaling molecule involved in activating cellular processes for growth and defense against biotic and abiotic stress. It has been shown that specific cellular responses can be induced by cell wall fragments thus considered as a signaling molecule (Ayers *et al.*, 1976; Aziz *et al.*, 2007). These plant cell-based signaling molecules which stimulate innate immunity responses has been named host-associated molecular patterns or damage-associated molecular patterns, in analogy to pathogen-associated molecular patterns (PAMPs) (Zipfel *et al.*, 2006; Galletti *et al.*, 2009). For example, pectin-derived oligogalacturonides (OGs) with a chain length between 9 and 15 galacturonic acid residues induce transcriptional reprogramming, stomatal closure, ethylene production, cell wall reinforcement and ROS production (Hahn *et al.*, 1981; Nothnagel *et al.*, 1983; Simpson *et al.*, 1998; Ridley *et al.*, 2001; Osorio *et al.*, 2007). OGs are capable of inhibiting root morphogenesis by inhibiting auxin-induced gene expression of *ROLB* in transgenic leaf explants (Bellincampi *et al.*, 1996). Pectin is also a target for many microbial cell wall-degrading enzymes during pathogen attack, the possible roles of OGs in plant defense mechanisms have been well investigated. The biological activity of OGs seems to depend on their degree of polymerization, methylation, and conformation (Seifert and Blaukopf, 2010). In parallel, expression of fungal polygalacturonases, enzymes that hydrolyze the homogalacturonan of the plant cell wall into OGs, leads to constitutively activated plant defense responses and to a reduction in sensitivity to auxin (Bellincampi *et al.*, 1996; Denoux *et al.*, 2008). Apart from their structural role, xyloglucan-derived OGs may also participate in cell wall signaling during developmental processes. Xyloglucan nonasaccharides (XG9s) have been shown to inhibit auxin-induced stem elongation in pea (York *et al.*, 1984). This process appears to be highly specific since XG10s or XG8s failed to reproduce the same result. This observation suggests the existence of a XG9 receptor that is implicated in regulation of auxin-induced growth. However, these findings could not be confirmed in *Arabidopsis*, since the xyloglucan fucosyl transferase mutant *mur2*, which produces xyloglucan lacking fucose, does not show a visible phenotype (Vanzin *et al.*, 2002). This result can be explained by a putative species-dependent process or by the possibility that one of the other 10 fucosyl transferase family members fulfills the function in *Arabidopsis*. Another carbohydrate that is thought to play a role in signaling at the cell wall is xylogen, a highly glycosylated cell wall molecule that acts as an extracellular developmental signal (Motosé *et al.*, 2004). Xylogen was found to promote tracheid differentiation *in vitro* and, together

with its paralogs, to be required for normal vascular differentiation *in planta*. Xylogen is a hybrid GPI-anchored arabinogalactan protein (AGP) and nonspecific lipid transfer protein. AGPs are proteins implicated in signaling processes during cell proliferation and survival, pattern formation and growth, as well as plant microbe interactions (Seifert and Roberts, 2007). Their potential to bind to β -glycan polymers together with their plasma membrane localization via GPI anchors put them in a strategic position to mediate interactions between cell wall polymers and cell signaling. In mammalian cells, GPI-anchored proteins have been implicated in mediating cell-cell interactions by interacting with other proteins that contain transmembrane domains (Ellis *et al.*, 2010). Although there is no available evidence, it is conceivable that GPI-anchored AGPs and/or their soluble forms interact with plasma membrane-bound receptor kinases or with receptors in neighboring cells in plants.

1.2 The role of cell wall signaling in plant morphogenesis

Plant morphogenesis at the cellular level is attributed to fundamental cellular processes like cell division, cell expansion. Since plant cells are glued together through their sharing cell wall, there is no cell migration possible to achieve concerted growth and development (Dupuy *et al.*, 2008). Thus, morphogenesis in higher plants is tightly controlled by the cell wall to facilitating a process of local cell division, selective cell expansion and differentiation (Wolf, 2018; Cosgrove, 2005; Wolf *et al.*, 2012a; Wolf and Höfte, 2014). The plant cell wall is deposited between two adjacent cells at the end of cell division and due to different growth rate, a mechanical force is generated that might have an impact on morphogenesis. (Mirabet *et al.*, 2011). Moreover, just before dividing, cells need to increase in volume, which is achieved by controlled cell wall biosynthesis and remodeling (Lipka *et al.*; Cosgrove, 2001, 2005; Cosgrove and J., 2014). Plant cells expand by depositing cell wall through the process of ‘polymer creep’ in which cellulose microfibrils and matrix polysaccharides slide within the wall to increase its surface area (Cosgrove., 2016; Xiao *et al.*, 2016b). Plant cell expansion includes wall hydration, turgor-driven wall relaxation, mechanosensing and wall cross-linking, and deposition of new wall materials (Wolf *et al.*, 2012a,b). To achieve proper growth and homeostasis during morphogenesis, as well as to assure cell wall fortifications in response to extrinsic challenges, cell wall monitoring system must exist to detect changes in cell wall state and activate downstream responses (Bidhendi and Geitmann; Hématy *et al.*, 2007, 2008; Wolf *et al.*, 2012a; Hamann, 2015; Wolf, 2017). Conventionally, cell wall monitoring pathways have been named cell wall integrity (CWI) signaling.

The CWI signaling mechanism in yeast involves cell surface receptors acting as CWI sensors which pass over information about extracellular wall status to intracellular regulatory pathways (Levin, 2005).

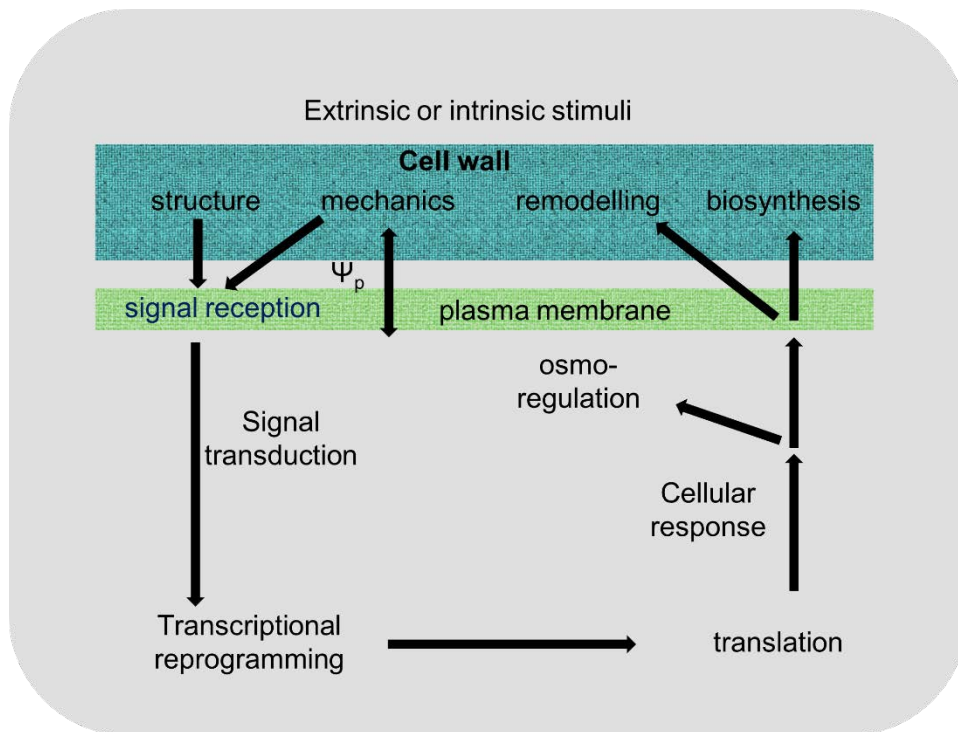


Figure 2. Model of the plant cell wall integrity maintenance system. Extrinsic and intrinsic stimuli are received at the plasma membrane through cell wall sensors and signal is transduced to transcriptional and translational machinery for adaptation and activating responses accordingly. Change in turgor pressure (Ψ_p) is perceived as a signal for cell wall perturbation. The responses include cell wall fortification, cell wall remodeling mediated through various enzymatic processes.

The first information about such surveillance system came from research in yeast where weakening of the cell wall through pharmacologically inhibiting cell wall biosynthesis forced single yeast cells to reinforce their wall to prevent bursting (Levin, 2005; Fujikura *et al.*, 2014). In yeast three different cell wall monitoring systems have been characterized: mating induced death 1 (MID1) calcium channel protein 1 (CCH1) mechano-perception based pathway, the high osmolarity glycerol (HOG) pathway, and the CWI maintenance mechanism (Levin, 2005). In MID1 CCH1 mediated mechano-perception pathway, it is suggested that an osmotic shock-like response is generated because of turgor pressure causing plasma membrane to stretch upon weakening of cell wall. The Ca^{2+} /calmodulin-dependent protein phosphatase CALCINEURIN and calcineurin-responsive zinc finger 1 (CRZ1) initiate calcium ion pulse upon a perception of stretch in the plasma membrane, followed by the expression of genes such as *FK506 Sensitivity (FKS2)*, which encodes a glucan synthase (Garrett-Engle *et al.*, 1995;

Batiza *et al.*, 1996). In the classical example of a similar response upon cell wall weakening, the mating factor induces an influx of calcium ions through the calcium channels CCH1 and MID1 (Garrett-Englele *et al.*, 1995; Locke *et al.*, 2000). MID1 is a glycosylated transmembrane protein that induces stretch-activated calcium influx in both yeast and heterologous systems (Iida *et al.*, 1994; He *et al.*, 1999). The HOG pathway involves two different hyperosmotic stress sensors, Synthetic high osmolarity-sensitive protein 1 (SHO1), and Synthetic Lethal of N-end rule 1 (SLN1)/ tYrosine Phosphatase Dependent 1 (YPD1)/ Suppressor of Sensor Kinase 1 (SSK1) (Posas *et al.*, 1998). Both SHO1 and SLN1 sensors transduce signals to the MAPKinase HOG1, which results in inactivation of the transcriptional response via Suppressor of Kre Null 7 (SKN7), which in turn induces *FKS2* expression (Alberts *et al.*, 1998; Levin, 2005). The low osmolarity keeps SLN1 inactive while an increase in osmolarity activates SLN1 and triggers the activation of the HOG response genes, leading to the biosynthesis and retention of glycerol as a compatible intracellular solute (Luyten *et al.*, 1995; Tamas *et al.*, 1999; Reiser *et al.*, 2003).

In contrast to yeast, CWI signaling in the plant is not well understood. In recent years, there has been an increasing number of findings that indicate the existence of CWI maintenance mechanism in plants. The initial idea about CWI in plant originated with suppressor screen of cellulose biosynthesis defective mutant *prc1-1* in Arabidopsis, which has a mutation in primary cellulose biosynthesis gene *CESA6*. The *CESA6* is part of cellulose biosynthesis machinery *CESA* complex and plants lacking *CESA6* activity show reduced hypocotyl growth, ectopic lignification and elevated transcript level of defense-related gene *PDF1.2* and *VSP1*. The suppressor allele of *prc1-1* was able to partially rescue hypocotyl growth defect and suppress ectopic lignification and elevated *PDF1.2* and *VSP1* transcripts without affecting cellulose content (Shedletzky *et al.*, 1990; Burton *et al.*, 2000; Cano-Delgado *et al.*, 2000; Ellis, 2002; Cano-Delgado *et al.*, 2003; Manfield *et al.*, 2004; Hématy *et al.*, 2007; Bischoff *et al.*, 2009; Largo-Gosens *et al.*, 2014; Xiao *et al.*, 2016). With this observation, it could be safely inferred that signaling and cell wall surveillance are required to orchestrate these responses. In addition, presumably signaling-mediated compensatory responses have been observed to genetic impairment of xyloglucan biosynthesis (Xiao *et al.*, 2016) and in lignin biosynthesis mutants (Voxeur and Höfte, 2016a). Again, the yeast cell wall integrity signaling field offers a useful model demonstrating the feasibility of this approach. An exciting recent example that builds on earlier studies (Beňová-Kákošová *et al.*, 2006) is provided by the observation that oligosaccharides produced by an endo- β -mannanase suppress cell wall thickening in the xylem of Populus, controlling the switch from primary to secondary cell wall deposition (Zhao *et al.*, 2013). Thus, cell wall-derived signals affect stress

responses, but can also regulate developmental processes. Irrespective of their function, all cell wall signaling pathways share the requirement that information has to be transmitted from the outside across the plasma membrane to the inside of the cell, where a response can be orchestrated. Numerous possibilities to transduce signals are conceivable (Figure 2), such as gated ion channels, arabinogalactan proteins (AGPs), proteins that connect the cell wall and the cytoskeleton, mechanosensory analogous to yeast MID1, and osmosensors (Nakagawa *et al.*, 2007b; Seifert and Blaukopf, 2010; Denness *et al.*, 2011a; Hamilton *et al.*, 2015). For instance, it has been demonstrated recently that MECHANOSENSITIVE CHANNEL OF SMALL CONDUCTANCE-LIKE 8, a protein from Arabidopsis homologous to the mechanosensitive channel of small conductance from Escherichia coli, senses and response to changes in osmotic potential in the pollen (Hamilton *et al.*, 2015). However, many of the known cell wall signaling components seem to operate in pathways featuring a member of the large family of receptor kinases (RKs) to transmit signals from the outside to the inside of the cell.

Plant RKs form expanded gene families with >600 and 1000 members in Arabidopsis and rice, respectively (Shiu and Bleecker, 2001a,b; Tor *et al.*, 2009). The majority of which are, to date, orphan receptors without a known ligand or downstream intracellular targets. Generally, RKs contain an N-terminal signal peptide, a variable extracellular domain (ECD), a single-pass transmembrane domain (TM), and a cytosolic protein kinase domain (KD) that is related to animal Pelle/IRAK-4 kinases (Shiu and Bleecker, 2001a,b; Tor *et al.*, 2009). The largest subgroup among RLKs is formed by proteins with a leucine-rich repeat extracellular domain (LRR-RLKs), and individual members of this group have essential roles in many aspects of plant development and immunity (Li and Chory, 1997; Li *et al.*, 2002; Wang *et al.*, 2005; Zipfel *et al.*, 2006). The typical event starts with binding of an extracellular ligand to cell surface receptor that induces a conformational change leading to the activation of the protein kinase activity, thereby initiating a cascade of subsequent signal transduction events. In Arabidopsis, several families of RK have been shown to involved in cell wall signaling, but currently, it is unclear whether cell wall components are actual ligands of these proteins. So far only wall-associated kinases (WAKs) have been shown to directly bind to a cell wall carbohydrate in vitro (Kohorn *et al.*, 2006b,a). Moreover, it has also been reported that WAK1 is tightly bound to a cell wall fraction and is specifically localized to the plasma membrane-cell wall interface (He *et al.*, 1999). Plant RLKs can be categorized into two classes depending on their role in growth and development or in plant immune signaling. The first class comprises hormone receptors, such as BRI1, regulating brassinosteroid related development, or surface receptor determining the developmental fate of cells

like CLV1 controlling apical meristem proliferation and ER regulating organ initiation and elongation (Clark *et al.*, 1997; Li and Chory, 1997). The second category includes RLKs involved in plant-microbe interactions and stress responses. These include FLS2, involved in bacterial elicitor flagellin perception, and the above mentioned WAKs, that are linked to defense responses and cell expansion (Brutus *et al.*, 2010; Gómez and Boller, 2000; Anderson *et al.*, 2001; Li *et al.*, 2009). The different RLK families that are possibly involved in CWI signaling are discussed in figure 3.

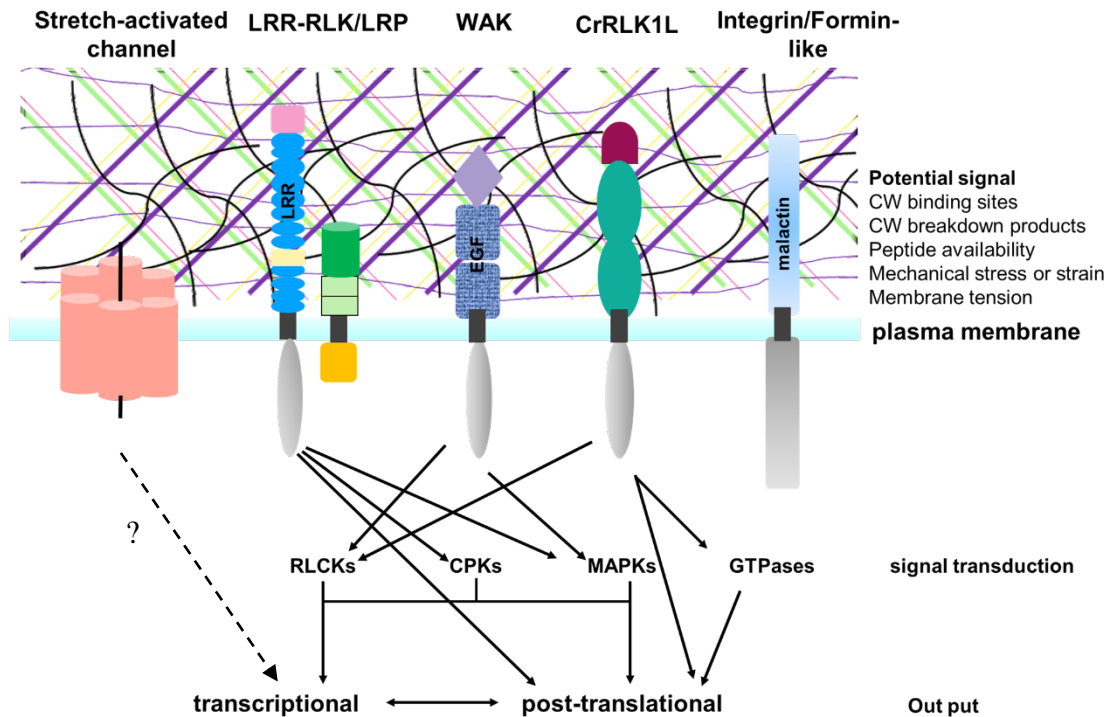


Figure 3. Overview of selected potential cell wall-related signaling receptors and signals. Based on existing data, RLKs, such as LRR-RLKs, WAKs, and CrRLK1Ls, play the most prominent role in signal transduction upon cell wall-related cues. However, other cell walls and plasma membrane-localized proteins are well suited to play a role in cell wall perception, e.g. stretch-activated ion channels, proteins homologous or analogous to animal integrins and formins, putative mechanosensory (not shown), AGPs (not shown), and LRR-extensins (not shown). Note that among the depicted receptor families, only WAK1 and FORMIN HOMOLOGY 1 have been shown to physically interact with the wall. Signaling downstream from the plasma membrane receptors can involve intracellular protein kinases of the RLCK, calcium-dependent protein kinase (CPK), mitogen-activated protein kinase (MAPK), or small GTPase protein families.

1.3 CWI sensor proteins in plant

1.3.1 *Catharanthus roseus* RLK1-like kinases

Members of *Catharanthus roseus* receptor-like kinase1-like (CrRLK1L) subfamily constitute the most studied group of receptor-like kinases in the context of cell wall signaling (Wolf and Höfte, 2014; Wolf *et al.*, 2014; Nissen *et al.*, 2016). This could be because of the existence of putative carbohydrate-binding domains within their cell wall-facing ECD. There is also resounding genetic evidence relating CrRLK1L receptors to cell wall homeostasis, mechanoreception, cell wall integrity maintenance, and growth control (Wolf and Höfte, 2014; Wolf *et al.*, 2014; Nissen *et al.*, 2016) The CrRLK1L gene family includes 17 members in Arabidopsis, among which seven have been allocated a function including *THE1* and *FERONIA* (Huck *et al.*, 2003; Hématy *et al.*, 2007). The domain structure analysis reveals they consist of a signal peptide, a divergent ECD of ~400 amino acids, a juxtamembrane (JT) region required for binding of the co-receptors LORELEI/LORELEI-LIKE-GPI-ANCHORED PROTEIN 1, TM, and a highly conserved cytoplasmic serine/threonine KD with a more divergent C-terminal tail of unknown function. The ECD also shares some homology with malectin (Boisson-Dernier *et al.*, 2011), a protein originally described to be involved in ER quality control in *Xenopus laevis* (Feng *et al.*, 2018). Remarkably, malectin is able to interact with di-glucose motifs of N-linked oligoglycans and is structurally close to carbohydrate-binding modules of glycosyltransferases (Feng *et al.*, 2018). It promotes the notion that the homologous CrRLK1L domain might mediate cell wall binding in plants (Boisson-Dernier *et al.*, 2011).

1.3.1.1 THESEUS1

THE1 was identified in a suppressor screen of the CESA6 mutant *prc1-1* (Hématy *et al.*, 2007). The loss-of-function allele *the1-1* was able to rescue the dwarf phenotype and ectopic lignification of many *cesa* mutants without affecting cellulose deficiency. This observation places *THE1* as a possible component of CWI signaling in Arabidopsis. Furthermore, *THE1* is also required for isoxaben-induced ROS production and to repress JA production upon isoxaben treatment (Denness *et al.*, 2011b) The transcriptional reprogramming in *prc1* depends on *THE1* signaling, hinting at a role of *THE1* in cell wall cross-linking. Taken together, these results suggest the participation of *THE1* in facilitating the response to cell wall distress. It is conceivable that *THE1*-mediated ROS production leads to the inhibition of cell growth, perhaps through cell wall cross-linking. Surprisingly, loss-of-function allele *the1-1* do not show noticeable phenotypes in normal growth conditions (Hématy *et al.*, 2007). Thus,

it remains to be established in which developmental or stress-related processes the THE1 is involved. Moreover, It will be exciting to see whether THE1 interacts with wall-derived carbohydrates through its malectin domains and whether it binds additional ligands as demonstrated for the best-characterized CrRLK1L, FERONIA.

1.3.1.2 FERONIA

FERONIA (FER) was initially described as needed for fertilization since the loss of activity results into the accumulation of supernumerary pollen tubes that failed to discharge in female gametophyte (Rotman *et al.*, 2003; Huck *et al.*, 2003). It is localized to the filiform apparatus of the two synergid cells that form the entry point for the pollen tube (Escobar-Restrepo *et al.*, 2007). Moreover, the *fer* mutants show various growth and developmental defects like defective root hair growth, stunted plant height, hypersensitive root growth during high salinity (Wolf and Höfte, 2014). The pleiotropic phenotype of *fer* mutant could be explained on the basis of fact that, FER has been shown to involved in several hormone pathways such as abscisic acid, auxin, ethylene, and BR signaling , as well as defence and mechanical signaling (Guo *et al.*, 2009; Keinath *et al.*, 2010; Deslauriers and Larsen, 2010; Duan *et al.*, 2010; Kessler *et al.*, 2010; Yu *et al.*, 2012; Shih *et al.*, 2014). Recently, the FER ectodomain was shown to bind to the secreted peptide RAPID ALKALINIZATION FACTOR 1 (RALF1) (Haruta *et al.*, 2014). RALF1 peptide is known to induce several cellular processes, such as increase in apoplastic pH, a transient increase in cytoplasmic calcium, a concomitant cessation of growth, and the differential phosphorylation of many proteins, including FER itself. The *fer* mutant is insensitive to RALF1 induced cellular responses, suggest FER is the receptor for RALF1 (Pearce *et al.*, 2001; Haruta *et al.*, 2008, 2014, 2018). Interestingly, FER is also known to facilitate the response towards mechanical stress and root growth of *fer* mutant is hypersensitive to mechanical impediments. However presently, it is uncertain if FER-mediated mechano-responses depend on the availability/release of RALF peptides (Pearce *et al.*, 2001; Haruta *et al.*, 2008, 2014, 2018). Nevertheless, the available data so far suggests that FER being required to sense both extrinsic and intrinsic mechanical cues to coordinate growth responses (Haruta *et al.*, 2014, 2018) and thus indicate that mechanosensing is required for supracellular growth coordination.

1.3.1.3 ANXUR1/2

ANXUR1 (ANX1) and ANXUR2 (ANX2) are the closest homologs of FER and mainly expressed in the male gametophyte (Boisson-Dernier *et al.*, 2009; Miyazaki *et al.*, 2009). The loss in activity of ANX1 and 2 results into strongly reduced fertility and premature pollen tube burst, whereas

overexpression of ANX1 or 2 inhibited pollen tube growth (Miyazaki *et al.*, 2009). It is essential for pollen tube cell wall integrity (Miyazaki *et al.*, 2009). The ANX1, 2 also promote the generation of ROS in pollen tube through the pollen-expressed NADPH oxidases respiratory burst oxidase homologs (RBOH) RBOHH and RBOHJ. NADPH oxidase-mediated ROS, in turn, are required to maintain functional calcium dynamics during pollen tube growth. Interestingly, a marked increase in cytoplasmic calcium preceded the premature pollen tube burst in *anx1 anx2* (Miyazaki *et al.*, 2009), similar to the calcium spike induced by exogenous ROS application before rupture (Duan *et al.*, 2010). Thus, both elevated and reduced levels of ROS lead to pollen tube burst, although the underlying mechanism in both cases is not understood yet.

1.3.2 Wall-associated kinases (WAKS)

Arabidopsis genome contains five *WAK* gene arranged in a genes cluster at chromosome 1 and 17 *WAK*-like genes (Kohorn, 2001). The *WAK* proteins are characterized by an intracellular serine-threonine kinase domain and an extracellular domain with epidermal growth factor repeats (He *et al.*, 1996, Kohorn, 2001). The extracellular domain of *WAKs* has been shown to bind covalently with pectic homogalacturonan and noncovalently to Ca²⁺ cross-linked OGs *in vitro* (Wagner and Kohorn, 2001, Decreux and Messiaen, 2005). However, the mechanisms by which *WAKs* interact with the cell wall are still not clarified. In a recent finding, *WAK1* was shown to be the receptor for OGs in Arabidopsis (Brutus *et al.*, 2010). In addition, the *WAK1* extracellular domain can be pelleted *in vitro* with Ca²⁺ cross-linked homogalacturonan, suggesting that interaction of *WAKs* is not restricted to short fragments such as OGs (Decreux and Messiaen, 2005). *WAK2* has been shown to be required for sugar-independent growth. The root growth in loss-of-function *wak2* mutant is dependent on the sucrose availability in the growth media and *wak2* phenotypic defect is rescued by adding sugar or sorbitol (Kohorn *et al.*, 2006). *WAK2* has also been shown to important for normal expression of vacuolar invertase, an enzyme that hydrolyzes sucrose into glucose and fructose (Kohorn *et al.*, 2006). This observation suggests a role of *WAK2* in regulating the balance of cell wall carbohydrates, which act as an energy source and as osmotically active compounds. *WAKs* may thus provide a molecular mechanism linking cell wall sensing (via pectin attachment) to regulation of solute metabolism, which in turn is known to be involved in turgor maintenance in growing cells.

1.3.3 Proline-rich Extensin-like Receptor Kinases (PERKs)

The proline-rich extensin-like receptor kinase (PERK) family comprises of 15 members in Arabidopsis (Shiu and Bleecker, 2003). PERKs poses a proline-rich extracellular domain similar to Extensin, embedded in the cell wall like that of the WAKs (Nakhamchik *et al.*, 2004). PERKs are shown localized at the plasma membrane (Silva and Goring, 2002; Nakhamchik *et al.*, 2004). The functional characterization of *PERKs* suggests the involvement of this gene family in cell elongation and development (Haffani *et al.*, 2006; Humphrey *et al.*, 2007). The downregulation of *PERK* expression using anti-sense approach leads to floral organ defect and in addition, *perk13* mutants exhibit cell elongation defect in the root (Humphrey *et al.*, 2007). *BnPERK1* is the first reported *PERK* from *Brassica napus* and its expression is rapidly induced upon wounding (Silva and Goring, 2002). Similar to the WAKs, PERK4 is an active protein kinase localized to the plasma membrane, and its extraction from plant material is increased by pectinase treatment (Bai *et al.*, 2009). More recently, PERK4 has been shown to specifically required for the abscisic acid (ABA)-dependent influx of Ca²⁺ in seeds and roots (Haffani *et al.*, 2006). There has been ample evidence supporting the notion that PERKs have roles in development and stress responses, however further work is needed in order to demonstrate their direct involvement in signaling during cell wall perturbations.

1.3.4 Leucine-Rich Repeat Receptor Kinases (LRR-RKs)

LRR-RKs form the biggest group of RKs in Arabidopsis, with at least 220 members (Shiu and Bleecker, 2003). They are known to play fundamental roles in cell-cell communication during development, hormone perception, abiotic and biotic stress responses (Torii, 2004). Several LRR-RKs have functions in plant growth and development for example, a LRR-RK CLAVATA1 (CLV1), and CLAVATA2 (CLV2) along with its ligand CLAVATA3 (CLV3), controls the balance between cell proliferation and cell differentiation in the shoot meristem (Jeong *et al.*, 1999; Trotochaud *et al.*, 2000). ERECTA plays an important role in organ elongation (Torii *et al.*, 1996). BRASSINOSTEROIDS INSENSITIVE1 (BRI1) is involved in growth-promoting brassinosteroid signaling (Li and Chory, 1997; Nam and Li, 2002; Wang *et al.*, 2005). The LRR-RKs, SOMATIC EMBRYOGENESIS RECEPTOR KINASES 1 and 2 (SERK1 and SERK2), are crucial for the anther development (Colcombet *et al.*, 2005). Plant LRR-RKs also function as pattern recognition receptors in host innate immunity. FLAGELLIN SENSITIVE 2 (FLS2) and EF-Tu receptor (EFR) play a role in bacterial elicitor perception (Gómez-Gómez and Boller, 2000; Zipfel *et al.*, 2006). Two other LRR-RKs FEI1 and FEI2 have been shown to involve in maintaining cell wall integrity during high osmolar growth

condition. The *fei1* and *fei2* loss-of-function mutants show sucrose and salt content-sensitive anisotropic cell expansion defects and also show a deficiency in cellulose (Xu *et al.*, 2008). Interestingly the kinase domain of is dispensable for FEI function since the inactive kinase domain of FEI1 was able to fully complement the *fei1fei2* double mutant phenotype.

1.3.5 Leguminous L-Type Lectin RLKs (LecRKs)

Leguminous L-type Lectin RLKs are a group of 45 RLKs proteins which are capable of binding carbohydrates via their tripeptide lectin motifs (Gouget *et al.*, 2006; Bouwmeester *et al.*, 2011). The lectin motif also called arginine-glycine-aspartate (RGD) motif, is a tripeptide sequence present in various animal extracellular matrix proteins (Gouget *et al.*, 2006). In plants it is known to facilitate plasma membrane detachment from the cell wall during plasmolysis, suggesting a role in cell wall-plasma membrane adhesion (Canut *et al.*, 1998). The *LEKRR79* interacts with the tripeptide motif RGD in IPI-O, an Arg-X-Leu-Arg (RXLR) effector from *Phytophthora infestans* (Bouwmeester *et al.*, 2011). RGD peptides can dissociate PM-cell wall Hechtian strands which are formed during plasmolysis (Canut *et al.*, 1998). *P.infestans* can disrupt cell wall-plasma membrane connections through the RGD domain on IPI-O (Gouget *et al.*, 2006). The *LecRLKs* are expressed at very low levels during plant development but on pathogen attach they are transcriptionally up-regulated (Bouwmeester *et al.*, 2011). Interestingly, the receptor LecRK-1.9 has been identified as a receptor for RGD peptides. The knockout mutant of LecRK1.9 shows reduced callose deposition, reduced membrane-wall contacts and increased pathogen susceptibility (Bouwmeester *et al.*, 2011).

1.3.6 Histidine Kinases (HKs)

Histidine kinases (HKs) are a very interesting group of protein that acts as sensors of environmental and intrinsic stimuli in bacteria, amoeba, yeast, and plants. They are known to form a two-component system: the membrane-bound histidine kinase (HK) acting as an environmental sensor and a phospho-relay system to translate the signal (Romir *et al.*, 2010). Eight HKs have been identified in Arabidopsis and have been associated with various development and defense pathways like osmosensing (AHK1), megagametophyte development (CKI1), ethylene signaling (ETR1 and ERS1), cytokinin receptors (AHK2, AHK3 and AHK4/CRE1), salt sensitivity and resistance against bacterial and fungal infection (AHK5) (Kakimoto, 1996; Gamble *et al.*, 2002; Pham *et al.*, 2012). Moreover, several HKs have also been shown to partake in responses to abiotic stresses such as temperature, salt, changes in osmolarity and drought (Wohlbach *et al.*, 2008; Tran *et al.*, 2010; Jeon *et al.*, 2010).

1.3.7 Mechanosensitive Receptors and Ion Channels

A living being has to respond to physical forces such as touch, sound, and osmotic stress. These extrinsic stimuli have to be perceived and interpreted into biochemical signals that can be observed by the cell. As stated earlier, the plasma membrane is mechanically associated with the cell wall by turgor pressure, plasma membrane stretch due to variations in turgor pressure may be a general mechanism to report cell wall integrity and performance to the cell interior. In *E.coli* the mechanosensitive channels of small conductance (*MscS*) are well-characterized mechanosensitive channels for osmosensitivity (Haswell and Meyerowitz, 2006; Haswell *et al.*, 2008). The stretching of the membrane opens *MscS* channels and lets ions pass through, consequently an increase in cytoplasmic Ca²⁺ levels and relief of osmotic pressure (Jensen and Haswell, 2012). In *Arabidopsis* 10 *MscS*-like (*MSL*) genes have been identified and 6 in *Oryza sativa* (rice) (Haswell and Meyerowitz, 2006). The *MSL* protein harbors conserved motifs critical for mechano-sensitive function (Jensen and Haswell, 2012). It has been shown that the *MSL3* from *Arabidopsis* can rescue an *E.coli mscs* mutant from osmotic shock indicating that the *MSL3* protein functions as a mechano-sensor (Haswell and Meyerowitz, 2006). In another example, *MCA1* provides the best evidence of possible functional similarities between the yeast and plant CWI systems. Originally *MCA1* was identified as a gene which is up-regulated during the S-phase of the cell cycle (Menges *et al.*, 2002). In a functional complementation study, it was shown that the yeast *mid1/cch1* double knock out could be partially complemented by plant *MCA* despite the low conservation between the two genes (10% identity and 41% similarity) (Nakagawa *et al.*, 2007a). Interestingly the *MCA1* can function on its own, unlike the yeast proteins that require the complete MID1/CCH1 complex to confer stretch activation (Nakagawa *et al.*, 2007a). Moreover, the loss of function mutant failed to grow through increasing agar concentrations due to a loss of mechano-sensing ability (Nakagawa *et al.*, 2007). The localization study showed that *MCA1*-GFP localized to the plasma membrane in *Arabidopsis* root cells (Nakagawa *et al.*, 2007a) and regulates Ca²⁺ influx during growth.

1.3.8 Other candidate proteins involved in cell wall signaling

Besides RLKs and MscSs, other candidate proteins also have been identified that could be involved in cell wall signaling in plants. Formin proteins represent the best-known example. They participate in the organization of actin microfilaments in *Arabidopsis*. The extracellular extensin-like domain-containing ARABIDOPSIS THALIANA FORMIN HOMOLOGY1 (ATFH1) is localized at the plasma membrane and has been shown to form a bridge between the actin cytoskeleton and the cell

wall (Martinière *et al.*, 2011). Similar to the mechanosensory protein integrin in mammalian cells, ATFH1 might directly connect the cell wall and the cytoskeleton. In Arabidopsis, NDR1 is a transmembrane protein that shares structural homology to mammalian integrin proteins, and is known to provide disease resistance against bacterial and fungal pathogens (Century *et al.*, 1995, Coppinger *et al.*, 2004, Knepper *et al.*, 2011). It was shown that plasmolysis in *ndr1-1* mutants results in the complete detachment of the plasma membrane from the cell wall. The *ndr1-1* mutants yield spherical protoplasts with no remaining attachments, i.e., convex plasmolysis contrary to concave plasmolysis in wild-type. Available evidence suggests a dual role for NDR1 in regulating primary cellular functions in Arabidopsis through maintaining the integrity of the cell wall-plasma membrane connection and as a critical signaling element of the responses upon pathogen attack.

1.4 Downstream signaling processes involved in the response to CWD

1.4.1 Ca²⁺ and ROS

Ca²⁺ ion and reactive oxygen species (ROS) are two important ion fluxes known to involve in various developmental and defense-related processes. The existing data advocate similarity between cell wall signaling in defense response to cell perturbation and cell wall remodeling related to developmental processes. For example, during root hair growth pattern of ROS burst and increase in extracellular pH alongside Ca²⁺ ion flux has been reported that relates to the pattern observed in the cell wall burst response in Arabidopsis root cells (Monshausen *et al.*, 2007, 2008; Takeda *et al.*, 2008; Shih *et al.*, 2014). This overlap in between two processes could be explained by assuming that rapid cell wall expansion is perceived at the plasma membrane, causing an elevation in intracellular Ca²⁺ followed by the production of ROS and alkalinization of the apoplast. It has also been shown that suppressing Ca²⁺ and ROS results in cell bursting (Foreman and Dolan; Monshausen *et al.*, 2008). Ca²⁺ fluxes may be first induced by mechano-sensitive channels that respond to increased membrane tension during cell wall growth.

The ROS signaling network is evolutionarily preserved among most living organisms. It acts as one of the first molecules to transduce signal-regulating a diverse set of biological processes such as growth and response to biotic and abiotic stimuli (Mittler *et al.*, 2011). NADPH oxidases are the key enzyme for apoplastic ROS production and they are represented by transmembrane RBOHs in Arabidopsis. Arabidopsis genome has ten *RBOH* genes and they all exhibit the same domain structure. The RBOHs comprises of a core C-terminal region that contains the transmembrane domains and the functional

oxidase domain responsible for superoxide generation, and an additional N-terminal regulatory region where Ca²⁺-binding and phosphorylation domains are present (Mittler *et al.*, 2011; Suzuki *et al.*, 2011). The RBOH-derived ROS has also been linked to plant defenses in response to pathogen attacks and regulation of signaling related to abiotic stresses such as heat, drought, cold, high-light intensity, salinity or wounding (Lu *et al.*, 1996; Torres *et al.*, 2002; Mittler *et al.*, 2011).

1.4.2 CBI induced cell wall damage and response

In recent years, impairing cellulose biosynthesis has become a popular method to study cell wall integrity signaling in Arabidopsis. Plant cells respond to alteration in cellulose content in the cell wall. Cellulose is synthesized by cellulose synthase (CESA) complexes at the plasma membrane (Richmond and Somerville, 2000). The effects of reduced production of cellulose on plant growth and development have been studied by analyzing mutants with defects in genes encoding CESA subunits involved in primary cell wall biosynthesis (Fagard *et al.*, 2000; Ellis, 2002; Cano-Delgado *et al.*, 2003). Alternatively, various pharmacological agents can be applied for specifically inhibiting cellulose biosynthesis and similar response could be observed.

Isoxaben is a broad-leaf herbicide compound and is known as a very potent inhibitor of cellulose biosynthesis (Lefebvre *et al.*, 1987). Isoxaben specifically inhibits the incorporation of glucose units into the acid-insoluble cell wall fraction without affecting cellulase protein (Heim *et al.*, 1990). Moreover, at the cellular level isoxaben has shown to induce rapid disappearance of YFP:CESA6 from PM into an intracellular vesicle and thereby disrupting the CESA complex (Paredes, 2006). Thus, it has been proposed to be a specific inhibitor of cellulose biosynthesis (Heim *et al.*, 1990b; Coriocoet *et al.*, 1991; Paredes, 2006)). The isoxaben treatment results in cell swelling and bursting in the elongation zone of the Arabidopsis root. This phenotypic consequence is due to increased turgor that could not be held back by the weakened cell wall. Isoxaben induced cell wall perturbation could not be observed in the isoxaben resistant mutant *ixr1* and *ixr2*. The *ixr* mutations appear to directly affect the herbicide target since resistant lines show no alterations in uptake or detoxification of the herbicide (Heim *et al.*, 1991). The *IXR* genes were found to encode the subunits of the cellulose synthesis complex CESA3 and CESA6, respectively (Fagard *et al.*, 2000). Taken together, these findings suggest that isoxaben specifically inhibits cellulose biosynthesis by affecting the CESA complex.

As previously discussed, cellulose biosynthesis inhibition results in several physiological responses such as epidermal root cell bulgings, ROS production, ectopic lignification, callose deposition in

cotyledons JA and SA accumulation and transcriptional upregulation of defense-related genes such as *VSP1* and *PDF1.2* (Fagard *et al.*, 2000; Ellis, 2002; Cano-Delgado *et al.*, 2003; Hamann *et al.*, 2009). These physiological responses are osmosensitive and hexose sugar dependent and can be attenuated with the addition of sorbitol (Hamann *et al.*, 2009; Engelsdorf *et al.*, 2018). These observations led to the hypothesis that isoxaben-induced CBI mimics the effects of a hypo-osmotic shock. The transcriptional upregulation of drought-stress response genes such as *TCH4*, *ERD1* and *RD26* support this hypothesis. Moreover, proteins that are involved in water transport such as *TIP2;3* and *PIP2;4* were down-regulated by CBI in liquid culture grown seedlings (Alexandersson *et al.*, 2005). This finding suggests that change in turgor pressure may be sensed by specific mechano-sensor proteins which then activate responses to cell wall damage. Surprisingly, upon isoxaben treatment, the expression of several genes involved in photosynthesis and starch metabolism appeared to be downregulated (Denness *et al.*, 2011; Wormit *et al.*, 2012) however, in mutants of *MCA1*, *RBOHDF*, and *CRE1* the expression of those genes upon CBI did not change. It suggests a role of the mechanosensory machinery in mediating the changes in transcript levels of photosynthesis and starch metabolism genes induced by isoxaben.

1.5 The STRUBBELIG signaling pathway and its role in plant morphogenesis

1.5.1 STRUBBELIG is atypical RK

STRUBBELIG (SUB) is a leucine-rich repeat-receptor kinase of length 768 aa with a predicted molecular mass of 84.5 kDa. SUB contains N' terminus signal peptide of 24 aa, a SUB domain shared between the LRR-V members, six LRRs, a proline-rich region, a transmembrane domain (TM), a juxta-membrane domain (JM), and a carboxyl-terminal kinase domain (KD) (Kwak *et al.*, 2005; Chevalier *et al.*, 2005; Vaddepalli *et al.*, 2011) (Figure 4) SUB has been shown as atypical receptor kinase as it does not show any in-vitro kinase activity. Moreover, mutations in conserved amino acid residues known to interfere with kinase activity in typical kinases also do not affect SUB-wild-type function in planta

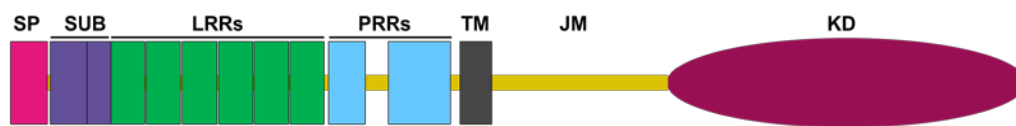


Figure 4. Overview of the domain architecture of SUB.

Abbreviations: JM, juxtamembrane domain; KD, kinase domain; LRR, leucine-rich repeat; PRR, proline-rich repeat; SP, signal peptide; SUB, SUB-domain; TM, transmembrane domain. Length of SUB protein: 768 amino acids. Scale bar : 50 aa.

(Chevalier *et al.*, 2005; Vaddepalli *et al.*, 2011). Interestingly, the kinase domain is indispensable for its function that suggests it might be involved in scaffolding to other proteins. Thus SUB represents an atypical receptor kinase as enzymatic activity of its kinase domain is not required for its function *in vivo* (Chevalier *et al.*, 2005; Vaddepalli *et al.*, 2011).

1.5.2 SUB regulates tissue morphogenesis in Arabidopsis

SUB regulates various aspects of plant growth and development. A plant lacking functional activity of *SUB* shows a pleiotropic phenotype including integument outgrowth, mis-organised sepals and petals,

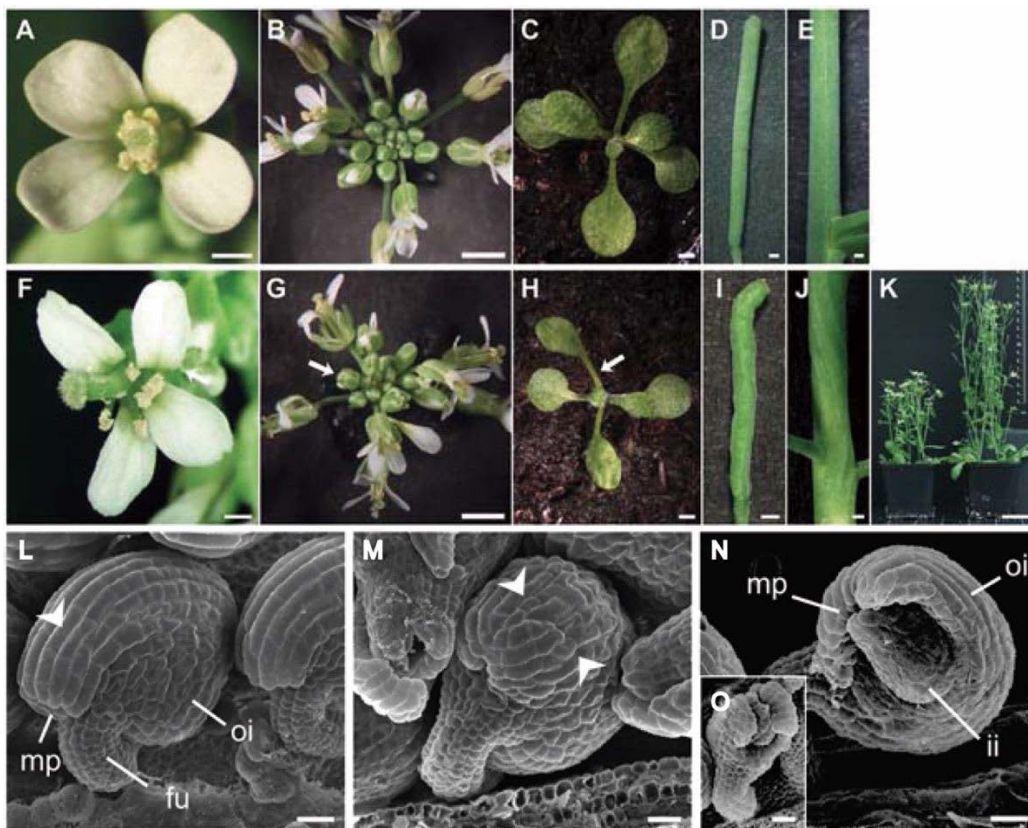


Figure 5. Phenotype comparison of the overall above-ground morphology of *Ler* and *sub-1*. (A-E) Wild-type *Ler*. (F-K) *sub-1*. (A, F) An open stage 13 flower from a 30-day old plant. Note the misorientation of petals due to twisting in the basal end of the petal structure (arrows). (F) Petals can also show small notches. (B, G) Top view of a 30-day inflorescence. (G) Flower phyllotaxis is irregular. Arrows mark prematurely opened flower buds. (C, H) Top view of a 12-day rosette. (H) Leaf petioles can be twisted (arrow). (D, I) Morphology of mature siliques. (E, J) A lateral view of a section of stems from a 30-day plant. (K) Plant height *sub-1* (left) in comparison to *Ler* (right). (L-N) Scanning electron micrographs of stage 4 ovules. (L) Wild-type *Ler*. The arrow marks one of the elongated cells of the distal outer integument. (M) *sub-1*. A mild phenotype is shown. Note the irregular size and shape of cells at the distal outer integument (arrowheads, compare to (L)). (N, O) *sub-1*. Strong phenotypes are depicted. Note the half-formed outer integument. (O) Shows an example where the outer integument shows several gaps. Scale bars: (A, D, E, F, I, J) 0.5 mm, (B, C, G, H) 2 mm, (K) 3 cm, (L, M, N, O) 20 μ m. Modified from (Fulton *et al.*, 2009).

twisted carpels and siliques and stunted plant height (Schneitz *et al.*, 1997; Chevalier *et al.*, 2005; Fulton *et al.*, 2009) (Figure 5). Initially, SUB was identified for its role in ovule development (Schneitz *et al.*, 1997; Chevalier *et al.*, 2005).

In addition, *sub* mutants have also been reported to show temperature-sensitive leaf development defects (Lin *et al.*, 2012). Under high ambient temperature (30°C) the *sub-2* mutants displayed impaired blade development, asymmetric leaf shape, and altered venation patterning, but these defects were less pronounced at normal growth temperature (22°C) (Lin *et al.*, 2012). At the cellular level, occasional periclinal divisions in the L2 layer of stage-3 floral meristem were observed, and the shape of the L2 layer cells seemed more irregular in *sub-1* mutant (Figure 6). The horizontal stem sections of 30-day old *sub-1* stem revealed reduced number of epidermal, cortex, and pith cells. The pith cells, in particular, appeared smaller. Furthermore, SUB is also known as SCM and it helps unspecified root epidermal cells to interpret their position in relation to underlying cortical cells and establish root hair cell identities (Kwak *et al.*, 2005; Kwak and Schiefelbein, 2008) (Figure 6).

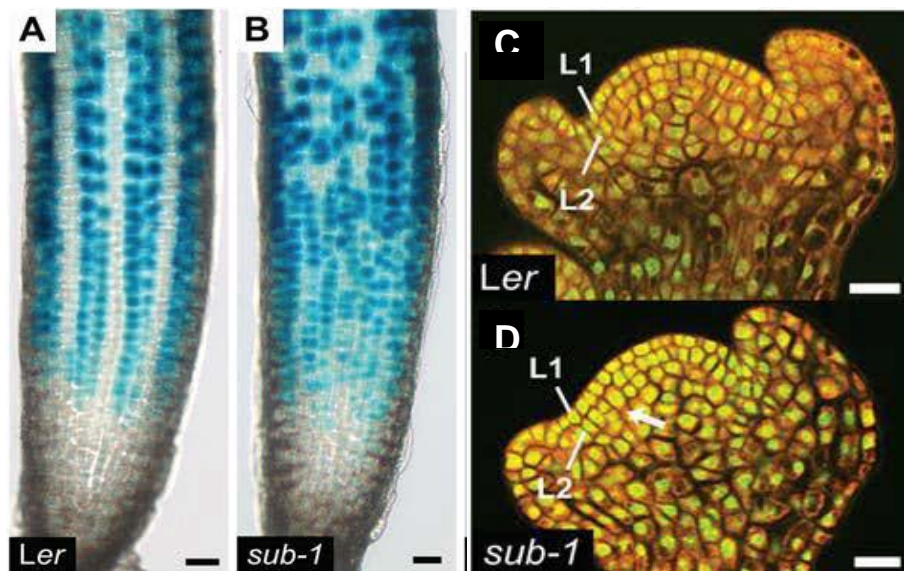


Figure 6. Sub-cellular phenotype comparison of the *Ler* and *sub-1*.

(A, C) Wild-type *Ler*. (B, D) *sub-1*. (A, B) Root hair cell patterning marked with non root hair cell-specific pGL2:GUS reporter. Notice the mis patterned root cells in *sub-1*(B). (C, D) Floral meristem stained with propidium iodide. The arrowhead indicates anticlinal cell division in L2 layer of *sub-1*(D) Scale bars: 5μm Modified from (Fulton *et al.*, 2009).

1.5.3 Novel components in the SUB signaling pathway

To elucidate the molecular mechanism of the SUB signaling pathway, additional candidate gene involved in the SUB pathway were identified. Using a forward genetic approach, EMS- mutagenized plants were scored for the *sub* phenotyped and three additional genetic factors were identified, *QUIRKY* (*QKY*), *ZERZAUST* (*ZET*), and *DETORQUEO* (*DOQ*) (Fulton *et al.*, 2009). *DOQ* is also known as *ANGUSTIFOLIA* (*AN*) in Arabidopsis (Bai *et al.*, 2013). The *qky-8*, *zet-2*, and *doq-1* mutants showed a *sub*-like phenotype and cellular defects, in outer integument development, floral organ shape, stem twisting, the floral meristem, and root hair patterning. The *qky-8* mutation was identified in gene encoding for multiple C2 domains and transmembrane region protein (MCTP) *QKY* which is localized at plasmodesmata (PD) (Fulton *et al.*, 2009). The other two candidates were identified as cell wall-localized β -1,3 glucanase *ZET* and cytoplasm localized *AN* (Bai *et al.*, 2013; Vaddepalli *et al.*, 2017). *QKY*, *ZET*, and *AN* were proven to contribute to *SUB*-dependent organogenesis and shed light on the mechanisms, which are dependent on signaling through the atypical receptor-like kinase *SUB* (Fulton *et al.*, 2009).

1.5.4 SUB:EGFP is enriched at plasmodesmata and interacts with QKY at PD

The translational fusion protein, SUB:EGFP has been shown to localize at PM in root epidermis cell of Arabidopsis root (Yadav *et al.*, 2008). Interestingly, SUB:EGFP also shows punctate pattern along PM (Vaddepalli *et al.*, 2014). In the light of PD localization of *QKY*, it led to the speculative if SUB:EGFP puncta are PD spots. On further analysis it has been revealed that SUB:EGFP is enriched at PD (Figure 7) (Vaddepalli *et al.*, 2014). Moreover, the PD localization of SUB:EGFP is further supported by immunogold electron microscopy. Thus, SUB is not only localized to the PM but also present at PD (Yadav *et al.*, 2008; Vaddepalli *et al.*, 2014), channels interconnecting most plant cells (Otero *et al.*, 2016; Sager and Lee, 2018). In co-localisation and interaction study it has been shown that SUB:EGFP colocalize and interact with mCherry:*QKY* specifically at PD (Figure 7) (Vaddepalli *et al.*, 2014). In line with a function in RLK-mediated control of PD-based intercellular communication SUB and *QKY* function in a non-cell-autonomous manner (Yadav *et al.*, 2008; Vaddepalli *et al.*, 2014) indicating that SUB signaling involves a yet unknown factor that moves between cells.

SUB can be found in internal compartments as well (Yadav *et al.*, 2008; Kwak and Schiefelbein, 2008; Vaddepalli *et al.*, 2011; Wang *et al.*, 2016). *SUB* is glycosylated in the endoplasmic reticulum (ER) (Hüttner *et al.*, 2014), subject to ER-associated protein degradation (Fulton *et al.*, 2009; Hüttner

et al., 2014). It was recently shown that ovules of plants homozygous for a hypomorphic allele of *HAPLESS13* (*HAP13*) preferentially accumulate signal from a functional SUB:EGFP reporter in the cytoplasm, rather than the PM (Wang *et al.*, 2016). *HAP13/AP1M2* encodes the $\mu 1$ subunit of the adaptor protein (AP) complex AP1 that is present at the TGN/EE network and is involved in post-Golgi vesicular trafficking to the PM, vacuole and cell-division plane (Park *et al.*, 2009; Teh *et al.*, 2013; Wang *et al.*, 2013). Interestingly, the ovules of plants with reduced *HAP13/AP1M2* activity show *sub*-like integuments (Wang *et al.*, 2016). These results indicate that the AP1 complex is involved in subcellular distribution of SUB in a functionally relevant manner.

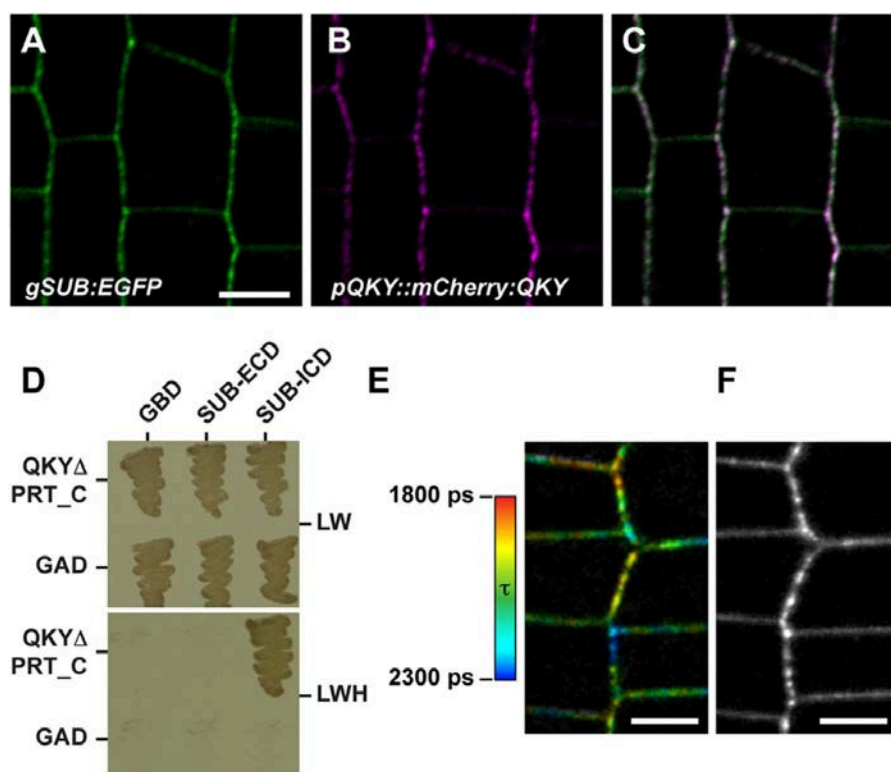


Figure 7. Interaction between SUB and QKY.

(A-C) Confocal micrographs of 6-day root epidermis cells of plants transgenic for both gSUB:EGFP and pQKY::mCherry:QKY reporters. (A) gSUB:EGFP signal. (B) pQKY::mCherry:QKY signal. (C) Overlay of A and B. Punctate signals overlap. (D) Yeast two-hybrid assay involving a QKY variant, including all four C2 domains but lacking the PRT_C domain (QKY Δ PRT_C) fused to the GAL4 activating domain (GAD) and the extracellular domain (ECD) or intracellular domain (ICD) of SUB fused to the GAL4 DNA-binding domain (GBD), respectively. Growth on -LW panel indicates the successful transformation of both plasmids and on -LWH panel indicates presence or absence of interaction. (E,F) FRET-FLIM analysis in root epidermal cells of Arabidopsis plants stably transformed with SUB:EGFP and mCherry:QKY reporters. (E) Fluorescence lifetime image. Color bar denotes the false-color code for SUB:EGFP fluorescence lifetimes (τ). (F) Confocal micrograph depicting SUB:EGFP signal. Scale bars: 5 μ m. Adopted from (Vaddepalli *et al.*, 2014)

1.5.5 SUB signaling affects cell wall biochemistry

In the quest to find additional candidate genes, *ZET* was isolated as genetic component of SUB signaling pathway. *ZET* is atypical cell wall-localized β -1,3 glucanase, which involved in floral organ morphogenesis similar to SUB (Vaddepalli *et al.*, 2017). The Fourier-transformed infrared spectroscopy (FTIR) analysis of cell wall material from *sub-1* mutant suggest *SUB* is involved in cell wall biochemistry. Interestingly, the *zet-2*, *qky-8*, and *sub-1* mutants showed notable and near-identical FTIR spectra deviation from wild type. Thus, it indicates that *ZET*, *SUB*, and *QKY* directly or

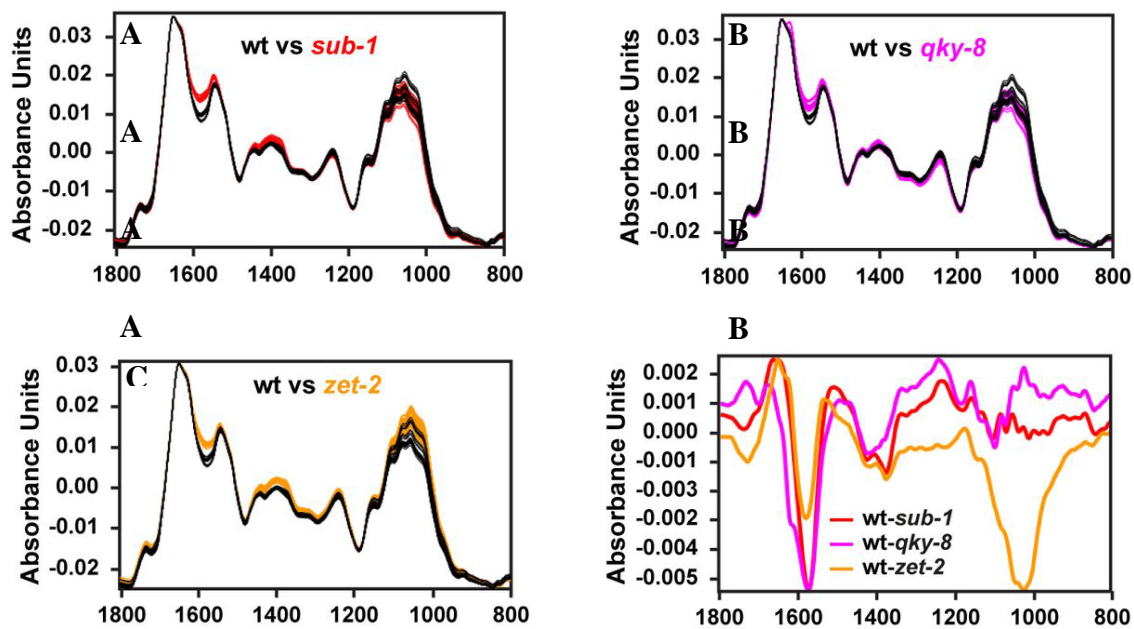


Figure 8. SUB signaling affects cell wall chemistry. FTIR analysis. Each of the three top panels shows an overlay of the spectra of three biological replicates, with ten technical replicates each, for the indicated genotype (total of 30 spectra each). The bottom panel depicts the difference spectra obtained by digital subtraction from the wild type of the average spectra of the indicated genotypes. Adopted from (Vaddepalli *et al.*, 2017).

indirectly influence cell wall composition in an overlapping fashion. Moreover, the whole-genome transcriptomic analysis revealed that many genes responsive to SUB-mediated signal transduction relate to cell wall remodeling (Fulton *et al.*, 2009).

1.6 Objectives

SUB play pivotal roles in plant morphogenesis during several developmental stages of Arabidopsis. Although, it has been almost two-decade since *SUB* was identified for its role in floral organ morphogenesis, however molecular mechanism underlying SUB signaling pathway is not well understood. In this study, I wanted to examine the role of the *SUB* in cell wall signaling associated with growth and defense of plant. The physiological and cellular analysis was performed to gain a better understanding of various *SUB* mediated downstream response to CWD due to CBI. Using a combination of genetic, cell biological and pharmacological approaches, I provide evidence that cell wall damage-induced cellular responses require SUB.

In addition, I was also interested to find additional candidates in the SUB signaling pathway. The later part of the thesis deals with the detailed analysis of putative candidates in the SUB signaling pathway. During the screening process, I found *KIN7.4*, WAKs, TOR1, and *CHC2* genetically and physically interact with SUB. The molecular and functional characterization of *KIN7.4* revealed that *KIN7.4* is positive regulator of root hair patterning.

2 Materials and Methods

2.1 Plant work, plant genetics, and plant transformation

Arabidopsis thaliana (L.) Heynh. var. Columbia (Col-0) and var. Landsberg (*erecta* mutant) (*Ler*) were used as wild-type strains. Plants were grown as described earlier (Fulton *et al.*, 2009). The *sub-1*, *qky-8* (all in *Ler*), and the *sub-9* and *qky-11* mutants (Col) have been characterized previously (Chevalier *et al.*, 2005; Fulton *et al.*, 2009; Vaddepalli *et al.*, 2011; Vaddepalli *et al.*, 2014). The *prc1-1* (Fagard *et al.*, 2000), *the1-1* (Hématy *et al.*, 2007), and *ixr2-1* (Desprez *et al.*, 2002) alleles were also described previously. The *sub-21* (Col) allele was generated using a CRISPR/Cas9 system in which the egg cell-specific promoter pEC1.2 controls Cas9 expression (Wang *et al.*, 2015). The single guide RNA (sgRNA) 5'-TAATAACTTGTATATCAACTT-3' binds to the region +478 to +499 of the *SUB* coding sequence. The sgRNA was designed according to the guidelines outlined in (Xie *et al.*, 2014). The mutant carries a frameshift mutation at position 495 relative to the *SUB* start AUG, which was verified by sequencing. The resulting predicted short SUB protein comprises 67 amino acids. The first 39 amino acids correspond to SUB and include its predicted signal peptide of 29 residues, while amino acids 40 to 67 represent an aberrant amino acid sequence. The additional mutant alleles of the candidate gene studied in chapter 3 have been listed in table no.1. The pUBQ::gSUB:mCherry plasmid used to generate the *SUB* overexpression lines L1 and O3 was generated previously (Vaddepalli *et al.*, 2014). Wild-type and mutant plants were transformed with different constructs using *Agrobacterium* strain GV3101/pMP90 (Koncz and Schell, 1986; Sambrook *et al.*, 1989) and the floral dip method (Clough and Bent, 1998). Transgenic T1 plants were selected on Kanamycin (50 µg/ml), Hygromycin (20 µg/ml) or Glufosinate (Basta) (10 µg/ml) plates and around 10 DAG, viable seedlings were transferred to soil for further inspection. Seedlings were grown on half-strength Murashige and Skoog (1/2 MS) agar plates (Murashige and Skoog, 1962). Before sowing seeds on 1/2 MS, they were surface sterilized in 3.5% (V/V) sodium hypochlorite (NaOCl) plus 0.1% (V/V) Triton X-100 for 10min on a rotator to prevent bacterial and fungal growth on plates. Seeds were washed three times with ddH₂O and stratified for 4d at 4°C prior to incubation. Dry seeds were sown on soil (Patzner Einheitserde, extra-gesiebt, Typ T, Patzner GmbH & Co. KG, Sinntal-Jossa, Germany) situated above a layer of perlite, stratified for 4 days at 4°C and then placed in a long day cycle (16 hrs light) using Philips SON-T Plus 400 Watt fluorescent bulbs. The light intensity was 120-150 µmol/m²sec. The plants were kept under a lid for 7-8 days to increase humidity (50-60%) and support equal germination.

Table 2 List of candidate genes screened with tDNA line no.

No.	Gene name/AGI	t-DNA line no.	t-DNA insertion
1	C2 domain (AT5G37740)	SALK_067530, SALK_080173, SALK_067530	Inside Gene
2	<i>CIPK12</i> (AT4G18700)	SALK_039846, SALK_039840, SAIL_669_B02	In Promoter
3	Unknown (AT3G11590)	SALK_044149	Inside Gene
4	<i>TRM22</i> (AT1g67040)	SALK_042024	Inside Gene
5	<i>LRR 1</i> (AT5g16590)	SAIL_412_D10, SALK_053366	In 5' UTR
6	<i>Dof</i> (AT5G66940)	SAIL_895_C05, SALK_002536	Inside Gene
7	<i>BOP2</i> (AT2G41370)	SAIL_767_G02	In 3' UTR
8	<i>Kinesin</i> (AT4G39050)	SALK_130786, SALK_130788	At 3' end of Gene
9	<i>EDA33</i> (AT4G00120)	SALK_085302, SALK_052009	In Promoter
10	<i>OBE1</i> (AT3G07780)	SALK_142374, SALK_076140	Inside Gene
11	<i>AGL2</i> (AT5G15800)	SALK_067923, SAIL_162_D09	Inside Gene
12	<i>AGO10</i> (AT5G43810)	SALK_047336, SAIL_162_D09	Inside Gene
13	<i>Dicer</i> (AT1G01040)	SAIL_442_D10, SALK_081595	Inside Gene
14	<i>FAT</i> (AT2G20830)	SALK_095219, SALK_02492	In Promoter
15	<i>60S Ribo</i> (AT3G07110)	SALK_106033 SALK_058172	Inside Gene
16	<i>ATPAP</i> (AT3G07130)	SAIL_529_D01	103 bp Upstream to Start codon

17	<i>BIR1</i> (AT5G48380)	SALK_008775C SAIL_1223_C08	Promoter, 5' UTR
18	<i>Clathrin</i> (AT3G08530)	SAIL_72_D_10, SALK_007180, SALK_042321	Inside Gene
19	Glycine rich protein (AT2G05540)	SAIL_255_A01	5' UTR
20	Glycolipid Transfer (AT3G21260)	SALK_000856, SALK_128685	Inside Gene
21	Homeobox (AT4G36740)	SALK_115125	Inside Gene
22	<i>WAK2</i> (AT1G21270)	SAIL-12_D05	Inside Gene
23	<i>ATMYB43</i>	SALK_107965	Inside Gene
24	Porins/ Auxin (AT5G15090)	SAIL_238_A01	Inside Gene
25	<i>ATPIN8</i> (AT5G15100)	SALK_107965	Inside Gene
26	<i>PRK2</i> (AT2G07040)	SALK_110661, SALK_110653	Inside Gene
27	<i>TOR1</i> (AT4G27060)	SALK_094291, SALK_024539	Inside Gene
28	<i>SYT1</i> (AT2G20990)	SAIL_775A_08	At 3' end of Gene
29	<i>Ribo S-17</i>	SALK_036518	Inside Gene
30	<i>Ribo-L28e</i>	SALK_74808	Inside Gene
31	Transposable Element	SALK_049609	Inside Gene
32	<i>NHL3</i> (AT5G06320)	SALK_035427, SALK_021767C, SALK_135329C, SALK_150318C	Inside Gene

2.2 Recombinant DNA work

For DNA and RNA work standard molecular biology techniques were used. DNA and RNA used for cloning were extracted from *Arabidopsis thaliana* using the NucleoSpin Plant II kit (Macherey-Nagel

GmbH und Co. KG) and the NucleoSpin RNA Plant kit (Macherey-Nagel GmbH und Co. KG). RNA was used as a template, mRNA was reverse transcribed into cDNA using the RevertAid 1st strand cDNA synthesis kit (Fermentas) and a poly-T primer according to the manufacturer's protocol. Cloning was performed using standard methods described in (Sambrook et al., 1989). PCR-fragments used for cloning were obtained using Q5 high-fidelity DNA polymerase (New England Biolabs, Frankfurt, Germany). Restriction enzymes and T4 DNA Ligase used for cloning were also received from NEB GmbH and used according to the manufacturer's protocols. PCR products were purified using the NucleoSpin Gel and PCR clean-up kit (Macherey-Nagel GmbH und Co. KG) according to the manufacturer's protocol. Plasmids were isolated with the NucleoSpin Plasmid kit (Macherey-Nagel GmbH und Co. KG) according to the manufacturer's protocol. *Escherichia coli* strain DH10 β was used for amplification of the plasmids. Bacteria were grown on corresponding selection media (Lysogeny broth). Antibiotics for bacterial selection were used at final concentrations as follows: Kanamycin 50 $\mu\text{g}/\text{mL}$; Ampicillin 100 $\mu\text{g}/\text{mL}$; Gentamycin 25 $\mu\text{g}/\text{mL}$; Spectinomycin 100 $\mu\text{g}/\text{mL}$; Tetracyclin 12.5 $\mu\text{g}/\text{mL}$; and Rifampicin 10 $\mu\text{g}/\text{mL}$. All PCR-based constructs were sequenced by MWG-Biotech AG following the company's standards. Sequencing results were aligned with geneious software to reference sequences received from The Arabidopsis Information Resource (TAIR, www.arabidopsis.org). The plasmids pCAMBIA2300 (www.cambia.org) and pGGZ001 (Lampropoulos *et al.*, 2013) were used as binary vectors. Details of the PCR reaction mix and steps involved in PCR using both Q5 high-fidelity DNA polymerase and Taq polymerase have been summarized in Table 1. Vectors used in this work are listed in Table 2. Detailed information for all oligonucleotides used in this study is listed in supplementary material Table S1.

Table 3 PCR reaction mix and cycler program.

Reaction mix for Q5® High-Fidelity DNA polymerase based PCR amplification

Components/reaction	Volume (μl)
5x Q5 Reaction buffer	10
2 mM dNTPs	5
10 μM Forward primer	2.5
10 μM Reverse primer	2.5
Q5 High-Fidelity DNA polymerase (2 U/ μl)	0.5

Template DNA (100 ng made upto 2.5 μ l)	2.5	
Sterile double distilled water	to 50	
PCR Cycler program for Q5 polymerase		
Temperature	Time	Cycles
98 °C	30 sec	1 cycle
98 °C	15 sec	25 - 35 cycles
X °C	10 sec	
72 °C	30 sec/kb	
72 °C	3 min	1 cycle
Reaction mix for Taq polymerase based PCR amplification		
Components/reaction	Volume (μl)	
10x Standard <i>Taq</i> Reaction buffer	2.5	
2 mM dNTPs	2.5	
10 μ M Forward primer	0.5	
10 μ M Reverse primer	0.5	
Taq polymerase (5 U/ μ l)	0.125	
Template DNA (100 ng made up to 1 μ l)	1	
Sterile double distilled water	17.875	
PCR Cycler program for Taq polymerase		
Temperature	Time	Cycles
95 °C	2 min	1 cycle
95 °C	20 seconds	30 - 40 cycles
X °C	20 seconds	
72 °C	1 min/ kb	
72 °C	5 min	1 cycle

Table 4 Plasmid vectors used in this work.

Name	Purpose	Description
------	---------	-------------

pGADT7-GW	Yeast two-hybrid interaction test	Express a protein of interest fused to a GAL4 activation domain
pGBKT7-GW	Yeast two-hybrid interaction test	Express a protein fused to GAL4 DNA binding domain
pGGA000	GG entry vector	Entry vector for promoter region of interest
pGGB003	GG entry with N-decoy	Entry vector carrying N-decoy in case no D-tag is needed
pGGC000	GG entry vector	Entry vector for CDS of interest
pGGD001	GG entry vector with linker-GFP	Entry vector carrying GFP as C-tag
pGGE009	GG entry with tUBQ	Entry vector carrying terminator of <i>UBQ10</i>
pGGF005	GG entry with Hygromycin-R	Entry vector carrying Hygromycin resistance for plant selection
pGGZ001	GG destination vector	Destination vector, binary vector for plant transformation
pCambia3300	Binary vector for plant transformation	

2.3 Arabidopsis genomic DNA extraction and genotyping PCR

DNA was extracted from a small piece of leaf tissue of diameter ~ less than 1 cm. Leaf disk was freeze in liquid nitrogen and ground to a fine powder (Qiagen grinder or pestle). The powdered tissue was suspended in 500 µl gDNA extraction buffer and incubated for 15 min at 65°C using a thermomixer at 1000 rpm after brief vortexing. 300 µl chloroform was added and mixed thoroughly by inverting Eppendorf tubes. The mixture was centrifuged for 10 min at 13000 rpm. 400 µl of the supernatant was transferred into a new tube (make sure to avoid any interphase junk). 280 µl of isopropanol was added to the supernatant (70% vol of supernatant), mixed by inversion, incubated 5 min at room temperature and centrifuged for 15 min at 12000 rpm. The pellet was washed with 1 ml ice-cold 70% ethanol, dried completely and resuspended in 50 µl 5 mM Tris-HCl PH 5.8 or ddH₂O. The entire preparation was stored at 4 °C until use. PCR-based genotyping was performed with the genotyping primer combinations. The genotyping primers have been listed in table no.2

2.4 RNA extraction from the plant material and cDNA synthesis

Total RNA was isolated from the 7-day old seedlings using the kit according to the instructions given in the manufacturer's manual. Purified total RNA in RNase- free water were quantified and analyzed for purity using the NanoPhotometer P330 (Implen GmbH). Isolated RNA was stored at -80 °C until use. First-strand cDNA synthesis was performed using the RevertAid 1st strand cDNA synthesis kit (Thermo Scientific) accordingly. Details of the reaction mix and steps involved in the cDNA synthesis have been summarized in Table3.

Table 5 Reaction mix and steps involved in cDNA synthesis.

Reaction mix for the cDNA synthesis

Components per reaction		Volume (µl)
5x Reaction Buffer		4
RiboLock RNase Inhibitor (20 U/µl)		1
10 mM dNTP Mix		2
RevertAid M-MuLV RT (200 U/µl)		1
Oligo (dT)18 primer		1
Template RNA		1 µg
Nuclease-free water		to 20µl
Steps for cDNA synthesis		
Step	Temperature (°C)	Incubation time (min)
Step 1	42	60
Step 2	70	5
Step 3	4	forever

2.5 Generation of various reporter constructs

2.5.1 Construction of Y2H vectors

The backbone vectors for the yeast two-hybrid (Y2H) analysis were pGADT7 AD (AD) and pGBKT7 BD (BD). The Coding sequences of *WAK2*, *KIN7.4*, *KIN7.2* and *TOR1* was amplified from Col-0

cDNA with respective primer (primer list is in supplementary data). Amplicons were purified and digested for cloning into AD. In order to map KIN7.4 interaction domains by yeast-two-hybrid assay, various truncated fragments of KIN7.4 were generated by PCR and ligated into pGADT7. *SUB* intracellular domain fused to the GAL4 DNA-binding domain (GBD) was described previously (Vaddepalli *et al.*, 2014). Coding sequences of *SUB* juxta, *SUB* juxta 1st and *SUB* juxta 2nd and *SUB* kinase domain were cloned into pGBDT7 by former lab members. All constructs were verified by sequencing.

List of yeast two hybrid vectors

Y2H vector	Restriction enzyme	Primer no.
TOR-AD	<i>NdeI/XmaI</i>	4140/4139
TOR-BD	<i>NdeI/XmaI</i>	4150/4151
KIN7.4-AD	<i>XmaI/SacI</i>	4230/4231
KIN7.4-BD	<i>NcoI/XmaI</i>	4232/4233
KIN7.2-AD	<i>XmaI/SacI</i>	4226/4227
KIN7.2-BD	<i>NcoI/XmaI</i>	4228/4229
KIN7.4 A -AD	<i>XmaI/SacI</i>	4230/4511
KIN7.4 A -BD	<i>NcoI/XmaI</i>	4232/4512
KIN7.4 B-AD	<i>XmaI/SacI</i>	4513/4231
KIN7.4 B-BD	<i>NcoI/XmaI</i>	4514/4233
KIN7.4-ATP-AD	<i>XmaI/XmaI</i>	4574/4575
KIN7.4-Motor-AD	<i>XmaI/XmaI</i>	4576/4577
KIN7.4-Stalk-AD	<i>XmaI/XmaI</i>	4578/4579
KIN7.4-Zn-AD	<i>XmaI/XmaI</i>	4580/4581
WAK2-ECD-AD	<i>XmaI/NdeI</i>	4157/4158
WAK2-ICD-AD	<i>NdeI/XmaI</i>	4155/4156

2.5.2 Generation of root hair patterning construct pGL2::GUS:EGFP pGGZ001

The pGL2::GUS:EGFP construct was assembled using the GreenGate system (Lampropoulos *et al.*, 2013). The promoter region of *GL2* (AT1G79840) was amplified with primer pGL2_F1 and pGL2_R1 from genomic Col-0 DNA. The internal *BsaI* site was removed during the procedure as described in (Lampropoulos *et al.*, 2013). The *GUS* coding sequence was amplified from plasmid pBI121 (Jefferson *et al.*, 1987) with primer *GUS_F* and *GUS_R*, digested with *BsaI* and used for further cloning. Vectors were further assembled with pGGA006, pGGB003, pGGD001, pGGE009, and pGGF005 (all kindly provided by Jan Lohmann) to pGGZ001::pGL2:GUS:EGFP:tUBQ.

2.5.3 Generation of *KIN7.4* promoter reporter construct pKIN7.4::NLS-GUS:EGFP:tKIN7.4

The pKIN7.4::NLS-GUS:EGFP:tKIN7.4 construct was assembled using the GreenGate system. The promoter of *KIN7.4* was amplified using primers 4461, 4462, 4463, and 4464 from Col-0 genomic DNA. The PCR product was cloned in to green gate promoter module entry vector. In the same manner terminator was also amplified using primers 4465,4466,4467 and 4468 primers and cloned in to green gate terminator module. Vector were further assembled with pGGA0K4, pGGB003, pGGD001, pGGE0K4 and pGGF005 to pGGZ001:pKIN7.4::NLS:GUS:EGFP:tKIN7.4.

2.5.4 pKIN7.4::EGFP:gKIN7.4:tKIN7.4 pCambia3300

The promoter was amplified from Col-0 genomic DNA with primer pair 4551 and 4552. The PCR product was cloned in to pCAMBIA3300 using *XmaI* restriction enzyme. In the second step,the terminator was amplified from Col-0 genomic DNA with primer pair 4549 and 4550. The PCR product was cloned in to pCAMBIA3300:pKIN7.4 using *PmeI* restriction enzyme resulting into plasmid pCAMBIA3300:pKIN7.4:tKIN7.4. In thrid step complete genomic region of *KIN7.4* was amplified from Col-0 genomic DNA with primer pair 4551 and 4552 and PCR product was cloned in to pCAMBIA3300:pKIN7.4:tKIN7.4. using *SbfI* and *PmeI* restriction enzyme. In final step EGFP was amplified from greengate EGFP module plasmid using primer pair 4543 and 4544. The PCR product was cloned into pCAMBIA3300:pKIN7.4:gKIN7.4:tKIN7.4 plasmid using *XmaI* and *SbfI* restriction enzyme resulting into final pKIN7.4::EGFP:gKIN7.4:tKIN7.4 pCAMBIA3300.

2.6 Yeast-two-hybrid (Y2H) assay

For Y2H, the above-mentioned GAD- and GBD-fusion constructs were co-transformed into yeast strain AH109 (MATa, trp1-901, leu2-3, 112, ura3-52, his3-200, gal4Δ, gal80Δ, LYS2::GAL1UAS-GAL1TATA-HIS3,MEL1, GAL2UAS-GAL2TATA-ADE2, URA3::MEL1UAS-MEL1TATA-lacZ) (Clontech/TaKaRa, USA). Transformants were selected after 3 days growth on synthetic complete medium lacking leucine and tryptophan (–LW) at 30 °C. To test for interaction, transformants were streaked on yeast synthetic drop-out (SD) plates lacking leucine, tryptophan, and histidine (–LWH) supplemented with 2.5 mM 3-amino-1,2,4-triazole for 2 days at 30 °C.

2.7 Scanning electron microscopy (SEM)

For scanning electron microscopy analysis, carpel was obtained from freshly open flower buds and dissected before suspending in fixative (2% glutaraldehyde (SIGMA G5882), 69% acetone, 29% H₂O) overnight. Fixed ovules were washed with 70% acetone (4×15 minute, followed by 6×30 minute). During fixation II, ovules were washed for 15 minutes in 50% acetone in 50mM cacodylate buffer pH 7.0, followed by 10 minutes in 25% acetone in 50mM cacodylate buffer, 10 minutes in 10% acetone/cacodylate buffer, and finally, washed with 50mM cacodylate for 5 minutes. Washed ovules were then treated with 2% osmium-tetroxide in 50mM cacodylate buffer for 2 hours. Osmium tetroxide was removed by washing 2 times with 50mM cacodylate buffer, and then followed with a 10-minute wash with 10% acetone/cacodylate buffer. In the end, the ovules were passed through an acetone series (10%, 20%, 40%, 60%, and 70%) for 30 minutes each and stored at 4°C. Fixed ovules were passed through a minimum of three 100% acetone washes before critical point drying. Specimens were mounted on stubs and dissected using fine tip needle. The tissues were coated with gold particles and examined with the TM3000 tabletop scanning electron microscope (HITACHI). Scanning electron microscopy was performed essentially as reported previously (Schneitz et al., 1997; Sieburth and Meyerowitz, 1997).

2.8 Confocal laser scanning microscopy (CLSM)

To assess the cellular structure of floral meristems samples were stained with modified pseudo-Schiff propidium iodide (mPS-PI) (Truernit *et al.*, 2008). Confocal laser scanning microscopy was performed with an Olympus FV1000 setup using an inverted IX81 stand and FluoView software (FV10-ASW version 01.04.00.09) (Olympus Europa GmbH, Hamburg, Germany) equipped with a water-corrected 40x objective (NA 0.9) at 3x digital zoom. For SUB:EGFP subcellular localization upon drug treatments or colocalization with endosomal markers confocal laser scanning microscopy was performed on epidermal cells of root meristems located about 8 to 12 cells above the quiescent center using a Leica TCS SP8 X microscope equipped with GaAsP (HyD) detectors. The following objectives were used: a water-corrected 63x objective (NA 1.2), a 40x objective (NA 1.1), and a 20x immersion objective (NA 0.75). Scan speed was set at 400 Hz, line average at between 2 and 4, and the digital zoom at 4.5 (colocalization with FM4-64), 3 (drug treatments) or 1 (root hair patterning). EGFP fluorescence excitation was done at 488 nm using a multi-line argon laser (3 percent intensity) and detected at 502 to 536 nm. FM4-64 fluorescence was excited using a 561 nm laser (1 percent intensity) and detected at 610 to 672 nm. For the direct comparisons of fluorescence intensities, laser, pinhole,

and gain settings of the confocal microscope were kept identical when capturing the images from the seedlings of different treatments. The intensities of fluorescence signals at the PM were quantified using Leica LAS X software (version 3.3.0.16799). For the measurement of the fluorescence levels at the PM optimal optical sections of root cells were used for measurements. On the captured images the fluorescent circumference of an individual cell (ROI, region of interest) was selected with the polygon tool. The mean pixel intensity readings for the selected ROIs were recorded and the average values were calculated. For determination of colocalization, the distance from the center of each EGFP spot to the center of the nearest FM4-64, mCherry or mRFP signal was measured by hand on single optical sections using ImageJ/Fiji software (Schindelin *et al.*, 2012). If the distance between two puncta was below the resolution limit of the objective lens (0.24 μm) the signals were considered to colocalize (Ito *et al.*, 2012). Arabidopsis seedlings were covered with a 22×22 mm glass coverslip of 0.17 mm thickness (No. 1.5H, Paul Marienfeld GmbH & Co. KG, Lauda-Königshofen, Germany). Images were adjusted for color and contrast using ImageJ/Fiji software.

2.9 Three-dimensional ovule imaging using CLSM and MorphoGraphX

Carpel was obtained from appropriate flower buds and dissected before suspending in fixative 4% paraformaldehyde (PFA) in 1×PBS pH7.3 for one to two hours at room temperature with gentle agitation or overnight at 40C. The fixed tissues were washed twice for 1 min in 1 x PBS. Then the tissues were transferred to ClearSee solution at room temperature with gentle agitation for overnight or more. Cleared ovules were stained with (0.1 %) SCRI Renaissance 2200 (SR2200) stain (Musielak *et al.*, 2015) in 1x PBS for 30 min. Subsequently, the ovules were transferred to ClearSee solution for another 30 min before imaging (Ursache *et al.*, 2018). Ovules were mounted on slides and dissected from the carpel wall. For imaging, a Leica TCS SP8 X microscope with 63 x glycerol objective was used. SR2200 was excited with a 405-nm laser line and emission recorded between 415 and 476 nm (405/415–476). The confocal images of the ovules were used to construct a 3D image with MorphoGraphX 2.0 (Barbier de Reuille *et al.*, 2015).

2.10 Phenotyping flower organ

Whole flowers and silique micrographs were obtained using an Olympus SZX12 stereomicroscope equipped with an XC CCD camera and Cell Sense Dimension software. Whole plant pictures were taken with a Nikon COOLPIX B500 digital camera (NIKON CORP.). Images were manipulations such

as brightness and contrast, were carried out using ImageJ/Fiji and Adobe Photoshop CS6 software (Adobe System Inc.).

2.11 Drug treatments

The transgenic *sub-1/pSUB:SUB:EGFP* seeds were used. Isoxaben (ISX), DCB, Thoxtomin A (Thx), Latriclelin-B (Lat-B), oryzalin were obtained from Sigma-Aldrich and used from stock solutions in DMSO (1 mM ISX, DCB, Thx, Lat-B, oryzalin) FM4-64 was purchased from Molecular Probes (2 mM stock solution in water). For FM4-64 staining seedlings were incubated in 4 μ M FM4-64 in liquid 1/2 MS medium for 5 minutes prior to imaging.

2.12 Immunoprecipitation and western blot analysis

500 mg of 7-day wild-type or transgenic seedlings were lysed using a TissueLyser II (Qiagen) and homogenized in 1 ml lysis buffer A (50mM Tris-HCl pH7.5, 100 mM NaCl, 0.1 mM PMSF, 0.5% Triton X-100, protease inhibitor mixture (Roche)). The cell lysate was mildly agitated for 15 min on ice and centrifuged for 15 minutes at 13000 g. For lines carrying GFP-tagged proteins, the supernatant was incubated with GFP-TRAP_MA magnetic agarose beads (ChromoTek) for 2 hours at 4°C. Beads were concentrated using a magnetic separation rack. Samples were washed four times in buffer B (50mM Tris-HCl pH7.5, 100 mM NaCl, 0.1 mM PMSF, 0.2% Triton X-100, protease inhibitor mixture (Roche)). Bound proteins were eluted from beads by heating the samples in 30 μ l 2x Laemmli buffer for 5 minutes. Samples were separated by SDS-PAGE and analyzed by immunoblotting according to standard protocols. Primary antibodies included mouse monoclonal anti-GFP antibody GST (Invitrogen/Thermo Fisher Scientific), mouse monoclonal anti-MBP antibody (Agrisera). Secondary antibodies were obtained from Pierce/ThermoFisher Scientific: goat anti-rabbit IgG antibody (1858415) and goat anti-mouse IgG antibody (1858413).

2.13 Growth media, growth conditions and frequently used buffers

Ingredients are dissolved in deionized H₂O, and all growth media need to be autoclaved.

For DNA gel electrophoresis

5x TBE running buffer (pH should be 8.3)

450 mM Tris Base

400 mM boric acid

10 mM EDTA pH 8

<p>For DNA extraction 100 mM Tris/HCl pH 8 250 mM NaCl 25 mM EDTA pH 8 0.5% (v/v) SDS</p>
<p>For Glycine-SDS polyacrylamide gel electrophoresis according to Laemmli Protein lysis buffer 50 mM Tris/HCl pH 7.5 150 mM NaCl 0.1 mM PMSF protein inhibitor cocktail 0.5% (v/v) Triton-X 100</p>
<p>Coomassie R-250 staining solution 0.25% (w/v) Coomassie Brilliant Blue R-250 0.50% (v/v) Ethanol 10% (v/v) Glacial acetic acid</p>
<p>Coomassie R-250 destaining solution 0.50% (v/v) Ethanol 10% (v/v) Glacial acetic acid</p>
<p>10x SDS running buffer 0.25 M Tris 2 M Glycine 1% (w/v) SDS</p>
<p>For transfer and immunodetection of proteins 10x Transfer buffer 40 mM Tris base 40 mM Glycine</p>
<p>TBST buffer 0.1% (w/v) Tween 20 in TBS buffer</p>
<p>TBS buffer 10 mM Tris/HCl (pH 7.4) 150 mM Sodium chloride</p>
<p>Blocking buffer 5% (w/v) Skim milk powder in TBST buffer</p>
<p>For standard molecular biology/cloning</p>
<p>Lysogeny broth (LB) medium 1% tryptone, 0.5% yeast extract, 10% NaCl, (0.9% bacto agar)</p>
<p>For plant tissue culture ½ Murashige-Skoog medium 0.22% MS medium powder, (1% sucrose), 0.9% Agar (plant cell culture tested)</p>
<p>For yeast growth culture YPD medium 2% tryptone, 1% yeast extract, (2.4% bacto agar), 2% glucose</p>
<p>SD-LW 0.67% yeast nitrogen base (double drop-out; SD lacking leucine and tryptophan), 2% glucose, (2% bacto agar)</p>

SD-LWH

0.67% yeast nitrogen base (triple drop-out; SD lacking leucine, tryptophan and histidine), 2% glucose, (2% bacto agar)

SD media might be supplemented with 5-10 mM 3-AT

2.14 Bioinformatics

Protein domain searches were conducted using the PFAM database. Bioinformatic analysis was mainly performed using Geneious software. Alignments were generated with Geneious software using a ClustalW algorithm with BLOSUM62 matrix. Sequencing results were analyzed in Geneious software using the map to reference tool with Geneious Mapper and highest sensitivity.

2.15 Cellulose quantification

Seedlings were grown on square plates with half-strength MS medium and 0.3% sucrose supplemented with 0.9% agar for seven days. Cellulose content was measured following the Updegraff method essentially as described (Kumar and Turner, 2015; Updegraff, 1969) with minor modifications as outlined here. Following the acetic nitric treatment described in (Kumar and Turner, 2015) samples were allowed to cool at room temperature and transferred into 2 ml Eppendorf safe lock tubes. Samples were then centrifuged at 14000 rpm at 15°C for 15 min. The acetic nitric reagent was removed carefully without disturbing the pelleted material at the bottom of the tube. 1 ml of double-distilled H₂O was added, and the sample was left on the bench for 10 min at room temperature followed by centrifugation at 14000 rpm at 15°C for 15 min. After aspirating off the H₂O 1 ml acetone was added and the samples were incubated for another 15 min, followed by centrifugation at 14000 rpm at 15°C for 15 min. Afterward, acetone was removed, and samples were air-dried overnight. Then the protocol was continued as described in (Kumar and Turner, 2015).

2.16 ROS, lignin, and callose staining

Intracellular ROS accumulation in root meristems was estimated using the H₂DCFDA fluorescent stain essentially as described (Juárez *et al.*, 2015). Seeds were grown on square plates with half-strength MS medium and 1% sucrose supplemented with 0.9% agar. The seeds were stratified for two days at 4°C and incubated for seven days at 22°C under long-day conditions, at a 10 degree inclined position. Seven days-old seedlings were first transferred into multi-well plates containing half-strength liquid MS medium supplemented with 1% sucrose for two hours. Then medium was exchanged with liquid

medium containing either DMSO (mock) or 600nM isoxaben without disturbing seedlings. 10 min prior to each time point seedlings were put in the dark and the liquid medium was supplemented with 100 μ M H₂DCFDA staining solution. Images were acquired with a confocal microscope. For quantification a defined region of interest (ROI) located 500 μ m above the root tip (excluding the root cap) was used in all samples. Staining for lignin (phloroglucinol) and callose (aniline blue) was performed as described in (Van der Does *et al.*, 2017) and (Schenk and Schikora, 2015) respectively. ROS, phloroglucinol and aniline blue staining were quantified on micrographs using ImageJ software (Rueden *et al.*, 2017).

2.17 Hypocotyl and root measurements

For measuring etiolated hypocotyl length, seedlings were grown for five days on half-strength MS agar supplemented with 0.3 % sucrose. Seedlings were photographed and hypocotyl length was measured using ImageJ. For root growth assays, seedlings were grown for seven days in long-day conditions at 21°C on half-strength MS agar supplemented with 0.3 % sucrose. Plates were inclined at 10 degrees. Root length was measured using ImageJ. For root growth recovery assays seedlings were grown on half-strength MS agar supplemented with 0.3 % sucrose. Seeds were stratified for two days followed by incubation at 21°C in long-day conditions for seven days. Plates were inclined at 10 degrees. Individual seedlings were transferred to plates containing either 0.01 percent DMSO (mock) or 600 nM isoxaben for 24 hours. After treatment, seedlings were transferred onto half-strength MS agar plates supplemented with 0.3 % sucrose. The position of the root tip was marked under a dissection microscope. Root length was measured every 24 hours for up to three days. For root cell bulging assays seedlings were grown for seven days in long-day conditions at 21°C on half-strength MS agar supplemented with 0.3 % sucrose. Plates were inclined at 10 degrees. Individual seedlings were first transferred into liquid medium for two hours habituation followed by treatment with 600 nM isoxaben for up to seven hours. To take images, seedlings were stained with 4 μ M FM4-64 for 10 minutes and imaged using confocal microscopy. Confocal micrographs were acquired at each time point. All hypocotyl length or root measurements were performed in double-blind fashion.

2.18 Statistics

Statistical analysis was performed with PRISM8 software (GraphPad Software, San Diego, USA).

2.19 Microscopy and artwork

Images of seedlings exhibiting phloroglucinol staining were taken on a Leica MZ16 stereomicroscope equipped with a Leica DFC320 digital camera. Images of hypocotyl and root length were taken on a Leica SAPO stereomicroscope equipped with a Nikon Coolpix B500 camera. Aniline blue-stained cotyledons and root cell bulging were imaged with an Olympus FV1000 setup using an inverted IX81 stand and FluoView software (FV10-ASW version 01.04.00.09) (Olympus Europa GmbH, Hamburg, Germany) equipped with a 10x objective (NA 0.3). For assessing cell bulging a projection of a 5 μm z-stack encompassing seven individual optical sections was used. Aniline blue fluorescence was excited at 405 nm using a diode laser and detected at 425 to 525 nm. H₂DCFDA and EGFP fluorescence excitation was done at 488 nm using a multi-line argon laser and detected at 502 to 536 nm. For the direct comparisons of fluorescence intensities, laser, pinhole and gain settings of the confocal microscope were kept identical when capturing the images from the seedlings of different treatments. Scan speeds were set at 400 Hz and line averages at between 2 and 4. Measurements on digital micrographs were done using ImageJ software (Rueden *et al.*, 2017). Images were adjusted for color and contrast using Adobe Photoshop CC software (Adobe, San Jose, USA).

3 Results

3.1 The receptor kinase STRUBBELIG promotes the response to cellulose deficiency in *Arabidopsis thaliana*

3.1.1 *SUB* does not affect cellulose production

In previous work, the FTIR analysis of cell wall fraction reveals *SUB* mutants are defective in cell wall biochemistry (Vaddepalli *et al.*, 2017). To explain the molecular mechanism responsible for altered cell wall biochemistry of *SUB* mutants, I first analyzed if *SUB* is affecting cellulose biosynthesis. To this end, I checked transcript levels of *CESA1*, *CESA3*, and *CESA6* and its homologous *CESA2* and *CESA5* in wild-type and *sub* mutants with the help of quantitative real-time polymerase chain reaction (qRT-PCR). The qRT-PCR result showed no significant difference in the transcript level of *CESA1*, *CESA3*, and *CESA6* and its homolog *CESA2*, and *CESA5* between *sub* and wild-type (Figure 9 A).

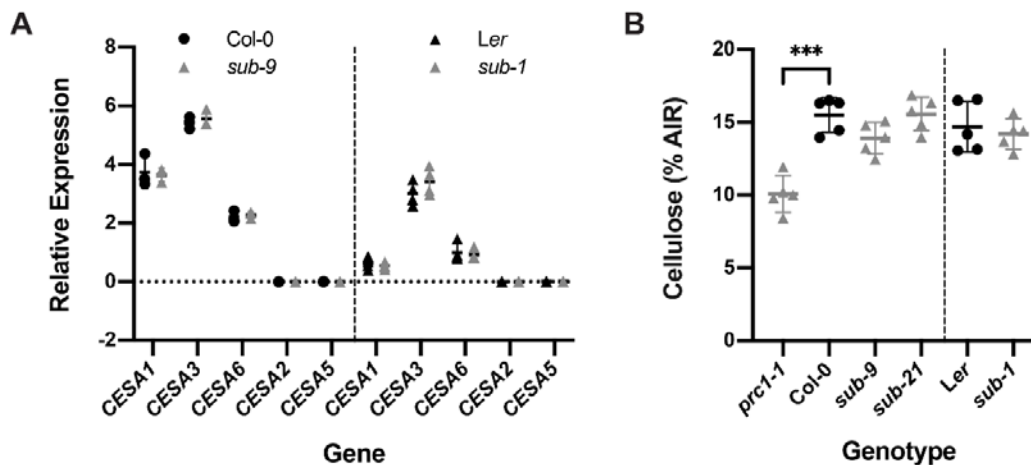


Figure 9. Effects of *SUB* on cellulose content in seven-day-old seedlings.

(A) Gene expression levels of primary cell wall *CESA* genes in wild type and *sub* as assessed by qRT PCR. Individual *CESA* genes and genotypes are indicated. Mean \pm SD is shown. Data points designate results of individual biological replicates. The experiment was performed two times with similar results. (B) Estimation of cellulose content. Genotypes are indicated. Data points indicate the results of individual biological replicates. Mean \pm SD is shown. Asterisks represent statistical significance ($P < 0.0001$, unpaired t test, two-tailed P values).

In the next step, to corroborate transcript analysis results I also quantified total cellulose content in wild type and *sub*. Cellulose content from seven-day-old seedlings was quantified using the Updegraff method (Updegraff, 1969; Kumar and Turner, 2015). I could not observe any differences in the amount of cellulose between *sub* and wild-type (Figure 9 B) however similar to previous finding cellulose biosynthesis deficient mutant *prc1-1* shows a significant difference of cellulose content with Col

(Fagard *et al.*, 2000). Taken together the results indicate that *SUB* does not affect cellulose biosynthesis in young seedlings.

3.1.2 *SUB* promotes the isoxaben-induced CWD response

Next, I hypothesized that *SUB* is involved in cell wall integrity signaling and thereby facilitating cell wall remodeling. To test this hypothesis, I first analyzed *SUB* on various parameter characterized for cell wall integrity, for example, ROS accumulation, induction of marker genes ectopic lignin, and callose deposition upon cell wall damage (CWD).

3.1.2.1 *SUB* promotes early ROS accumulation upon CBI

To detect if *SUB* is involved in early ROS production upon treatment with cellulose biosynthesis inhibitor drug isoxaben. Seven-day-old seedlings of wild-type and *sub-9* were exposed to 600nM isoxaben or DMSO in a time-course experiment for up to 120 min in 30 minutes' intervals. Upon treatment, I measured the fluorescence intensity of the intracellular ROS probe H₂DCFDA in roots (Henry *et al.*, 2015, Juárez *et al.*, 2015). I noticed an increase in H₂DCFDA signal in wild-type Col seedlings treated for 30 minutes with isoxaben compared to untreated seedlings (Figure 10 A, B). The signal intensity of the probe continues to increased further in seedlings exposed for 60 minutes. This signal intensity remained for up to 120 minutes of continuous exposure to isoxaben. However, in *sub-9* seedlings, we noticed a slight increase in H₂DCFDA signal only after 60 minutes (Figure10 A, C). Moreover, signal intensity was noticeably reduced in comparison to the wild type. In comparison to the mock-treated *sub-9* seedlings, isoxaben-treated *sub-9* seedlings continued to show an enhanced signal intensity for up to 120 minutes of exposure, while the relative difference to signal levels of mock-treated seedlings was never as prominent as in wild type. Thus, it is safe to infer *sub-9* mutants showed a delayed onset of H₂CDFDA signal appearance and overall reduced signal intensity for the time frame analyzed. The results show that cellulose biosynthesis inhibition upon isoxaben leads to

accumulation of intracellular ROS in roots cells within 30 minutes of application. This isoxaben induced early intracellular ROS accumulation is dependent on *SUB*.

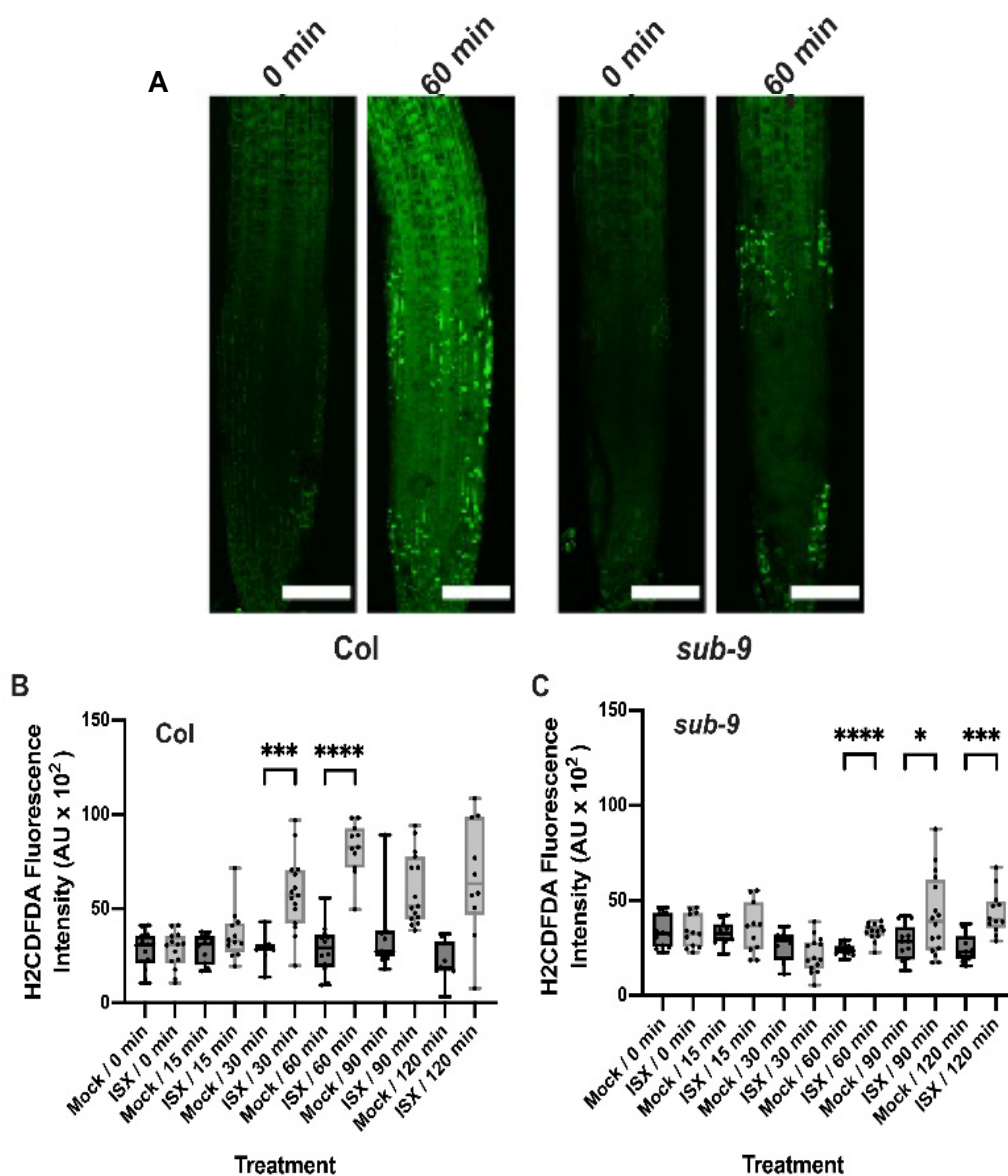


Figure 10. *SUB* affect on isoxaben-induced ROS production.

(A) Confocal micrographs depicting H₂CFDA signal in root tips of six-day-old seedlings treated with 600 nM isoxaben for the specified time. Genotypes are indicated. Note reduced signal in *sub-9*. (B, C) Quantification of results depicted in (A). Genotypes are indicated. Box and whisker plots are shown. $10 \leq n \leq 14$. Asterisks represent statistical significance (****, $P < 0.0001$; *** $P < 0.002$, * $P < 0.05$, unpaired t test, two-tailed P values). Experiments were performed three times with similar results.

3.1.2.2 *SUB* promotes upregulation of defense marker gene transcription upon CBI

After establishing the role of *SUB* in isoxaben induced early ROS production, I decided to test if *SUB* activity is required for transcriptional regulation of several marker genes, known to respond to isoxaben-induced CBI within eight hours (Hamann *et al.*, 2009). To this end, with the help of my colleague Jin Gao and Xia Chen I performed qRT-PCR experiments for defense marker genes. Total RNA from seven days-old liquid-grown seedlings treated with 600 nM isoxaben for eight hours was subject for qRT-PCR experiment. I noticed that isoxaben-induced upregulation of *CCR1*, *PDF1.2*, and *TCH4* was attenuated in *sub-9* mutants compared to wild type (Figure 11). However, I did not detect a significant change in the upregulation of other tested marker genes, including *VSP1*, *FRK1*, *CYP81F2*, *TIP2:3*, and *RBOHD*, in *sub-9* seedlings. The results indicate that *SUB* is required in a quantitative fashion for the isoxaben-induced transcriptional upregulation of several marker genes.

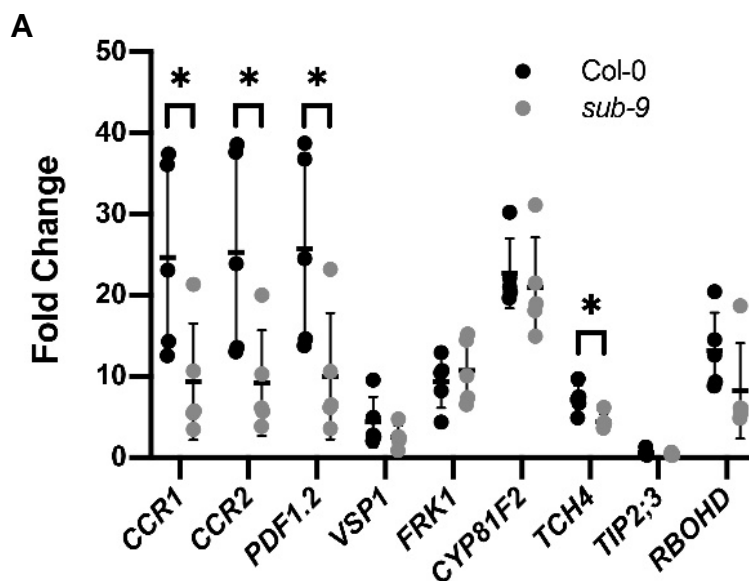


Figure 11. *SUB* effects on isoxaben-induced marker gene expression accumulation.

(A) Gene expression levels of several CBI marker genes by qPCR upon exposure of seven-day-old seedlings to 600 nM isoxaben for eight hours. The results from five biological replicates are shown. Marker genes and genotypes are indicated. Mean \pm SD is presented. Asterisks represent statistical significance (*, $P < 0.05$, unpaired t test, two-tailed P values). The experiment was repeated twice with similar results.

3.1.2.3 *SUB* promotes ectopic lignin accumulation upon CBI

Isoxaben-induced CBI eventually results in the alteration of cell wall biochemistry as evidenced for example by the ectopic accumulation of lignin and callose (Hamann *et al.*, 2009). So in the next step, I analyzed if *SUB* affects ectopic lignification upon application of isoxaben. Using the phloroglucinol

staining method (Mitra and Loqué, 2014) I then estimated lignin accumulation in six-day-old liquid-grown seedlings treated with 600 nM isoxaben for 12 hours. I noticed reduced phloroglucinol signal in the root elongation zone of *sub-1* seedlings in comparison to *Ler* wild type (Figure 12A, B). I also analyzed *sub-9* mutant allele in Col background and noticed reduced phloroglucinol signal in *sub-9* seedlings although the effect was less prominent. However, in our hands, Col wild-type plants exhibited an overall weaker phloroglucinol staining indicating that isoxaben-induced lignin accumulation does not occur to the same level as in *Ler* (Figure 12A, B). The reduced lignin accumulation in *SUB* loss of function mutant background regardless of ecotype suggests *SUB* could be directly involved in the genetic pathway required for isoxaben induced lignification. Furthermore, to test our notion we analyzed three independent *SUB* overexpression line for ectopic lignin accumulation upon isoxaben treatment. I could detect significantly increased phloroglucinol staining in two out of three *SUB* over-expressing lines (pUBQ::SUB:mCherry, lines L1, O3) (Figure 12A, B). From obtained results, it could be inferred that *SUB* is part of a genetic pathway involved in ectopic lignification upon cell wall perturbation due to isoxaben.

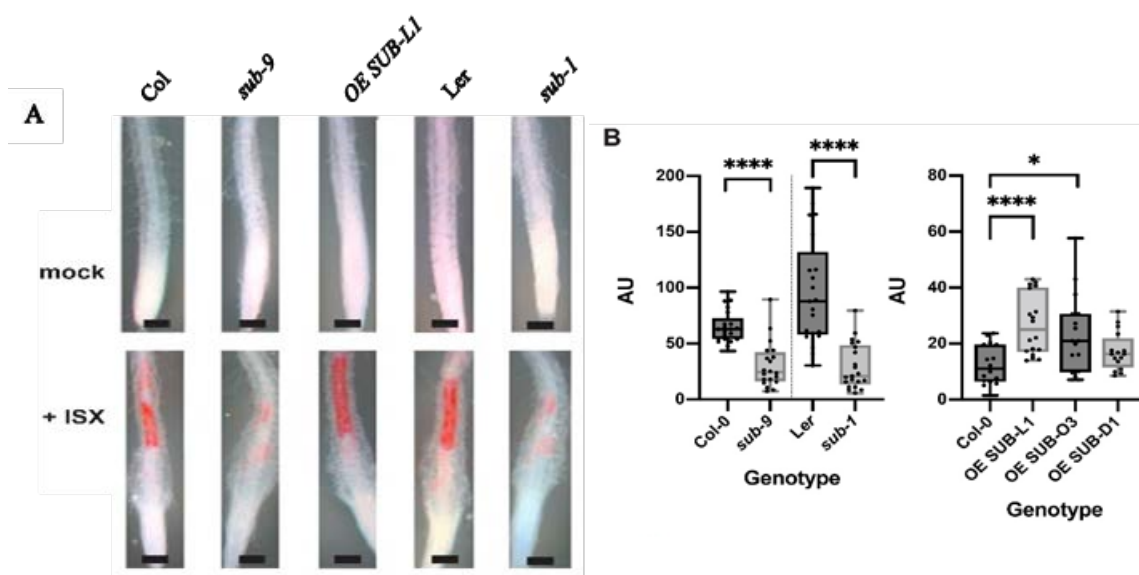


Figure 12. *SUB* affects isoxaben-induced ectopic lignification. (A) Phloroglucinol signal strength indicating lignin accumulation in roots of six-day-old seedlings exposed to 600 nM isoxaben for 12 hours. Genotypes: Col, *sub-9* (Col), pUBQ::gSUB:mCherry (line L1), Ler, and *sub-1* (Ler). (B) Quantification of the results depicted in (A). Left panel shows results obtained from different sub mutants in the Col or Ler background. Right panel depicts results from three independent pUBQ::gSUB:mCherry transgenic lines overexpressing *SUB* (Col, lines L1, O3, D1). Box and whisker plots are shown. $16 \leq n \leq 21$. Asterisks represent statistical significance (* $P < 0.02$, ****, $P < 0.0001$; unpaired t test, two-tailed P values).

3.1.2.4 *SUB* promotes callose accumulation upon CBI

In previous research, it has been reported that CBI for 24 hours leads to accumulation of callose in cotyledons of wild-type seedlings (Hamann *et al.*, 2009.). Thus, I analyzed if *SUB* is also required for this response. To this end, I transferred seven days-old plate-grown seedlings to liquid medium without isoxaben for 12 hours for habituation to accommodate seedlings in new environment. Subsequently, the medium was exchanged, and seedlings were kept in 600 nM isoxaben containing liquid medium for another 24 hours. Afterward, seedlings were fixed and stained with aniline blue following standard protocol mentioned (Schenk and Schikora, 2015). As expected, I observed prominent aniline blue staining in cotyledons of *Ler* and *Col* wild-type seedlings upon isoxaben treatment (Figure 13 A, B). However, I noticed strongly reduced aniline blue staining in cotyledons of isoxaben-treated *sub-1* and *sub-4* (both in *Ler*) as well as *sub-9* and *sub-21* (both in *Col*). In contrast, we detected stronger aniline blue staining in *SUB* overexpressors (lines L1, O3) (Figure 13 A, B). Taken together, our results suggest that *SUB* is required for the isoxaben-induced formation of callose in cotyledon and it could be rather direct participation of *SUB* for isoxaben induced callose accumulation.

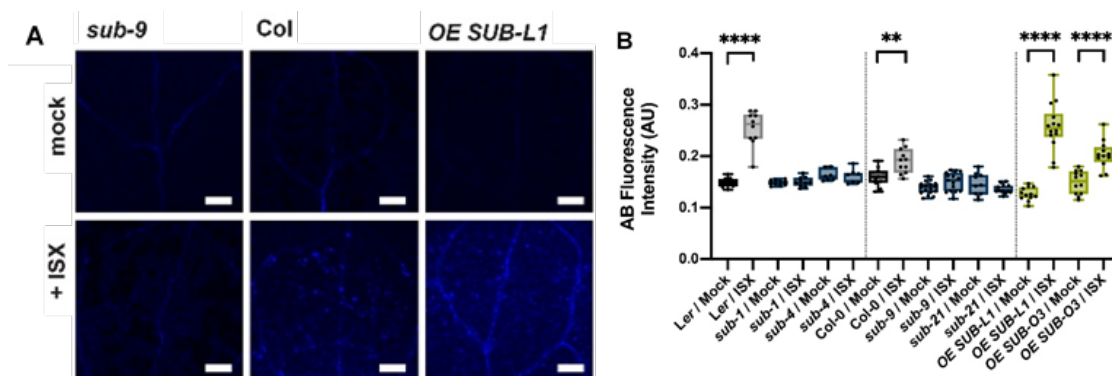


Figure 13. *SUB* affects isoxaben-induced callose accumulation.

(A) Confocal micrographs show cotyledons of seven-day-old *sub-9*, *Col*, and pUBQ::*gSUB*:mCherry (line L1) seedlings treated with mock or 600 nM isoxaben for 24 hours. Aniline blue fluorescence signal strength indicates callose accumulation. (B) Quantification of the results depicted in (A). Left panel shows results obtained from *sub* mutants in *Ler* background. Center panels indicate results obtained from *sub* mutants in *Col* background. Right panel depicts results from two independent pUBQ::*gSUB*:mCherry transgenic lines overexpressing *SUB* (*Col*, lines L1, O3). Box and whisker plots are shown. $7 \leq n \leq 18$. Asterisks represent statistical significance (****, $P < 0.0001$; **, $P < 0.004$, unpaired t test, two-tailed P values). The experiment was performed three times with similar results. Scale bars: (A) 0.1 mm; (C) 0.2 mm.

3.1.3 The *SUB*-mediated CBI response is sensitive to sorbitol

In previous research it has been reported that isoxaben-induced CWD response is sensitive to turgor pressure, as indicated by the suppression of lignin or callose accumulation in the presence of osmotica, such as sorbitol (Engelsdorf *et al.*, 2018, Wormit *et al.*, 2012, Hamann *et al.*, 2009). So in next step, I decided to test if *SUB* mediated responses to CBI is osmosensitive. To this end, I analyzed if *SUB* affects a turgor-sensitive CBI response. I compared isoxaben-induced accumulation of lignin and callose in six-day-old Col, *sub-9*, and *pUBQ::SUB:mCherry* seedlings in the presence of 300 mM sorbitol (Figure 14). I observed that sorbitol suppressed lignin and callose accumulation in all tested genotypes, including *SUB* overexpressing lines that result in hyperaccumulation of lignin or callose in the absence of sorbitol. I noticed that providing 300mM sorbitol along with isoxaben suppresses lignin and callose accumulation in all genotype analyzed. For lignin accumulation I did not notice any phloroglucinol stain in any observed samples (Figure 14 A) although our control samples showed staining signal (image not is shown) suggesting that the experiment worked per se. Similarly, for callose accumulation isoxaben treated seedlings do not differ than mock-treated seedlings in aniline blue signal intensity (Figure 14B, C). Taking together these results indicate that *SUB* contributes to a turgor-sensitive CBI response.

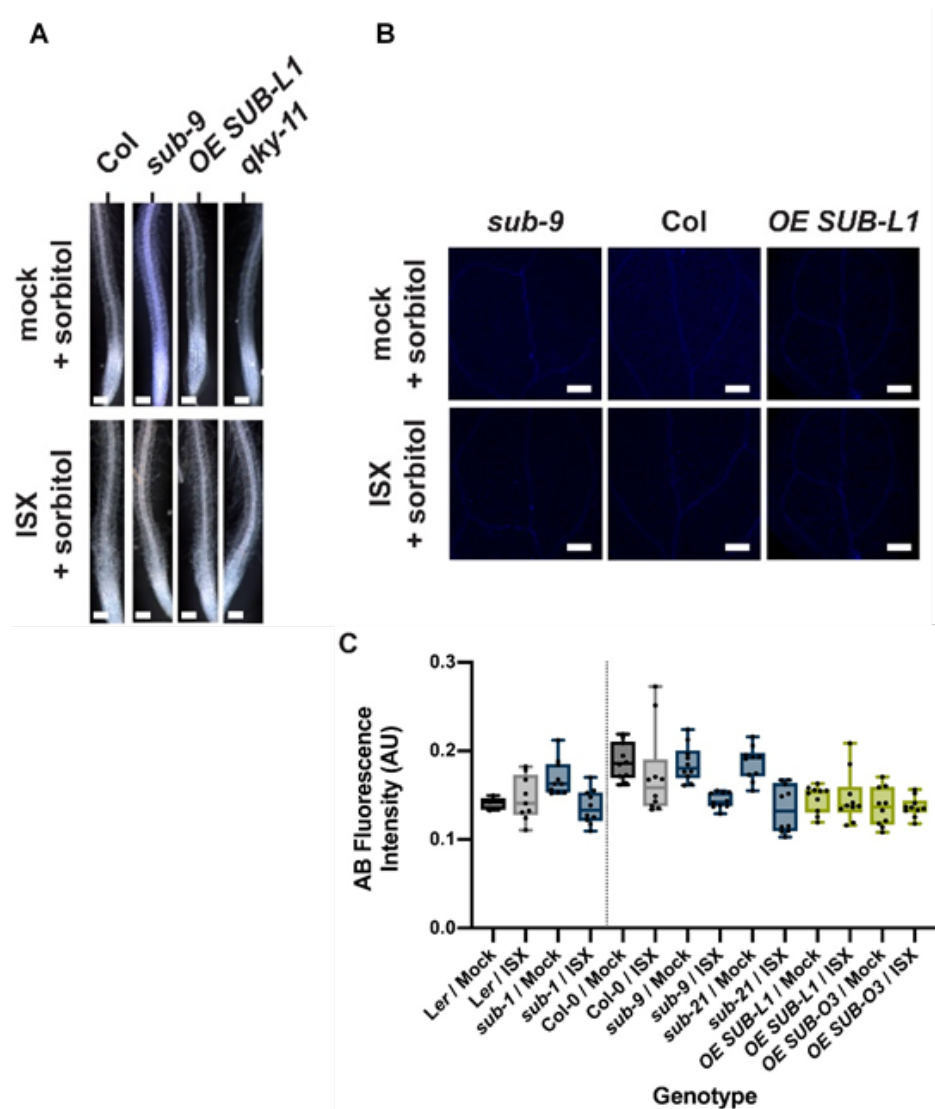


Figure 14. The effects of sorbitol on lignin and callose accumulation upon isoxaben exposure. (A) Phloroglucinol signal strength indicating lignin accumulation in roots of six-day-old seedlings exposed to mock/300 mM sorbitol or to 600 nM isoxaben/300 mM sorbitol for 12 hours. Genotypes: Col, *sub-9* (Col), pUBQ::gSUB:mCherry (line L1), *qky-11* (Col). Note absence of detectable signal. Minimum 10 roots per genotype were analyzed and experiment was performed three times with similar results (B) Confocal micrographs show cotyledons of seven-day-old *sub-9*, Col, and pUBQ::gSUB:mCherry (Col, line L1) seedlings treated with mock/300 mM sorbitol or 600 nM isoxaben/300 mM sorbitol for 24 hours. Aniline blue fluorescence signal strength indicates callose accumulation. No increase in signal intensity can be observed in isoxaben-treated seedlings. (C) Quantification of the results depicted in (B). Left panel depicts results obtained from *sub-1* mutants in Ler background. Right panel shows results obtained from *sub* mutants in Col background and also depicts results from two independent pUBQ::gSUB:mCherry transgenic lines overexpressing SUB (Col, lines L1, O3). Box and whisker plots are shown. $5 \leq n \leq 10$. No statistically significant differences were observed (unpaired t tests, two-tailed P values). The experiment was performed three times with similar results. Scale bars: (A) 0.1 mm; (C) 0.2 mm.

3.1.4 *SUB* attenuates isoxaben-induced cell swelling and promotes root growth recovery

After confirming the role of *SUB* in cell wall integrity signaling, I next asked if the participation of *SUB* in cell wall signaling has any biological relevance to isoxaben-induced cell wall perturbation. It has been known that exposure of seedlings to isoxaben result into reduced microfibril formation in the cell wall and eventually results in the shortening and swelling of cells of the root epidermis (Engelsdorf *et al.*, 2018). So I hypothesized if *SUB* is involved in monitoring cell wall perturbation and thereby facilitating remodeling and fortification process, *sub* seedlings should be hypersensitive to isoxaben treatment. To test the hypothesis I analyzed the effect of 600nM isoxaben on contour of epidermal cell in elongation zone of root meristem in time course fashion. I transferred six days-old plate grown seedlings into a mock-solution or a solution containing 600 nM isoxaben for up to seven hours. I then analyze the timing of the initial appearance of altered cellular morphology of root epidermal cells. In addition, I also examined the severity of the phenotype. Notably, I did not observe any obvious morphological alterations in mock-treated wild-type or mutant seedlings (Figure 15). In Col wild-type seedlings cell shortening and swelling appeared first during a five to six-hour interval after the start of the treatment (Figure 15) (44/96 seedlings total, n = 4), as reported previously (Engelsdorf *et al.*, 2018). Upon isoxaben application to *sub-9* or *sub-21* seedlings, however, I detected similar alterations already during a three to four-hour interval after initiating isoxaben treatment (*sub-9*: 23/57, n = 2; *sub-21*: 20/46, n = 2). In addition, I noticed that *sub* mutants exhibited more prominent cellular alterations after seven hours of isoxaben treatment in comparison to wild type (Figure 15).

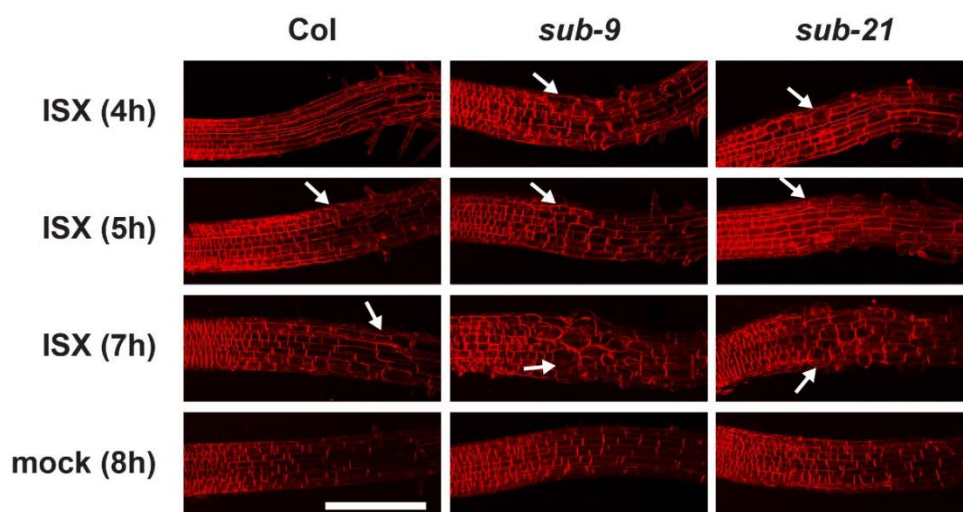


Figure 15. Root epidermal cell shape changes upon isoxaben treatment.

Six-day-old seedlings counter-stained with the membrane stain FM4-64 are shown. Confocal micrographs depict the region where the elongation zone flanks the root meristem. Time of exposure in hours to 600 nM isoxaben (ISX) or mock are indicated as are the genotypes. Arrows denote aberrant cell shapes. Scale bar: 0.1 mm.

In the second experiment, I took advantage of previously established root growth recovery assay. In wild-type seedlings, a 24-hour exposure to isoxaben results in a temporary stop of root growth followed by rapid recovery (Engelsdorf *et al.*, 2018). Thus, I also analyzed the role of *SUB* in root growth recovery upon a 24-hour treatment with isoxaben. First I grew wild-type and various mutant seedlings on plates for six days, transferred the seedlings onto plates containing 600 nM isoxaben for 24 hours, then transferred back the seedlings to recovery plates lacking isoxaben, and subsequently monitored the percentage of seedlings that continued root growth every 24 hours for up to 72 hours (Table 5). I used *ixr2-1* mutants as control. I noticed that 98 percent of *ixr2-1* seedlings recovered root growth already within 24 hours indicating that the treatment did not generally interfere with the seedling's ability to recover root growth. I then tested wild-type seedlings. I noticed that 46 percent of *Ler* or 39 percent of *Col* seedlings had resumed root growth after 24 hours. By 72 hours, 86 percent of *Ler* and 90 percent of *Col* seedlings had recovered root growth. By contrast, a significantly reduced fraction of *sub-1* and *sub-4* mutants had resumed root growth when compared to wild-type *Ler* (Table 5). The *sub-9* and *sub-21* mutants also showed reduced root growth recovery in comparison to *Col* although *sub-21* appeared less affected than *sub-9*. Importantly, *ixr2-1 sub-9* mutants behaved identically to *ixr2-1* single mutants at all-time points scored. The finding indicates that *ixr2-1* is epistatic to *sub-9* and that the observed isoxaben-induced decrease in root growth recovery in *sub-9* mutants relates to the herbicide. Taken together, the result suggests that *sub* mutants are hypersensitive to isoxaben treatment and that *SUB* promotes root growth recovery and represses cell size and shape changes in root epidermal cells during the isoxaben-induced CWD response.

Table 6 Root growth recovery after isoxaben treatment

Genotype	N total ^a	24 h ^b	48 h ^b	72 h ^b
<i>Ler</i>	110	45.5	69.1	85.5
<i>sub-1</i>	82	24.4 ^{**}	50.0 [*]	64.6 ^{**}
<i>sub-4</i>	76	17.1 ^{**}	39.5 ^{****}	52.6 ^{****}
<i>qky-8</i>	87	37.9 ^{ns}	64.4 ^{ns}	88.5 ^{ns}
Col-0	142	38.7	65.5	90.1
<i>sub-9</i>	88	23.9 [*]	45.5 ^{**}	70.5 ^{**}
<i>sub-21</i>	72	26.4 ^{ns}	51.4 ^{ns}	68.1 ^{**}
<i>qky-11</i>	81	37.0 ^{ns}	64.2 ^{ns}	92.6 ^{ns}
<i>ixr2-1</i>	83	97.6 ^{****}	97.6 ^{****}	97.6 ^{ns}
<i>sub-9 ixr2-1</i>	77	100.0 ^{****}	100.0 ^{****}	100.0 ^{**}
<i>the1-1</i>	78	41.0 ^{ns}	69.2 ^{ns}	88.5 ^{ns}

Percentages of root growth recovery of plate-grown, seven-day-old seedlings after transient exposure to 600 nM isoxaben for 24 hours. The top four sample rows list genotypes that are in *Ler* background. The bottom seven sample rows list genotypes that are in *Col* background.

^aTotal number of samples. Cases per class and time point were pooled from three independent experiments. For each biological replicate, $22 \leq n \leq 32$ seedlings were analyzed per genotype and time point. ^bStatistical significance (mutant vs respective wild type): na, not applicable; ns, not significant; * $P < 0.05$; ** $P < 0.005$; **** $P < 0.0001$; (Fisher's exact test; two-sided).

3.1.5 *SUB* attenuates root growth in *prc1-1*

As in previous experiments, there has been sufficient evidence to support role of *SUB* in isoxaben induced cellular response. Moreover, *SUB* is also required to sustain the morphological defects arising due to cellulose biosynthesis inhibition. Since pharmacological agents may have uncertain secondary effects it becomes necessary to corroborate the results with genetic experiments. *PRC1* encodes the CESA6 subunit of cellulose synthase (Fagard *et al.*, 2000) and *prc1-1* loss-of-function mutants show reduced cellulose levels (Fagard *et al.*, 2000). To test if *SUB* also affects a biological process in a scenario where cellulose reduction is induced genetically I compared root length in *sub-9*, *sub-21*, and *prc1-1* single and *sub-9 prc1-1* double mutants (Figure 16 A, B). I found that root length of *sub-9* or *sub-21* did not deviate from wild type while root length of *prc1-1* was markedly smaller in comparison to wild type, confirming previous results (Fagard *et al.*, 2000). Interestingly, I observed that *sub-9*

prc1-1 exhibited a significantly longer root than *prc1-1* though *sub-9 prc1-1* roots were still notably smaller than wild type roots. The results indicate that *SUB* contributes to root growth inhibition in *prc1-1*.

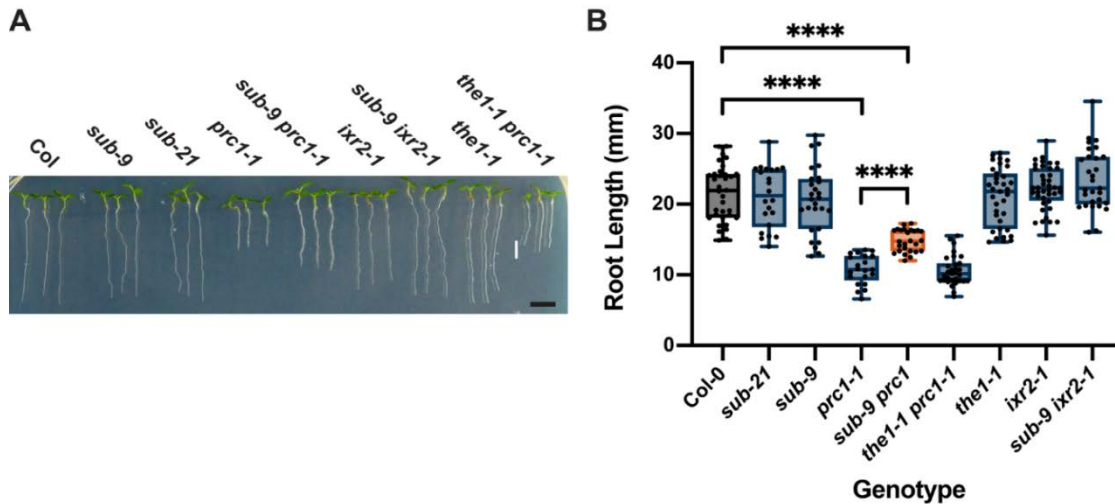


Figure 16. *SUB* effect on root growth inhibition in *prc1-1*.

(A) Root length in seven-day-old seedlings grown on plates under long-day conditions (16 hours light). Genotypes are indicated. Note the partial rescue of root length in *sub-9 prc1-1* but not in *the1-1 prc1-1*. (B) Quantification of the data shown in (A). Box and whisker plots are shown. $21 \leq n \leq 40$. Asterisks represent statistical significance (****, $P < 0.0001$; unpaired t test, two-tailed P values). The experiment was performed three times with similar results. Scale bars: 0.5 mm.

3.1.6 *SUB* and *THE1* share partially overlapping functions

THE1 is a central regulator of the isoxaben-induced CBI response (Engelsdorf *et al.*, 2018, Gonneau *et al.*, 2018, Van der Does *et al.*, 2017). My data indicate that *SUB* and *THE1* have overlapping but also distinct functions in this process. For example, *SUB* and *THE1* control isoxaben-induced lignin accumulation in the root (Engelsdorf *et al.*, 2018, Van der Does *et al.*, 2017). However, in contrast to *THE1*, *SUB* did not affect *FRK1* induction by isoxaben (Van der Does *et al.*, 2017). I also found that root growth recovery of *the1-1* seedlings upon transient exposure to isoxaben did not deviate from wild type (Table 5). Moreover, I failed to detect an effect of *THE1* on root growth inhibition in *prc1-1*, while *SUB* contributes to this process (Figure 16). We, therefore, explored further the relationship between *THE1* and *SUB*.

THE1 contributes to the reduction of hypocotyl length of cellulose-diminished *prc1-1* seedlings grown in the dark as evidenced by the partial recovery of hypocotyl elongation in *the1 prc1* double mutants (Hématy *et al.*, 2007). I compared *sub-9 prc1-1* to *the1-1 prc1-1* with respect to hypocotyl elongation in six-day-old etiolated seedlings and root length in seven-day-old light-grown seedlings

(Figure 17). I observed strongly reduced hypocotyl elongation in *prc1-1* in comparison to wild type and significant suppression of this reduction in *the1-1 prc1-1* double mutants (Figure 17 A, B) as described earlier (Hématy *et al.*, 2007). In contrast, hypocotyl length in *sub-9* mutants was not decreased, nor was there a partial reversal of reduced hypocotyl elongation in *sub-9 prc1-1* double mutants (Figure 17 A, B). The results indicate that *SUB* does not affect hypocotyl elongation in etiolated wild-type or *prc1-1* seedlings. Finally, I assessed the role of *THE1* in isoxaben-induced early ROS accumulation in root tips. I noticed no difference in H₂CDFDA signal intensity when comparing *the1-1* seedlings that had been treated with either mock or isoxaben for 30 minutes (Figure 17 C). By

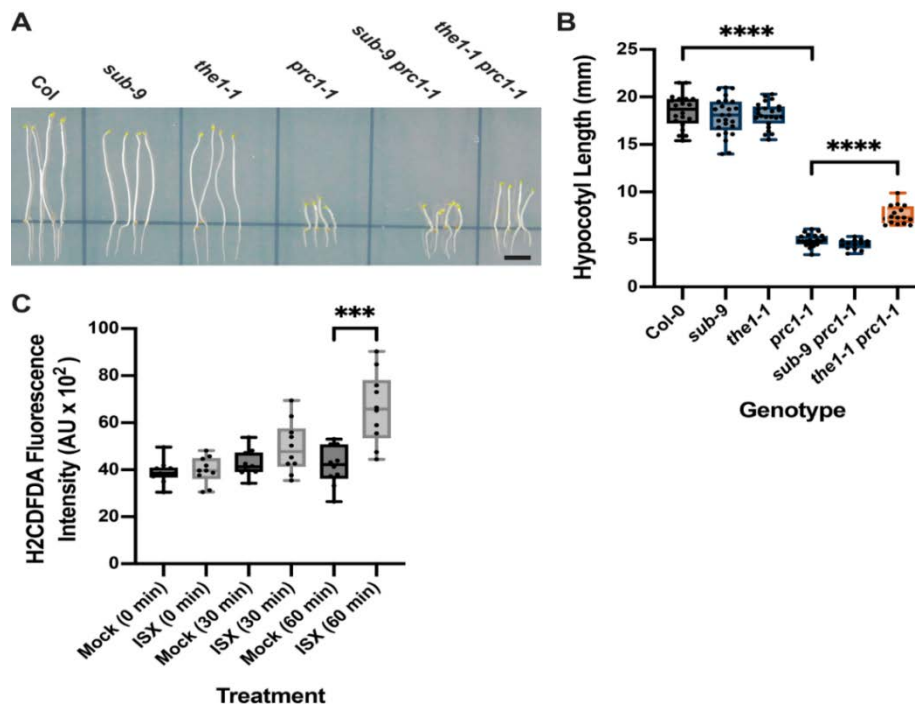


Figure 17. Influence of *THE1* on etiolated hypocotyl length of *prc1-1* and isoxaben-induced ROS accumulation in root tips.

(A) Hypocotyl elongation in six-day-old seedlings grown on plates in the dark. Genotypes are indicated. Note the partial rescue of hypocotyl elongation in *the1-1 prc1-1* but not in *sub-9 prc1-1*. (B) Quantification of the data shown in (A). Box and whisker plots are shown. $14 \leq n \leq 25$. Asterisks represent statistical significance (****, $P < 0.0001$; unpaired t test, two-tailed P values). The experiment was performed three times with similar results. (C) Quantification of H₂CDFDA signal indicating ROS accumulation in root tips of six-day-old *the1-1* seedlings exposed to mock or 600 nM isoxaben for the indicated time. Note the unaltered signal at 30 minutes exposure. Box and whisker plots are shown. $n = 10$. Asterisks represent statistical significance (***, $P = 0.0003$, unpaired t test, two-tailed P values). Experiments were performed three times with similar results. Scale bars: 0.5 mm.

contrast, isoxaben-induced reporter signal in the root tip became stronger than the mock-mediated signal at the 60 minute time point (Figure 17 C). Overall the results resemble the findings obtained

with *sub-9* mutants (Figure 10 C) although the response may be slightly less affected in *the1-1* in comparison to *sub-9*. In summary, *SUB* and *THE1* are required for ROS and lignin accumulation in roots and show partial overlap with respect to stress marker gene induction. *SUB* and *THE1* show opposite effects on growth inhibition of roots and hypocotyls in *prc1* mutants and their functions differ with respect to root growth recovery.

3.2 Morphogenesis in Arabidopsis during cellulose deficient condition is regulated by the activity of SUB

3.2.1 Isoxaben treatment reduces SUB transcriptionally and post-translationally

In the previous chapter, I demonstrated the participation of SUB signaling pathway in cell wall integrity signaling. Furthermore, I decided to look into the mechanistic detail of *SUB* mediated cell wall signaling. To this end, first I together with my colleague Jin Gao analyzed the effect of isoxaben on translational fusion SUB protein in a time-course experiment. Upon treatment with 600nM isoxaben in liquid grown seedlings I noticed considerably weaker pSUB::SUB:EGFP (SSE) reporter signal in comparison to reporter signal in DMSO mock-treated seedlings (Figure 18 A, B). The decrease of EGFP signal intensity could be observed at around five hours after the start of the treatment and it was significantly decreased after around eight hours. Although EGFP signal did not completely disappear but remained at about 50 percent of the intensity detected prior to the start of the isoxaben treatment. Next question I asked if isoxaben treatment also results in reduced endogenous *SUB* expression. My lab colleague Xia Chen analyzed *SUB* transcript expression by qRT-PCR in seedlings treated for eight hours with isoxaben. In line with the observed reduction in reporter expression, she also detected reduced *SUB* mRNA levels (Figure 18 C).

In the next step, I decided to test if prolonged exposure with sublethal dose of isoxaben treatment has a similar effect on *SUB* activity. In previous dose-response experiments testing the effect of isoxaben on growth inhibition of Arabidopsis seedlings, Heim *et al.* have revealed a tight response ranging from near normal growth to no growth in the narrow range of 1 to 10 nM isoxaben, with an I_{50} at 4.5 nM (Heim *et al.*, 1989). Thus, I decided to analyze seven-days-old pSUB::SUB:EGFP *sub-1* seedlings that were continuously grown on agar plates containing 3 to 5 nM isoxaben. In comparison to mock-treated samples, I observed a decreased reporter signal in the isoxaben dose-dependent manner (Figure 18 D, E). In a similar experiment, Xia Chen observed reduction of *SUB* transcript levels by about 50 percent in comparison to untreated seedlings (Figure 18 F). In summary, the results suggest that isoxaben induces a reduction in SSE signal as well as in *SUB* transcript.

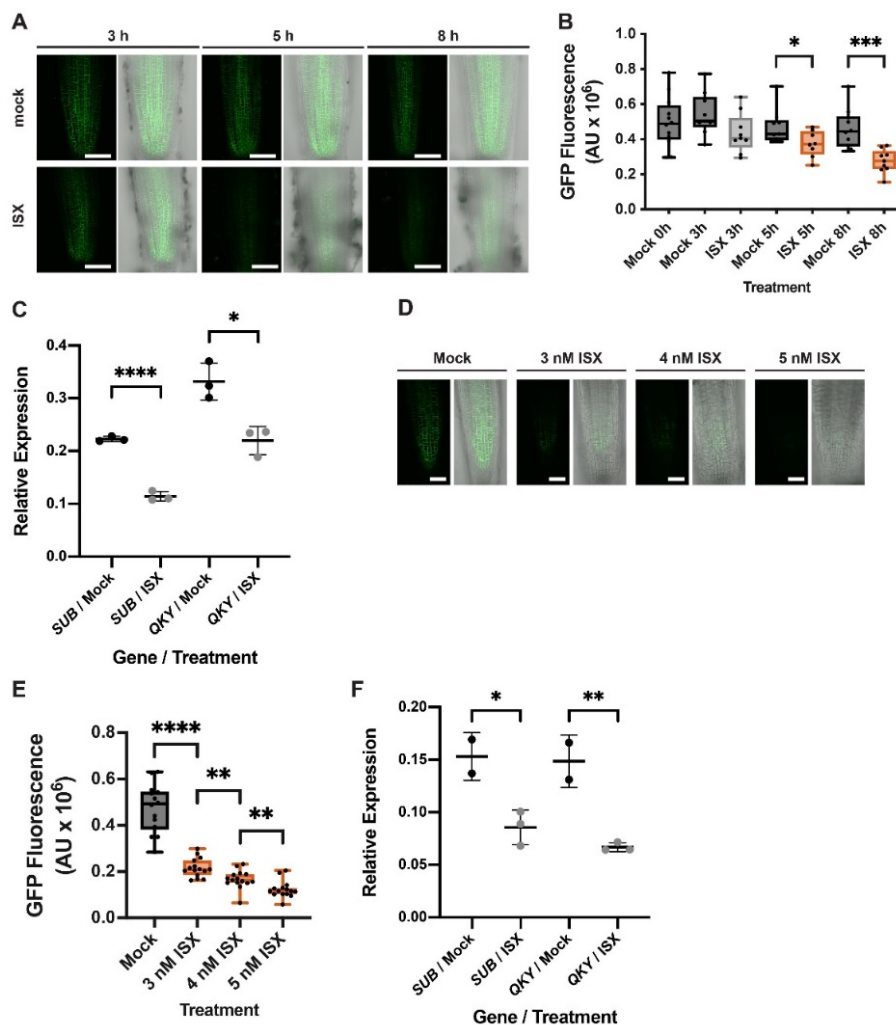


Figure 18. Effect of isoxaben treatment on *SUB*.

(A) and (D) show confocal micrographs depicting optical sections through roots of seven-day-old, seedlings. (A) Signal intensity of a functional pSUB::SUB:EGFP reporter upon exposure of liquid-grown seedlings to mock or 600 nM isoxaben. Duration of treatment and treatment are indicated. Imaging parameters between the mock and isoxaben treatments were identical. Note the reduction of signal in isoxaben-treated seedlings that starts at about five hours of treatment. (B) Quantification of the data shown in (A). Box and whiskers blots are shown. $8 \leq n \leq 12$. Asterisks represent statistical significance (*, $P < 0.04$; ***, $P < 0.0006$; unpaired t test, two-tailed P values). The experiment was performed three times with similar results. (C) Relative mRNA levels of *SUB* and *QKY* in seven days-old seedlings exposed to mock or 600 nM isoxaben for eight hours. Expression was detected by qPCR. Mean \pm SD is shown, $n = 3$. Asterisks represent statistical significance (*, $P < 0.02$; ****, $P < 0.0001$; unpaired t test, two-tailed P values). The experiment was performed three times with similar results. (D) Signal intensity of a functional pSUB::SUB:EGFP reporter upon exposure of plate-grown seedlings continuously exposed to mock or three, four, or five nM isoxaben. Duration of treatment and treatment are indicated. Imaging parameters between the mock and isoxaben treatments were identical. Note the reduced signal in isoxaben-treated seedlings. (E) Quantification of the data shown in (D). Box and whiskers blots are shown. $14 \leq n \leq 15$. Asterisks represent statistical significance (**, $P < 0.004$; ****, $P < 0.0001$; unpaired t test, two-tailed P values). The experiment was performed three times with similar results. (F) Relative expression of *SUB* and *QKY* in seven days-old seedlings grown on plates containing mock or 3 nM isoxaben. Expression was detected by qPCR. Mean \pm SD is shown, $2 \leq n \leq 3$. Asterisks represent statistical significance (*, $P < 0.03$; **, $P < 0.009$; unpaired t test, two-tailed P values). The experiment was performed three times with similar results. Scale bars: (A) 60 μm ; (D) 50 μm .

3.2.2 Exposing plants to sub-lethal doses of isoxaben induces *sub*-like root hair patterning defects

The observation that cellulose biosynthesis inhibition results in the downregulation of *SUB* raised the question if isoxaben treatment also results in a similar *sub* like phenotype. To address this issue, I first analyze the effect of isoxaben treatment on root hair cell patterning in six-day-old seedlings. To this end, I made use of Col plants carrying the pGL2::GUS:EGFP (GL2::EGFP) reporter. The *GLABRA2* (*GL2*) promoter drives expression in nonhair (N) cells but not in hair (H) cells of the root epidermis (Dolan *et al.*, 1994) and the expression pattern of a pGLS2::GUS or GL2::EGFP reporter thus serves as a convenient and faithful proxy for root hair patterning (Kwak *et al.*, 2005, Masucci *et al.*, 1996, Gao *et al.*, 2019). I analyzed six days-old wild-type seedlings first grown on regular plates for four days followed by growth in 3 nM isoxaben-containing plates for two days with the help of a confocal microscope. I noticed that 3nM isoxaben treated seedlings show prominent misexpression of reporter signal that resembled the expression pattern of the reporter in *sub-9* mutants (Figure 19 A-D) (Table 6) however mock-treated seedlings showed regular expression pattern. To corroborate my finding, I repeated the experiment with two different drugs 2,6-dichlorobenzonitrile (DCB) and Thaxtomin A, both drug cause CBI in Arabidopsis (Heim *et al.*, 1990, Scheible *et al.*, 2003, Tateno *et al.*, 2016). I treated wild-type seedlings with 200 nM DCB or 15 nM Thaxtomin A, both drugs induced *sub*-like expression pattern defects of the GL2::EGFP reporter (Figure 19 E, F). To complement our finding, I analyzed genetically defected in cellulose biosynthesis *prc1-1* mutants that carried the GL2::EGFP reporter but were not exposed to isoxaben. I noticed that *prc1-1* mutants exhibited a mild but consistent defect in the expression pattern of the reporter (Figure 19 G). These observations lead to question, if altered patterning of GL2::EGFP reporter is just consequence of over-active cell wall integrity signaling due to non-specific cell wall perturbation. It has been previously reported that changing in osmolarity of cell or disrupting the microtubule dynamics could also activate the cell wall integrity signaling machinery due to changes in turgor (Hamann *et al.*, 2009; Hamant and Haswell, 2017; Engelsdorf *et al.*, 2018). So to address the issue of specificity of cell wall perturbation I analyze the pattern of GL2::EGFP reporter in presence of high osmoticum or microtubule disrupting drugs. I did not notice any irregular reporter expression pattern in seedlings exposed to 150 mM NaCl, 175 nM oryzalin, or 100 nM latrunculin B (Figure 19 H-L). Furthermore proving osmotic support to *sub-9* did not

rescue its root hair patterning defect as treatment of *sub-9* *GL2::EGFP* seedlings with 100 nM sorbitol did not rescue the altered expression pattern of the reporter (Figure 19 I).

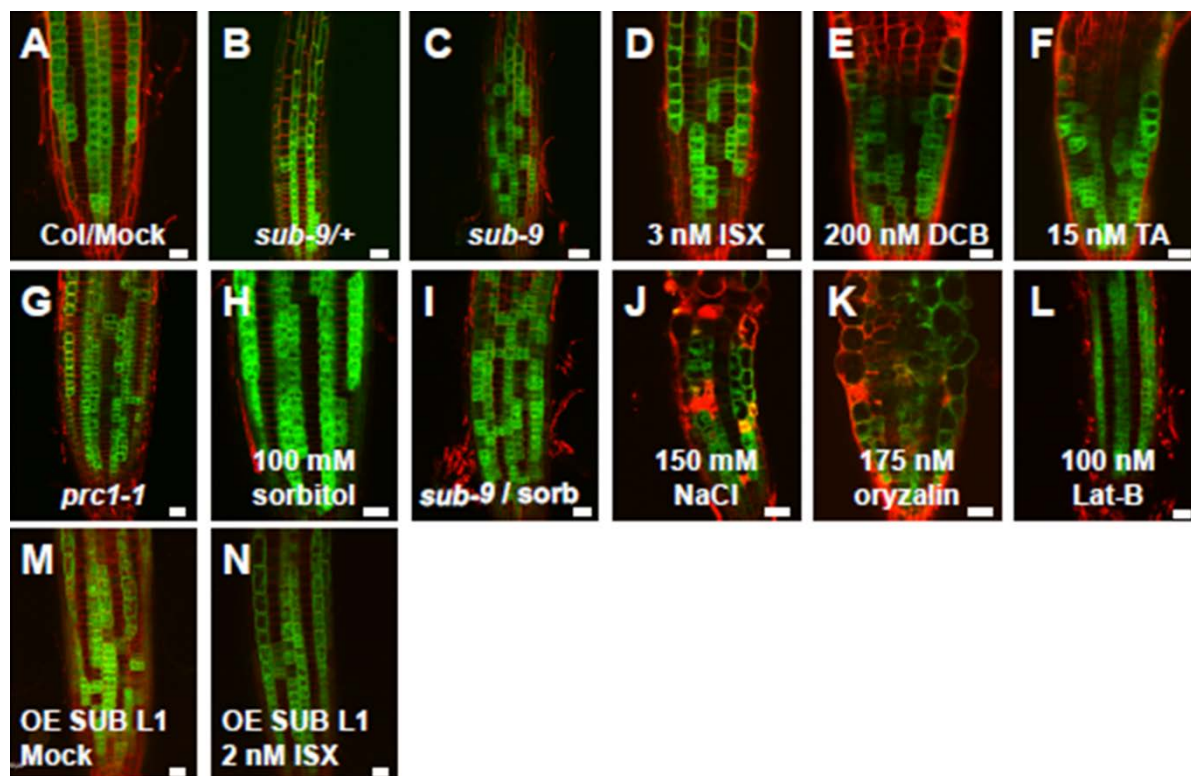


Figure 19. The consequence of reduced cellulose biosynthesis on the *GL2::EGFP* expression pattern. Confocal micrographs show optical sections through roots of seven-day-old seedlings showing the *GL2::EGFP* expression pattern. Genotypes and/or treatments are indicated. For quantification of some of the effects see Table X. (A) 10/10 roots analyzed showed this pattern. (B) 13/16. (C) 22/22. (D) 31/35. (E) 21/28. (F) 12/12. (G) 11/11. (H) 17/21. The remaining four roots showed the occasional single cell displacement in the reporter expression as also sometimes seen in wild type (Table 2). (I) 12/13. (J) 17/19. (K) 11/11. (L) 13/13. (M) 15/17. (N) 16/19. The experiment was performed three times with similar results. Scale bars: 20 μ m.

Table 7 Position-dependent pattern of *GL2::EGFP* reporter expression in root epidermal cells upon a 48 hour exposure to isoxaben.

Genotype	ISX [nM] ^a	H cells total ^b	H Position ^c	N cells total ^b	N Position ^c
Col	0	633	2.7	741	96.6
<i>sub-9</i>	0	548	33.6 ^d	615	74.8
Col	1	441	14.1 ^e	589	86.1
	2	375	26.7	459	78.7
	3	395	30.6	579	77.0
<i>SUB OE L1</i>	0	423	6.9	558	77.3
	1	616	4.7 ^f	663	95.9

	2	327	1.2 ^g	396	92.2
	3	401	16.7	445	86.7
<i>SUB OE O3</i>	0	508	4.7	701	82.2
	1	638	3.3 ^h	706	94.5
	2	320	3.4 ⁱ	396	92.4
	3	359	10.9	475	86.1

For each genotype and treatment at least 10 different roots of seven-days-old seedlings were analyzed.

^aIsoxaben (ISX) concentration in plate

^bTotal number of cells at H or N position scored

^cPercentage of cells at H or N position expressing the GL2::EGFP reporter

^dStatistical significance: *sub-9* vs Col (untreated), $P < 0.0001$.

^eStatistical significance: Col (1 nM ISX) vs Col (untreated), $P < 0.0001$.

^fStatistical significance: L1 (1 nM ISX) vs Col (untreated), $P = 0.0708$; L1 (1 nM ISX) vs Col (1 nM ISX), $P < 0.0001$. L1 (1 nM ISX) vs L1 (untreated), $P = 0.1686$.

^gStatistical significance: L1 (2 nM ISX) vs Col (untreated), $P = 0.1676$; L1 (2 nM ISX) vs Col (2 nM ISX), $P < 0.0001$, L1 (2 nM ISX) vs L1 (untreated), $P = 0.0001$.

^hStatistical significance: O3 (1 nM ISX) vs Col (untreated), $P = 0.6219$; O3 (1 nM ISX) vs Col (1 nM ISX), $P < 0.0001$; O3 (1 nM ISX) vs O3 (untreated), $P = 0.2241$.

ⁱStatistical significance: O3 (2 nM ISX) vs Col (untreated), $P = 0.5448$; O3 (2 nM ISX) vs Col (2 nM ISX), $P < 0.0001$; O3 (2 nM ISX) vs O3 (untreated), $P = 0.4785$.

Significance was estimated by a two-sided Fisher's exact test. The experiment was performed twice with similar results.

To confirm that the altered GL2::EGFP expression pattern in roots of isoxaben-treated wild-type seedlings indeed reflects root hair patterning defects. To this end, I compared the number of hair and nonhair cells in the N and H positions of the root epidermis, respectively, in untreated and treated wild type seedlings to the respective numbers in untreated *sub-9* roots. In untreated plate-grown wild-type plants, we found that 97.4 percent of cells at the H position were hair cells while only 1.9 percent of cells at the N position were hair cells (Table 7). In contrast, roots of wild-type seedlings grown on 3 nM isoxaben plates for seven days exhibited 67.7 percent hair cells in the H position and 24.4 percent hair cells in the N position. A similar value was observed for *sub-9* mutants, confirming previous results (Kwak *et al.*, 2005) (Table 7). Taken together, the results indicate that reduced cellulose biosynthesis leads to an altered expression of the GL2::EGFP reporter and a *sub*-like defect in root hair patterning.

Table 8 Distribution of root hair and nonhair cells in the root epidermis.

Genotype	roots ^a	H position ^b		N position ^b	
		Hair (%)	Nonhair (%)	Hair (%)	Nonhair (%)
Col-0	17	97.4 ± 3.3	2.6 ± 3.3	1.9 ± 2.8	98.1 ± 2.8
Col-0 / 3 nM ISX	17	67.7 ± 4.9	32.3 ± 4.8	24.4 ± 6.0	75.6 ± 6.0
<i>sub-9</i>	17	70.9 ± 4.1	29.8 ± 4.1	23.4 ± 4.1	76.6 ± 4.1

^aTotal number of different roots analyzed.

^bMean ± standard deviation. Total number of cells counted at H position: $321 \leq n \leq 442$. Total number of cells counted at N position: $472 \leq n \leq 561$. The experiment was repeated twice with similar results.

3.2.3 Exposing plants to sub-lethal doses of isoxaben induces *sub*-like floral defects

SUB is known to regulated morphogenesis of above ground floral organ as well as root (Chevalier *et al.*, 2005, Fulton *et al.*, 2009). So in the next step, I decided to explore further the effect of isoxaben on *SUB*-dependent floral organ morphogenesis. For that, I tested if isoxaben treatment also induces *sub*-like defects in flowers and ovules. To this end, I compared wild-type (*Ler*) and *sub-1* plants that were grown on soil in the presence of isoxaben. Plants were initially germinated and grown without any treatment. Just before the start of bolting I began watering wild-type plants with 100 to 500 nM isoxaben and continued watering with isoxaben in three-day intervals for two weeks. As it has previously been reported that stage 3 floral meristems of *sub* mutants show aberrant cell division planes in the L2 layer (Chevalier *et al.*, 2005, Fulton *et al.*, 2009) (floral stages according to (Smyth *et al.*, 1990), I collected floral primordia and stained them with propidium iodide. Isoxaben-treated wild-type Col plants revealed *sub* like L2 layer division plane defect (Figure 20 A-C) of floral meristems with propensity corresponding to increasing concentrations of isoxaben (Table 8). Additionally, I compared stage 13 flower morphology of isoxaben-treated *Ler* plants to flowers from untreated *sub-1* plants (Figure 20 D-F). I noticed similar *sub*-like flowers with altered arrangement of petals from isoxaben-treated plants. At last, I analyzed the ovule phenotype of isoxaben-treated wild-type plants. I observed *sub*-like defects in integument outgrowth in late stage 3 or early stage 4 ovules (ovule stages according to Schneitz *et al.*, 1995) (Fig. 20 G-I) (Table 9). Ovule defect was less pronounced with 100 nM isoxaben compared to treatment with 500 nM isoxaben (Table 9). The obtained results show that isoxaben also induces *sub*-like defects in floral and ovule development.

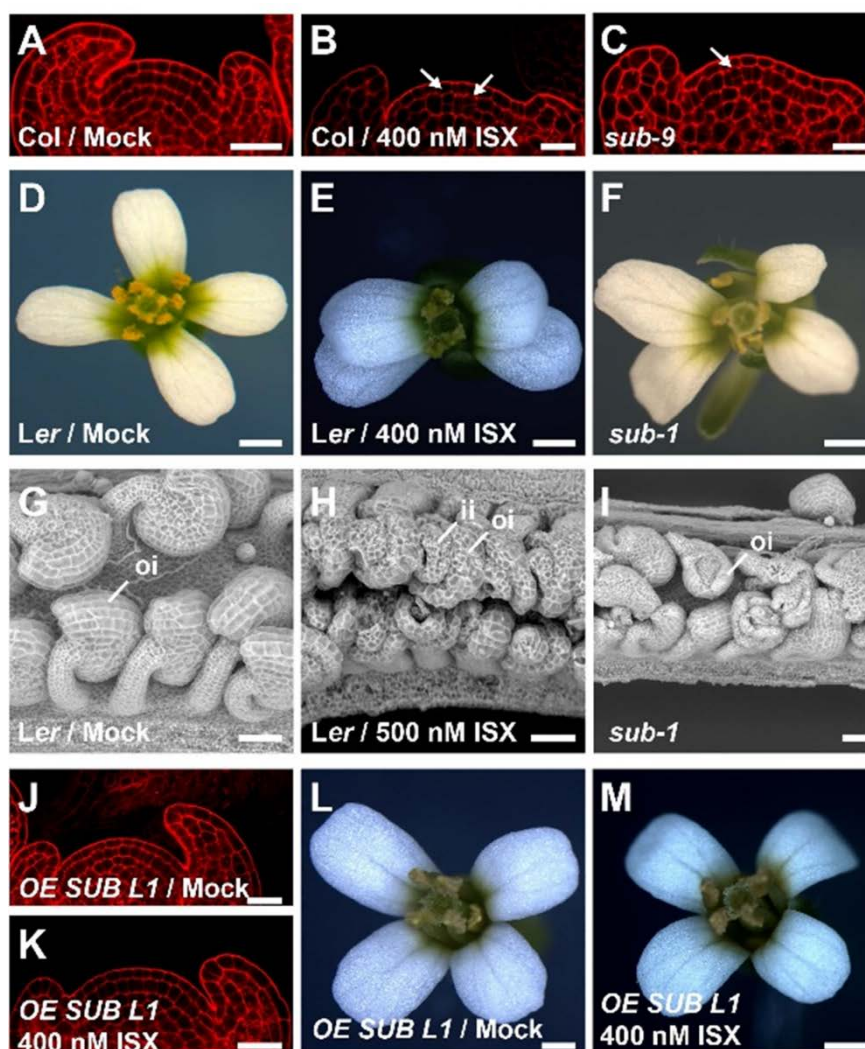


Figure 20. Influence of isoxaben treatment on floral and ovule morphogenesis. Genotypes and treatments are indicated. For a quantification of the effects see Table 8, 9. (A-C) Confocal micrographs depicting mid-optical sections through stage 3 floral meristems. Arrows indicate irregular periclinal cell divisions in L2. (D-F) Morphology of mature stage 13 or 14 flowers. (E, F) Compare to (D). Note the aberrant arrangement of petals. (G-I) Electron scanning micrographs depicting mature stage 3 or 4 ovules. (H, I) Compare to (G). Note aberrant integuments. (J, K) Confocal micrographs depicting mid-optical sections through stage 3 floral meristems. Note the regular cell division pattern in the L2 layer. (L, M) Note regular appearance of flowers. The experiment was performed three times with similar results. Abbreviations: ii, inner integument; oi, outer integument. Scale bars: (A) to (C) and (J), (K), 20 μ m; (D) to (F), and (L), (M), 0.5 mm; (G) to (I) 50 μ m.

3.2.4 Ectopic expression of *SUB* attenuates several detrimental effects of isoxaben

Taking all the above results into account I hypothesized that cellulose biosynthesis inhibition results in downregulation of *SUB*, and subsequently in a *sub*-like phenocopy, ectopic expression of *SUB* should counteract this outcome. To test this hypothesis I made use of two wild-type lines carrying a pUBQ::*SUB*:mCherry transgene (lines L1, O3) and crossed them into a wild-type line carrying the GL2::*EGFP* reporter. I first then analyzed the reporter signal in seven-days-old plate-grown seedlings that had been grown on normal plates for five days before being transferred to plates containing no isoxaben or 1 nM, 2 nM, or 3 nM isoxaben, respectively, for another 48 hours prior to analysis (Figure 19 M, N) (Table 6). Kwak *et al*, 2007 has previously reported that ectopic expression of *SUB* results in aberrant pGL2::*GUS* expression and a mild defect in root hair patterning (Kwak and Schiefelbein, 2007). I noticed that lines L1 and O3 both showed an altered expression pattern of the GL2::*EGFP* reporter in untreated root confirming the previous finding, with more cells in the H position and fewer cells in the N position exhibiting reporter signal compared to wild type (Fig. 19 M) (Table 6). In Col wild type seedlings upon 1 to 3 nM isoxaben treatment I observed noticeable and concentration-dependent increase in defects in the expression pattern of the reporter (Table 6). Interestingly, isoxaben-treated L1 and O3 lines show significant differences to wild type expression pattern of reporter signal. Exposing seedlings of both lines to 1 or 2 nM isoxaben resulted in GL2::*EGFP* patterns that resembled the pattern observed in untreated wild-type seedlings and that were less aberrant than the GL2::*EGFP* patterns observed in corresponding isoxaben-treated wild-type seedlings (Figure 19 M,N) (Table 6). Moreover, the defects were weaker when compared to the aberrations exhibited by untreated L1 or O3 lines. However, exposing both lines to 3 nM isoxaben resulted in defected expression pattern of the reporter but that was still less severe in comparison to wild-type plants treated with 3 nM isoxaben (Table 6). Taken together, these data indicate that ectopic *SUB* activity attenuates the effects of isoxaben on the expression pattern of the GL2::*EGFP* reporter in the root epidermis.

Next, I also tested if ectopic expression of *SUB* also alleviates the effects of isoxaben on floral development by cultivating lines L1 and O3 in the presence of different concentrations of isoxaben as described above. I noticed that floral meristem and ovule defects were reduced in both lines compared to wild type (Fig. 20 J-M) (Tables 8, 9). In summary, the results indicate that the effects of isoxaben on root hair patterning as well as floral and ovule development relate to the isoxaben-induced reduction of *SUB* activity.

Table 9 Number of periclinal cell divisions in L2 layer of stage 3 floral meristems of plants exposed to different concentrations of isoxaben.

Genotype	ISX [nM] ^a	N FM ^a	N PCD ^b	Percentage
Col	0	29	5	17.2
<i>sub-9</i>	0	31	14	45.2
Col	200	14	4	28.6
	300	21	8	38.1
	400	25	15	60.0
<i>SUB OE LI</i>	0	8	2	25.0
	400	27	6	22.2

^aNumber of floral meristems analyzed.

^bNumber of periclinal cell divisions observed.

The experiment was performed twice with similar results

Table 10 Comparison of integument defects between Col, *sub-9*, *sub-21*, and Col plants exposed to different concentrations of isoxaben.

Genotype	ISX [nM] ^a	N Ovules ^b	Defective Ovules ^c
Col	0	502	0.0
<i>sub-9</i>	0	629	44.2 ^d
<i>sub-21</i>	0	578	49.5 ^d
Col	200	547	13.5 ^e
	300	576	25.4
	400	563	34.3
	500	551	50.5
<i>SUB OE LI</i>	0	511	0.0
	200	593	2.4 ^{f,g}
	300	527	4.0 ^{g,h}

	400	573	8.7 ^h
	500	581	14.1 ^h
<i>SUB OE O3</i>	0	570	0.0
	200	587	1.9
	300	508	3.3
	400	571	8.4
	500	541	16.1

For each genotype and treatment at least 15 different carpels from four different plants were analyzed.

^aIsoxaben (ISX) concentration in water.

^bTotal number of ovules scored.

^cPercentage of ovules with *sub*-like integument defects.

^dStatistical significance: *sub* vs Col (untreated), $P < 0.0001$.

^eStatistical significance: Col (untreated) vs Col (200 nM ISX), $P < 0.0001$.

^fStatistical significance: Col (untreated) vs SUB OE L1 (200 nM ISX), $P = 0.0002$.

^gStatistical significance: Col (untreated) vs SUB OE L1 (300 nM ISX), $P < 0.0001$.

^hStatistical significance: Col (treated) vs SUB OE L1 (treated), $P < 0.0001$.

Significance was estimated by a two-sided Fisher's exact test. The experiment was performed three times with similar results.

3.3 Additional candidate genes involved in the *SUB* signaling pathway

After establishing the role of *SUB* in CBI induced cellular response and cellular architecture maintenance, I set out to find additional candidates involved in the *SUB* signaling pathway. I took into consideration two criteria for a candidate to be likely involved in the *SUB* signaling cascade. The first consideration was a potential physical interaction. In the canonical signaling pathway, two proteins have to physically interact or at least reside in close vicinity for propagating signaling cues. Due to the sophisticated nature of plant cell and limited available resources, it is difficult to isolate intact protein complexes from plant. With the advent of yeast two-hybrid (Y2H) system, it has become very convenient to find putative interactor of signaling component. The Y2H system also provides the opportunity to find domain-specific interactor of a protein. However, Y2H is a heterologous system and there have been several reports of false-positive result so independent validation of interaction is always recommended. The genetic interaction analysis is another method to find possible participants of the signaling component. The comparison of the single and double mutant phenotype of candidate gene reveals genetic interaction among them, for example, the positive regulators of signaling pathway show similar phenotype whereas phenotype of double mutant could reveal more complex nature individual signaling components.

The second factor I considered if the putative candidate is also localized or enriched at plasmodesmata by mining PD proteome data. *SUB* is known to localized at plasmodesmata along with plasma membrane. To form the *SUB* signaling protein complex, the putative candidate has to be in close vicinity to *SUB*.

By taking advantage of already available *SUB* yeast two-hybrid interactome data in the lab and various data search yield into list of 32 putative candidate genes (Table 1). The candidate gene was first screened for *sub* like floral organ phenotype in the single mutant background. In the next step, by crossing with *sub-9* and *qky-11*, double mutant plants were generated for each candidate gene. The double mutant plants were screened for suppression or enhancement of *sub-9* floral organ phenotype. In the compiled list of candidate genes, I found two microtubule-binding proteins *TORTIFOLIA* (*TOR1*) and *KINESIN7.4* (*KIN7.4*) (Table 10). *TOR1* is involved in stabilizing microtubule (Buschmann *et al.*, 2004) and mutant plant lacking functional TOR protein show anticlockwise stem and petiole twisting (Buschmann *et al.*, 2004; Wightman *et al.*, 2013). Kinesin is a motor protein known for cargo transport (Asada and Collings, 1997). *KIN7.4* is not well studied

although *KIN7.3* an ortholog of *KIN7.4* is reported to assist in microtubule polymerization (Moschou *et al.*, 2016). I also found several receptor-like kinases including *BAK1-interacting receptor like kinase (BIR1)*, *Pollen receptor like kinase 2 (PRK2)*, *Leucine-rich repeat 1(LRR1)* and *Wall associated kinase 2 (WAK2)* (Table 10). WAKs are known for transducing signal from cell membrane upon various biotic and abiotic stress (He *et al.*, 1999; Kohorn and Kohorn, 2012). The LRR1 is plasma membrane-localized kinase which is recently been reported for relocalization from the plasma membrane to plasmodesmata upon osmotic stress (Grison *et al.*, 2019). I also found CLATHRIN HEAVY CHAIN 2 (*CHC2*) an endocytosis machinery protein. *CHC2* is involved in embryonic and postembryonic development (Kitakura *et al.*, 2011) and ligand-mediated internalization of membrane receptors (Andres Ortiz-Morea *et al.*; Fendrych *et al.*, 2013; Mbengue *et al.*, 2016; Žárský, 2016).

Table 11 List of putative *SUB* signaling candidate genes

No.	Gene name	AGI code	Y2H bait/source database	Single mutant phenotype observed	Double mutant with <i>sub-9</i> or <i>qky-11</i> phenotype observed
1	<i>BAK1-interacting receptor like kinase (BIR1)</i>	AT5G48380	SUB split ubiquitin (Lalonde S et al; 2010)	No <i>sub-9</i> like floral organ phenotype	No change in <i>sub-9</i> floral organ phenotype
2	<i>Pollen receptor like kinase 2 (PRK2)</i>	AT2G07040	SUB split ubiquitin (Lalonde S et al; 2010)	No <i>sub-9</i> like floral organ phenotype	No change in <i>sub-9</i> floral organ phenotype
3	<i>Clathrin heavy chain 2 (CHC2)</i>	AT3G08530	SUB-ICD/ (Mukhtar MS et al; 2011)	No <i>sub-9</i> like floral organ phenotype	Rescue of <i>sub-9</i> floral organ phenotype
4	<i>Tortifolia 1 (TOR1)</i>	AT4G27060	SUB-ICD/ (Mukhtar MS et al; 2011)	Anticlockwise stem and petiole twisting	Rescue of <i>tor</i> phenotype
5	<i>Synaptotagmin1 (SYT1)</i>	AT2G20990	QKYΔTM (Lab database)	No <i>sub-9</i> like floral organ phenotype	No change in <i>sub-9</i> floral organ phenotype
6	<i>Wall associated Kinase 2 (WAK2)</i>	AT1G21270	SUB-ICD (Lab database)	No <i>sub-9</i> like floral organ phenotype	No change in <i>sub-9</i> floral organ phenotype
7	<i>TON1 recruiting motif 22 (TRM22)</i>	AT1G67040	SUB-ICD (Lab database)	No <i>sub-9</i> like floral organ phenotype	No change in <i>sub-9</i> floral organ phenotype
8	<i>KINESIN 7.4 (KIN7.4)</i>	AT4G39050	SUB-ICD/ (Mukhtar MS et al; 2011)	No <i>sub-9</i> like floral organ phenotype	Rescue of <i>sub-9</i> floral organ phenotype
9	<i>Leucine-rich repeat protein 1 (LRR1)</i>	AT5G16590	SUB-ICD (Lab database)	No <i>sub-9</i> like floral organ phenotype	No change in <i>sub-9</i> floral organ phenotype
10	<i>Blade on petiole 2 (BOP2)</i>	AT2G41370	SUB-ICD (Lab database)	No <i>sub-9</i> like floral organ phenotype	No change in <i>sub-9</i> floral organ phenotype

11	<i>Embryo sac development arrest 33 (EDA 33)</i>	AT4G00120	SUB-ICD (Lab database)	No <i>sub-9</i> like floral organ phenotype	No change in <i>sub-9</i> floral organ phenotype
12	<i>OBERON 1(OBE1)</i>	AT3G07780	SUB-ICD (Lab database)	No <i>sub-9</i> like floral organ phenotype	No change in <i>sub-9</i> floral organ phenotype
13	<i>CBL-interacting protein kinase 12 (CIPK12)</i>	AT4G18700	QKYΔTM (Lab database)	No <i>sub-9</i> like floral organ phenotype	No change in <i>sub-9</i> floral organ phenotype
14	<i>Calcium dependent lipid bining protein</i>	AT5G37370	QKYΔTM (Lab database)	No <i>sub-9</i> like floral organ phenotype	No change in <i>sub-9</i> floral organ phenotype
15	<i>Unkown protein</i>	AT3G15590	SUB-ICD (Lab database)	No <i>sub-9</i> like floral organ phenotype	No change in <i>sub-9</i> floral organ phenotype

To analyze the possible role of candidate genes, we obtained at least two independent t-DNA insertion mutant lines from the stock center for each gene (Table 10). All the t-DNA lines were genotyped for homozygous plant and t-DNA insertion site was further confirmed by sequencing. For some t-DNA line, insertion was found either very downstream of 3' terminator or very upstream of 5' Promoter than predicted site of insertion (Table 1). After careful sequencing analysis, homozygous t-DNA lines were grown in long-day condition and were analyzed for *sub* like floral organ phenotype. None of the t-DNA showed any *sub* like floral organ phenotype. That could be either because of redundant gene function or complex genetic interactions are difficult to score. Nevertheless, in the second step, all single mutants plant was crossed into *sub-9* to find more direct genetic interaction if any existed among them. In F1 population of all crossings showed wild type morphology suggesting recessive nature of mutation in either individual candidate gene. In the next step, F2 generation plants were screened for homozygous double mutant for each combination of the crossing. At least 300 plants per combination were grown in long-day condition. F2 population was first analyzed phenotypically for any observable change *sub* like floral organ morphology. Except *chc2-1sub-9* and *kin7.4-1 sub-9* none of F2 population showed any enhanced or suppressed *sub-9* phenotypes. For *chc2-1 sub-9*, 3/4 population of F2 plants showed wild type floral organ phenotype and 1/4 plants showed *sub-9* like. That suggests *SUB* negatively regulates *CHC2* for floral organ development. This genetic interaction is further characterized and published by lab colleague Jin (Gao *et al.*, 2019). The second genetic interaction I could observe was for *kin7.4-1 sub-9*, as again 3/4 population of F2 plants showed wild type floral organ

phenotype and $\frac{1}{4}$ plants showed *sub-9* like. This observation hints at *KIN7.4* being also negatively regulated by *SUB* during floral organ development. The more detail about role of *KIN7.4* in floral organ morphogenesis will be discussed in next chapter.

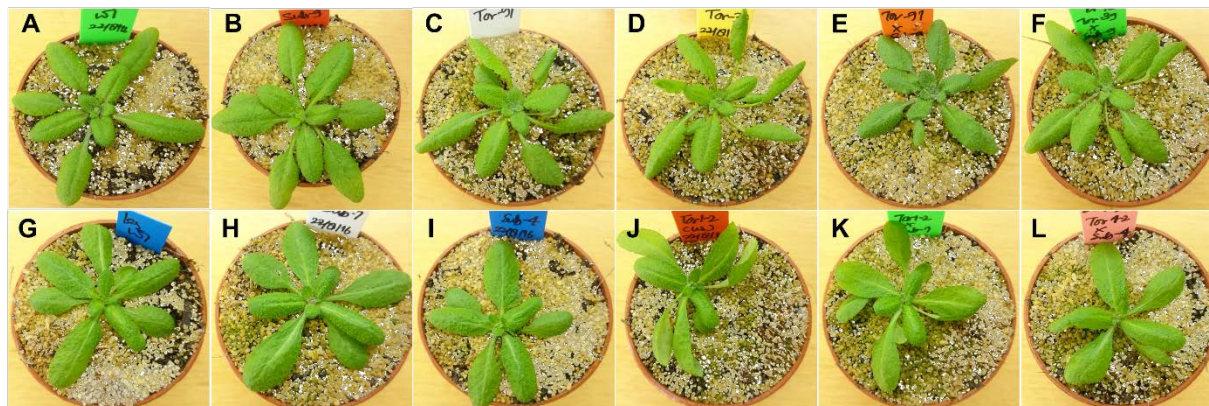


Figure 21. Twisted petiole organization of *tor* is attenuated in *tor sub* double mutant. Morphology of 3-weeks old seedlings showing straight petioles in wild type seedling Col (A) Ler (B), *sub-9* (B) *sub-1* (H) *sub-4* (I), anticlockwise twisted petiole in *tor-91*(C), *tor-39* (D), *tor1-1* (J). Notice the alleviated petiole twisting in *tor sub* (E, F, K, and L).

TORI was the third interesting candidate from list of putative candidates. I decided to analyze three independent mutant alleles, one EMS mutagenized line *tor1-2* in Ler ecotype and two t-DNA insertion lines *tor-39* and *tor-91* in Col background. None of these lines shows any *sub* like floral organ defect but I could confirm anticlockwise twisting phenotype in the petiole of *tor1-2*, *tor-39* and *tor-91* (Figure 21) (Buschmann *et al.*, 2004; Wightman *et al.*, 2013) however *sub* mutant did not show twisted petiole defect. Interestingly the *tor1-2 sub1* and *tor1-2 sub-4* double mutant showed reduced petiole twisting in Ler ecotype background (Figure 21) as well as in *tor-39 sub-9* and *tor-91 sub-9*. The twisting phenotype was more prominent in *tor-39* and *tor1-2* alleles while in double mutant with *tor-91 sub-9* showed nearly wild type petiole arrangement and *tor-39 sub-9* still shows some reminiscence of *tor* phenotype. These phenotypic observations suggest *SUB* is epistatic to *TOR* with respect to petiole twisting.

The fourth interesting candidate was *WAK2*, *WAKs* have been already been reported for their role in cell elongation, cell expansion and plant defense upon pathogen attack (Verica *et al.*, 2003; Kohorn *et al.*, 2006a, 2012, 2014; Li *et al.*, 2009). Upon analysis of *wak2* mutant alleles, I found that none of *wak2* single or *wak2-12 sub-9* double mutants showed any change in floral organ morphology. But in light of recently proven *SUB*'s role in CBI mediated defense pathway, I decided to further explore *WAKs* for their role *SUB* mediated tissue morphogenesis and in cell wall-associated signaling pathway.

This work was carried by Master's thesis student Barbara Leśniewska under my supervision. In her detailed phenotypic analysis, she could confirm that *WAK2* did not participate in *SUB* mediated floral organ morphogenesis using two independent loss of function *wak2* alleles. Interestingly for *WAK3*, she could show that the *wak3-1sub-9* double mutant shows rescue of the *sub-9* floral organ defect, ovule integument defect and periclinal division defect in floral meristem while *wak3-1* did not show any defect in floral organ. This observation suggests *SUB* to act as a negative regulator of *WAK3* for floral organ development. In case of *WAK1*, she could not generate any homozygous t-DNA insertion mutant and there is no mutant allele available in the database. Upon performing fecundity assay, she concluded that the *wak1-1* is embryo lethal. For further analysis of *WAK1*, I might have to devise inducible system for suppressing *WAK1* activity in temporal and spatial fashion. Taken together her results suggest there is complex genetic interaction between *SUB* and *WAKs* and for further characterization Barbara has taken up the project for her Ph.D. thesis in the lab.

3.3.1 Validation of interaction of promising candidate gene in Y2H

After analyzing the phenotype of all putative candidate genes, in the next step, I decided to validate the yeast two-hybrid interaction of promising candidate gene. *WAK2*, *TOR1*, *CHC2*, and *KIN7.4* were identified as an interesting candidate for their role in *SUB* mediated tissue morphogenesis. *CHC2* has already been shown to interact with *SUB* intracellular domain by our colleague Jin (Gao *et al.*, 2019), I will not discuss it further. To this end, I decided to perform a yeast two-hybrid experiment on these selected candidate genes. The coding sequences of *WAK2*, *TOR1*, and *KIN7.4* were cloned into yeast two-hybrid vectors. After successful cloning and transformation into yeast, one to one interaction studies between *SUB* and candidate genes were performed. Growth of yeast on double drop out medium containing plate confirmed the successful transformation of both GAL-AD and GAL-DB plasmids into single yeast. For *WAK2*, in case when *WAK2* intracellular domain (*WAK2* ICD) was concomitantly transformed with *SUB* intracellular domain (*SUB* ICD), yeast were failed to grow on triple drop out plate (image not is shown) however they successfully formed colony when they harbor plasmid *WAK* ECD-AD along with *SUB* ECD-BD. None of yeast cell grew when empty *GAD* or

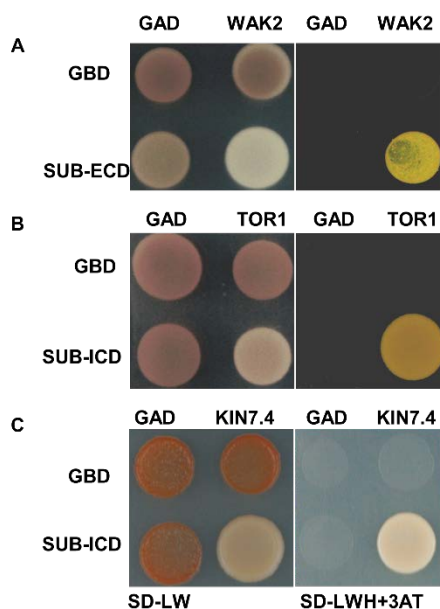


Figure 22. Yeast two-hybrid interaction of *SUB* with *WAK2*, *TOR1*, and *KIN7.4*

For Yeast two-hybrid assay *SUB*-ECD/ICD was cloned into pGBKT7, and *WAK2*-ECD, *TOR1*, and *KIN7.4* were cloned into pGADT7. Yeast AH109 cells were cotransformed with a combination of the indicated plasmids. To test protein-protein interactions, yeast cells were plated onto synthetic drop out $-His(H)/-Trp(W)/-Leu(L)$ medium including 10 mM 3-amino-1,2,4, -triazole and allowed to grow for 4 d at 30°C. Growth of yeast cells on SD-LWH plate suggests an interaction between subjected protein. Red color yeast colony mark the deficiency of adenine hemisulfate. AD-activation domain, BD-binding domain, *SUB* ECD- *SUB* extracellular domain, *SUB* ICD- *SUB* intracellular domain.

GDB vector was used in combination with other ORFs containing plasmids suggest there is no autoactivation or nonspecific growth of yeast cells. Our result indicates WAK2 extracellular domain interacts with SUB extracellular growth (Figure 22) while there is no interaction observed between intracellular domain of WAK2 and SUB. Additionally, TOR1 and KIN7.4 show interaction with intracellular domain SUB (Figure 22).

3.4 *SUB* signaling regulates microtubule organization

SUB signaling pathway mutant *sub-1*, *qky-8*, and *zet-1* have been shown to exhibit altered cell wall biochemistry (Vaddepalli *et al.*, 2017). Cortical microtubules (CMT) have been shown to respond to a defect in the cell wall (Hamant *et al.*, 2008). Moreover in *qky* mutant background misoriented microtubules were shown in the carpel (Trehin *et al.*, 2013). Since *SUB* mutants also show morphological defect with twisted siliques, carpels, and stem that could also be related to altered CMT. This notion encouraged me to explore if CMT in *sub* mutant is also affected. To this end I generated microtubule marker line mCherry-TUA5 (Gutierrez *et al.*, 2009) previously reported for visualizing CMT in Arabidopsis seedlings. Interestingly, the recovered transformants displayed severe growth defect and sterility. The similar observation has also been made in some earlier studies for the TUA5 based CMT marker lines (Xiao *et al.*, 2016). So in step, I generated MT marker transgenic lines expressing the RFP-TUB6 (Ambrose *et al.*, 2011) in the *Ler* and *Col* background. This time the obtained transformants did not show any twisting phenotype. The homozygous RFP-TUB6 expressing line was crossed into *sub* mutant background. After having all genetic material, seedlings were grown in long-day condition on MS half medium supplemented with 1% sucrose. Five-day old seedlings were analyzed with CLSM using 561 laser with 40X water objective. Maximum Z-projection images of CMT were acquired from the elongation zone of root epidermis. Microtubule orientation in different zones of 5 days old *Col* WT root (Figure 23, A-C) was different from each other. The root cap of *Col* (Figure 23, A) shows mostly transverse orientation to the longitudinal wall of the cell. While epidermal cell of meristematic zone shows radial patterning with occasional preprophase band and mitotic spindle. However, MTs in the transition zone was aligned transversally to the longitudinal axis of root. CMTs in root cap (Figure 23 D) and meristematic zone of the *sub-9* (Figure 23 E) did not show any major alignment difference compare to *Col* WT. But in transition zone *sub-9* epidermal cells (Figure 23, F) showed more radon organized CMTs in contrast to more transversely organized CMTs in *Col* WT.

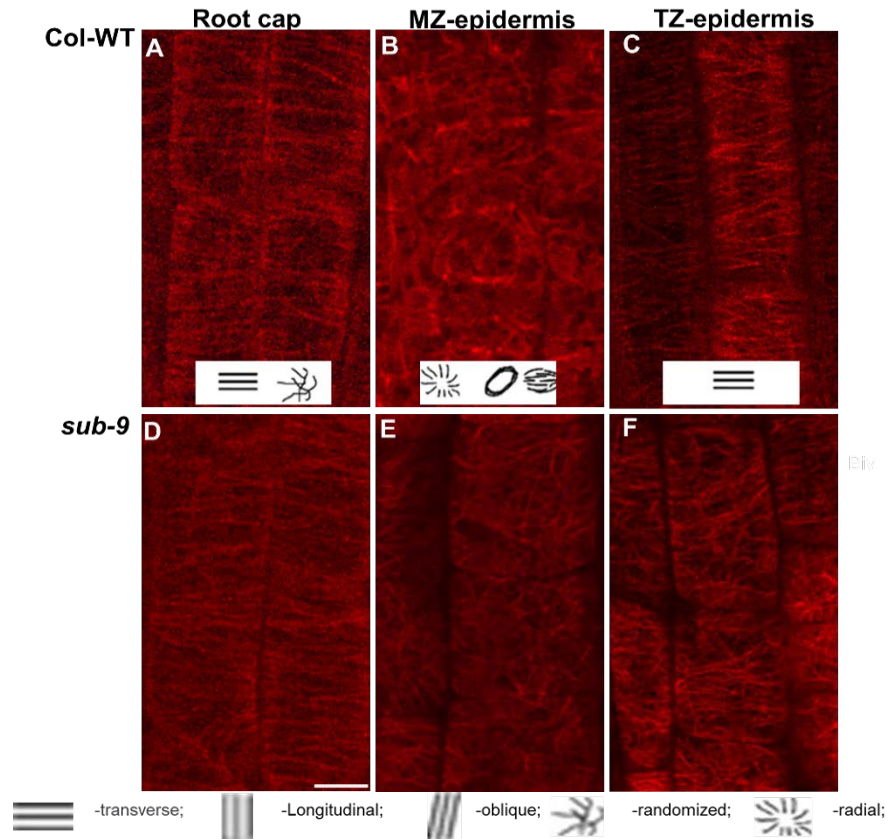


Figure 23. Cortical microtubule patterning in different zones of the Arabidopsis root. Maximum projections of Z-series images from root epidermal cells of 5-d-old Arabidopsis seedlings expressing RFP-TUB6 in Col-WT (A, B, C) and *sub-9* (D, E, F) backgrounds. The distribution of MT orientation relative to the longitudinal cell axis in epidermal cells is shown for root cap (A, D), Meristematic zone (B, E), and transition zone (C, F) cells in Col WT and *sub-9* seedlings ($n \geq 10$ roots per genotype analyzed). Schematic drawings in white inset of images A, B, and C represent MTs orientation relative to the primary root or root hair axis. Scale bar: 5 μ m.

A similar observation was also made in *Ler* background (Figure 24 A). *Ler* WT controls (Figure 24 A left panel) showed mostly transverse RFP-TUB6-labeled MTs. Whereas in *sub-1* MTs (Figure 24, A) appeared to be more disorganized. Further on, the orientation angle of MTs of 100 cells from ten different roots was measured in both background and plotted on the frequency graph after binning for 10 degrees orientation angle. In *Ler* background the highest frequency of MT were clustered at 90 degrees (Figure 24 B upper panel). *sub-1* as expected MTs were more dispersed (Figure 24 B lower panel). In conclusion *sub* mutant show CMT orientation defect in root epidermis cells.

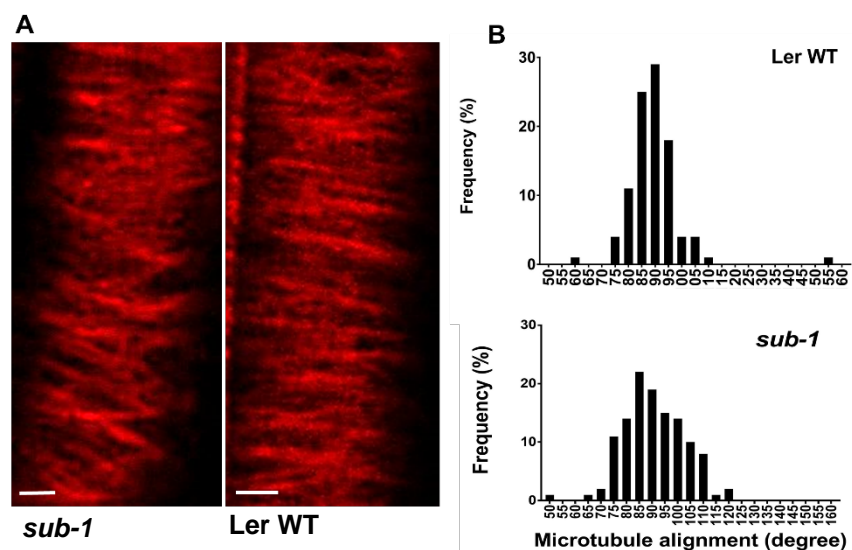


Figure 24. Organization of cortical microtubule in the elongation zone epidermal cell. A, RFP-TUB6 labeled CMT in Ler (A, left panel) *sub-1* (A, right panel). B, Quantification of cortical microtubule of Ler (B, Upper panel) and *sub-1* (B, Lower panel).

In light of the observed CMT orientation defects in of *sub* mutant, it was interesting to study microtubule-binding protein. Moreover, AtKin13a another kinesin from Arabidopsis has been shown to modulate cell wall synthesis and cell expansion (Fujikura *et al.*, 2014). So in next step I decided to characterize KIN7.4

3.5 Characterization of KINESIN 7.4 (KIN7.4) in Arabidopsis

3.5.1 In silico structure-function analysis of KIN7.4

To develop an understanding about the role of *KIN7.4* in plant development I first analyze domain structure. In silico structure analysis based on homology modeling reveals very conserve nature of *KIN7.4*. It contains 1055 amino acid (aa) that spans through four necessary domains viz Motor, neck, coiled-coil stalk, and tail domain required for a functional plant mortar protein (Figure 25) (Vinogradova *et al.*, 2009). The N-terminus motor domain contains 415 aa including 97 aa ATP binding motif that attaches kinesin to microtubules. The C-terminus tail domain is also known as cargo binding domain contains 50 aa and binds with cargo. (Vale, 2003). The middle region of 592 aa long between Motor domain and cargo binding domain is known as stalk. It harbors four coiled-coil domains of various length which connects the motor and tail domains. In previous studies, the coiled-coil domain has been reported for helping KIN to make a functional dimeric form (Ganguly and Dixit, 2019). The neck or neck linker is a few amino acids long connecting region between motor and stalk. The neck is important for transmitting the conformational change in the catalytic site during movement of KIN (Sablin *et al.*, 1998; Rice *et al.*, 1999). During the nucleotide hydrolysis cycle, the neck linker adopts distinct positions with respect to the motor domain, being either attached to the motor core or released.

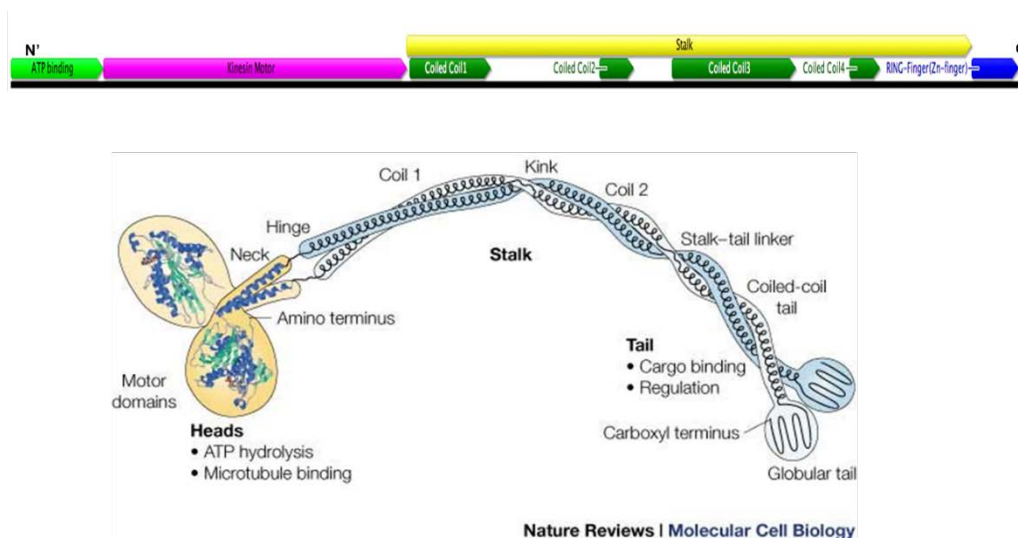


Figure 23. Schematic depiction of KIN7.4 domain structure.

KIN7.4 is consisting of N' Terminus ATP binding domain followed by a motor domain. It has cargo binding domain at C' terminus end and the central region is consisting of four coiled-coil domains. Modified from (Woehlke and Schliwa, 2000).

3.5.2 Phylogenetic analysis of KIN7.4

In Arabidopsis 61 kinesins are known to exist. They are classified into 14 families on the basis of their amino acid sequences in motor domain (Nebenführ and Dixit, 2018). To perform phylogenetic analysis, I took amino acid sequences of the motor domain that resulted in the *KIN7.4* into group 7 of the *KINESIN* superfamily (Supplementary figure 1). Group 7 has five Arabidopsis kinesin-*KIN7.1* (AT1G21730), *KIN7.2* (AT2G21380), *KIN7.3* (AT3G12020) *KIN7.4* (AT4G39050), and *KIN7.5* (AT5G06670). The *KIN7.1*, *KIN7.3* and *KIN7.5* genes are involved in the establishment of cell polarity in Arabidopsis (Moschou *et al.*, 2016). The functions of *KIN7.4* and *KIN7.2* is yet to be explored. As in previous work, Moschou *et al.* 2016, has also found *KIN7.4* to be in group 7. They named a member of this group according to their position on chromosome number. *KIN7.4* is located on chromosome number 4, thus it is *KIN7.4*. *CENP-E* is a founding member of group 7 and it is known to regulate microtubule dynamics during various stages of the cell cycle in animal (Sardar *et al.*, 2010). Since in phylogenetic tree *KIN7.4* and *KIN7.2* shares the same branching point with rest of group members. So in next step, I analyzed sequence identity at amino acid level using ClustalW algorithm and BLOSUM62 (BLSM62) matrix (Supplementary figure 2). I found that *KIN7.4* is more than 75% identical to *KIN7.2*. As it was expected, the motor domain of both proteins showed more than 90% similarity. But surprisingly C' terminus cargo binding domain of both proteins also showed very similar sequence identity. It suggests they could be involved in very similar cargo transport. However, in N' Terminus ATP binding domain, *KIN7.2* has some additional amino acid and sequence identity is less than 50 percent. Similarly the stalk domain also has some sporadic region with dissimilar amino acids and also some additional amino acid sequences in both KIN.

3.5.3 Expression analysis of KIN7.4

To examine if the Arabidopsis *KIN7.4* gene has a specific expression pattern during plant development and if co-expressed with *SUB*, the expression levels of *KIN7.4* and *SUB* were analyzed using the Klepikova atlas (Kilian *et al.*, 2007; Klepikova *et al.*, 2016). The mean normalized expression values revealed constant expression of *KIN7.4* during most of the developmental stages except for floral organ formation (Supplementary Data 3 A). The *KIN7.4* expression was strongly upregulated in petals of stage 11-13 flower whereas interestingly *SUB* expression was down-regulated in petal and upregulated in the carpel. *KIN7.2* showed stronger expression level throughout all developmental stages except in shoot apical meristem (Supplementary Data 3 C).

In addition to the above-mentioned Klepikova atlas for global transcript analysis, I extracted tissue-specific absolute expression values normalized to the median of ratio method as described in Anders and Huber (Anders and Huber, 2010) from TraVA database (Weblet Importer, Klepikova *et al.*, 2016). As previously reported by in-situ hybridization, I also found absolute expression values for *SUB* is higher in carpel and inflorescence meristem (Chevalier *et al.*, 2005). (Supplementary Data 3). *KIN7.4* and *KIN7.2* exhibited almost half absolute expression value in carpels and double in petals, in line to previous observation with the klepikova atlas (Supplementary data 3 A and C). Between flower stage 9 to 11, *SUB* and both *KIN* shows almost equal level of the transcript but with the progression of flower development stage, *SUB* transcript tends to decrease while both Kinesin showed increment in expression level. In inflorescence, meristem *SUB* showed a higher level of expression than both *KIN*. But in stage 2i-3iv ovule has an almost equal level of all three gene transcripts. Mature leaf and internode accumulated almost thrice amount of *KIN* transcript than *SUB* which is at its minimum level. In young silique *KIN* strongly expressed than *SUB*. In 7-day old seedling root meristem shows more expression of *SUB* than both *KIN* but in the later part of root *KIN* is strongly expressed and *SUB* is at its minimal level of expression. In seedling cotyledons and hypocotyl again *KIN7.4* is highly expressed than *KIN7.2* and *SUB*. In overall *SUB* is mostly expressed in very young developing tissues, but some reminiscent of *SUB* transcript is also been detected in mature tissue. While *KIN* is weakly expressed in young tissue and strongly present in mature tissues.

The next question I asked if *SUB* regulates *KIN7.4* expression. To address that I performed qRT-PCR. Since *KIN7.4* is best expressed in 7-day-old seedlings (Supplementary data 3) I choose seedling tissue for qRT-PCR analysis. Genomic DNA of *KIN7.4* comprises of several intermittent intron elements. To capture any alternatively spliced variant of transcript and avoid nonspecific amplification two different primer pairs were used. The primer pair P1 span through first exon and intron interval and Primer pair P2 covers second last exon-intron span at 3' end before stop codon. Mean normalized expression of both primer pairs showed same level in Col WT background suggested specific primer binding. There was no significant change observed in *KIN7.4* transcript in *sub-9* background indicating that *SUB* does not affect the transcription of *KIN7.4* (Figure 26).

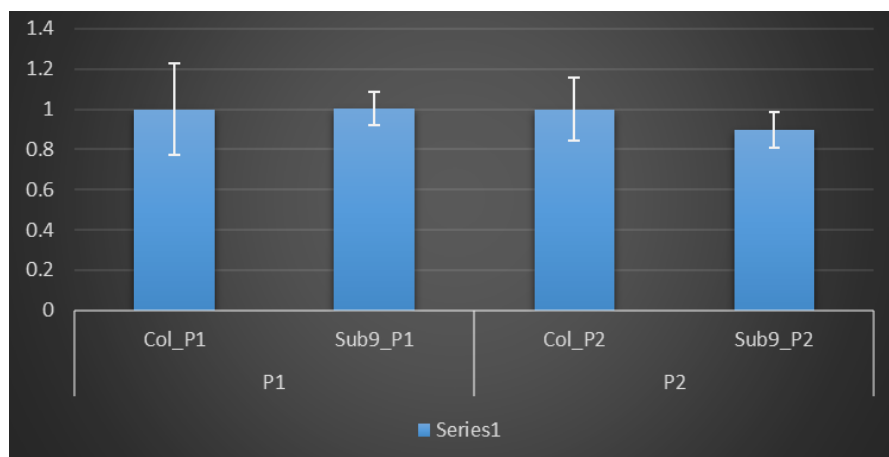


Figure 26. qRT-PCR analysis of *KIN7.4* expressions.

The transcript expression of *KIN7.4* in Col and *sub-9*, 7-days-old seedlings. *KIN7.4* is not altered in *sub-9* mutant seedling. P1 and P2 designate to primer pair 1 and 2.

3.5.4 Analysis of *KIN 7.4* promoter activity

To analyze promoter activity of *KIN7.4*, 2.9 kb nucleotide from upstream of the start codon to terminator of next gene was used as promoter sequences. For terminator 2.4 kb nucleotide downstream of stop codon to next gene was cloned. The reporter construct p*KIN7.4*:NLS GUS-EGFP:t*KIN7.4* was transformed and transgenic plants were screen. For analysis of *KIN7.4* promoter activity, 7-day old plate grown whole seedlings and whole inflorescence from 4-week old plants were used. Tissues were harvested and fixed for Gus staining according to the protocol (Li, 2011). The experiment was performed using six independent homozygous T3 lines.

For spatial resolution roots from 7-day old seedlings were analyzed in the confocal microscope. The EGFP reporter signal was strongly observed in root cap cells of the meristematic region (Figure 27), in epidermis cell, there was a very weak signal observed, however, vascular cells show relatively stronger signal in meristematic zone (Figure 27). An overall signal was most prominently observed in maturation and differentiation zone of the root.

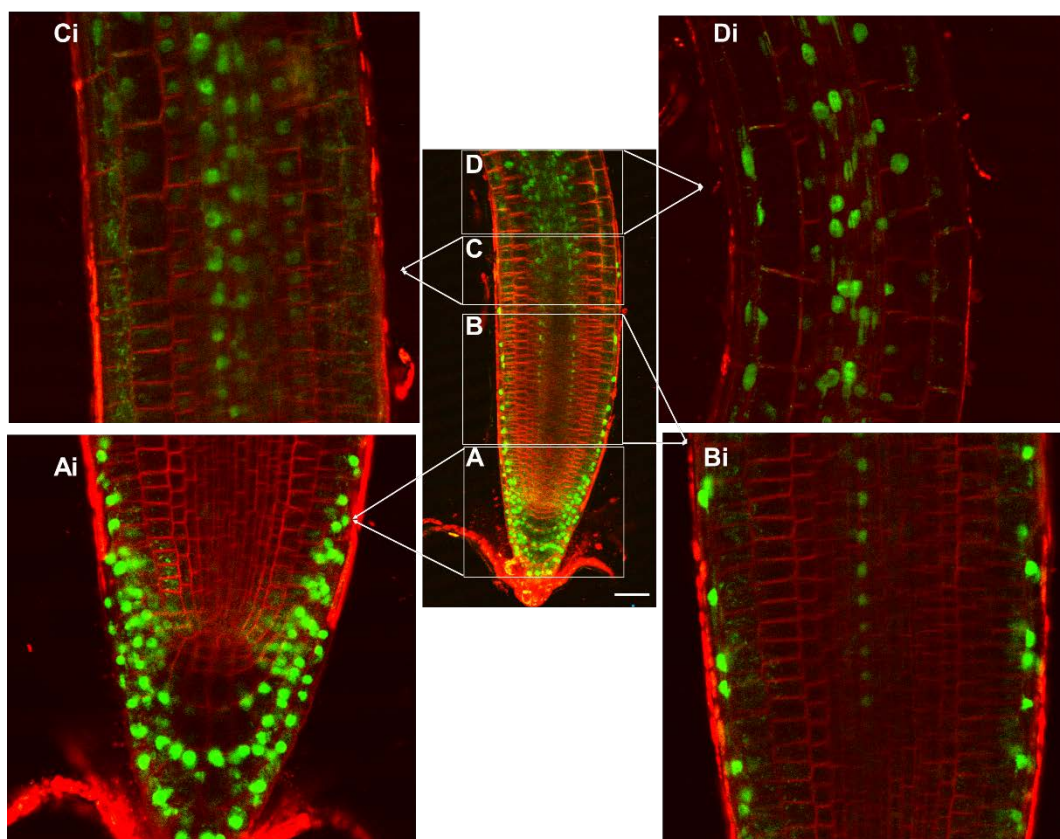


Figure 27. Promoter activity of KIN7.4 in 7-day-old root. The expression of pKIN7.4:NLS GUS-EGFP:tKIN7.4 in Col background. The reporter signal is observed in root cap cells (A), epidermal cells (B) vascular cells (C) and in the elongation zone (D).

3.5.5 Phenotypic characterization of *kin7.4* and *kin7.2* mutant alleles

3.5.5.1 Analysis of *kin7.4* and *kin7.2* mutant alleles

To determine the biological function of the candidate *KIN7.4*, I obtained several knockout or knock down mutant for both *KIN7.4* and *KIN7.2*. I received two independent t-DNA lines for each of the *KIN* genes from the Nottingham Arabidopsis Stock Centre (NASC). For *KIN7.4*, we named these lines *kin7.4-1* (SALK_130788) and *kin7.4-2* (SALK_026411), and for *KIN7.2*, *kin7.2-1* (SALK_1407078) and *kin7.2-2* (SALK_101917). The t-DNA insertion site was determined by genotyping PCR followed by sequencing according to SIGnAL guideline ('SIGnAL iSect Toolbox'). The SALK_130788 t-DNA is located at the beginning of third last exon (from ATG to downstream position no. 5623) and SALK_026411 t-DNA is integrated just before very last exon (From ATG to downstream position no. 6286) of *KIN7.4* (Figure 28). The qRT PCR analysis using primer pair spanning through first exon

these lines shows only $\frac{1}{4}$ th of transcript compare to Wild type plant. (Supplemental Figure 4). To obtain complete null allele I generated several crispr-cas lines. In this study, only two CRISPR-Cas lines *kin7.4-3* and *kin7.4-4* were used. *kin7.4-3* was created in *sub-9* mutant background and it has deletion of 40 nucleotides in just after first ATG and that also lead to an immediate stop codon (Figure 28). The *kin7.4-4* has an insertion of an ‘A’ nucleotide that leads to stop codon after the first 15 amino acid (Figure 28) (Supplemental Figure 5). For *kin7.2-1*, SALK_1407078 was detected within the ninth intron (from ATG to downstream position no. 2225), and SALK_101917 has insertion within the twentieth one intron (from ATG to downstream position no. 5557) (Figure 28). The qRT-PCR experiment revealed only 1/5th to wild type level transcript in *kin7.2-1* and no transcript in *kin7.2-2* when primer pair binding after t- DNA insertion site was used (Supplemental Figure 5). But there was no significant change observed in transcript when primer pair binding before t-DNA insertion was used. Since t-DNA inserted in motor domain for *kin7.2-1* and stalk domain in case of *kin7.2-2* so in principle both alleles are completely devoid of functional protein.

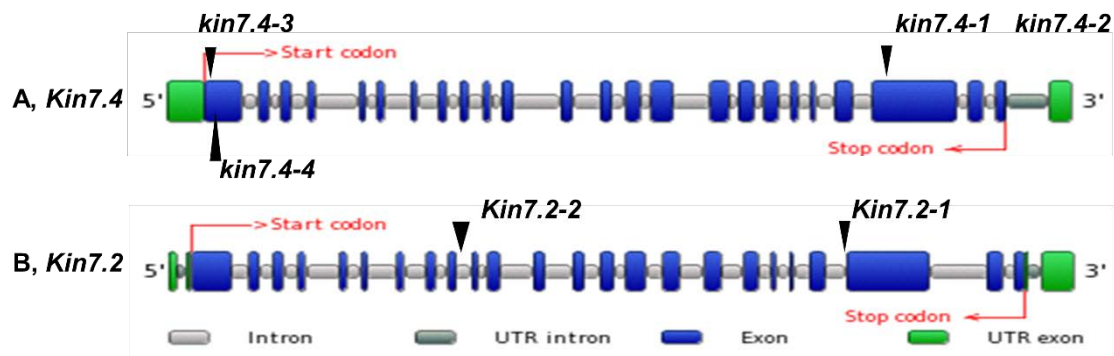


Figure 28. Gene structure of *KIN7.4* and *KIN7.2* including t-DNA insertion sites.

Green boxes represent UTRs, blue boxes exons, grey boxes introns, and black arrowheads indicate crispr cas generated mutation for *kin7.4-3* and *kin7.4-4* and for rest of alleles its T-DNA insertion site.

3.5.5.2 Analysis of floral organ morphology of *kin7.4* mutant alleles

In order to elucidate the role of *KIN7.4* in floral organ development, I first analyzed the floral organ morphology of homozygous knockdown mutants *kin7.4-1* and *kin7.4-2*. The four-week plant of both *kin7.4* mutant alleles showed no floral organ phenotype. The plant height, stem and silique twisting, floral organ were indistinguishable from Col WT plant (Figure 29, Table 11 and 12). Flowers were properly developed, without any obvious alterations. Long and straight siliques resembled WT morphology. In scanning electron microscopy of stage 4 ovule from both *kin7.4* alleles, I did not

observe any *sub-9* like outer integument defected ovules. Subsequently, *kin7.4-1* and *kin7.4-2* mutants were tested for cellular patterning in L1/L2 cells of stage 2 to 4 floral meristems (Figure 29, Table 11). Homozygous *kin7.4* mutant plants preserved typical cell shape and anticlinal cell division in the L1 and L2 cells of floral meristems (Table 11). Interestingly, floral meristems of *kin7.4-1* and *kin7.4-2* showed a slightly higher percentage of periclinal cell division planes. However, double mutant analysis of *sub-9 kin7.4-1* revealed rescue of *sub-9* floral organ phenotype (Figure 29 E, J, O, T and Table 11 and 12). Flowers maintained their natural shape and size. Twisting of carpels and later siliques were not observed (Figure 29 J). The appearance together with the number of mature and fertilized ovules in siliques did not significantly differ from wild-type plants (Figure 29, Table 12). Furthermore, at the cellular level, *sub-9 kin7.4-1* preserved unchanged morphology and an anticlinal, rather than periclinal cell division in L1 and L2 layers of floral meristems (Figure 29 O). Interestingly double mutant analysis with other alleles of *kin7.4* (*kin7.4-2*, *kin7.4-3*, and *kin7.4-4*) showed no change in *sub-9* floral organ phenotype. It suggests *kin7.4-1* acts as a dominant-negative form of KIN7.4.

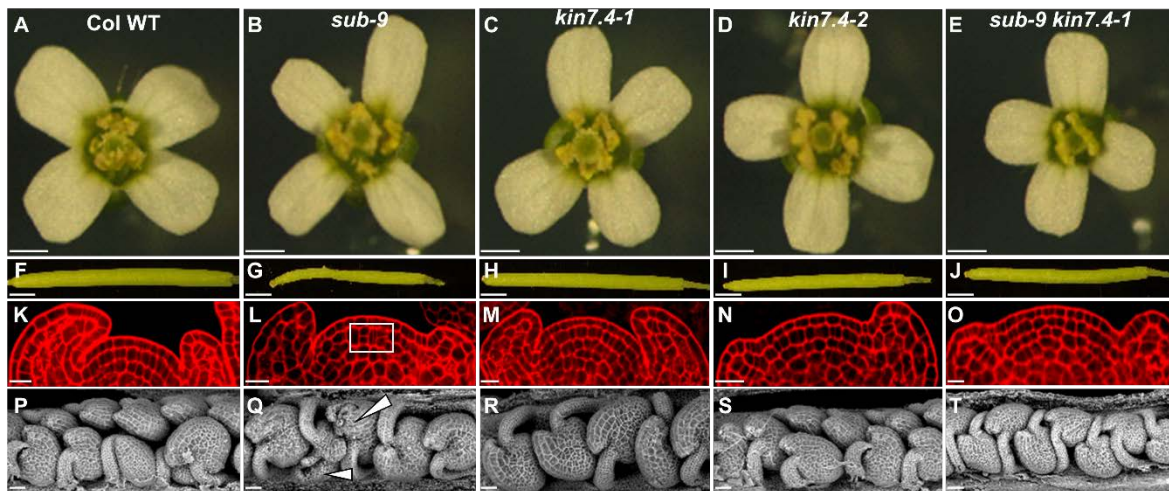


Figure 29. Phenotype comparison between Col-0, *sub-9*, *kin7.4-1*, *kin7.4-2* and *sub-9 kin7.4-1*. (A) to (E) Morphology of mature stage 13 or 14 flowers stages according to (Smyth et al., 1990)) (F) to (J) Morphology of siliques. (K) to (O) Central region of stage 3 floral meristems stained with pseudo-Schiff propidium iodide (mPS-PI). (L) square white box indicates aberrant cell division planes. (P) to (T) Scanning electron micrographs of stage 4 ovules (stages according to (Schneitz *et al.*, 1995)) (Q) Note the aberrant outer integument (arrow). (D, I, N, S) Note the defects of the *sub-9* phenotypes were partially rescued in *sub-9 kin7.4-1* double mutants. Scale bars: (A) to (E) 0.5 mm, (F) to (J) 1 mm, (K) to (O) 10 μ m. (P) to (T) 50 μ m.

Table 12 Number of periclinal cell divisions in the L2 layer of stage 3 floral meristems

Genotype	NPCD ^a	Percentage	NFM ^b
Col	9	16.36	55
<i>sub-9</i>	22	37.28	59
<i>kin7.4-1</i>	12	19.35	62
<i>kin7.4-2</i>	7	17.07	41
<i>sub-9 kin7.4-1</i>	14	21.53	65
<i>kin7.2-1</i>	8	19.35	49
<i>kin7.2-2</i>	7	17.07	37
<i>sub-9 kin7.2-1</i>	14	21.53	43

^aNumber of periclinal cell divisions observed

^bNumber of floral meristems observed

Table 13 Comparison of integument defects between Col, *sub-9*, *kin7.4-1*, *kin7.4-2* and *sub-9 kin7.4-1* mutants.

Genotype	N total	N with defects	Percentage
Col	300	0	0
<i>sub-9</i>	250	60	24
<i>kin7.4-1</i>	200	0	0
<i>kin7.4-2</i>	230	0	0
<i>sub-9 kin7.4-1</i>	250	13	5.2
<i>kin7.2-1</i>	160	0	0
<i>kin7.2-2</i>	184	0	0
<i>sub-9 kin7.2-1</i>	215	48	22.32

3.5.5.3 Analysis of floral organ morphology of *kin7.2* mutant alleles

In previous section homology modeling of KIN7.4 and KIN7.2 suggests very identical nature of the protein. So in the next step, I decided to analyze the floral organ morphology of *kin7.2* mutants. The *kin7.2-1* and *kin7.2-2* mutants also did not show any *sub-9* like floral organ phenotype (Figure 30). The above-ground part of the plants showed no detectable abnormality, making them indistinguishable

from wild-type plants. Flowers were developed in wild type fashion, without any alterations. Siliques were devoid of any twisting and appeared to be wild type morphology. Furthermore ovule of *kin7.2* mutants showed no morphological difference to wild type ovule neither any resemblance to *sub-9* outer integument defect (Figure 30 Table 12). At cellular level of stage 2 to 4 floral meristem cell division plane in L2 layer was also preserved to anticlinal division (Figure 30 Table 11). Unlike *kin7.4-1* double mutant of *sub-9 kin7.2-1* did not show rescue of floral organ phenotype. None of floral organ analyzed showed any alteration to *sub-9* morphological defect (Figure 30 Table 11 and 12).

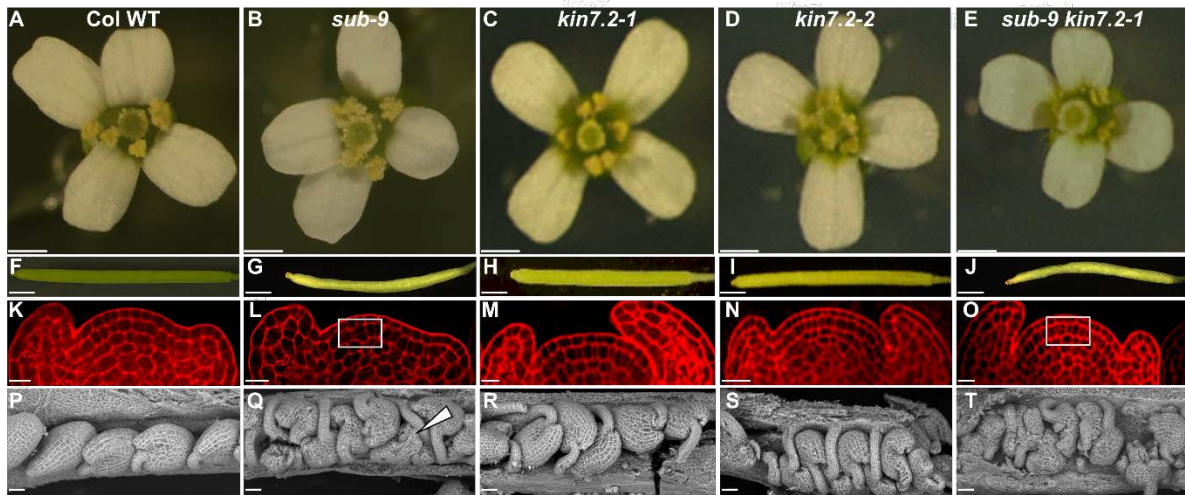


Figure 30. Phenotype comparison between Col-0, *sub-9*, *kin7.2-1*, *kin7.2-2* and *sub-9 kin7.2-1*. (A) to (E) Morphology of mature stage 13 or 14 flowers (stages according to (Smyth et al., 1990)) (F) to (J) Morphology of siliques. (K) to (O) Central region of stage 3 floral meristems stained with pseudo-Schiff propidium iodide (mPS-PI). (L) square white box indicates aberrant cell division planes. (P) to (T) Scanning electron micrographs of stage 4 ovules (stages according to (Schneitz et al., 1995)) (Q) Note the aberrant outer integument (arrow). (D, I, N, S) Note the non rescued defects of the *sub-9* phenotypes in *sub-9 kin7.2-1* double mutants. Scale bars: (A) to (E) 0.5 mm, (F) to (J) 1 mm, (K) to (O) 10 μ m. (P) to (T) 50 μ m.

3.5.5.4 Analysis of floral organ morphology of *kin7.4 kin7.2* double mutant

Since a single mutant of *KIN7.4* and *KIN7.2* do not show any floral organ phenotype (figure 29, 30). So in the next step, I decided to generate double mutant of *kin7.4 kin7.2* in all possible allelic combinations. All the combinatorial double mutants showed very similar morphology, so here data is presented only for *kin7.4-1 kin7.2-1*. The homozygous double were observed for the above-ground morphological defect. These double mutant did not deviate from wild type growth appearance including plant height (data not shown). The floral organ sepals, petals did not show any twisting

(Figure 31). Silique grew straight and to the length of the wild-type plant (figure 31). I also did not observe any deformed ovule (Figure 31 M, N, O, and P).

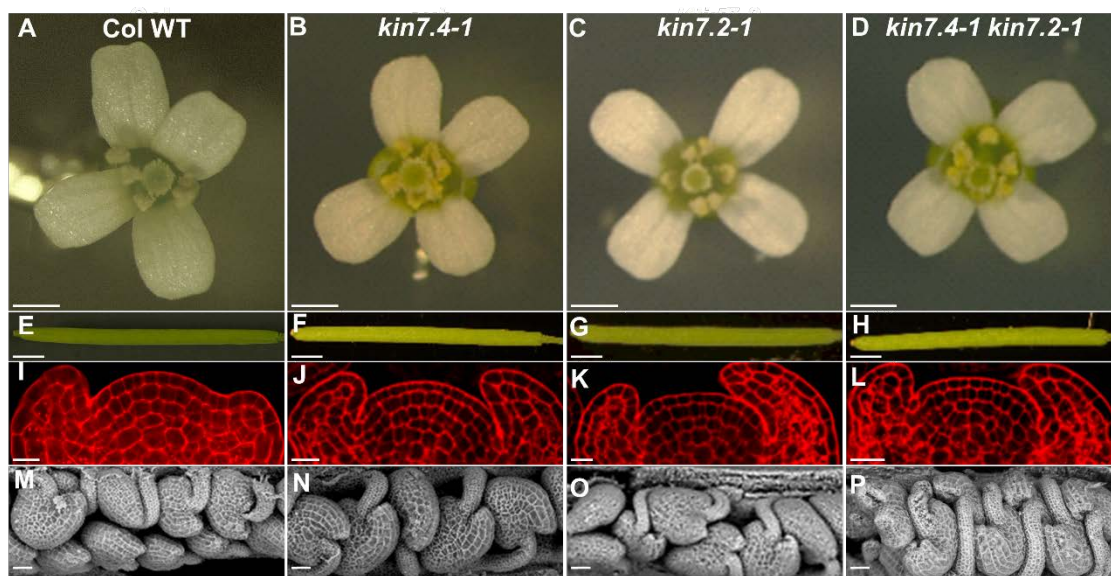


Figure 31. Phenotype comparison between Col-0, *kin7.4-1*, *kin7.2-1*, and *kin7.4-1 kin7.2-1*. (A) to (D) Morphology of mature stage 13 or 14 flowers (stages according to (Smyth *et al.*, 1990)) (E) to (H) Morphology of siliques. (I) to (L) Central region of stage 3 floral meristems stained with pseudo-Schiff propidium iodide (mPS-PI). (M) to (P) Scanning electron micrographs of stage 4 ovules (stages according to (Schneitz *et al.*, 1995)) Scale bars: (A) to (D) 0.5 mm, (E) to (H) 1 mm, (I) to (L) 10 μ m. (M) to (P) 50 μ m.

3.5.5.5 Analysis of root hair patterning (RHP) in *kin7*

SUB also regulates root hair cell patterning in Arabidopsis root (Kwak *et al.*, 2005). So in the next step, we set to explore root hair cell arrangement in *kin* mutant background. The nonhair cell-specific marker pGL2:GUS:EGFP (Lin and Schiefelbein, 2001; Gao *et al.*, 2019) were introduced into all single and double *kin* mutants by genetic crossing. Homozygous mutant plants harboring root hair cell patterning (RHP) marker were screen by genotyping PCR using primer spanning through GUS-EGFP and then further propagated. For RHP analysis seeds were grown on square plate with half-strength MS medium supplemented with 1% sucrose in continuous light for 5 days. Seedlings were stained with plasma membrane marker dye FM4-64 (4 μ m) for 10 min. Image of the meristematic zone of root was acquired with CLSM using 20x objective lens. For each line minimum, 15 roots were analyzed, the representative image is shown here (Figure 32). As expected, Col WT roots showed very distinct and defined expression pattern of EGFP in the non root hair cells. Although occasionally few hair cells also showed EGFP expression. On contrary *sub-9* roots were completely devoid of patterning as previously reported by several researchers (Gao *et al.*, 2019; Kwak *et al.*, 2005; Kwak and Schiefelbein,

2008; Jones et al., 2014; Song et al., 2019). *kin7.4* mutants showed similar *sub-9* like mis-patterned expression of EGFP except for *kin7.4-2* (Figure 32 D) probably because in this allele t-DNA insertion is at the very end of C' terminus tail domain. The *kin7.4-1* showed expression pattern defect of EGFP. Several non EGFP expressing cells could be observed in between two continuous line EGFP expressing non root hair cells wherever neighboring root hair cells also showed EGFP signal. Since *kin7.4-1* is also a knockdown mutant and probably able to make truncated protein that could be partially active. There has been previous report where motor domain alone is sufficient for its wildtype function (Rice et al., 1999; Moschou et al., 2016; Ganguly et al., 2017; Popchok et al., 2017; De Keijzer et al., 2017). To analyze RHP in *kin7.4* null mutant pGL2:GUS-EGFP marker was introduced into *kin7.4-3 sub-9* CRISPR Cas generated double mutant by crossing into *kin7.4-1* pGL2:GUS-EGFP line. In heterozygous situation neither *sub-9* nor *kin7.4-1* showed RHP defect (figure not shown). However F1 population (17 roots) *kin7.4-1^{+/-} kin7.4-3^{+/-} sub-9^{+/-}* showed strong root hair cell patterning defect (Figure 32 E). All the 17 roots observed show very similar mis patterning of EGFP expression in epidermal cell profile of root meristematic zone. To find genetic interaction between *SUB* and *KIN 7.4* double mutants for root hair patterning *sub-9 kin7.4-1* and *sub-9 kin7.4-2* double mutants were also analyzed. I did not observe any visual difference in comparison to the *sub-9* RHP defect in (Figure 32 F) although EGFP expression pattern in *sub-9 kin7.4-1* appears to be less affected and similar to *kin7.4-1* single mutant. But in the case of *sub-9 kin7.4-2* expression pattern of EGFP stayed as *sub-9* (Figure 32 G). It suggests *sub-9* is epistatic for root hair patterning in *kin7.4-2 sub-9* double mutant. For precise

inference of genetic interaction more detailed microscopic analysis of root hair patterning in all genetic backgrounds needs to be analyzed.

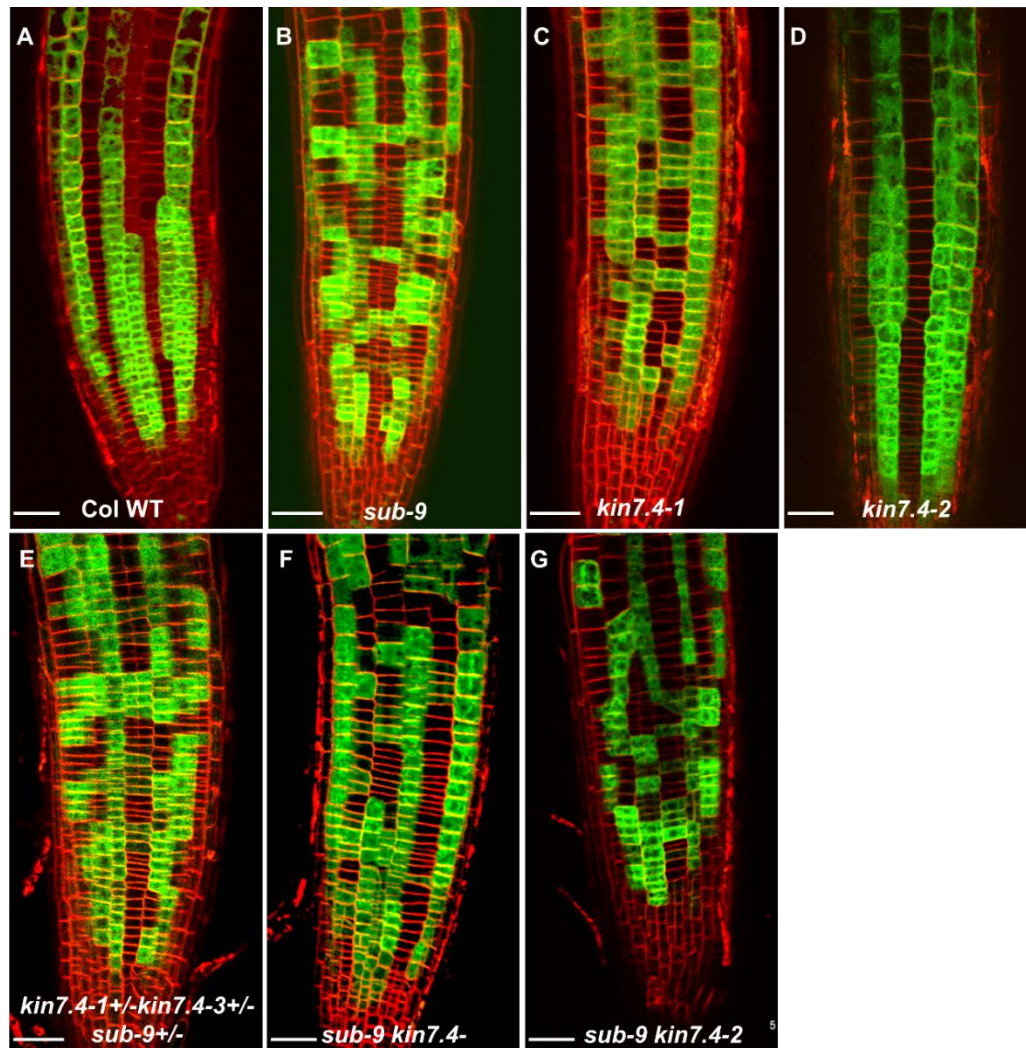


Figure 32. Expression pattern of pGL2::GUS:EGFP in Col wild-type, *sub-9*, *kin7.4-1*, *kin7.4-2*, *kin7.4-1+/- kin7.4-3+/- sub-9+/-*, *sub-9 kin7.4-1* and *sub-9 kin7.4-2* mutants. Note the straight line expression pattern of reporter in Col (A) and *kin7.4-2* (D). The irregular expression pattern of reporter in *sub-9* (B), *kin7.4-1* and in double mutants (E,F, and G). Minimum 15 roots were analyzed per genotype. Scale bar: (A) to (G) 20 μ m.

Interestingly *Kin7.2* mutants do not show any defect in the expression pattern of RHP maker (Figure 33 B, C). Both mutant allele *kin7.2-1* and *kin7.2-2* show very similar wild type like an expression of EGFP in epidermal cell profile of root.

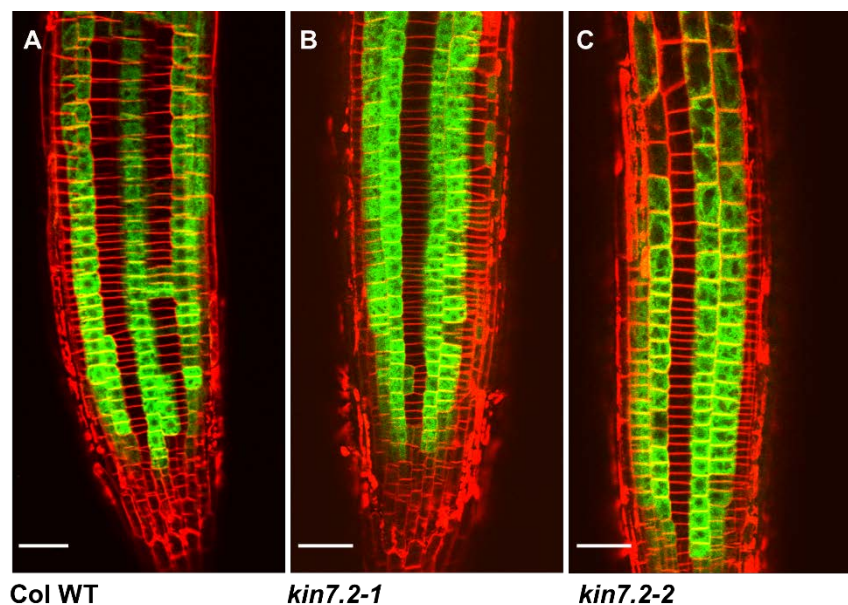


Figure 33. Expression pattern of pGL2::GUS:EGFP in wild-type, *kin7.1-1*, and *kin7.2-2* mutants. Confocal micrograph depicting rescue of root hair patterning in *kin7.1-1* (B) and *kin7.2-2* (C). Minimum 15 roots were analyzed per genotype. Scale bar: (A) to (C) 20 μ m.

3.5.6 Complementation of *kin7.4* mutant phenotype

To determine the root hair patterning defect seen in the *kin7.4-1* mutant is a consequence of the loss of *KIN7.4* function, I transformed a wild-type copy of the *KIN7.4* into the homozygous mutants and tested for complementation of the phenotype. The root hair patterning defect was fully rescued in 11/18 transformants in the *kin7.4-1* background (Figure 34) while 5/18 transformants show partial rescue with the occasional mis expression pattern of EGFP. Two transformants lines failed to rescue RHP defect in *kin7.4-1*. In these lines, it is possible either transgene got silenced by the host RNAi machinery or t-DNA was integrated partially into the plant genome. The complementation assay was performed only in *kin7.4-1* background for root hair patterning defect and in *sub-9 kin7.4-1* double mutant background for complementation of floral organ phenotype. But transformants in *sub-9 kin7.4-1* have not been carefully analyzed yet. Although cursory observation of T1 transformants showed twisted silique that otherwise appears straight in *sub-9 kin7.4-1* background. It suggests *KIN7.4* also complement floral organ defects. The *kin7.4-2* was omitted from the complementation experiment because it does not show any observable morphological defect.

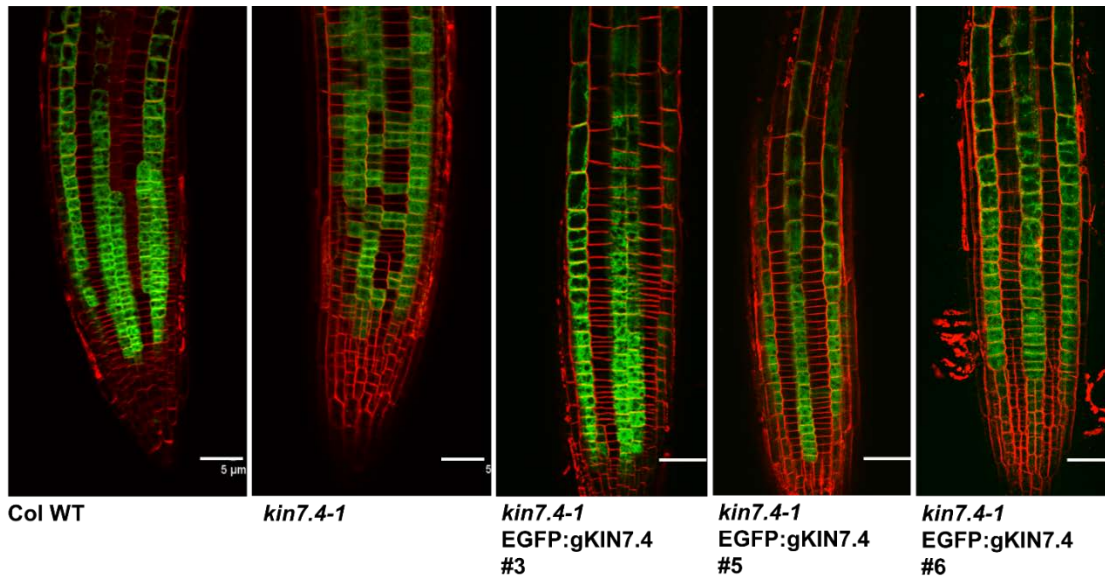


Figure 34. Complementation of *kin7.4*pGL2::GUS:EGFP with pKIN7.4::EGFP:gKIN7.4
Confocal micrograph depicting rescue of root hair patterning defect in *kin7.4-1* (B) in three independent complemented lines (C, D, E). Minimum 15 roots were analyzed per genotype. Scale bar: (A) to (E) 20 μm.

3.5.7 Subcellular distribution of EGFP:gKIN7.4 fusion protein.

After successful complementation of *kin7.4* mutant phenotype, I explored the subcellular localization of the functional EGFP:KIN7.4 fusion protein. As shown in the previous section *KIN7.4* is expressed in root and its promoter activity has also been observed throughout the root. Moreover, seedlings lacking functional *KIN7.4* showed root hair cell patterning defect in meristematic region of the 5-day old root. In order to investigate the subcellular localization of *KIN7.4*, I used the complemented line for RHP in *kin7.4-1* background harboring pKIN7.4::EGFP:gKIN7.4:tKIN7.4 construct. The root cells were first stained with the membrane marker FM4-64 for 10 mins. FM4-64 shows clear plasma membrane signal with some noticeable vesicle-like foci in cytoplasm (Figure 35 B, F). However EGFP shows more cytoplasmic vesicle-like structure and also distinct punctate pattern percolating or coalescing to the plasma membrane (Kin bodies) that some times colocalize with FM4-64. Interesting cytoplasmic EGFP foci appear to be bigger in size than FM4-64 leveled foci and they abundantly accumulate at the cell periphery (Figure 35 C, D). The cytoplasmic EGFP foci also occasionally

colocalizing with FM4-64 labeled vesicles (Figure 35 C, D, G). Three independent complementing homozygous lines were analyzed with similar observations.

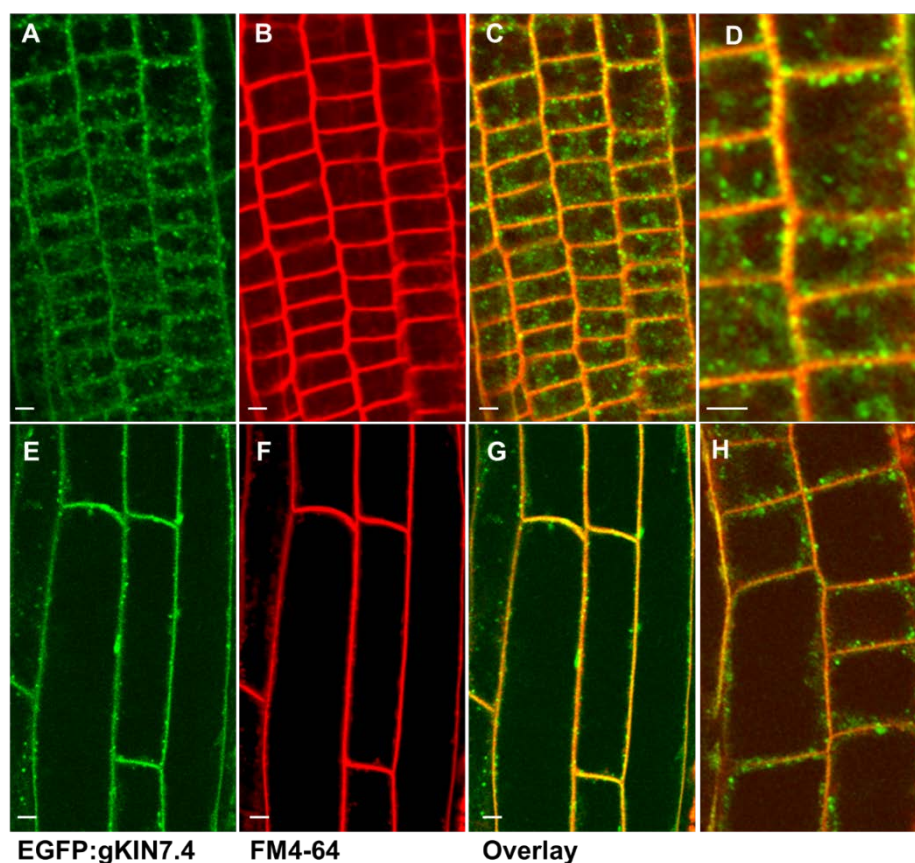


Figure 35. Sub-cellular distribution of EGFP:gKIN7.4 fusion protein in root. Confocal micrographs depicting the subcellular distribution of EGFP:gKIN7.4 fusion proteins under control of the native KIN7.4 promoter. (A) meristematic zone epidermal cell, (E) differentiation zone epidermal cell. (B) FM4-64 co-stained meristematic zone epidermal cell, (F) differentiation zone epidermal cell. (C) overlay of (A and B), (G) overlay of (E and F). (D) higher magnification of the region in (C). Scale bars: 5 μ m.

In the next step, to address possible microtubule localization of EGFP:gKIN7.4, RFP:TUB6 marker line was crossed. The resulting F1 plants were analyzed. The image was acquired using confocal microscope from transition zone root epidermis of the 5-days-old continuous light-grown seedling. The EGFP:gKIN7.4 showed similar cytoplasmic foci as discussed in the previous section (Figure 35 A). The RFP:TUB6 clearly marked transversely oriented microtubule (Figure 36 B). In the merged image panel (Figure 36 C) some EGFP:KIN7.4 foci appeared to colocalize with RFP:TUB6 marked microtubules. This observation is in line with the notion *KIN7.4* is microtubule-binding protein but more corroborative data are required for confirmation. Moreover, time-lapse imaging is also required to assess if *KIN7.4* is mobile kinesin.

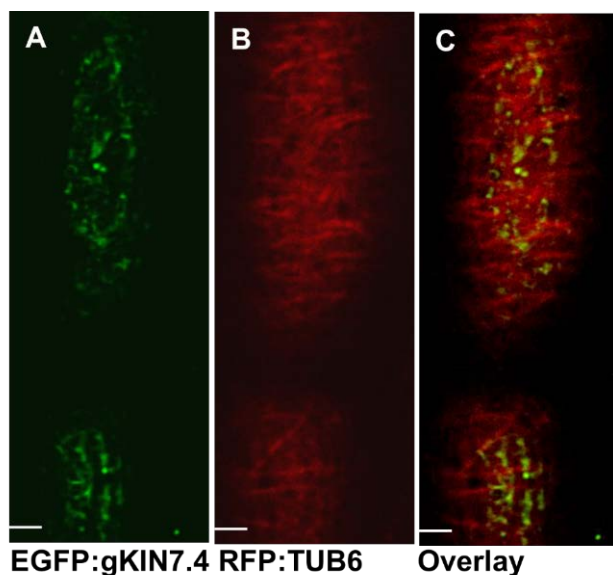


Figure 36. Co-localization of EGFP:gKIN7.4 with RFP-TUB6 in root epidermis cell. Confocal micrographs depicting the CMT decoration of EGFP:gKIN7.4 fusion proteins in root epidermis cell of the elongation zone. Scale bars: 5 μ m.

3.5.8 EGFP:gKIN7.4 is colocalizing with gSUB:mCherry in the root epidermis

KIN7.4 is a genetic component of the *SUB* signaling pathway for root hair patterning in Arabidopsis. Moreover, *KIN7.4* is also localized to the plasma membrane as discussed in the previous section raised the question if *KIN7.4* is also co-localizing with *SUB* at the root epidermis. To this end I crossed transgenic plants expressing pUBQ::SUB:mCherry and pKIN7.4::EGFP:KIN7.4. The resulting F1 population were analyzed using a confocal microscope. The image was acquired from the root epidermis cells in transition and early elongation zone of 5-day old seedlings. The mCherry signal showed the plasma membrane localization of *SUB* (Figure 37 B) as it has been reported in several different independent studies (Chevalier *et al.*, 2005; Vaddepalli *et al.*, 2014, 2017; Gao *et al.*, 2019; Song *et al.*, 2019), although in elongating root epidermis cell plasmodesmata puncta could not be observed very distinctively. However, EGFP:KIN7.4 consistently shows weak plasma membrane signal with the occasional bright spot along membrane and in cytoplasm collectively called “kin bodies” (Figure 37 A). The plasma membrane EGFP:KIN7.4 along with some population of membrane attached kin bodies are colocalizing with SUB:mCherry (Figure 37 C).

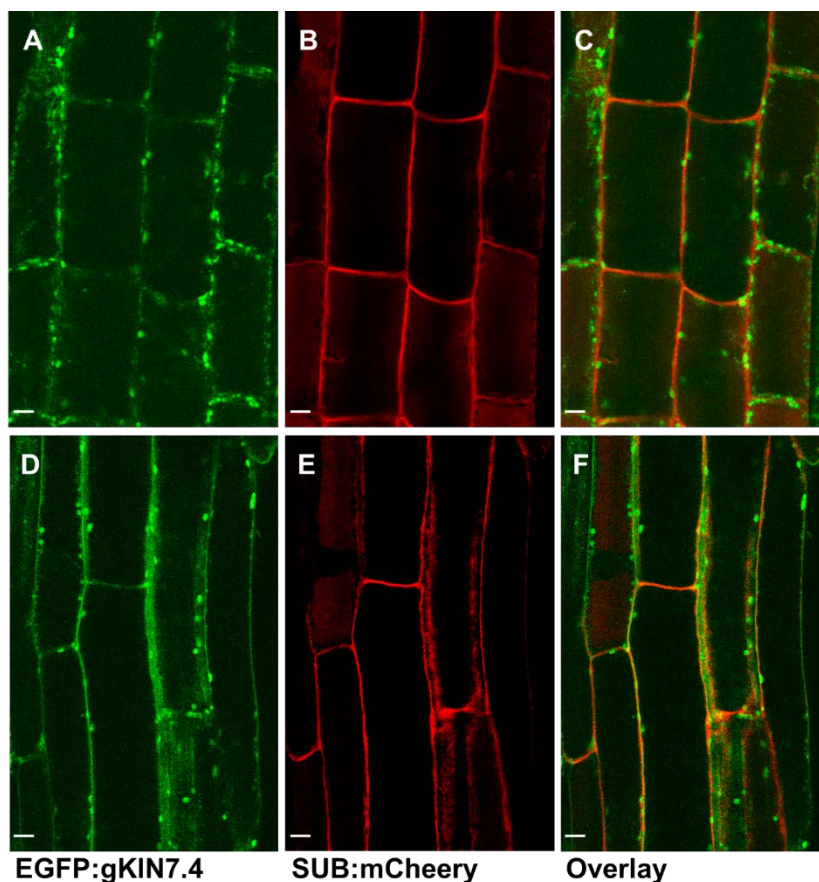


Figure 37. Co-localization of EGFP:gKIN7.4 with mCherry:gSUB in root epidermis cells. Confocal micrographs depicting the colocalization of EGFP:gKIN7.4 with SUB:mCherry (A-C) elongation zone epidermal cell, (D-E) differentiation zone epidermal cell. (C) overlay of (A and B), (F) overlay of (D and E) Scale bars: 5 μ m.

3.5.9 KIN7.4 interacts with SUB in yeast two-hybrid and in vitro

Genetic and molecular analysis so far support that KIN7.4 could be involved in SUB mediated intercellular signaling. To further investigate the direct physical interaction between SUB and KIN7.4 I performed yeast two-hybrid assays. The bait construct expressing the GAL4 DNA-binding domain (GDB) fused to either SUB intracellular domain (DB-SUB-ICD) or full-length KIN7.4 (DB-KIN7.4) or KIN7.2 (DB-KIN7.2). In the next step, the bait construct was tested for interaction with a prey construct expressing the GAL4 AD (GAD) fused to full-length either KIN 7.4 (AD-KIN7.4) or KIN 7.2 (AD-KIN 7.2). Growth of yeast on double drop out selective media was observed for all combination. But on triple drop out selective media yeast did not grow in combination when empty GAD or GDB vector was used. Any yeast growth also could not be observed when SUB-ICD-DB was used with AD-KIN 7.2 (Figure 38) otherwise rest combination grew well. These results indicated that

KIN 7.4 directly interacts with SUB-ICD in yeast. KIN 7.4 and KIN 7.2 also interact with each other and with themselves. So they can form homo and heterodimer in yeast.

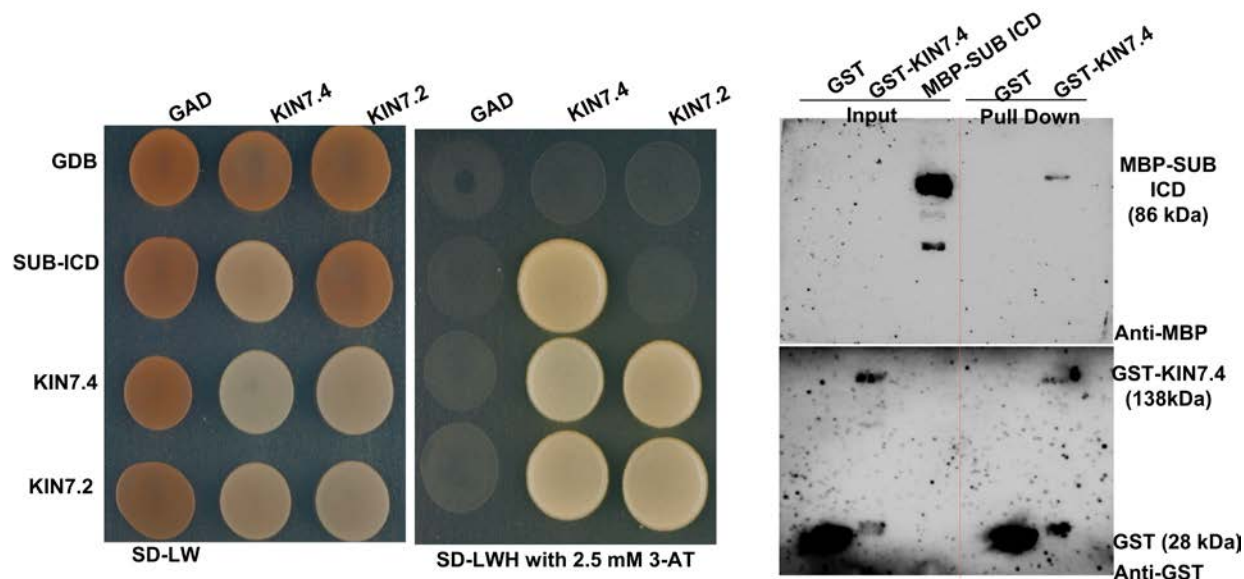


Figure 38. Yeast two-hybrid and in vitro pull-down assay.

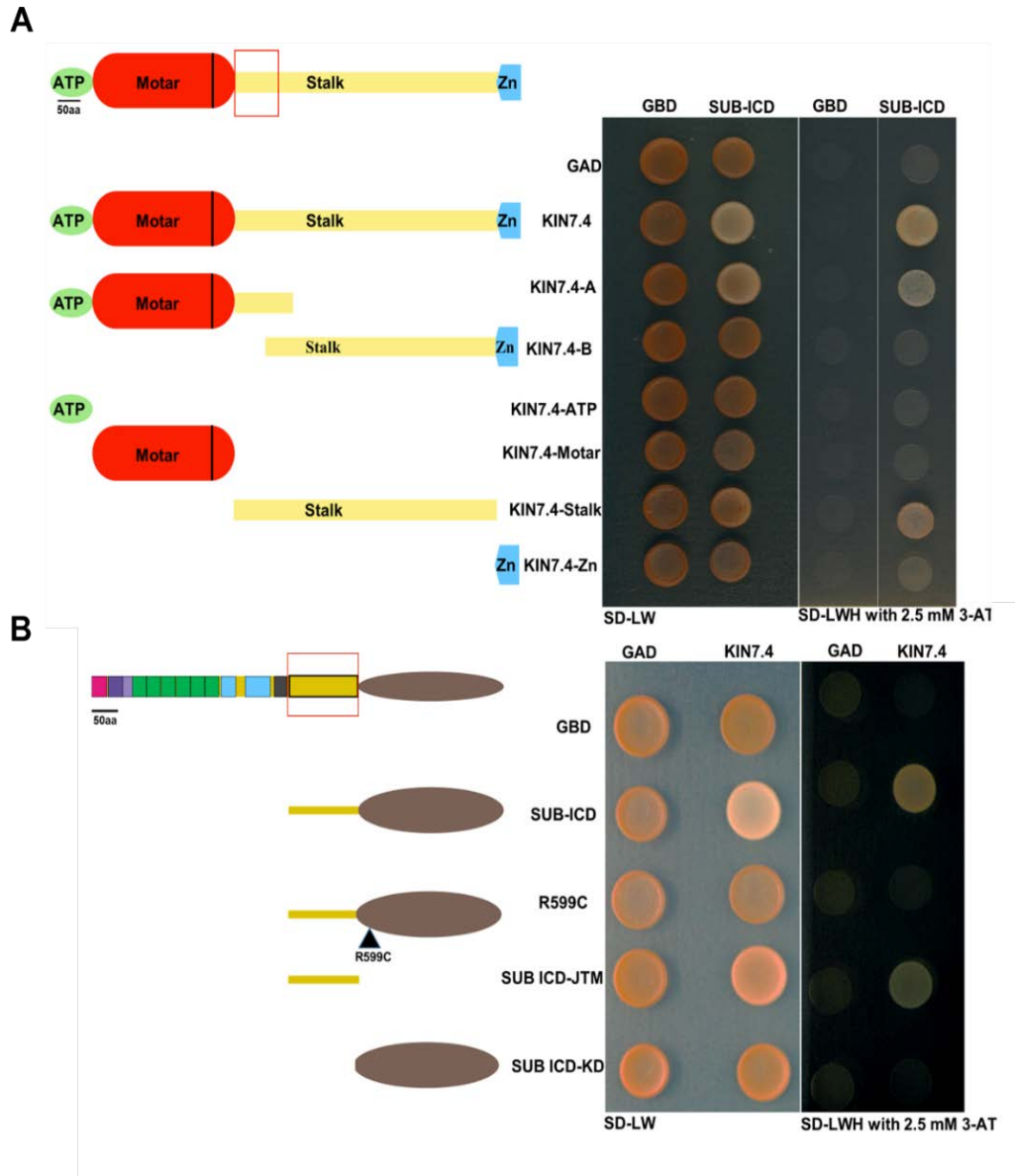
(A) yeast two-hybrid assay, The full-length KIN7.4, KIN7.2, and SUB-ICD were used for yeast-two-hybrid. Growth on -LW panel indicates successful transformation of both plasmids and on -LWH panel indicates presence or absence of interaction. Empty vectors, GAD and GBD, were used as negative controls. (B) in vitro pull-down assay.

In next step, to confirm the interaction between KIN 7.4 and SUB-ICD I also performed in vitro pull-down assay together with Andrea Bayer (Bachelor student). For pull-down assay GST, GST-KIN 7.4, and MBP-SUB-ICD recombinant proteins were expressed and purified from *E.Coli* and an estimated 100ug of each protein was used for the assay. After pull-down assay, the resulting proteins were subject to western blot (WB). The blot was first probed anti-MBP antibody and developed in phospho-imager using ECL solution. In second step, after treating with mild alkaline stripping buffer same blot was again probed with anti-GST antibody. On western blot, all proteins were detected though MBP- SUB, and GST-KIN7.4 show some additional bands of degraded protein with lower molecular weight (Figure 38). Moreover input panel also confirms specificity of both antibodies as they do not cross-react. However in the pull-down MBP-SUB-ICD was only detected when used together with GST-KIN7.4. I did not observe a corresponding band to MBP-SUB-ICD in GST control. Consistent with the yeast two-hybrid results, I could show MBP-SUB-ICD was pulled down by GST-KIN7.4

(Figure 38). However an important input control to show there is no nonspecific binding of MBP-SUB-ICD with GST is lacking. So more confirmation is required.

3.5.10 Mapping of protein domains involved in the SUB-ICD and KIN7.4 interaction

To examine which protein domains of KIN7.4 and SUB- ICD are critical for the interaction, I performed yeast two-hybrid assays. I fused the full-length or different truncations of SUB-ICD (Figure 39) to the Gal4-DNA binding domain to generate bait vectors and full-length KIN7.4 or truncated version to the GAL4 activation domain to generate the prey vector. Y2H assays indicated that full-length SUB-ICD interacts with full-length KIN7.4 as it was discussed in the previous section. Interestingly, deletion of the Kinase domain (SUB-ICD-KD) does not affect this interaction (Figure 39), whereas a point mutation in the kinase domain (R599C) eliminated the interaction between SUB-ICD and KIN7.4 (Figure 39). These results support the notion that the juxta membrane domain (SUB-ICD-JTM) is involved in its interaction with KIN7.4. Similarly, to determine which protein domain of KIN7.4 is responsible for its interaction with SUB-ICD, I divided the KIN7.4 into its individual domain and into two equal halves Kin7.4-A and Kin7.4-B with 50 amino acid overlapping in middle region (Figure 39). The result indicates that 59 amino acid region of stalk domain close to motor domain is necessary for interaction in yeast cells (Figure 39).



4 Discussion

In previous work, *SUB* was shown to be important for tissue morphogenesis in Arabidopsis. It regulates several developmental processes, including floral morphogenesis, integument outgrowth, leaf development, and root hair patterning (Chevalier *et al.*, 2005; Kwak *et al.*, 2005; Lin *et al.*, 2012). *SUB* signaling genetic component *ZERZAUST* (*ZET*), encoding a predicted cell wall-localized β -1,3 glucanase, to be involved in *SUB* signal transduction (Fulton *et al.*, 2009; Vaddepalli *et al.*, 2017). Moreover, the whole-genome transcriptomic analysis revealed that many genes responsive to *SUB*-mediated signal transduction relate to cell wall remodeling (Fulton *et al.*, 2009) and *sub*, *qky* and *zet* mutants share overlapping defects in cell wall biochemistry (Vaddepalli *et al.*, 2017). Thus, apart from functionally connecting RK-mediated signal transduction and PD-dependent cell-cell communication *SUB*-signaling also relates to cell wall biology. In the present study, I explored the connection between the cell wall and the *SUB* signaling.

4.1 *SUB* participates in the response to changes cell wall

The data provided in this work establishes a novel role for *SUB* in cell wall stress signaling. The cell wall stress in this study is induced by a reduction in cellulose biosynthesis, a major carbohydrate component of the cell wall. Cell wall biosynthesis inhibition is achieved by the application of several known pharmacological agents for example isoxaben, DCB and thaxtomin A. The cell wall modification including remodeling and fortification during plant development and stress responses which relies on complex and largely unknown signaling pathways (Hamann, 2015; Sampathkumar *et al.*, 2014; Voxeur and Höfte, 2016; Wolf, 2017). To present date only a few cell surface receptor kinases, including *THE1*, *MIK2*, and *FEI2*, have shown to play an important role in CBI-induced cell wall damage response like ectopic lignification, callose, and phytohormone JA, SA accumulation (Engelsdorf *et al.*, 2018; Gonneau *et al.*, 2018; Hématy *et al.*, 2007; Van der Does *et al.*, 2017). Thus, data provided here establishes *SUB* signal transduction as a new component in the molecular framework mediating the CWD response due to CBI.

Role of ROS in cell wall signaling has been long implicated, upon the perception of cell wall perturbation by cell surface receptors, simultaneously activates *NADPH/RESPIRATORY BURST OXIDASES* and thereby the production of ROS. Previous work on cellular response to isoxaben-induced CWD response revealed ROS production and the detected ROS response depended on *NADPH/RBOHD*, *RBOHF*, and *THE1* (Hamann *et al.*, 2009; Denness *et al.*, 2011). Denness et al have

detected ROS production in luminol-based time-course assays involving entire seedlings. ROS production could be detected after around three to four hours following the application of isoxaben (Denness *et al.*, 2011). Using a confocal microscope-based method enabling tissue-level resolution, I could show that fluorescence of the ROS probe H₂CDFDA in the root meristem becomes detectable within 30 minutes of treatment. The obtained data indicate that *SUB* affects the early ROS production response to isoxaben-induced CWD. In this experiment, I have shown for the first time the isoxaben-dependent change in H₂CDFDA fluorescence signal in root meristem cell. It represents the earliest available marker of the isoxaben-induced CWD response so far and indicates that the response occurs much earlier than has previously been appreciated. The transcript analysis of defense marker gene in presence of isoxaben suggest that *SUB* is required for full induction of *CCR1*, *PDF1.2*, or *TCH4*. Additionally, the data also indicate that *SUB* plays a central role in the promotion of CBI-induced accumulation of lignin and callose. Thus *SUB* specifically promotes cell wall remodeling upon CBI.

Interestingly, *SUB* basically becomes irrelevant for these canonical CBI stress responses upon application of sorbitol in addition to isoxaben. This observation suggests that *SUB* mediates an osmosensitive cell wall stress response. The notion had been culminating among plant stress biologist that a mechanical stimulus initiates the CBI induced CWD response, associated with a weakening of the cellulose framework. It could result in a stretching of the plasma membrane relative to the cell wall (Kohorn *et al.*, 2006; Engelsdorf and Hamann, 2014; Haswell and Verslues, 2015; Nissen *et al.*, 2016; Engelsdorf *et al.*, 2018). Taken together I speculate that *SUB* signaling might involve as yet unknown mechano-sensitive factors. The obtained results together meet the criteria that have been established for a CBI-induced CWD response (Engelsdorf *et al.*, 2018; Hamann *et al.*, 2009).

Interestingly, for lignin and callose accumulation upon isoxaben treatment *sub*-loss-of-function mutants (*sub-1*, *sub-9*, and *sub-21*) and gain-of-function (*pUBQ::SUB:mCherry*) mutants showed reciprocal effects. The *sub* mutants showed less lignin and callose accumulation whereas the several independent *pUBQ::SUB:mCherry* lines showed higher levels of lignin or callose accumulation, respectively upon application of isoxaben. So on the basis of genetic evidence presented here, I put forward the model that *SUB* represents an important regulator of isoxaben-induced lignin and callose accumulation and thus cell wall composition.

4.1.1 *SUB* is required for tissue morphogenesis in cellulose deficient condition

Data shown here clearly demonstrate that *SUB* plays a biologically relevant role in CWD signaling activated in cellulose deficiency. In the first line of support, I showed that *SUB* attenuates isoxaben-induced cell bulging in the epidermal cells of the meristem-transition zone boundary of the root. In second evidence, *SUB* promotes root growth recovery upon transient exposure of seedlings to isoxaben. The third data where *SUB* has been shown involved in root growth inhibition that is a consequence of a genetic reduction of cellulose content. In precise, root length of *sub-9 prc1-1* double mutant seedlings is less reduced in comparison to the root length of *prc1-1* single mutant seedlings. Collectively, the data shown here support the idea that *SUB* plays a central role in CBI-induced CWD signaling.

4.1.2 The relation of *SUB* to *THE1* and *MIK2*

Next question is the relative of *SUB* mediated cell wall signaling to other known RK genes contributing to the response of CBI-induced cell wall stress, such as *THE1* and *MIK2*. Comparing our result of *SUB* mediated cell response upon isoxaben treatment with published reports on other cell wall sensors, I found overlapping but also distinct function. *SUB*, *THE1*, and *MIK2* all promote isoxaben-induced ectopic lignin production. The three genes are also required for full induction of certain stress marker genes. However, my data indicate that *SUB* is not required for the induction of *FRK1* and *CYP81F2* genes, while *THE1* and *MIK2* control *FRK1* expression, and *MIK2* also affect the expression of *CYP81F2* (Van der Does *et al.*, 2017). I did not observe any effect of *THE1* on root growth recovery. In addition, I also did not observe altered hypocotyl length of *sub-9 prc1-1* in contrast to *the1-1* suggesting that *SUB* does not affect hypocotyl growth inhibition in etiolated *prc1-1* seedlings, whereas *THE1* is reported on several occasions to inhibit hypocotyl growth in *prc1-1* (Hématy *et al.*, 2007). Interestingly, our data on root growth suggest that *SUB* contributes to root growth inhibition in *prc1-1*. But our evidence does not support a function for *THE1* in this process. The root length of *the1-1 prc1-1* double mutants did not deviate from the root length observed for *prc1-1* single mutants. Finally, I also did not observe the left-ward root skewing in *sub* seedlings that is characteristic of *mik2* mutants (Van der Does *et al.*, 2017). Hence data provided here suggest that *SUB* has both overlapping but also distinct functions with *THE1* and *MIK2*. As the most parsimonious explanation, I propose that *SUB* contributes to CBI-induced cell wall stress signaling in a pathway that is separate from *THE1* and *MIK2* signaling.

4.2 Isoxaben treatment results in *SUB* downregulation

Surprisingly, the data presented here also reveals a negative effect of inhibition of cellulose biosynthesis on *SUB* mediated tissue morphogenesis pathways, such as floral morphogenesis, ovule development, and root hair patterning. During the experiment, I observed that the application of sub-lethal concentrations of isoxaben to wild-type plants results in a *sub*-like phenocopy in a dose-dependent manner. Upon 600 nM isoxaben treatment in seedlings I noticed reduced SUB:EGFP reporter signal and decrease in reporter signal intensity starts at 5hour after treatment. We also observed a reduction in endogenous *SUB* mRNA and *QKY* levels indicating that isoxaben-induced CWD eventually results in the transcriptional downregulation of *SUB* and *QKY*. This observation raises speculation if the *sub*-like defects upon isoxaben treatment are indeed the result of downregulated *SUB* activity in that case ectopic expression of *SUB* should counteract the effect. I observed that ectopic expression of *SUB* attenuates the detrimental effects of isoxaben on root hair patterning and floral morphogenesis as revealed by the much-reduced phenotypes of two independent pUBQ::*SUB*:mCherry lines exposed to similar concentrations of isoxaben than wild-type plants. The obtained result suggests that the noticed developmental *sub*-like defects are caused by the downregulation of *SUB* activity. However, it also raises the question of why the ectopic expression of the only *SUB* counteracts the developmental effects of isoxaben when *SUB* and *QKY* both are subjected to downregulation. By considering two findings into account this conundrum can be explained. First, it has been shown that *QKY* function can be bypassed by increasing gene dosage of *SUB* as *qky* mutants carrying a pSUB::*SUB*:EGFP reporter show much weaker floral phenotypes (Vaddepalli *et al.*, 2014). Second, the applied isoxaben dose did not lead to a complete depletion of *QKY* transcripts. I propose that ectopic expression of *SUB* also bypasses the requirement for developmental *QKY* activity during isoxaben-induced CWD stress.

4.3 Novel Candidate factors of the *SUB* signaling pathway

In our quest to elucidate up and downstream candidate members of the *SUB* signaling pathway, I found some interesting candidate. In the list of putative candidates we had several cell surface receptor-like kinases, for example, *WAK2*, *BIR1*, *LRR1*, and *PRK1* that have been reported to involve in tissue morphogenesis. In the phenotypic analysis, I could not observe any floral organ defect in *wak2*, *bir1*, *lrr1*, and *prk1* t-DNA insertion lines. Moreover, they also do not affect *sub-9* phenotype in double mutant combination. In part, it could be because the t-DNA insertions are not in the coding region for *bir1*, *lrr1*, and *prk1*. Another explanation is that homolog of these candidate genes might be acting

redundantly. Although in light of the newfound role of *SUB* signaling pathway these genes might be working in CWD response. It will be interesting in the future to explore the function of these genes in CBI induced CWD response.

For *WAKs* however, I could not observe any phenotypic alterations in floral organs for *wak2-12*, *wak3-1*. In double mutants interestingly *wak3-1 sub-9* but not *wak2-12 sub-9* showed wild type flowers, ovules and floral meristems contrary to *sub-9* defective flowers and ovules. *WAKs* have been shown to be involved in cellular responses to various biotic and abiotic stress (He *et al.*, 1999; Kohorn and Kohorn, 2012). My data first time revealed that the involvement of *WAK3* in floral organ morphogenesis and it also suggests that although *WAKs* are highly similar, there is functional distinction among them. However, to make any concrete conclusion more functional analysis is required. It is tantalizing to hypothesize the scenario where *SUB* is acting as the central regulator of *WAKs* function in a context-dependent process.

In the compiled list of candidate genes, we had two microtubule-binding proteins *TOR1* and *KIN7.4*. *TOR1* is involved in stabilizing microtubule (Buschmann *et al.*, 2004) and mutant plant, lacking functional *TOR1* protein show anticlockwise stem and petiole twisting (Buschmann *et al.*, 2004; Wightman *et al.*, 2013). All *tor* mutant show anticlockwise twisting in petiole organization and did not show any *sub* like floral organ phenotype. In double mutants, *sub* floral organ phenotype was not altered but the plant was showing ameliorated anticlockwise twisting. It suggests *sub* is epistatic to *tor1* for petiole twisting. The yeast two-hybrid interaction data suggest *SUB* interacts with *TOR1*. With limited data available here it is difficult to speculate further about possible mechanism of *SUB* and *TOR1* interaction in plants.

4.4 SUB signaling regulates microtubule organization

In previous research *SUB* signaling pathway mutants *sub-1*, *qky-8*, and *zet-1* have been shown with altered cell wall biochemistry (Vaddepalli *et al.*, 2017). It is a canonical belief that the cytoskeleton and cell wall correspond to each other. Cortical microtubules have been shown to respond to changes in cell wall defects (Hamant *et al.*, 2008). It has also been shown that treatment of isoxaben ultimately leads to a change in microtubule orientation (Panteris *et al.*, 2013, 2014). In *qky* mutant background mis oriented microtubule has already been shown in carpel wall (Trehin *et al.*, 2013). Taking all previous studies into consideration, *sub* mutants were expected to exhibit microtubule defect. In my analysis, the first observation was that root epidermis cells of different zone had different CMT

orientation. The root cap cells of WT shows mostly transverse orientation to the longitudinal wall of cell. While epidermal cell of early meristematic zone shows radial patterning with occasional preprophase band and mitotic spindle. However, MTs in transition zone were aligned transversally to the longitudinal axis of root. These observations were in line with previous studies (Panteris *et al.*, 2014). In *sub* mutants, I did not observe any major change CMT orientation of the root cap in comparison to wild type and it was expected because *SUB* does not express in root cap cells. Interestingly, *sub* mutants showed CMT orientation defect in epidermal cells of transition zone. CMTs were randomly organized in the *sub* mutants in contrast to transversely organized CMTs in WT. Since *SUB* is strongly expressed in meristematic zone, so it is plausible to propose that *SUB* is involved in maintaining CMT orientation in tissue specific manner. There are few possibilities to correlate *SUB* with microtubule, first *SUB* could directly interact with microtubule to provide tethering with PM. The second possibility is that some of the unknown *SUB* signaling factors may be bridging *SUB* with microtubule, for example, TOR1, and KIN7.4. The third possibility is CMT defect in *sub* mutants could be an indirect consequence of altered cell wall biochemistry. In conclusion, the data presented shows that *sub* mutant has altered microtubule orientation in root epidermis cell. This result may correlate with hypersensitivity of *sub* mutant to isoxaben induced root bulging.

4.5 Characterization of KINESIN 7.4

4.5.1 In silico analysis of KIN7.4 and KIN7.2

In silico analysis based on homology modeling revealed that KIN7.4 contains all conserved domain structure known for a functional kinesin in Arabidopsis. KIN 7.4 contains all four necessary Motor, neck, coiled-coil stalk, and tail domain required for a functional plant motor protein suggesting a vital role in plant morphogenesis. The presence of motor domain at N' terminus along with additional ATP binding domain raises speculation if it is conventionally involved in anterograde transport. The C-terminus tail domain contains globular cargo binding domain which is known to binds with cargo (Vale, 2003) in animal system. The middle stalk domain is most likely to be involved in the regulation of its function by dimer formation. The coiled-coil domains which connect the motor and tail domains are known to involve in autoinhibition activity. In earlier reports, the coiled-coil domain also has been reported for helping kinesin to make a functional dimeric form (Ganguly and Dixit, 2015). The neck is important for transmitting the conformational change in the catalytic site during movement of kinesin (Sablin *et al.*, 1998; Rice *et al.*, 1999).

The phylogenetic analysis of *KIN7.4* using motor domain sequences placed *KIN7.4* into group 7 of the Kinesin superfamily. CENP-E is a founding member of group 7 and involved maintaining microtubule dynamics during various stages of the cell cycle in animal (Sardar *et al.*, 2010). Group 7 has four more members *KIN7.1*, *KIN7.2*, *KIN7.3*, and *KIN7.5* in Arabidopsis. The *KIN7.1*, *KIN7.3* and *KIN7.5* genes are involved in the establishment of cell polarity in Arabidopsis (Moschou *et al.*, 2016). Data provided in the thesis suggests functions of *KIN7.4* is positive regulator of root hair patterning, however we could not address the functional role of *KIN7.2*. Since in phylogenetic tree *KIN7.4* and *KIN7.2* shares the same branching point with rest of group members. In ClustalW analysis I found that *KIN7.4* is more than 75% identical to *KIN7.2* at amino acid level. As expected motor domain of both proteins shows more than 90% similarity. But surprisingly C' terminus cargo binding domain of both proteins also show very similar sequence identity. It suggests they could be involved in very similar cargo transport. However in N' terminus ATP binding domain, *KIN7.2* has some additional amino acid and sequence identity is less than 50%. Similarly the stalk also has some sporadic region on with dissimilar or some additional amino acid sequences in both kinesin.

4.5.2 Expression analysis of *KIN7.4* and *KIN7.2*

The expression analysis of *KIN7.4* and *SUB* using Klepikova atlas (Kilian *et al.*, 2007; Klepikova *et al.*, 2016) revealed that *KIN7.4* gene has specific expression pattern during plant development and co-expressed with *SUB*. Moreover, the expression data also indicate the antagonist relationship between *SUB* and *KIN7.4* transcripts during floral organ development. Additionally, the *KIN7.2* shows stronger transcript expression level throughout all floral developmental stages except in shoot apical meristem where it is absent. My study of transcript expression analysis was also complemented with another method. In the second approach, the quantitative analysis of absolute expression normalized to median of ratio suggests relatively higher abundance of *SUB* transcript in carpel and inflorescence meristem tissue. The similar observation has been reported for *SUB* using in situ hybridization method (Chevalier *et al.*, 2005) and thus provides strong support to expression database TreVA. The qRT-PCR analysis data revealed that there is no significant change in transcript level in the *sub-9* background.

The *KIN7.4* promoter activity analysis indicates the spatial pattern of *KIN7.4* expression. The promoter-reporter transgenic line showed a relatively strong signal in root cap, but surprisingly epidermis cell of early meristematic region shows very weak but noticeable reporter signal. However vascular cells show prominent signal in meristematic zone. The most prominent signal was observed in maturation and differentiation zone of root. The data reveals that *KIN7.4* promoter is active in root,

stronger activity is observed in later part of root. In wholesome the expression analysis suggest that *SUB* may not be involved in transcriptional regulation of *KIN7.4*. However, there is overlap in expression pattern at various developmental stages.

4.5.3 Analysis of floral organ morphology of *kin7.4* and *kin7.2* mutant alleles

To analyze the role of *KIN7.4* in floral organ development two independent t-DNA insertion lines were examined. In my analysis I could not observe any *sub-9* like floral organ defect in *kin7.4-1* and *kin7.4-2* single mutant. Both *kin7.4* alleles showed no above-ground phenotypic defect and were almost indistinguishable from Col WT plant. Interestingly, *sub-9 kin7.4-1* double mutant showed rescue of *sub-9* floral organ defect. However, CRISPR Cas generated null mutants *kin7.4-3* and *kin7.4-4* did not show rescue of *sub* floral organ defect in double mutant combination. This observation led us to speculate that *kin7.4-1* might be acting as a dominant-negative form of *KIN7.4*. If it is the case then ectopic expression of truncated form of *KIN7.4* mimicking *kin7.4-1* should result in *sub* like floral organ defect. But in the absence of further data we have to limit our speculation. In conclusion, our data suggest *KIN7.4* either does not participate in floral organ morphogenesis or its homolog *KIN7.2* participate in floral organ redundantly in absence of *KIN7.4*.

The phenotypic analysis of floral organ from *kin7.2* revealed that the *kin7.2-1* and *kin7.2-2* mutants also did not exhibit any *sub-9* like floral organ phenotype. Moreover, in contrast to *kin7.4-1* double mutant of *kin7.2-1 sub-9* did not show rescue of *sub-9* floral organ phenotype. So far it is obvious from our data that knocking out activity of any *KIN7.4* or *KIN7.2* alone does not interfere with floral organ morphogenesis. Analysis of *kin7.4-1 kin7.2-1* double mutant again did not yield into any *sub-9* floral organ defect. All the allelic combinatorial double mutants showed very similar phenotype. These double mutant did not deviate from wild type growth appearance including plant. Data presented here suggest that *KIN7.4* and *KIN7.2* do not participate in floral organ morphogenesis in natural growth condition. Albeit it can not be completely eliminated if they participate in yet to discover context-dependent pathway or if they exhibit microscopic phenotype that we failed to score.

4.5.4 Role of *KIN7.4* and *KIN7.2* for root hair cell patterning (RHP)

In order to find if *KIN7.4* and *KIN7.2* are involved in regulating RHP, expression pattern of nonhair cell-specific reporter pGL2:GUS:EGFP signal were analyzed in single and double *kin7.4* and *kin7.2* mutants. The *kin7.4-1* shows expression pattern defect of reporter signal similar to *sub-9* root however

in *kin7.4-2* reporter signal appear to be more wild type like. It is probably because in this allele t-DNA insertion is at the very end of C' terminus tail domain and it is able to make function KIN7.4 protein. In addition trans heterozygous *kin7.4-1^{+/-} kin7.4-3^{+/-} sub-9^{+/-}* all roots (n=17) analysed were showing strong RHP defect where as, in heterozygous situation neither *sub-9* nor *kin7.4-1* showed any RHP defect. With this observation it appears *KIN7.4* does take part in regulating patterning of root hair cells. In double mutant *sub-9 kin7.4-1* and *sub-9 kin7.4-2* reporter signal is equally mis patterned similar to either of *sub-9* or *kin7.4-1* single mutant. I did not observe any enhancement of RHP that suggests both *SUB* and *KIN 7.4* is in similar genetic pathway for root hair cell patterning. At this time point it is difficult to say what is upstream or downstream in genetic order for RHP pathway. Interestingly *Kin7.2* mutants do not show any defection in the expression pattern of RHP marker. Both mutant allele *kin7.2-1* and *kin7.2-2* show very similar wild type like expression of reporter signal epidermal cell profile of root suggest *KIN7.2* does not control root hair patterning.

4.5.5 Genetic complementation of *kin7.4* mutant phenotype

In transgene complementation assay using genomic DNA with its cis-regulatory elements confirms our finding *KIN7.4* is indeed regulating root hair patterning. I notice more than 60 percent *kin7.4-1* mutant plant carrying transgene copy of *KIN7.4* were able to maintain regular expression pattern of non root hair cell reporter signal while 27 percent shows partial rescue. Two transformants lines failed to rescue RHP defect in *kin7.4-1*. In these lines, it is possible either transgene got silenced with host RNAi machinery or t-DNA was integrated into more complex region of genomic DNA of the plant. Complementation assay in *sub-9 kin7.4-1* double mutant background for floral organ phenotype indicate *KIN7.4* is also active in floral organ and providing wild type copy of *KIN7.4* protein would overcome the negative effect of truncated version of the protein. The second T-DNA insertion allele *kin7.4-2* was omitted from complementation assay because it does not show any observable morphological defects.

4.5.6 Subcellular distribution of EGFP: KIN7.4 fusion protein.

The localization study of *KIN7.4* using functional reporter showed the more cytoplasmic vesicle-like structure and also distinct punctate pattern percolating or coalescing to the plasma membrane (Kin bodies) occasionally colocalizing with FM4-64. This observation suggests EGFP:*KIN7.4* is localized at the cell cortex and could be tether to membrane. It also shows cytoplasmic vesicle-like structures. The similar observation has been made for microtubule-associated protein CLASP. The CLASP

protein is enriched at sites of endoplasmic microtubule-cortex attachment and is required for stable EMT tethering and growth into the cell cortex (Le and Ambrose, 2018). Interestingly cytoplasmic EGFP foci appear to be bigger in size than FM4-64 leveled foci and they are abundantly accumulated at the cell periphery. The cytoplasmic EGFP foci also occasionally colocalizing with FM4-64 leveled vesicles.

In colocalization study using RFP:TUB6 microtubule reporter line, EGFP:gKIN7.4 shows similar cytoplasmic foci as discussed in the previous section. The RFP:TUB6 clearly marked transversely oriented microtubule. In the merged image panel some EGFP:KIN7.4 foci appeared to be colocalized with RFP:TUB6 marked microtubules. This observation is in line with the notion *KIN7.4* is microtubule-binding protein but the more corroborative data is required to put the point firmly. Moreover, time-lapse imaging is also required to assess if *KIN7.4* is mobile kinesin.

4.5.7 EGFP:gKIN7.4 is colocalizing with gSUB:mCherry in the root epidermis

Our data in previous data establishes *KIN7.4* is a genetic component of the *SUB* signaling pathway for root hair patterning in *Arabidopsis*. Moreover, *Kin7.4* is also localized to the plasma membrane as discussed in the previous section. This compelled the idea if *KIN7.4* is also co-localizing to *SUB* in the root epidermis. To explore the idea, then I analyzed transgenic plant co-expressing pUBQ::SUB:mCherry and pKIN7.4::EGFP:KIN7.4 generated through genetic crossing. The mCherry signal shows the plasma membrane localization of *SUB* as it has been reported in several different independent studies (Chevalier *et al.*, 2005; Vaddepalli *et al.*, 2014, 2017; Gao *et al.*, 2019; Song *et al.*, 2019), although in elongating root epidermis cell plasmodesmata puncta could not be observed very distinctively. Additionally EGFP:KIN7.4 consistently shows weak plasma membrane signal with the occasional bright spot along the membrane and in cytoplasm collectively called as kin bodies. An overlay image the plasma membrane EGFP:KIN7.4 along with some population of membrane attached kin bodies were colocalizing with SUB:mCherry.

4.5.8 KIN7.4 interacts with SUB in yeast two-hybrid and in vitro

Genetic and molecular analysis so far support that *KIN7.4* could be involved in *SUB* mediated signaling for tissue morphogenesis in *Arabidopsis*. To further investigate the direct physical interaction between *SUB* and *KIN7.4* targeted yeast-two-hybrid (Y2H) assay was performed. The obtained Y2H results suggest *SUB* intracellular domain interact with *KIN7.4* but not with *KIN7.2*. Moreover, *KIN7.4* and

KIN7.2 interact among themselves making dimer and also with each other. Interaction of KIN7.4 with itself in yeast two-hybrid confirms the idea that KIN works in dimeric form and propels the notion that KIN7.4 would also be working in the dimeric form in plants. The Y2H result could not be confirmed with in-vitro pull-down assay. However, in pull-down assay we could successfully pull out free-floating MBP tagged SUB-ICD from assay buffer using GST tagged KIN7.4 on sepharose bead but not with GST alone bound to sepharose bead. But an important input control to show there is no nonspecific binding of MBP-SUB-ICD with GST is missing. So from our result, it can not be firmly concluded.

4.5.9 Mapping of protein domain involved in SUB-KIN7.4 interaction

Y2H assays indicated that full-length SUB-ICD interacts with full-length KIN7.4 as it was discussed in the previous section. Interestingly for SUB deletion of the Kinase domain (SU-ICD-KD) does not affect this interaction whereas point mutation in the kinase domain (R599C) eliminated the interaction between SUB-ICD and KIN7.4. This observation supports the concept that the interaction with KIN7.4. occur via Juxta membrane domain (SUB-ICD-JTM) and R599C probably interfere with proper protein folding. Similarly, in KIN7.4, 59 amino acid of stalk domain next to motor domain is important for its interaction with SUB-ICD. In light of the previous finding of mechanism of Kin7.4 regulation, our Y2H data suggests that SUB is positively regulating KIN7.4 by interacting with the stalk domain. Stalk domain has been reported to contribute to dimer formation and thus making function KINESIN protein. So one hypothesis could be SUB might regulate dimer formation of KIN by interacting with the stalk domain.

4.6 Working model of SUB signaling pathway

The presented data indicate that *SUB* is mediating multiple pathways involved in development as well as in CWD signaling induced by sub-lethal doses of isoxaben. They also indicate that the CWD response eventually attenuates *SUB* signaling via the transcriptional downregulation of *SUB* and *QKY*. At least two possible scenarios can explain the findings. In the first scenario, *SUB* is downregulated in a quantitative manner by isoxaben-induced CWD signaling. The partial downregulation leaves some remaining *SUB* activity in place. This residual *SUB* activity would be sufficient for further *SUB*-dependent CWD signaling. The scenario assumes that less *SUB* activity is required for CWD signaling in comparison to the function of *SUB* during development. In another plausible scenario, *SUB* activity is required during a restricted time period following the initiation of CWD signaling, for example, to

fully set in motion the stress response. Eventually, however, *SUB* function may become less important or even entirely irrelevant. It will be very interesting to address these issues in future work. Whatever the outcome, the collective data strongly suggest that *SUB*-mediated signal transduction is an important component of the isoxaben-induced CWD response mediating plant survival. At the same time *SUB* activity is subject to control the growth and development versus stress responses.

Furthermore, in developmental pathway my data also support the notion that *SUB* is involved in two distinct tissue-specific processes: control of floral organ morphogenesis and root hair cell patterning. For floral organ development *SUB* is negatively regulating *WAK3* and *CHC 2* while in root cells it promotes activity of *KIN7.4* and *CHC2*.

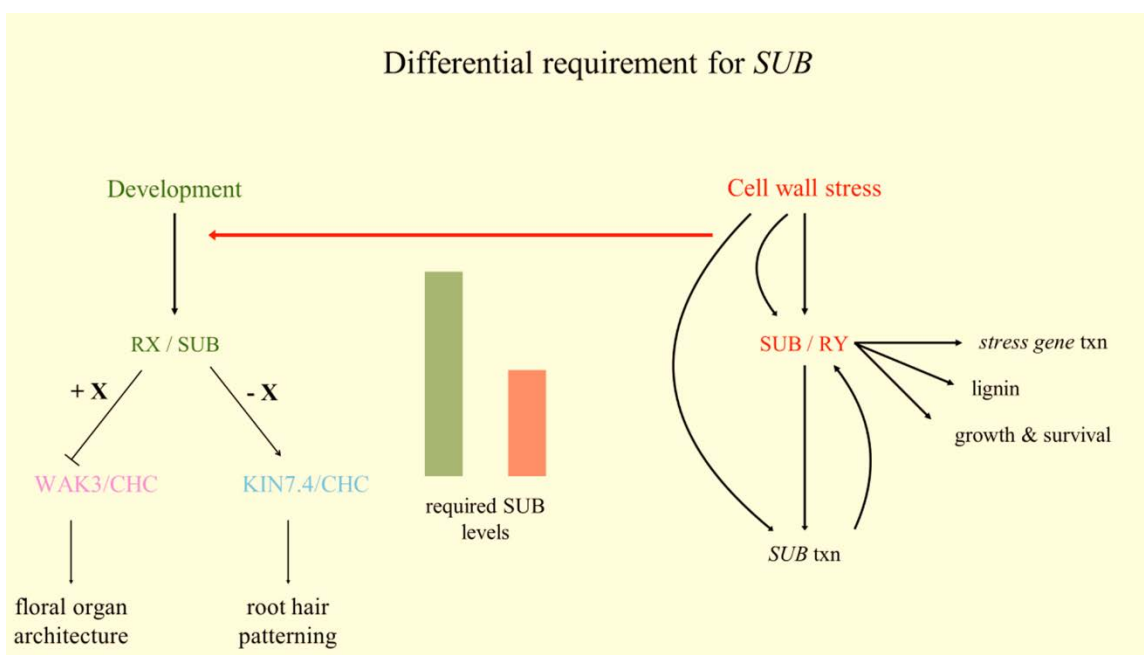


Figure 40. A schematic representation of *SUB* signaling pathway in development and cell wall stress. *SUB* is involved in plant morphogenesis (green) and cell wall stress response (Red). In-plant morphogenesis pathway higher activity of *SUB* is required. Upon cell wall stress, the developmental pathway of *SUB* signaling is closed off by downregulating *SUB* activity. For CWD response a lesser amount of *SUB* is required. For development pathway, In floral organ *WAK3* and *CHC* is negatively regulated whereas in root *SUB* promotes *KIN7.4* and *CHC* for root hair cell patterning.

5 Conclusion

Plant cell wall remodeling is the central aspect of multiple processes required for cell growth and stress responses. For a plant tissue morphogenesis and to cope-up with various biotic and abiotic stresses, the plant cell wall has to be continuously remodeled. To monitor the change in the cell wall architecture a surveillance mechanism exists in the plant. The cell wall monitoring mechanism in return coordinates across cells in growing tissue, for an organ to attain its regular size and shape. Plant pathogens must break through the cell wall thereby generating wall-derived factors that can induce defense responses. There is only limited knowledge regarding the system that monitors the composition and status of the cell wall. In this thesis work, I have provided further insight into cell wall monitoring mechanism.

The data presented here indicate that *SUB* signaling in mediating multiple pathways involved in development as well as in CBI induced CWD responses. The *SUB* is required for ROS, ectopic lignin, and callose accumulation upon isoxaben treatment. The data also indicate that *SUB* promotes transcriptional reprogramming in cellulose deficient condition as optimal induction of several defense marker genes does not occur in *sub* mutant. Further analysis indicates that the CWD response eventually attenuates *SUB* signaling via the transcriptional downregulation of *SUB*. The collective data strongly suggest that *SUB*-mediated signal transduction is an important component of the isoxaben-induced CWD response mediating plant survival. At the same time, *SUB* activity is subject to control that balances growth and development versus stress responses.

In *SUB* mediated plant morphogenesis I have found several additional candidates. The genetic and yeast two-hybrid interaction with *KIN7.4* and *TOR1* indicates possible role of *SUB* in microtubule dynamics. The functional characterization of *KIN7.4* suggests that it is a positive regulator of root hair cell patterning. Interestingly, In floral organ, *WAK3* and *CHC* are negatively regulated whereas in root *SUB* promotes *KIN7.4* and *CHC* for root hair cell patterning.

6 References

1. Albersheim P (2010) Plant Cell Walls. doi: 10.1201/9780203833476
2. Alberts AS, Bouquin N, Johnston LH, Treisman R (1998) Analysis of RhoA-binding proteins reveals an interaction domain conserved in heterotrimeric G protein beta subunits and the yeast response regulator protein Skn7. *J Biol Chem* 273:8616–8622. doi: 10.1074/jbc.273.15.8616
3. Alexandersson E, Fraysse L, Sjövall-Larsen S, et al (2005) Whole gene family expression and drought stress regulation of aquaporins. *Plant Mol Biol* 59:469–484. doi: 10.1007/s11103-005-0352-1
4. Alonso JM, Stepanova AN, Leisse TJ, et al (2003) Genome-wide insertional mutagenesis of *Arabidopsis thaliana*. *Science* 301:653–657. doi: 10.1126/science.1086391
5. Ambrose C, Allard JF, Cytrynbaum EN, Wasteneys GO (2011) A CLASP-modulated cell edge barrier mechanism drives cell-wide cortical microtubule organization in *Arabidopsis*. *Nat Commun* 2:430. doi: 10.1038/ncomms1444
6. Anders S, Huber W (2010) Differential expression analysis for sequence count data. *Genome Biol* 11: R106. doi: 10.1186/gb-2010-11-10-r106
7. Anderson CM, Wagner TA, Perret M, et al (2001) WAKs: cell wall-associated kinases linking the cytoplasm to the extracellular matrix. *Plant Mol Biol* 47:197–206.
8. Antolín-Llovera M, Ried MK, Parniske M (2014) Cleavage of the SYMBIOSIS RECEPTOR-LIKE KINASE ectodomain promotes complex formation with Nod factor receptor 5. *Curr Biol* 24:422–427. doi: 10.1016/j.cub.2013.12.053
9. Asada T, Collings D (1997) Molecular motors in higher plants. *Trends Plant Sci* 2:29–37. doi: 10.1016/S1360-1385(96)10051-0
10. Ayers AR, Valent B, Ebel J, Albersheim P (1976) Host-pathogen interactions: xi. Composition and structure of wall-released elicitor fractions. *Plant Physiol* 57:766–774. doi: 10.1104/pp.57.5.766
11. Aziz A, Gauthier A, Bézier A, et al (2007) Elicitor and resistance-inducing activities of beta-1,4 cellodextrins in grapevine, comparison with beta-1,3 glucans and alpha-1,4 oligogalacturonides. *J Exp Bot* 58:1463–1472. doi: 10.1093/jxb/erm008
12. Bacete L, Mélida H, Miedes E, Molina A (2018) Plant cell wall-mediated immunity: cell wall changes trigger disease resistance responses. *Plant J* 93:614–636. doi: 10.1111/tpj.13807
13. Bai L, Zhang G, Zhou Y, et al (2009) Plasma membrane-associated proline-rich extensin-like receptor kinase 4, a novel regulator of Ca signalling, is required for abscisic acid responses in *Arabidopsis thaliana*. *Plant J* 60:314–327. doi: 10.1111/j.1365-313X.2009.03956.x
14. Bai Y, Vaddepalli P, Fulton L, et al (2013) ANGUSTIFOLIA is a central component of tissue morphogenesis mediated by the atypical receptor-like kinase STRUBBELIG. *BMC Plant Biol* 13:16. doi: 10.1186/1471-2229-13-16
15. Balasubramanian S, Schneitz K. NOZZLE regulates proximal-distal pattern formation, cell proliferation and early sporogenesis during ovule development in *Arabidopsis thaliana*. *Development*. 2000;127: 4227–4238.

16. Baluska F, Jasik J, Edelmann HG, et al (2001) Latrunculin B-induced plant dwarfism: Plant cell elongation is F-actin-dependent. *Dev Biol* 231:113–124. doi: 10.1006/dbio.2000.0115
17. Baluska F, Samaj J, Wojtaszek P, et al (2003) Cytoskeleton-plasma membrane-cell wall continuum in plants. Emerging links revisited. *Plant Physiol* 133:482–491. doi: 10.1104/pp.103.027250
18. Batiza AF, Schulz T, Masson PH (1996) Yeast respond to hypotonic shock with a calcium pulse. *J Biol Chem* 271:23357–23362. doi: 10.1074/jbc.271.38.23357
19. Bellincampi D, Cardarelli M, Zaghi D, et al (1996) Oligogalacturonides prevent rhizogenesis in rolb-transformed tobacco explants by inhibiting auxin-induced expression of the rolb gene. *Plant Cell* 8:477–487. doi: 10.1105/tpc.8.3.477
20. Bender KW, Wang X, Cheng GB, et al (2015) Glutaredoxin AtGRXC2 catalyses inhibitory glutathionylation of Arabidopsis BRI1-associated receptor-like kinase 1 (BAK1) in vitro. *Biochem J* 467:399–413. doi: 10.1042/BJ20141403
21. Benová-Kákosová A, Digonnet C, Goubet F, et al (2006) Galactoglucomannans increase cell population density and alter the protoxylem/metaxylem tracheary element ratio in xylogenic cultures of *Zinnia*. *Plant Physiol* 142:696–709. doi: 10.1104/pp.106.085712
22. Besson S, Dumais J (2014) Stochasticity in the symmetric division of plant cells: when the exceptions are the rule. *Front Plant Sci* 5:538. doi: 10.3389/fpls.2014.00538
23. Bidhendi AJ, Geitmann A (2016) Relating the mechanics of the primary plant cell wall to morphogenesis. *J Exp Bot* 67:449–461. doi: 10.1093/jxb/erv535
24. Bischoff V, Cookson SJ, Wu S, Scheible W-R (2009) Thaxtomin A affects CESA-complex density, expression of cell wall genes, cell wall composition, and causes ectopic lignification in *Arabidopsis thaliana* seedlings. *J Exp Bot* 60:955–965. doi: 10.1093/jxb/ern344
25. Blume YB, Krasylenko YA, Demchuk OM, Yemets AI (2013) Tubulin tyrosine nitration regulates microtubule organization in plant cells. *Front Plant Sci* 4:530. doi: 10.3389/fpls.2013.00530
26. Boisson-Dernier A, Kessler SA, Grossniklaus U (2011) The walls have ears: the role of plant CrRLK1Ls in sensing and transducing extracellular signals. *J Exp Bot* 62:1581–1591. doi: 10.1093/jxb/erq445
27. Boisson-Dernier A, Roy S, Kritsas K, et al (2009) Disruption of the pollen-expressed FERONIA homologs ANXUR1 and ANXUR2 triggers pollen tube discharge. *Development* 136:3279–3288. doi: 10.1242/dev.040071
28. Bonawitz ND, Kim JI, Tobimatsu Y, et al (2014) Disruption of Mediator rescues the stunted growth of a lignin-deficient *Arabidopsis* mutant. *Nature* 509:376–380. doi: 10.1038/nature13084
29. Bouton S, Leboeuf E, Mouille G, et al (2002) QUASIMODO1 encodes a putative membrane-bound glycosyltransferase required for normal pectin synthesis and cell adhesion in *Arabidopsis*. *Plant Cell* 14:2577–2590. doi: 10.1105/tpc.004259
30. Bouwmeester K, de Sain M, Weide R, et al (2011) The lectin receptor kinase LecRK-I.9 is a novel *Phytophthora* resistance component and a potential host target for a RXLR effector. *PLoS Pathog* 7: e1001327. doi: 10.1371/journal.ppat.1001327

31. Braam J (1992) Regulated expression of the calmodulin-related TCH genes in cultured *Arabidopsis* cells: induction by calcium and heat shock. *Proc Natl Acad Sci USA* 89:3213–3216. doi: 10.1073/pnas.89.8.3213
32. Braidwood L, Breuer C, Sugimoto K (2014) My body is a cage: mechanisms and modulation of plant cell growth. *New Phytol* 201:388–402. doi: 10.1111/nph.12473
33. Braybrook SA, Peaucelle A (2013) Mechano-chemical aspects of organ formation in *Arabidopsis thaliana*: the relationship between auxin and pectin. *PLoS ONE* 8: e57813. doi: 10.1371/journal.pone.0057813
34. Bruno F, Reis D, Pigosso LL, et al (2014) responsible for the impaired growth and morphogenesis of *Paracoccidioides brasiliensis* induced by N-glycosylation inhibition. 1–11.
35. Brutus A, Sicilia F, Macone A, et al (2010) A domain swap approach reveals a role of the plant wall-associated kinase 1 (WAK1) as a receptor of oligogalacturonides. *Proc Natl Acad Sci USA* 107:9452–9457. doi: 10.1073/pnas.1000675107
36. Burton RA, Gibeaut DM, Bacic A, et al (2000) Virus-induced silencing of a plant cellulose synthase gene. *Plant Cell* 12:691–706. doi: 10.1105/tpc.12.5.691
37. Burton RA, Gidley MJ, Fincher GB (2010) Heterogeneity in the chemistry, structure and function of plant cell walls. *Nat Chem Biol* 6:724–732. doi: 10.1038/nchembio.439
38. Buschmann H, Fabri CO, Hauptmann M, et al (2004) Helical growth of the *Arabidopsis* mutant *tortifolia1* reveals a plant-specific microtubule-associated protein. *Curr Biol* 14:1515–1521. doi: 10.1016/j.cub.2004.08.033
39. Caño-Delgado A, Penfield S, Smith C, et al (2003) Reduced cellulose synthesis invokes lignification and defense responses in *Arabidopsis thaliana*. *Plant J* 34:351–362. doi: 10.1046/j.1365-313x.2003.01729.x
40. Caño-Delgado AI, Metzlauff K, Bevan MW (2000) The *eli1* mutation reveals a link between cell expansion and secondary cell wall formation in *Arabidopsis thaliana*. *Development* 127:3395–3405.
41. Canut H, Carrasco A, Galaud JP, et al (1998) High affinity RGD-binding sites at the plasma membrane of *Arabidopsis thaliana* links the cell wall. *Plant J* 16:63–71. doi: 10.1046/j.1365-313x.1998.00276.x
42. Carraca, L. P. V., 2012, Functional characterization of cell wall damage response genes in *Arabidopsis thaliana*: Imperial College London, doi: 10.25560/11644.
43. Century KS (1995) locus of *Arabidopsis thaliana* that is required for disease resistance. *92:6597–6601*.
44. Chaiwanon J, Wang W, Zhu J-Y, et al (2016) Information integration and communication in plant growth regulation. *Cell* 164:1257–1268. doi: 10.1016/j.cell.2016.01.044
45. Chaudhary A, Chen X, Gao J, et al (2019) The *Arabidopsis* receptor kinase STRUBBELIG regulates the response to cellulose deficiency. *BioRxiv*. doi: 10.1101/775775
46. Chaudhary A, Gao J, Schneitz K (2018) The genetic control of ovule development. Reference module in life sciences. doi: 10.1016/B978-0-12-809633-8.20737-1

47. Chen J, Yu F, Liu Y, et al (2016) FERONIA interacts with ABI2-type phosphatases to facilitate signaling cross-talk between abscisic acid and RALF peptide in Arabidopsis. *Proc Natl Acad Sci USA* 113:E5519-27. doi: 10.1073/pnas.1608449113
48. Chen Y, Hu D, Yabe R, et al (2011) Role of malectin in Glc (2) Man (9) GlcNAc (2)-dependent quality control of α 1-antitrypsin. *Mol Biol Cell* 22:3559–3570. doi: 10.1091/mbc.E11-03-0201
49. Cheung AY, Wu H-M (2011) THESEUS 1, FERONIA and relatives: a family of cell wall-sensing receptor kinases? *Curr Opin Plant Biol* 14:632–641. doi: 10.1016/j.pbi.2011.09.001
50. Chevalier D, Batoux M, Fulton L, et al (2005) STRUBBELIG defines a receptor kinase-mediated signaling pathway regulating organ development in Arabidopsis. *Proc Natl Acad Sci USA* 102:9074–9079. doi: 10.1073/pnas.0503526102
51. Clark SE, Williams RW, Meyerowitz EM (1997) The CLAVATA1 gene encodes a putative receptor kinase that controls shoot and floral meristem size in Arabidopsis. *Cell* 89:575–585. doi: 10.1016/s0092-8674(00)80239-1
52. Clough SJ, Bent AF (1998) Floral dip: a simplified method for *Agrobacterium*-mediated transformation of *Arabidopsis thaliana*. *The Plant Journal* 16:735–743. doi: 10.1046/j.1365-313x.1998.00343.x
53. Colcombet J, Boisson-Dernier A, Ros-Palau R, et al (2005) Arabidopsis SOMATIC EMBRYOGENESIS RECEPTOR KINASES1 and 2 are essential for tapetum development and microspore maturation. *Plant Cell* 17:3350–3361. doi: 10.1105/tpc.105.036731
54. Conte I, Labriola C, Cazzulo JJ, et al (2003) The interplay between folding-facilitating mechanisms in *Trypanosoma cruzi* endoplasmic reticulum. *Mol Biol Cell* 14:3529–3540. doi: 10.1091/mbc.e03-04-0228
55. Cosgrove DJ (2001) Plant cell walls: wall-associated kinases and cell expansion. *Curr Biol* 11: R558-9. doi: 10.1016/s0960-9822(01)00342-6
56. Cosgrove DJ (2005) Growth of the plant cell wall. *Nat Rev Mol Cell Biol* 6:850–861. doi: 10.1038/nrm1746
57. Cosgrove DJ (2014) Re-constructing our models of cellulose and primary cell wall assembly. *Curr Opin Plant Biol* 22:122–131. doi: 10.1016/j.pbi.2014.11.001
58. Cosgrove DJ (2016) Plant cell wall extensibility: connecting plant cell growth with cell wall structure, mechanics, and the action of wall-modifying enzymes. *J Exp Bot* 67:463–476. doi: 10.1093/jxb/erv511
59. Côté F, Hahn MG (1994) Oligosaccharins: structures and signal transduction. *Plant Mol Biol* 26:1379–1411. doi: 10.1007/bf00016481
60. Côté F, Ham KS, Hahn MG, Bergmann CW (1998) Oligosaccharide elicitors in host-pathogen interactions. Generation, perception, and signal transduction. *Subcell Biochem* 29:385–432. doi: 10.1007/978-1-4899-1707-2_13
61. Couto D, Zipfel C (2016) Regulation of pattern recognition receptor signalling in plants. *Nat Rev Immunol* 16:537–552. doi: 10.1038/nri.2016.77

62. Cvrcková F, De Virgilio C, Manser E, et al (1995) Ste20-like protein kinases are required for normal localization of cell growth and for cytokinesis in budding yeast. *Genes Dev* 9:1817–1830. doi: 10.1101/gad.9.15.1817
63. Dagenbach EM, Endow SA (2004) A new kinesin tree. *J Cell Sci* 117:3–7. doi: 10.1242/jcs.00875
64. Daher FB, Braybrook SA (2015) How to let go: pectin and plant cell adhesion. *Front Plant Sci* 6:523. doi: 10.3389/fpls.2015.00523
65. de Keijzer J, Kieft H, Ketelaar T, et al (2017) Shortening of microtubule overlap regions defines membrane delivery sites during plant cytokinesis. *Curr Biol* 27:514–520. doi: 10.1016/j.cub.2016.12.043
66. Denness L, McKenna JF, Segonzac C, et al (2011) Cell wall damage-induced lignin biosynthesis is regulated by a reactive oxygen species- and jasmonic acid-dependent process in *Arabidopsis*. *Plant Physiol* 156:1364–1374. doi: 10.1104/pp.111.175737
67. Denninger P, Bleckmann A, Lausser A, et al (2014) Male-female communication triggers calcium signatures during fertilization in *Arabidopsis*. *Nat Commun* 5:4645. doi: 10.1038/ncomms5645
68. Denoux C, Galletti R, Mammarella N, et al (2008) Activation of defense response pathways by OGs and Flg22 elicitors in *Arabidopsis* seedlings. *Mol Plant* 1:423–445. doi: 10.1093/mp/ssn019
69. Derbyshire P, McCann MC, Roberts K (2007) Restricted cell elongation in *Arabidopsis* hypocotyls is associated with a reduced average pectin esterification level. *BMC Plant Biol* 7:31. doi: 10.1186/1471-2229-7-31
70. Deslauriers SD, Larsen PB (2010) FERONIA is a key modulator of brassinosteroid and ethylene responsiveness in *Arabidopsis* hypocotyls. *Mol Plant* 3:626–640. doi: 10.1093/mp/ssq015
71. Desprez T, Juraniec M, Crowell EF, et al (2007) Organization of cellulose synthase complexes involved in primary cell wall synthesis in *Arabidopsis thaliana*. *Proc Natl Acad Sci USA* 104:15572–15577. doi: 10.1073/pnas.0706569104
72. Desprez T, Vernhettes S, Fagard M, et al (2002) Resistance against herbicide isoxaben and cellulose deficiency caused by distinct mutations in same cellulose synthase isoform CESA6. *Plant Physiol* 128:482–490. doi: 10.1104/pp.010822
73. Di Matteo A, Giovane A, Raiola A, et al (2005) Structural basis for the interaction between pectin methylesterase and a specific inhibitor protein. *Plant Cell* 17:849–858. doi: 10.1105/tpc.104.028886
74. Diévarat A, Dalal M, Tax FE, et al (2003) CLAVATA1 dominant-negative alleles reveal functional overlap between multiple receptor kinases that regulate meristem and organ development. *Plant Cell* 15:1198–1211. doi: 10.1105/tpc.010504
75. Dolan L, Janmaat K, Willemsen V, et al (1993) Cellular organisation of the *Arabidopsis thaliana* root. *Development* 119:71–84.

76. Duan Q, Kita D, Johnson EA, et al (2014) Reactive oxygen species mediate pollen tube rupture to release sperm for fertilization in *Arabidopsis*. *Nat Commun* 5:3129. doi: 10.1038/ncomms4129
77. Duan Q, Kita D, Li C, et al (2010) FERONIA receptor-like kinase regulates RHO GTPase signaling of root hair development. *Proc Natl Acad Sci USA* 107:17821–17826. doi: 10.1073/pnas.1005366107
78. Dupuy L, Mackenzie J, Haseloff J (2010) Coordination of plant cell division and expansion in a simple morphogenetic system. *Proc Natl Acad Sci USA* 107:2711–2716. doi: 10.1073/pnas.0906322107
79. Duval I, Beaudoin N (2009) Transcriptional profiling in response to inhibition of cellulose synthesis by thaxtomin A and isoxaben in *Arabidopsis thaliana* suspension cells. *Plant Cell Rep* 28:811–830. doi: 10.1007/s00299-009-0670-x
80. Elliott RC, Betzner AS, Huttner E, et al (1996) AINTEGUMENTA, an APETALA2-like gene of *Arabidopsis* with pleiotropic roles in ovule development and floral organ growth. *Plant Cell* 8:155–168. doi: 10.1105/tpc.8.2.155
81. Ellis C, Karafyllidis I, Wasternack C, Turner JG (2002) The *Arabidopsis* mutant *cev1* links cell wall signaling to jasmonate and ethylene responses. *Plant Cell* 14:1557–1566. doi: 10.1105/tpc.002022
82. Engelsdorf T, Gigli-Bisceglia N, Veerabagu M, et al (2018) The plant cell wall integrity maintenance and immune signaling systems cooperate to control stress responses in *Arabidopsis thaliana*. *Sci Signal*. doi: 10.1126/scisignal. aao3070
83. Escobar-Restrepo J-M, Huck N, Kessler S, et al (2007) The FERONIA receptor-like kinase mediates male-female interactions during pollen tube reception. *Science* 317:656–660. doi: 10.1126/science.1143562
84. Fagard M, Desnos T, Desprez T, et al (2000) PROCUSTE1 encodes a cellulose synthase required for normal cell elongation specifically in roots and dark-grown hypocotyls of *Arabidopsis*. *Plant Cell* 12:2409–2424.
85. Fendrych M, Synek L, Pecenková T, et al (2013) Visualization of the exocyst complex dynamics at the plasma membrane of *Arabidopsis thaliana*. *Mol Biol Cell* 24:510–520. doi: 10.1091/mbc. E12-06-0492
86. Feng W, Kita D, Peaucelle A, et al (2018) The feronia receptor kinase maintains cell-wall integrity during salt stress through ca^{2+} signaling. *Curr Biol* 28:666-675.e5. doi: 10.1016/j.cub.2018.01.023
87. Foreman J (2001) Root hairs as a model system for studying plant cell growth. *Ann Bot* 88:1–7. doi: 10.1006/anbo.2001.1430
88. Foreman J, Demidchik V, Bothwell JHF, et al (2003) Reactive oxygen species produced by NADPH oxidase regulate plant cell growth. *Nature* 422:442–446. doi: 10.1038/nature01485
89. Francis KE, Lam SY, Copenhaver GP (2006) Separation of *Arabidopsis* pollen tetrads is regulated by QUARTET1, a pectin methylesterase gene. *Plant Physiol* 142:1004–1013. doi: 10.1104/pp.106.085274

90. Franck CM, Westermann J, Boisson-Dernier A (2018a) Plant malectin-like receptor kinases: from cell wall integrity to immunity and beyond. *Annu Rev Plant Biol* 69:301–328. doi: 10.1146/annurev-arplant-042817-040557
91. Franck CM, Westermann J, Boisson-Dernier A, et al (2018b) Annual review of plant biology plant malectin-like receptor kinases: from cell wall integrity to immunity and beyond rlk: receptor-like kinase. *Glycobiology* 26:950–960.
92. Fry SC (2011) Plant cell walls. From chemistry to biology. *Ann Bot* 108: viii–ix. doi: 10.1093/aob/mcr128
93. Fujikura U, Elsaesser L, Breuninger H, et al (2014) Atkinesin-13A modulates cell-wall synthesis and cell expansion in *Arabidopsis thaliana* via the THESEUS1 pathway. *PLoS Genet* 10: e1004627. doi: 10.1371/journal.pgen.1004627
94. Fulton L, Batoux M, Vaddepalli P, et al (2009) DETORQUEO, QUIRKY, and ZERZAUST represent novel components involved in organ development mediated by the receptor-like kinase STRUBBELIG in *Arabidopsis thaliana*. *PLoS Genet* 5: e1000355. doi: 10.1371/journal.pgen.1000355
95. Gallego-Giraldo L, Jikumaru Y, Kamiya Y, et al (2011) Selective lignin downregulation leads to constitutive defense response expression in alfalfa (*Medicago sativa* L.). *New Phytol* 190:627–639. doi: 10.1111/j.1469-8137.2010.03621.x
96. Galletti R, De Lorenzo G, Ferrari S (2009) Host-derived signals activate plant innate immunity. *Plant Signal Behav* 4:33–34. doi: 10.4161/psb.4.1.7224
97. Galli C, Bernasconi R, Soldà T, et al (2011) Malectin participates in a backup glycoprotein quality control pathway in the mammalian ER. *PLoS ONE* 6: e16304. doi: 10.1371/journal.pone.0016304
98. Gamble RL, Qu X, Schaller GE (2002) Mutational analysis of the ethylene receptor ETR1. Role of the histidine kinase domain in dominant ethylene insensitivity. *Plant Physiol* 128:1428–1438. doi: 10.1104/pp.010777
99. Ganguly A, DeMott L, Dixit R (2017) The *Arabidopsis* kinesin-4, FRA1, requires a high level of processive motility to function correctly. *J Cell Sci* 130:1232–1238. doi: 10.1242/jcs.196857
100. Ganguly A, Dixit R (2013) Mechanisms for regulation of plant kinesins. *Curr Opin Plant Biol* 16:704–709. doi: 10.1016/j.pbi.2013.09.003
101. Gao J, Chaudhary A, Vaddepalli P, et al (2019) The *Arabidopsis* receptor kinase STRUBBELIG undergoes clathrin-dependent endocytosis. *J Exp Bot* 70:3881–3894. doi: 10.1093/jxb/erz190
102. Gao M, Wang X, Wang D, et al (2009) Regulation of cell death and innate immunity by two receptor-like kinases in *Arabidopsis*. *Cell Host Microbe* 6:34–44. doi: 10.1016/j.chom.2009.05.019
103. Garrett-Engele P, Moilanen B, Cyert MS (1995) Calcineurin, the Ca²⁺/calmodulin-dependent protein phosphatase, is essential in yeast mutants with cell integrity defects and in mutants that lack a functional vacuolar H⁽⁺⁾-ATPase. *Mol Cell Biol* 15:4103–4114. doi: 10.1128/mcb.15.8.4103

104. Gigli-Bisceglia N, Engelsdorf T, Strnad M, et al (2018) Cell wall integrity modulates *Arabidopsis thaliana* cell cycle gene expression in a cytokinin- and nitrate reductase-dependent manner. *Development*. doi: 10.1242/dev.166678
105. Gómez-Gómez L, Boller T (2000) FLS2: an LRR receptor-like kinase involved in the perception of the bacterial elicitor flagellin in *Arabidopsis*. *Mol Cell* 5:1003–1011. doi: 10.1016/s1097-2765(00)80265-8
106. Gonneau M, Desprez T, Martin M, et al (2018) Receptor kinase THESEUS1 is a rapid alkalization factor 34 receptor in *Arabidopsis*. *Curr Biol* 28:2452-2458.e4. doi: 10.1016/j.cub.2018.05.075
107. Gouget A, Senchou V, Govers F, et al (2006) Lectin receptor kinases participate in protein-protein interactions to mediate plasma membrane-cell wall adhesions in *Arabidopsis*. *Plant Physiol* 140:81–90. doi: 10.1104/pp.105.066464
108. Gravino M, Savatin DV, Macone A, De Lorenzo G (2015) Ethylene production in *Botrytis cinerea*- and oligogalacturonide-induced immunity requires calcium-dependent protein kinases. *Plant J* 84:1073–1086. doi: 10.1111/tpj.13057
109. Green PB (1962) Mechanism for plant cellular morphogenesis. *Science* 138:1404–1405. doi: 10.1126/science.138.3548.1404
110. Grierson C, Nielsen E, Ketelaarc T, Schiefelbein J (2014) Root hairs. *Arabidopsis Book* 12:e0172. doi: 10.1199/tab.0172
111. Grison MS, Kirk P, Brault ML, et al (2019) plasma membrane-associated receptor-like kinases relocate to plasmodesmata in response to osmotic stress. *Plant Physiol* 181:142–160. doi: 10.1104/pp.19.00473
112. Guo H, Li L, Ye H, et al (2009) Three related receptor-like kinases are required for optimal cell elongation in *Arabidopsis thaliana*. *Proc Natl Acad Sci USA* 106:7648–7653. doi: 10.1073/pnas.0812346106
113. Gustin MC, Zhou XL, Martinac B, Kung C (1988) A mechanosensitive ion channel in the yeast plasma membrane. *Science* 242:762–765. doi: 10.1126/science.2460920
114. Gutierrez R, Lindeboom JJ, Paredes AR, et al (2009) *Arabidopsis* cortical microtubules position cellulose synthase delivery to the plasma membrane and interact with cellulose synthase trafficking compartments. *Nat Cell Biol* 11:797–806. doi: 10.1038/ncb1886
115. Haffani YZ, Silva-Gagliardi NF, Sewter SK, et al (2006) Altered expression of PERK receptor kinases in *Arabidopsis* leads to changes in growth and floral organ formation. *Plant Signal Behav* 1:251–260.
116. Hahn MG, Darvill AG, Albersheim P (1981) Host-Pathogen Interactions: XIX. The endogenous elicitor, a fragment of a plant cell wall polysaccharide that elicits phytoalexin accumulation in soybeans. *Plant Physiol* 68:1161–1169. doi: 10.1104/pp.68.5.1161
117. Halter T, Imkamp J, Mazzotta S, et al (2014) The leucine-rich repeat receptor kinase BIR2 is a negative regulator of BAK1 in plant immunity. *Curr Biol* 24:134–143. doi: 10.1016/j.cub.2013.11.047

118. Hamann T (2015) The plant cell wall integrity maintenance mechanism--a case study of a cell wall plasma membrane signaling network. *Phytochemistry* 112:100–109. doi: 10.1016/j.phytochem.2014.09.019
119. Hamann T, Bennett M, Mansfield J, Somerville C (2009) Identification of cell-wall stress as a hexose-dependent and osmosensitive regulator of plant responses. *Plant J* 57:1015–1026. doi: 10.1111/j.1365-313X.2008.03744.x
120. Hamant O, Haswell ES (2017) Life behind the wall: sensing mechanical cues in plants. *BMC Biol* 15:59. doi: 10.1186/s12915-017-0403-5
121. Hamant O, Heisler MG, Jönsson H, et al (2008) Developmental patterning by mechanical signals in *Arabidopsis*. *Science* 322:1650–1655. doi: 10.1126/science.1165594
122. Hamilton ES, Jensen GS, Makshev G, et al (2015) Mechanosensitive channel MSL8 regulates osmotic forces during pollen hydration and germination. *Science* 350:438–441. doi: 10.1126/science.aac6014
123. Han Z, Sun Y, Chai J (2014) Structural insight into the activation of plant receptor kinases. *Curr Opin Plant Biol* 20:55–63. doi: 10.1016/j.pbi.2014.04.008
124. Haruta M, Monshausen G, Gilroy S, Sussman MR (2008) A cytoplasmic Ca²⁺ functional assay for identifying and purifying endogenous cell signaling peptides in *Arabidopsis* seedlings: identification of AtRALF1 peptide. *Biochemistry* 47:6311–6321. doi: 10.1021/bi8001488
125. Haruta M, Sabat G, Stecker K, et al (2014) A peptide hormone and its receptor protein kinase regulate plant cell expansion. *Science* 343:408–411. doi: 10.1126/science.1244454
126. Haruta M, Tan LX, Bushey DB, et al (2018) Environmental and genetic factors regulating localization of the plant plasma membrane h⁺-atpase. *Plant Physiol* 176:364–377. doi: 10.1104/pp.17.01126
127. Haswell ES, Meyerowitz EM (2006) MscS-like proteins control plastid size and shape in *Arabidopsis thaliana*. *Curr Biol* 16:1–11. doi: 10.1016/j.cub.2005.11.044
128. Haswell ES, Peyronnet R, Barbier-Brygoo H, et al (2008) Two MscS homologs provide mechanosensitive channel activities in the *Arabidopsis* root. *Curr Biol* 18:730–734. doi: 10.1016/j.cub.2008.04.039
129. He ZH, Cheeseman I, He D, Kohorn BD (1999) A cluster of five cell wall-associated receptor kinase genes, Wak1-5, are expressed in specific organs of *Arabidopsis*. *Plant Mol Biol* 39:1189–1196. doi: 10.1023/a:1006197318246
130. Hebert DN (2012) An MBoC favorite: Malectin: a novel carbohydrate-binding protein of the endoplasmic reticulum and a candidate player in the early steps of protein N-glycosylation. *Mol Biol Cell* 23:2236. doi: 10.1091/mbc.E12-02-0156
131. Helenius A (1994) How N-linked oligosaccharides affect glycoprotein folding in the endoplasmic reticulum. *Mol Biol Cell* 5:253–265. doi: 10.1091/mbc.5.3.253
132. Hématy K, Höfte H (2008) Novel receptor kinases involved in growth regulation. *Curr Opin Plant Biol* 11:321–328. doi: 10.1016/j.pbi.2008.02.008

133. Hématy K, Sado P-E, Van Tuinen A, et al (2007) A receptor-like kinase mediates the response of Arabidopsis cells to the inhibition of cellulose synthesis. *Curr Biol* 17:922–931. doi: 10.1016/j.cub.2007.05.018
134. Hernández-Blanco C, Feng DX, Hu J, et al (2007) Impairment of cellulose synthases required for Arabidopsis secondary cell wall formation enhances disease resistance. *Plant Cell* 19:890–903. doi: 10.1105/tpc.106.048058
135. Höfte H (2015) The yin and yang of cell wall integrity control: brassinosteroid and FERONIA signaling. *Plant Cell Physiol* 56:224–231. doi: 10.1093/pcp/pcu182
136. Hok S, Danchin EGJ, Allasia V, et al (2011) An Arabidopsis (malectin-like) leucine-rich repeat receptor-like kinase contributes to downy mildew disease. *Plant Cell Environ* 34:1944–1957. doi: 10.1111/j.1365-3040.2011.02390.x
137. Holland N, Holland D, Helentjaris T, et al (2000) A comparative analysis of the plant cellulose synthase (CesA) gene family. *Plant Physiol* 123:1313–1324. doi: 10.1104/pp.123.4.1313
138. Hou S, Liu Z, Shen H, Wu D (2019) Damage-Associated Molecular Pattern-Triggered Immunity in Plants. *Front Plant Sci* 10:646. doi: 10.3389/fpls.2019.00646
139. Hua J, Sakai H, Nourizadeh S, et al (1998) EIN4 and ERS2 are members of the putative ethylene receptor gene family in Arabidopsis. *Plant Cell* 10:1321–1332. doi: 10.1105/tpc.10.8.1321
140. Huang KM, Snider MD (1995) Isolation of protein glycosylation mutants in the fission yeast *Schizosaccharomyces pombe*. *Mol Biol Cell* 6:485–496. doi: 10.1091/mbc.6.5.485
141. Hubbard SR, Till JH (2000) Protein tyrosine kinase structure and function. *Annu Rev Biochem* 69:373–398. doi: 10.1146/annurev.biochem.69.1.373
142. Huck N, Moore JM, Federer M, Grossniklaus U (2003) The Arabidopsis mutant *feronia* disrupts the female gametophytic control of pollen tube reception. *Development* 130:2149–2159. doi: 10.1242/dev.00458
143. Humphrey TV, Bonetta DT, Goring DR (2007) Sentinels at the wall: cell wall receptors and sensors. *New Phytol* 176:7–21. doi: 10.1111/j.1469-8137.2007.02192.x
144. Humphrey TV, Haasen KE, Aldea-Brydges MG, et al (2015) PERK-KIPK-KCBP signalling negatively regulates root growth in Arabidopsis thaliana. *J Exp Bot* 66:71–83. doi: 10.1093/jxb/eru390
145. Huse M, Kuriyan J (2002) The conformational plasticity of protein kinases. *Cell* 109:275–282. doi: 10.1016/s0092-8674(02)00741-9
146. Hüttner S, Veit C, Vavra U, et al (2014) A context-independent N-glycan signal targets the misfolded extracellular domain of Arabidopsis STRUBBELIG to endoplasmic-reticulum-associated degradation. *Biochem J* 464:401–411. doi: 10.1042/BJ20141057
147. Iida H, Nakamura H, Ono T, et al (1994) MID1, a novel *Saccharomyces cerevisiae* gene encoding a plasma membrane protein, is required for Ca²⁺ influx and mating. *Mol Cell Biol* 14:8259–8271. doi: 10.1128/mcb.14.12.8259

148. Jaillais Y, Hothorn M, Belkhadir Y, et al (2011) Tyrosine phosphorylation controls brassinosteroid receptor activation by triggering membrane release of its kinase inhibitor. *Genes Dev* 25:232–237. doi: 10.1101/gad.2001911
149. Jaillais Y, Vert G (2016) Brassinosteroid signaling and BRI1 dynamics went underground. *Curr Opin Plant Biol* 33:92–100. doi: 10.1016/j.pbi.2016.06.014
150. Jendretzki A, Wittland J, Wilk S, et al (2011) How do I begin? Sensing extracellular stress to maintain yeast cell wall integrity. *Eur J Cell Biol* 90:740–744. doi: 10.1016/j.ejcb.2011.04.006
151. Jensen GS, Haswell ES (2012) Functional analysis of conserved motifs in the mechanosensitive channel homolog MscS-Like2 from *Arabidopsis thaliana*. *PLoS ONE* 7:e40336. doi: 10.1371/journal.pone.0040336
152. Jeon J, Kim NY, Kim S, et al (2010) A subset of cytokinin two-component signaling system plays a role in cold temperature stress response in *Arabidopsis*. *J Biol Chem* 285:23371–23386. doi: 10.1074/jbc.M109.096644
153. Jeong S, Trotochaud AE, Clark SE (1999) The *Arabidopsis* CLAVATA2 gene encodes a receptor-like protein required for the stability of the CLAVATA1 receptor-like kinase. *Plant Cell* 11:1925–1934. doi: 10.1105/tpc.11.10.1925
154. John M, Röhrig H, Schmidt J, et al (1997) Cell signalling by oligosaccharides. *Trends Plant Sci* 2:111–115. doi: 10.1016/S1360-1385(97)01005-4
155. Johnson LN, Noble ME, Owen DJ (1996) Active and inactive protein kinases: structural basis for regulation. *Cell* 85:149–158. doi: 10.1016/s0092-8674(00)81092-2
156. Jones AM, Xuan Y, Xu M, et al (2014) Border control--a membrane-linked interactome of *Arabidopsis*. *Science* 344:711–716. doi: 10.1126/science.1251358
157. Kakimoto T (1996) CKI1, a histidine kinase homolog implicated in cytokinin signal transduction. *Science* 274:982–985. doi: 10.1126/science.274.5289.982
158. Keegstra K (2010) Plant cell walls. *Plant Physiol* 154:483–486. doi: 10.1104/pp.110.161240
159. Keinath NF, Kierszniowska S, Lorek J, et al (2010) PAMP (pathogen-associated molecular pattern)-induced changes in plasma membrane compartmentalization reveal novel components of plant immunity. *J Biol Chem* 285:39140–39149. doi: 10.1074/jbc.M110.160531
160. Kessler SA, Shimosato-Asano H, Keinath NF, et al (2010) Conserved molecular components for pollen tube reception and fungal invasion. *Science* 330:968–971. doi: 10.1126/science.1195211
161. Ketela T, Green R, Bussey H (1999) *Saccharomyces cerevisiae* mid2p is a potential cell wall stress sensor and upstream activator of the PKC1-MPK1 cell integrity pathway. *J Bacteriol* 181:3330–3340.
162. Kilian J, Whitehead D, Horak J, et al (2007) The AtGenExpress global stress expression data set: protocols, evaluation and model data analysis of UV-B light, drought and cold stress responses. *Plant J* 50:347–363. doi: 10.1111/j.1365-313X.2007.03052.x

163. Kitakura S, Vanneste S, Robert S, et al (2011) Clathrin mediates endocytosis and polar distribution of PIN auxin transporters in Arabidopsis. *Plant Cell* 23:1920–1931. doi: 10.1105/tpc.111.083030
164. Klepikova AV, Kasianov AS, Gerasimov ES, et al (2016) A high resolution map of the Arabidopsis thaliana developmental transcriptome based on RNA-seq profiling. *Plant J* 88:1058–1070. doi: 10.1111/tpj.13312
165. Kohorn BD, Kobayashi M, Johansen S, et al (2006a) An Arabidopsis cell wall-associated kinase required for invertase activity and cell growth. *Plant J* 46:307–316. doi: 10.1111/j.1365-313X.2006.02695.x
166. Kohorn BD, Kobayashi M, Johansen S, et al (2006b) Wall-associated kinase 1 (WAK1) is crosslinked in endomembranes, and transport to the cell surface requires correct cell-wall synthesis. *J Cell Sci* 119:2282–2290. doi: 10.1242/jcs.02968
167. Kohorn BD, Kohorn SL (2012) The cell wall-associated kinases, WAKs, as pectin receptors. *Front Plant Sci* 3:88. doi: 10.3389/fpls.2012.00088
168. Kohorn BD, Kohorn SL, Saba NJ, Martinez VM (2014) Requirement for pectin methyl esterase and preference for fragmented over native pectins for wall-associated kinase-activated, EDS1/PAD4-dependent stress response in Arabidopsis. *J Biol Chem* 289:18978–18986. doi: 10.1074/jbc.M114.567545
169. Kohorn BD, Kohorn SL, Todorova T, et al (2012) A dominant allele of Arabidopsis pectin-binding wall-associated kinase induces a stress response suppressed by MPK6 but not MPK3 mutations. *Mol Plant* 5:841–851. doi: 10.1093/mp/ssr096
170. Kollárová K, Zelko I, Henselová M, et al (2012) Growth and anatomical parameters of adventitious roots formed on mung bean hypocotyls are correlated with galactoglucomannan oligosaccharides structure. *ScientificWorldJournal* 2012:797815. doi: 10.1100/2012/797815
171. Kovtun Y, Chiu WL, Tena G, Sheen J (2000) Functional analysis of oxidative stress-activated mitogen-activated protein kinase cascade in plants. *Proc Natl Acad Sci USA* 97:2940–2945. doi: 10.1073/pnas.97.6.2940
172. Kwak S-H, Shen R, Schiefelbein J (2005) Positional signaling mediated by a receptor-like kinase in Arabidopsis. *Science* 307:1111–1113. doi: 10.1126/science.1105373
173. Lampugnani ER, Khan GA, Somssich M, Persson S (2018) Building a plant cell wall at a glance. *J Cell Sci*. doi: 10.1242/jcs.207373
174. Landrein B, Kiss A, Sassi M, et al (2015) Mechanical stress contributes to the expression of the STM homeobox gene in Arabidopsis shoot meristems. *elife* 4:e07811. doi: 10.7554/eLife.07811
175. Largo-Gosens A, Hernández-Altamirano M, García-Calvo L, et al (2014) Fourier transform mid infrared spectroscopy applications for monitoring the structural plasticity of plant cell walls. *Front Plant Sci* 5:303. doi: 10.3389/fpls.2014.00303
176. Laufs P, Grandjean O, Jonak C, et al (1998) Cellular parameters of the shoot apical meristem in Arabidopsis. *Plant Cell* 10:1375–1390. doi: 10.1105/tpc.10.8.1375

177. Le PY, Ambrose C (2018) CLASP promotes stable tethering of endoplasmic microtubules to the cell cortex to maintain cytoplasmic stability in Arabidopsis meristematic cells. PLoS ONE 13:e0198521. doi: 10.1371/journal.pone.0198521
178. León J, Shulaev V, Yalpani N, et al (1995) Benzoic acid 2-hydroxylase, a soluble oxygenase from tobacco, catalyzes salicylic acid biosynthesis. Proc Natl Acad Sci USA 92:10413–10417. doi: 10.1073/pnas.92.22.10413
179. Levin DE (2005) Cell wall integrity signaling in *Saccharomyces cerevisiae*. Microbiol Mol Biol Rev 69:262–291. doi: 10.1128/MMBR.69.2.262-291.2005
180. Leydon AR, Tsukamoto T, Dunatunga D, et al (2015) Pollen tube discharge completes the process of synergid degeneration that is initiated by pollen tube-synergid interaction in Arabidopsis. Plant Physiol 169:485–496. doi: 10.1104/pp.15.00528
181. Li C, Wu HM, Cheung AY (2016) FERONIA and her pals: functions and mechanisms. Plant Physiol 171:2379–2392. doi: 10.1104/pp.16.00667
182. Li H, Zhou S-Y, Zhao W-S, et al (2009) A novel wall-associated receptor-like protein kinase gene, OsWAK1, plays important roles in rice blast disease resistance. Plant Mol Biol 69:337–346. doi: 10.1007/s11103-008-9430-5
183. Li J, Chory J (1997) A putative leucine-rich repeat receptor kinase involved in brassinosteroid signal transduction. Cell 90:929–938. doi: 10.1016/s0092-8674(00)80357-8
184. Li J, Wen J, Lease KA, et al (2002) BAK1, an Arabidopsis LRR receptor-like protein kinase, interacts with BRI1 and modulates brassinosteroid signaling. Cell 110:213–222. doi: 10.1016/s0092-8674(02)00812-7
185. Li X (2011) Histostaining for tissue expression pattern of promoter-driven gus activity in Arabidopsis. Bio Protoc. doi: 10.21769/BioProtoc.93
186. Lin L, Zhong S-H, Cui X-F, et al (2012) Characterization of temperature-sensitive mutants reveals a role for receptor-like kinase SCRAMBLED/STRUBBELIG in coordinating cell proliferation and differentiation during Arabidopsis leaf development. Plant J 72:707–720. doi: 10.1111/j.1365-3113X.2012.05109.x
187. Lin W, Li B, Lu D, et al (2014) Tyrosine phosphorylation of protein kinase complex BAK1/BIK1 mediates Arabidopsis innate immunity. Proc Natl Acad Sci USA 111:3632–3637. doi: 10.1073/pnas.1318817111
188. Lin W, Ma X, Shan L, He P (2013) Big roles of small kinases: the complex functions of receptor-like cytoplasmic kinases in plant immunity and development. J Integr Plant Biol 55:1188–1197. doi: 10.1111/jipb.12071
189. Lin Y, Schiefelbein J (2001) Embryonic control of epidermal cell patterning in the root and hypocotyl of Arabidopsis. Development 128:3697–3705.
190. Lindner H, Müller LM, Boisson-Dernier A, Grossniklaus U (2012) CrRLK1L receptor-like kinases: not just another brick in the wall. Curr Opin Plant Biol 15:659–669. doi: 10.1016/j.pbi.2012.07.003
191. Liners F, Thibault JF, Van Cutsem P (1992) Influence of the degree of polymerization of oligogalacturonates and of esterification pattern of pectin on their recognition by monoclonal antibodies. Plant Physiol 99:1099–1104. doi: 10.1104/pp.99.3.1099

192. Lipka E, Gadeyne A, Stöckle D, et al (2014) The phragmoplast-orienting kinesin-12 class proteins translate the positional information of the preprophase band to establish the cortical division zone in *Arabidopsis thaliana*. *Plant Cell* 26:2617–2632. doi: 10.1105/tpc.114.124933
193. Locke EG, Bonilla M, Liang L, et al (2000) A homolog of voltage-gated Ca(2+) channels stimulated by depletion of secretory Ca(2+) in yeast. *Mol Cell Biol* 20:6686–6694. doi: 10.1128/mcb.20.18.6686-6694.2000
194. Long J, Barton MK (2000) Initiation of axillary and floral meristems in *Arabidopsis*. *Dev Biol* 218:341–353. doi: 10.1006/dbio.1999.9572
195. Lu D, Lin W, Gao X, et al (2011) Direct ubiquitination of pattern recognition receptor FLS2 attenuates plant innate immunity. *Science* 332:1439–1442. doi: 10.1126/science.1204903
196. Lu P, Porat R, Nadeau JA, O'Neill SD (1996) Identification of a meristem L1 layer-specific gene in *Arabidopsis* that is expressed during embryonic pattern formation and defines a new class of homeobox genes. *Plant Cell* 8:2155–2168. doi: 10.1105/tpc.8.12.2155
197. Luyten K, Albertyn J, Skibbe WF, et al (1995) Fps1, a yeast member of the MIP family of channel proteins, is a facilitator for glycerol uptake and efflux and is inactive under osmotic stress. *EMBO J* 14:1360–1371. doi: 10.1002/j.1460-2075.1995.tb07122.x
198. Ma X, Xu G, He P, Shan L (2016) SERKing coreceptors for receptors. *Trends Plant Sci* 21:1017–1033. doi: 10.1016/j.tplants.2016.08.014
199. Macho AP, Lozano-Durán R, Zipfel C (2015) Importance of tyrosine phosphorylation in receptor kinase complexes. *Trends Plant Sci* 20:269–272. doi: 10.1016/j.tplants.2015.02.005
200. Macho AP, Schwessinger B, Ntoukakis V, et al (2014) A bacterial tyrosine phosphatase inhibits plant pattern recognition receptor activation. *Science* 343:1509–1512. doi: 10.1126/science.1248849
201. Manfield IW, Orfila C, McCartney L, et al (2004) Novel cell wall architecture of isoxaben-habituated *Arabidopsis* suspension-cultured cells: global transcript profiling and cellular analysis. *Plant J* 40:260–275. doi: 10.1111/j.1365-313X.2004.02208.x
202. Mao D, Yu F, Li J, et al (2015) FERONIA receptor kinase interacts with S-adenosylmethionine synthetase and suppresses S-adenosylmethionine production and ethylene biosynthesis in *Arabidopsis*. *Plant Cell Environ* 38:2566–2574. doi: 10.1111/pce.12570
203. Marc J, Granger CL, Brincat J, et al (1998) A GFP-MAP4 reporter gene for visualizing cortical microtubule rearrangements in living epidermal cells. *Plant Cell* 10:1927–1940. doi: 10.1105/tpc.10.11.1927
204. Martin MV, Fiol DF, Sundaresan V, et al (2013) oiwa, a female gametophytic mutant impaired in a mitochondrial manganese-superoxide dismutase, reveals crucial roles for reactive oxygen species during embryo sac development and fertilization in *Arabidopsis*. *Plant Cell* 25:1573–1591. doi: 10.1105/tpc.113.109306
205. Martinière A, Gayral P, Hawes C, Runions J (2011) Building bridges: formin1 of *Arabidopsis* forms a connection between the cell wall and the actin cytoskeleton. *Plant J* 66:354–365. doi: 10.1111/j.1365-313X.2011.04497.x

206. Martins S, Dohmann EMN, Cayrel A, et al (2015) Internalization and vacuolar targeting of the brassinosteroid hormone receptor BRI1 are regulated by ubiquitination. *Nat Commun* 6:6151. doi: 10.1038/ncomms7151
207. Masachis S, Segorbe D, Turrà D, et al (2016) A fungal pathogen secretes plant alkalizing peptides to increase infection. *Nat Microbiol* 1:16043. doi: 10.1038/nmicrobiol.2016.43
208. Mbengue M, Bourdais G, Gervasi F, et al (2016) Clathrin-dependent endocytosis is required for immunity mediated by pattern recognition receptor kinases. *Proc Natl Acad Sci USA* 113:11034–11039. doi: 10.1073/pnas.1606004113
209. Menges M, Hennig L, Gruissem W, Murray JAH (2002) Cell cycle-regulated gene expression in Arabidopsis. *J Biol Chem* 277:41987–42002. doi: 10.1074/jbc.M207570200
210. Michel BE, Kaufmann MR (1973) The osmotic potential of polyethylene glycol 6000. *Plant Physiol* 51:914–916. doi: 10.1104/pp.51.5.914
211. Mirabet V, Das P, Boudaoud A, Hamant O (2011) The role of mechanical forces in plant morphogenesis. *Annu Rev Plant Biol* 62:365–385. doi: 10.1146/annurev-arplant-042110-103852
212. Mittler R, Vanderauwera S, Suzuki N, et al (2011) ROS signaling: the new wave? *Trends Plant Sci* 16:300–309. doi: 10.1016/j.tplants.2011.03.007
213. Miyazaki S, Murata T, Sakurai-Ozato N, et al (2009) ANXUR1 and 2, sister genes to FERONIA/SIRENE, are male factors for coordinated fertilization. *Curr Biol* 19:1327–1331. doi: 10.1016/j.cub.2009.06.064
214. Mohnen D (2008) Pectin structure and biosynthesis. *Curr Opin Plant Biol* 11:266–277. doi: 10.1016/j.pbi.2008.03.006
215. Monshausen GB, Bibikova TN, Messerli MA, et al (2007) Oscillations in extracellular pH and reactive oxygen species modulate tip growth of Arabidopsis root hairs. *Proc Natl Acad Sci USA* 104:20996–21001. doi: 10.1073/pnas.0708586104
216. Monshausen GB, Messerli MA, Gilroy S (2008) Imaging of the Yellow Cameleon 3.6 indicator reveals that elevations in cytosolic Ca²⁺ follow oscillating increases in growth in root hairs of Arabidopsis. *Plant Physiol* 147:1690–1698. doi: 10.1104/pp.108.123638
217. Moon RT, Bowerman B, Boutros M, Perrimon N (2002) The promise and perils of Wnt signaling through beta-catenin. *Science* 296:1644–1646. doi: 10.1126/science.1071549
218. Moscattello R, Mariani P, Sanders D, Maathuis FJM (2006) Transcriptional analysis of calcium-dependent and calcium-independent signalling pathways induced by oligogalacturonides. *J Exp Bot* 57:2847–2865. doi: 10.1093/jxb/erl043
219. Moschou PN, Gutierrez-Beltran E, Bozhkov PV, Smertenko A (2016) Separase promotes microtubule polymerization by activating cenp-e-related kinesin kin7. *Dev Cell* 37:350–361. doi: 10.1016/j.devcel.2016.04.015
220. Motose H, Sugiyama M, Fukuda H (2004) A proteoglycan mediates inductive interaction during plant vascular development. *Nature* 429:873–878. doi: 10.1038/nature02613
221. Mravec J, Kračun SK, Rydahl MG, et al (2017) An oligogalacturonide-derived molecular probe demonstrates the dynamics of calcium-mediated pectin complexation in cell walls of tip-growing structures. *Plant J* 91:534–546. doi: 10.1111/tbj.13574

222. Muller EM, Locke EG, Cunningham KW (2001) Differential regulation of two Ca²⁺ influx systems by pheromone signaling in *Saccharomyces cerevisiae*. *Genetics* 159:1527–1538.
223. Müller S, Han S, Smith LG (2006) Two kinesins are involved in the spatial control of cytokinesis in *Arabidopsis thaliana*. *Curr Biol* 16:888–894. doi: 10.1016/j.cub.2006.03.034
224. Nakagawa T, Kurose T, Hino T, et al (2007a) Development of series of gateway binary vectors, pGWBs, for realizing efficient construction of fusion genes for plant transformation. *J Biosci Bioeng* 104:34–41. doi: 10.1263/jbb.104.34
225. Nakagawa Y, Katagiri T, Shinozaki K, et al (2007b) *Arabidopsis* plasma membrane protein crucial for Ca²⁺ influx and touch sensing in roots. *Proc Natl Acad Sci USA* 104:3639–3644. doi: 10.1073/pnas.0607703104
226. Nakhamchik A, Zhao Z, Provarnt NJ, et al (2004) A comprehensive expression analysis of the *Arabidopsis* proline-rich extensin-like receptor kinase gene family using bioinformatic and experimental approaches. *Plant Cell Physiol* 45:1875–1881. doi: 10.1093/pcp/pch206
227. Nam KH, Li J (2002) BRI1/BAK1, a receptor kinase pair mediating brassinosteroid signaling. *Cell* 110:203–212. doi: 10.1016/s0092-8674(02)00814-0
228. Nebenführ A, Dixit R (2018) Kinesins and myosins: molecular motors that coordinate cellular functions in plants. *Annu Rev Plant Biol* 69:329–361. doi: 10.1146/annurev-arplant-042817-040024
229. Ngo QA, Vogler H, Lituiev DS, et al (2014) A calcium dialog mediated by the FERONIA signal transduction pathway controls plant sperm delivery. *Dev Cell* 29:491–500. doi: 10.1016/j.devcel.2014.04.008
230. Nissen KS, Willats WGT, Malinovsky FG (2016) Understanding *crrlk11* function: cell walls and growth control. *Trends Plant Sci* 21:516–527. doi: 10.1016/j.tplants.2015.12.004
231. Nothnagel EA, McNeil M, Albersheim P, Dell A (1983) Host-pathogen interactions : xxii. a galacturonic acid oligosaccharide from plant cell walls elicits phytoalexins. *Plant Physiol* 71:916–926. doi: 10.1104/pp.71.4.916
232. Oh M-H, Kim HS, Wu X, et al (2012) Calcium/calmodulin inhibition of the *Arabidopsis* BRASSINOSTEROID-INSENSITIVE 1 receptor kinase provides a possible link between calcium and brassinosteroid signalling. *Biochem J* 443:515–523. doi: 10.1042/BJ20111871
233. Oh M-H, Wang X, Kota U, et al (2009) Tyrosine phosphorylation of the BRI1 receptor kinase emerges as a component of brassinosteroid signaling in *Arabidopsis*. *Proc Natl Acad Sci USA* 106:658–663. doi: 10.1073/pnas.0810249106
234. Okada K, Ueda J, Komaki MK, et al (1991) Requirement of the auxin polar transport system in early stages of *arabidopsis* floral bud formation. *Plant Cell* 3:677–684. doi: 10.1105/tpc.3.7.677
235. O'Neill M, Albersheim P, Darvill A (1990) The pectic polysaccharides of primary cell walls. *Carbohydrates*. Elsevier, pp 415–441
236. Ortiz-Morea FA, Savatin DV, Dejonghe W, et al (2016) Danger-associated peptide signaling in *Arabidopsis* requires clathrin. *Proc Natl Acad Sci USA* 113:11028–11033. doi: 10.1073/pnas.1605588113

237. Osorio S, Castillejo C, Quesada MA, et al (2008) Partial demethylation of oligogalacturonides by pectin methyl esterase 1 is required for eliciting defence responses in wild strawberry (*Fragaria vesca*). *Plant J* 54:43–55. doi: 10.1111/j.1365-313X.2007.03398.x
238. Otero S, Desvoyes B, Peiró R, Gutierrez C (2016) Histone H3 dynamics reveal domains with distinct proliferation potential in the *Arabidopsis* root. *Plant Cell* 28:1361–1371. doi: 10.1105/tpc.15.01003
239. Paniagua C, Posé S, Morris VJ, et al (2014) Fruit softening and pectin disassembly: an overview of nanostructural pectin modifications assessed by atomic force microscopy. *Ann Bot* 114:1375–1383. doi: 10.1093/aob/mcu149
240. Panteris E, Adamakis I-DS, Daras G, et al (2013) Differential responsiveness of cortical microtubule orientation to suppression of cell expansion among the developmental zones of *Arabidopsis thaliana* root apex. *PLoS ONE* 8:e82442. doi: 10.1371/journal.pone.0082442
241. Panteris E, Adamakis I-DS, Daras G, Rigas S (2015) Cortical microtubule patterning in roots of *Arabidopsis thaliana* primary cell wall mutants reveals the bidirectional interplay with cell expansion. *Plant Signal Behav* 10:e1028701. doi: 10.1080/15592324.2015.1028701
242. Paredez AR, Somerville CR, Ehrhardt DW (2006) Visualization of cellulose synthase demonstrates functional association with microtubules. *Science* 312:1491–1495. doi: 10.1126/science.1126551
243. Park M, Song K, Reichardt I, et al (2013) *Arabidopsis* μ -adaptin subunit AP1M of adaptor protein complex 1 mediates late secretory and vacuolar traffic and is required for growth. *Proc Natl Acad Sci USA* 110:10318–10323. doi: 10.1073/pnas.1300460110
244. Pearce G, Moura DS, Stratmann J, Ryan CA (2001) Production of multiple plant hormones from a single polyprotein precursor. *Nature* 411:817–820. doi: 10.1038/35081107
245. Peaucelle A, Braybrook SA, Le Guillou L, et al (2011) Pectin-induced changes in cell wall mechanics underlie organ initiation in *Arabidopsis*. *Curr Biol* 21:1720–1726. doi: 10.1016/j.cub.2011.08.057
246. Peaucelle A, Louvet R, Johansen JN, et al (2008) *Arabidopsis* phyllotaxis is controlled by the methyl-esterification status of cell-wall pectins. *Curr Biol* 18:1943–1948. doi: 10.1016/j.cub.2008.10.065
247. Pelletier S, Van Orden J, Wolf S, et al (2010) A role for pectin de-methylesterification in a developmentally regulated growth acceleration in dark-grown *Arabidopsis* hypocotyls. *New Phytol* 188:726–739. doi: 10.1111/j.1469-8137.2010.03409.x
248. Pelloux J, Rustérucci C, Mellerowicz EJ (2007) New insights into pectin methylesterase structure and function. *Trends Plant Sci* 12:267–277. doi: 10.1016/j.tplants.2007.04.001
249. Pham J, Liu J, Bennett MH, et al (2012) *Arabidopsis* histidine kinase 5 regulates salt sensitivity and resistance against bacterial and fungal infection. *New Phytol* 194:168–180. doi: 10.1111/j.1469-8137.2011.04033.x
250. Philip B, Levin DE (2001) Wsc1 and Mid2 are cell surface sensors for cell wall integrity signaling that act through Rom2, a guanine nucleotide exchange factor for Rho1. *Mol Cell Biol* 21:271–280. doi: 10.1128/MCB.21.1.271-280.2001

251. Popchock AR, Tseng K-F, Wang P, et al (2017) The mitotic kinesin-14 KlpA contains a context-dependent directionality switch. *Nat Commun* 8:13999. doi: 10.1038/ncomms13999
252. Posas F, Takekawa M, Saito H (1998) Signal transduction by MAP kinase cascades in budding yeast. *Curr Opin Microbiol* 1:175–182. doi: 10.1016/s1369-5274(98)80008-8
253. Pradhan Mitra P, Loqué D (2014) Histochemical staining of *Arabidopsis thaliana* secondary cell wall elements. *J Vis Exp*. doi: 10.3791/51381
254. Rajavel M, Philip B, Buehrer BM, et al (1999) Mid2 is a putative sensor for cell integrity signaling in *Saccharomyces cerevisiae*. *Mol Cell Biol* 19:3969–3976. doi: 10.1128/mcb.19.6.3969
255. Rasmussen CG, Bellinger M (2018) An overview of plant division-plane orientation. *New Phytol* 219:505–512. doi: 10.1111/nph.15183
256. Rasmussen CG, Wright AJ, Müller S (2013) The role of the cytoskeleton and associated proteins in determination of the plant cell division plane. *Plant J* 75:258–269. doi: 10.1111/tbj.12177
257. Reddy N, Yang Y (2005) Biofibers from agricultural byproducts for industrial applications. *Trends Biotechnol* 23:22–27. doi: 10.1016/j.tibtech.2004.11.002
258. Reiser V, Raitt DC, Saito H (2003) Yeast osmosensor Sln1 and plant cytokinin receptor Cre1 respond to changes in turgor pressure. *J Cell Biol* 161:1035–1040. doi: 10.1083/jcb.200301099
259. Reymond P, Grünberger S, Paul K, et al (1995) Oligogalacturonide defense signals in plants: large fragments interact with the plasma membrane in vitro. *Proc Natl Acad Sci USA* 92:4145–4149. doi: 10.1073/pnas.92.10.4145
260. Rice S, Lin AW, Safer D, et al (1999) A structural change in the kinesin motor protein that drives motility. *Nature* 402:778–784. doi: 10.1038/45483
261. Ridley BL, O'Neill MA, Mohnen D (2001) Pectins: structure, biosynthesis, and oligogalacturonide-related signaling. *Phytochemistry* 57:929–967. doi: 10.1016/S0031-9422(01)00113-3
262. Romir J, Harter K, Stehle T (2010) Two-component systems in *Arabidopsis thaliana*--A structural view. *Eur J Cell Biol* 89:270–272. doi: 10.1016/j.ejcb.2009.11.007
263. Rotman N, Rozier F, Boavida L, et al (2003) Female control of male gamete delivery during fertilization in *Arabidopsis thaliana*. *Curr Biol* 13:432–436. doi: 10.1016/s0960-9822(03)00093-9
264. Ryan CA (1988) Oligosaccharides as recognition signals for the expression of defensive genes in plants. *Biochemistry* 27:8879–8883. doi: 10.1021/bi00425a001
265. Sablin EP, Case RB, Dai SC, et al (1998) Direction determination in the minus-end-directed kinesin motor ncd. *Nature* 395:813–816. doi: 10.1038/27463
266. Sablowski R (2016) Coordination of plant cell growth and division: collective control or mutual agreement? *Curr Opin Plant Biol* 34:54–60. doi: 10.1016/j.pbi.2016.09.004
267. Sager RE, Lee J-Y (2018) Plasmodesmata at a glance. *J Cell Sci*. doi: 10.1242/jcs.209346
268. Sardar HS, Luczak VG, Lopez MM, et al (2010) Mitotic kinesin CENP-E promotes microtubule plus-end elongation. *Curr Biol* 20:1648–1653. doi: 10.1016/j.cub.2010.08.001

269. Schallus T, Jaeckh C, Fehér K, et al (2008) Malectin: a novel carbohydrate-binding protein of the endoplasmic reticulum and a candidate player in the early steps of protein N-glycosylation. *Mol Biol Cell* 19:3404–3414. doi: 10.1091/mbc.e08-04-0354
270. Scheller HV, Ulvskov P (2010) Hemicelluloses. *Annu Rev Plant Biol* 61:263–289. doi: 10.1146/annurev-arplant-042809-112315
271. Schneitz K, Hülskamp M, Kopczak SD, Pruitt RE (1997) Dissection of sexual organ ontogenesis: a genetic analysis of ovule development in *Arabidopsis thaliana*. *Development* 124:1367–1376.
272. Schwessinger B, Roux M, Kadota Y, et al (2011) Phosphorylation-dependent differential regulation of plant growth, cell death, and innate immunity by the regulatory receptor-like kinase BAK1. *PLoS Genet* 7: e1002046. doi: 10.1371/journal.pgen.1002046
273. Seifert GJ, Blaukopf C (2010) Irritable walls: the plant extracellular matrix and signaling. *Plant Physiol* 153:467–478. doi: 10.1104/pp.110.153940
274. Seifert GJ, Roberts K (2007) The biology of arabinogalactan proteins. *Annu Rev Plant Biol* 58:137–161. doi: 10.1146/annurev.arplant.58.032806.103801
275. Sénéchal F, Wattier C, Rustérucci C, Pelloux J (2014) Homogalacturonan-modifying enzymes: structure, expression, and roles in plants. *J Exp Bot* 65:5125–5160. doi: 10.1093/jxb/eru272
276. Sessions A, Weigel D, Yanofsky MF (1999) The *Arabidopsis thaliana* MERISTEM LAYER 1 promoter specifies epidermal expression in meristems and young primordia. *Plant J* 20:259–263. doi: 10.1046/j.1365-313x.1999.00594.x
277. Shapiro BE, Tobin C, Mjolsness E, Meyerowitz EM (2015) Analysis of cell division patterns in the *Arabidopsis* shoot apical meristem. *Proc Natl Acad Sci USA* 112:4815–4820. doi: 10.1073/pnas.1502588112
278. Shedletsky E, Shmuel M, Delmer DP, Lamport DT (1990) Adaptation and growth of tomato cells on the herbicide 2,6-dichlorobenzonitrile leads to production of unique cell walls virtually lacking a cellulose-xyloglucan network. *Plant Physiol* 94:980–987. doi: 10.1104/pp.94.3.980
279. Shibuya N, Minami E (2001) Oligosaccharide signalling for defence responses in plant. *Physiological and Molecular Plant Pathology* 59:223–233. doi: 10.1006/pmpp.2001.0364
280. Shih H-W, Miller ND, Dai C, et al (2014) The receptor-like kinase FERONIA is required for mechanical signal transduction in *Arabidopsis* seedlings. *Curr Biol* 24:1887–1892. doi: 10.1016/j.cub.2014.06.064
281. Shiu SH, Bleecker AB (2001a) Plant receptor-like kinase gene family: diversity, function, and signaling. *Sci STKE* 2001:re22. doi: 10.1126/stke.2001.113.re22
282. Shiu SH, Bleecker AB (2001b) Receptor-like kinases from *Arabidopsis* form a monophyletic gene family related to animal receptor kinases. *Proc Natl Acad Sci USA* 98:10763–10768. doi: 10.1073/pnas.181141598
283. Shiu SH, Bleecker AB (2003) Expansion of the receptor-like kinase/Pelle gene family and receptor-like proteins in *Arabidopsis*. *Plant Physiol* 132:530–543. doi: 10.1104/pp.103.021964

284. Silva NF, Goring DR (2002) The proline-rich, extensin-like receptor kinase-1 (PERK1) gene is rapidly induced by wounding. *Plant Mol Biol* 50:667–685. doi: 10.1023/a:1019951120788
285. Simpson SD, Ashford DA, Harvey DJ, Bowles DJ (1998) Short chain oligogalacturonides induce ethylene production and expression of the gene encoding aminocyclopropane 1-carboxylic acid oxidase in tomato plants. *Glycobiology* 8:579–583. doi: 10.1093/glycob/8.6.579
286. Smith LG, Gerttula SM, Han S, Levy J (2001) TANGLED1: A microtubule binding protein required for the spatial control of cytokinesis in maize 7. 231–236.
287. Somerville C (2006) Cellulose synthesis in higher plants. *Annu Rev Cell Dev Biol* 22:53–78. doi: 10.1146/annurev.cellbio.22.022206.160206
288. Song JH, Kwak S-H, Nam KH, et al (2019) QUIRKY regulates root epidermal cell patterning through stabilizing SCRAMBLED to control CAPRICE movement in Arabidopsis. *Nat Commun* 10:1744. doi: 10.1038/s41467-019-09715-8
289. Sørensen I, Willats WGT (2011) Screening and characterization of plant cell walls using carbohydrate microarrays. *Methods Mol Biol* 715:115–121. doi: 10.1007/978-1-61779-008-9_8
290. Stein JC, Howlett B, Boyes DC, et al (1991) Molecular cloning of a putative receptor protein kinase gene encoded at the self-incompatibility locus of Brassica oleracea. *Proc Natl Acad Sci USA* 88:8816–8820. doi: 10.1073/pnas.88.19.8816
291. Su W, Liu Y, Xia Y, et al (2011) Conserved endoplasmic reticulum-associated degradation system to eliminate mutated receptor-like kinases in Arabidopsis. *Proc Natl Acad Sci USA* 108:870–875. doi: 10.1073/pnas.1013251108
292. Suzuki N, Sejima H, Tam R, et al (2011) Identification of the MBF1 heat-response regulon of Arabidopsis thaliana. *Plant J* 66:844–851. doi: 10.1111/j.1365-313X.2011.04550.x
293. Takeda S, Gapper C, Kaya H, et al (2008) Local positive feedback regulation determines cell shape in root hair cells. *Science* 319:1241–1244. doi: 10.1126/science.1152505
294. Tamás MJ, Luyten K, Sutherland FC, et al (1999) Fps1p controls the accumulation and release of the compatible solute glycerol in yeast osmoregulation. *Mol Microbiol* 31:1087–1104. doi: 10.1046/j.1365-2958.1999.01248.x
295. Teh O-K, Shimono Y, Shirakawa M, et al (2013) The AP-1 μ adaptin is required for KNOLLE localization at the cell plate to mediate cytokinesis in Arabidopsis. *Plant Cell Physiol* 54:838–847. doi: 10.1093/pcp/pct048
296. Tör M, Lotze MT, Holton N (2009) Receptor-mediated signalling in plants: molecular patterns and programmes. *J Exp Bot* 60:3645–3654. doi: 10.1093/jxb/erp233
297. Torii KU (2004) Leucine-rich repeat receptor kinases in plants: structure, function, and signal transduction pathways. *Int Rev Cytol* 234:1–46. doi: 10.1016/S0074-7696(04)34001-5
298. Torii KU, Mitsukawa N, Oosumi T, et al (1996) The Arabidopsis ERECTA gene encodes a putative receptor protein kinase with extracellular leucine-rich repeats. *Plant Cell* 8:735–746. doi: 10.1105/tpc.8.4.735

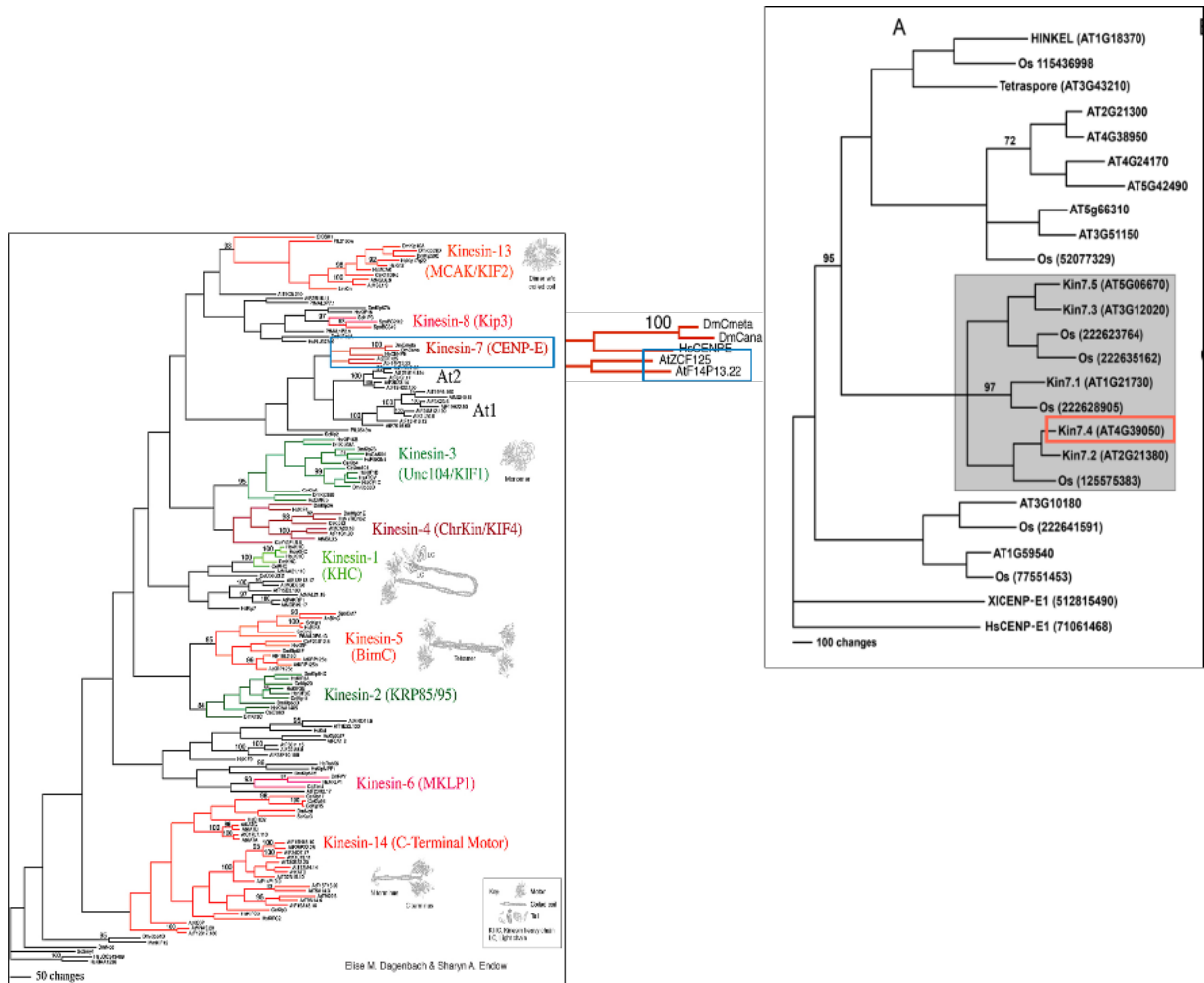
299. Torres MA, Dangl JL, Jones JDG (2002) Arabidopsis gp91phox homologues AtrbohD and AtrbohF are required for accumulation of reactive oxygen intermediates in the plant defense response. *Proc Natl Acad Sci USA* 99:517–522. doi: 10.1073/pnas.012452499
300. Tran L-SP, Shinozaki K, Yamaguchi-Shinozaki K (2010) Role of cytokinin responsive two-component system in ABA and osmotic stress signalings. *Plant Signal Behav* 5:148–150. doi: 10.4161/psb.5.2.10411
301. Trehin C, Schrempp S, Chauvet A, et al (2013) QUIRKY interacts with STRUBBELIG and PAL OF QUIRKY to regulate cell growth anisotropy during Arabidopsis gynoecium development. *Development* 140:4807–4817. doi: 10.1242/dev.091868
302. Trotochaud AE, Jeong S, Clark SE (2000) CLAVATA3, a multimeric ligand for the CLAVATA1 receptor-kinase. *Science* 289:613–617. doi: 10.1126/science.289.5479.613
303. Trouvelot S, Héloir M-C, Poinssot B, et al (2014) Carbohydrates in plant immunity and plant protection: roles and potential application as foliar sprays. *Front Plant Sci* 5:592. doi: 10.3389/fpls.2014.00592
304. Uehara T, Parzych KR, Dinh T, Bernhardt TG (2010) Daughter cell separation is controlled by cytokinetic ring-activated cell wall hydrolysis. *EMBO J* 29:1412–1422. doi: 10.1038/emboj.2010.36
305. Updegraff DM (1969) Semimicro determination of cellulose in biological materials. *Anal Biochem* 32:420–424. doi: 10.1016/S0003-2697(69)80009-6
306. Vaddepalli P, Fulton L, Batoux M, et al (2011) Structure-function analysis of STRUBBELIG, an Arabidopsis atypical receptor-like kinase involved in tissue morphogenesis. *PLoS ONE* 6:e19730. doi: 10.1371/journal.pone.0019730
307. Vaddepalli P, Fulton L, Wieland J, et al (2017) The cell wall-localized atypical β -1,3 glucanase ZERZAUST controls tissue morphogenesis in Arabidopsis thaliana. *Development* 144:2259–2269. doi: 10.1242/dev.152231
308. Vaddepalli P, Herrmann A, Fulton L, et al (2014) The C2-domain protein QUIRKY and the receptor-like kinase STRUBBELIG localize to plasmodesmata and mediate tissue morphogenesis in Arabidopsis thaliana. *Development* 141:4139–4148. doi: 10.1242/dev.113878
309. Vale RD (2003) The molecular motor toolbox for intracellular transport. *Cell* 112:467–480. doi: 10.1016/s0092-8674(03)00111-9
310. Vanzin GF, Madson M, Carpita NC, et al (2002) The mur2 mutant of Arabidopsis thaliana lacks fucosylated xyloglucan because of a lesion in fucosyltransferase AtFUT1. *Proc Natl Acad Sci USA* 99:3340–3345. doi: 10.1073/pnas.052450699
311. Verhertbruggen Y, Knox JP (2007) Pectic polysaccharides and expanding cell walls. In: Verbelen J-P, Vissenberg K (eds) *The expanding cell*. Springer Berlin Heidelberg, pp 139–158
312. Verica JA, Chae L, Tong H, et al (2003) Tissue-specific and developmentally regulated expression of a cluster of tandemly arrayed cell wall-associated kinase-like genes in Arabidopsis. *Plant Physiol* 133:1732–1746. doi: 10.1104/pp.103.028530

313. Vinogradova MV, Malanina GG, Reddy ASN, Fletterick RJ (2009) Structure of the complex of a mitotic kinesin with its calcium binding regulator. *Proc Natl Acad Sci USA* 106:8175–8179. doi: 10.1073/pnas.0811131106
314. Voxeur A, Höfte H (2016) Cell wall integrity signaling in plants: “To grow or not to grow that’s the question”. *Glycobiology* 26:950–960. doi: 10.1093/glycob/cww029
315. Wakabayashi K, Hoson T, Huber DJ (2003) Methyl de-esterification as a major factor regulating the extent of pectin depolymerization during fruit ripening: a comparison of the action of avocado (*Persea americana*) and tomato (*Lycopersicon esculentum*) polygalacturonases. *J Plant Physiol* 160:667–673. doi: 10.1078/0176-1617-00951
316. Walker KL, Müller S, Moss D, et al (2007) Arabidopsis TANGLED identifies the division plane throughout mitosis and cytokinesis. *Curr Biol* 17:1827–1836. doi: 10.1016/j.cub.2007.09.063
317. Wang J-G, Feng C, Liu H-H, et al (2016a) HAPLESS13-mediated trafficking of strubbelig is critical for ovule development in arabidopsis. *PLoS Genet* 12:e1006269. doi: 10.1371/journal.pgen.1006269
318. Wang J-G, Li S, Zhao X-Y, et al (2013) HAPLESS13, the Arabidopsis μ 1 adaptin, is essential for protein sorting at the trans-Golgi network/early endosome. *Plant Physiol* 162:1897–1910. doi: 10.1104/pp.113.221051
319. Wang R, Liu M, Yuan M, et al (2016b) The brassinosteroid-activated bri1 receptor kinase is switched off by dephosphorylation mediated by cytoplasm-localized pp2a b’ subunits. *Mol Plant* 9:148–157. doi: 10.1016/j.molp.2015.10.007
320. Wang X, Chory J (2006) Brassinosteroids regulate dissociation of BKI1, a negative regulator of BRI1 signaling, from the plasma membrane. *Science* 313:1118–1122. doi: 10.1126/science.1127593
321. Wang X, Li X, Meisenhelder J, et al (2005) Autoregulation and homodimerization are involved in the activation of the plant steroid receptor BRI1. *Dev Cell* 8:855–865. doi: 10.1016/j.devcel.2005.05.001
322. Welch MD, Drubin DG (1994) A nuclear protein with sequence similarity to proteins implicated in human acute leukemias is important for cellular morphogenesis and actin cytoskeletal function in *Saccharomyces cerevisiae*. *Mol Biol Cell* 5:617–632. doi: 10.1091/mbc.5.6.617
323. Wightman R, Chomicki G, Kumar M, et al (2013) SPIRAL2 determines plant microtubule organization by modulating microtubule severing. *Curr Biol* 23:1902–1907. doi: 10.1016/j.cub.2013.07.061
324. Willats WG, Orfila C, Limberg G, et al (2001) Modulation of the degree and pattern of methyl-esterification of pectic homogalacturonan in plant cell walls. Implications for pectin methyl esterase action, matrix properties, and cell adhesion. *J Biol Chem* 276:19404–19413. doi: 10.1074/jbc.M011242200
325. Woehlke G, Schliwa M (2000) Walking on two heads: the many talents of kinesin. *Nat Rev Mol Cell Biol* 1:50–58. doi: 10.1038/35036069

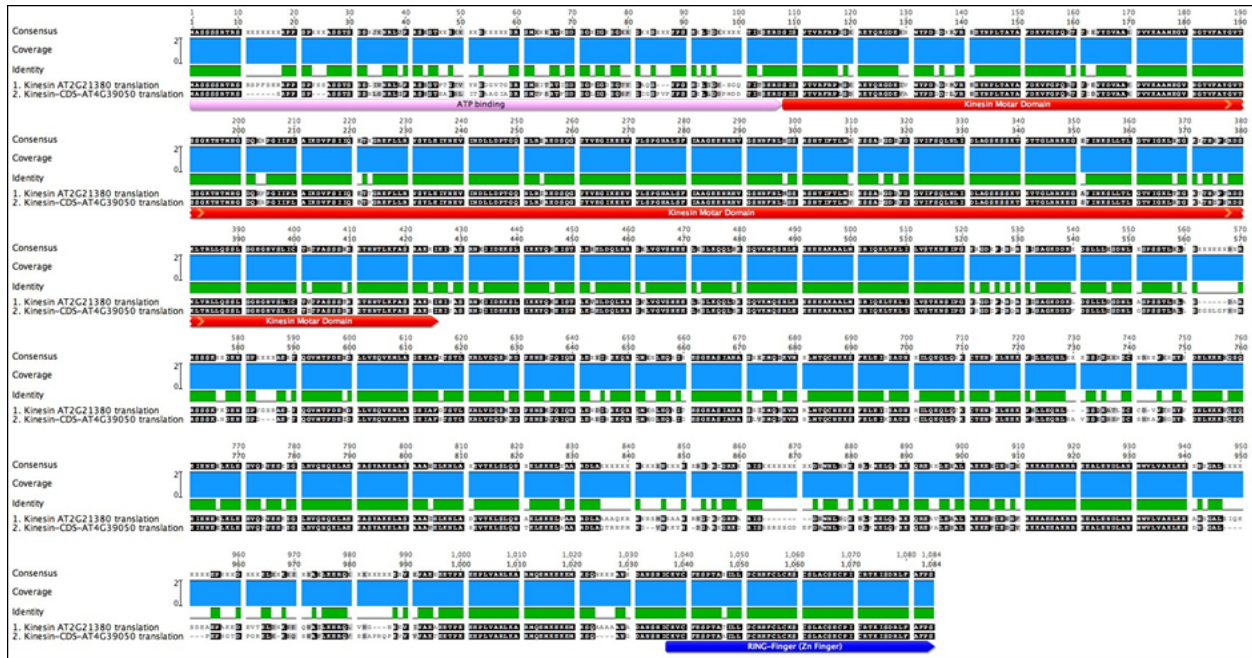
326. Wohlbach DJ, Quirino BF, Sussman MR (2008) Analysis of the Arabidopsis histidine kinase ATHK1 reveals a connection between vegetative osmotic stress sensing and seed maturation. *Plant Cell* 20:1101–1117. doi: 10.1105/tpc.107.055871
327. Wolf S (2017) Plant cell wall signalling and receptor-like kinases. *Biochem J* 474:471–492. doi: 10.1042/BCJ20160238
328. Wolf S, Hématy K, Höfte H (2012a) Growth control and cell wall signaling in plants. *Annu Rev Plant Biol* 63:381–407. doi: 10.1146/annurev-arplant-042811-105449
329. Wolf S, Höfte H (2014) Growth control: A saga of cell walls, ROS, and peptide receptors. *Plant Cell* 26:1848–1856. doi: 10.1105/tpc.114.125518
330. Wolf S, Mouille G, Pelloux J (2009) Homogalacturonan methyl-esterification and plant development. *Mol Plant* 2:851–860. doi: 10.1093/mp/ssp066
331. Wolf S, Mravec J, Greiner S, et al (2012b) Plant cell wall homeostasis is mediated by brassinosteroid feedback signaling. *Curr Biol* 22:1732–1737. doi: 10.1016/j.cub.2012.07.036
332. Wolf S, van der Does D, Ladwig F, et al (2014) A receptor-like protein mediates the response to pectin modification by activating brassinosteroid signaling. *Proc Natl Acad Sci USA* 111:15261–15266. doi: 10.1073/pnas.1322979111
333. Wu G, Wang X, Li X, et al (2011) Methylation of a phosphatase specifies dephosphorylation and degradation of activated brassinosteroid receptors. *Sci Signal* 4:ra29. doi: 10.1126/scisignal.2001258
334. Xiao C, Zhang T, Zheng Y, et al (2016) Xyloglucan deficiency disrupts microtubule stability and cellulose biosynthesis in Arabidopsis, altering cell growth and morphogenesis. *Plant Physiol* 170:234–249. doi: 10.1104/pp.15.01395
335. Xiong L, Ishitani M, Lee H, Zhu JK (2001) The Arabidopsis LOS5/ABA3 locus encodes a molybdenum cofactor sulfuryase and modulates cold stress- and osmotic stress-responsive gene expression. *Plant Cell* 13:2063–2083. doi: 10.1105/tpc.010101
336. Xu S-L, Rahman A, Baskin TI, Kieber JJ (2008) Two leucine-rich repeat receptor kinases mediate signaling, linking cell wall biosynthesis and ACC synthase in Arabidopsis. *Plant Cell* 20:3065–3079. doi: 10.1105/tpc.108.063354
337. Xu Y, Chang PFL, Liu D, et al (1994) Plant defense genes are synergistically induced by ethylene and methyl jasmonate. *Plant Cell* 6:1077–1085. doi: 10.1105/tpc.6.8.1077
338. Yadav RK, Fulton L, Batoux M, Schneitz K (2008) The Arabidopsis receptor-like kinase STRUBBELIG mediates inter-cell-layer signaling during floral development. *Dev Biol* 323:261–270. doi: 10.1016/j.ydbio.2008.08.010
339. Yamada K, Saijo Y, Nakagami H, Takano Y (2016) Regulation of sugar transporter activity for antibacterial defense in Arabidopsis. *Science* 354:1427–1430. doi: 10.1126/science.aah5692
340. Yang DC, Tan K, Joachimiak A, Bernhardt TG (2012) A conformational switch controls cell wall-remodelling enzymes required for bacterial cell division. *Mol Microbiol* 85:768–781. doi: 10.1111/j.1365-2958.2012.08138.x

341. Yapo BM, Robert C, Etienne I, et al (2007) Effect of extraction conditions on the yield, purity and surface properties of sugar beet pulp pectin extracts. *Food Chem* 100:1356–1364. doi: 10.1016/j.foodchem.2005.12.012
342. Yeats TH, Sorek H, Wemmer DE, Somerville CR (2016) Cellulose deficiency is enhanced on hyper accumulation of sucrose by a H⁺-coupled sucrose symporter. *Plant Physiol* 171:110–124. doi: 10.1104/pp.16.00302
343. Yeh Y-H, Panzeri D, Kadota Y, et al (2016) The arabidopsis malectin-like/LRR-RLK IOS1 is critical for bak1-dependent and bak1-independent pattern-triggered immunity. *Plant Cell* 28:1701–1721. doi: 10.1105/tpc.16.00313
344. York WS, Darvill AG, Albersheim P (1984) Elongation of Pea Stem Segments by a Xyloglucan Oligosaccharide'. *Journal of Biological Chemistry* 59:295–297.
345. Yu F, Qian L, Nibau C, et al (2012) FERONIA receptor kinase pathway suppresses abscisic acid signaling in Arabidopsis by activating ABI2 phosphatase. *Proc Natl Acad Sci USA* 109:14693–14698. doi: 10.1073/pnas.1212547109
346. Žárský V (2016) Clathrin in plant defense signaling and execution. *Proc Natl Acad Sci USA* 113:10745–10747. doi: 10.1073/pnas.1612925113
347. Zhao H, Shen ZM, Kahn PC, Lipke PN (2001) Interaction of alpha-agglutinin and a-agglutinin, *Saccharomyces cerevisiae* sexual cell adhesion molecules. *J Bacteriol* 183:2874–2880. doi: 10.1128/JB.183.9.2874-2880.2001
348. Zhao Y, Song D, Sun J, Li L (2013) Populus endo-beta-mannanase PtrMAN6 plays a role in coordinating cell wall remodeling with suppression of secondary wall thickening through generation of oligosaccharide signals. *Plant J* 74:473–485. doi: 10.1111/tpj.12137
349. Zipfel C, Kunze G, Chinchilla D, et al (2006) Perception of the bacterial PAMP EF-Tu by the receptor EFR restricts *Agrobacterium*-mediated transformation. *Cell* 125:749–760. doi: 10.1016/j.cell.2006.03.037
350. SIGnAL iSect Toolbox. <http://signal.salk.edu/isects.html>.
351. Weblet Importer. <http://travadb.org/samples/>.

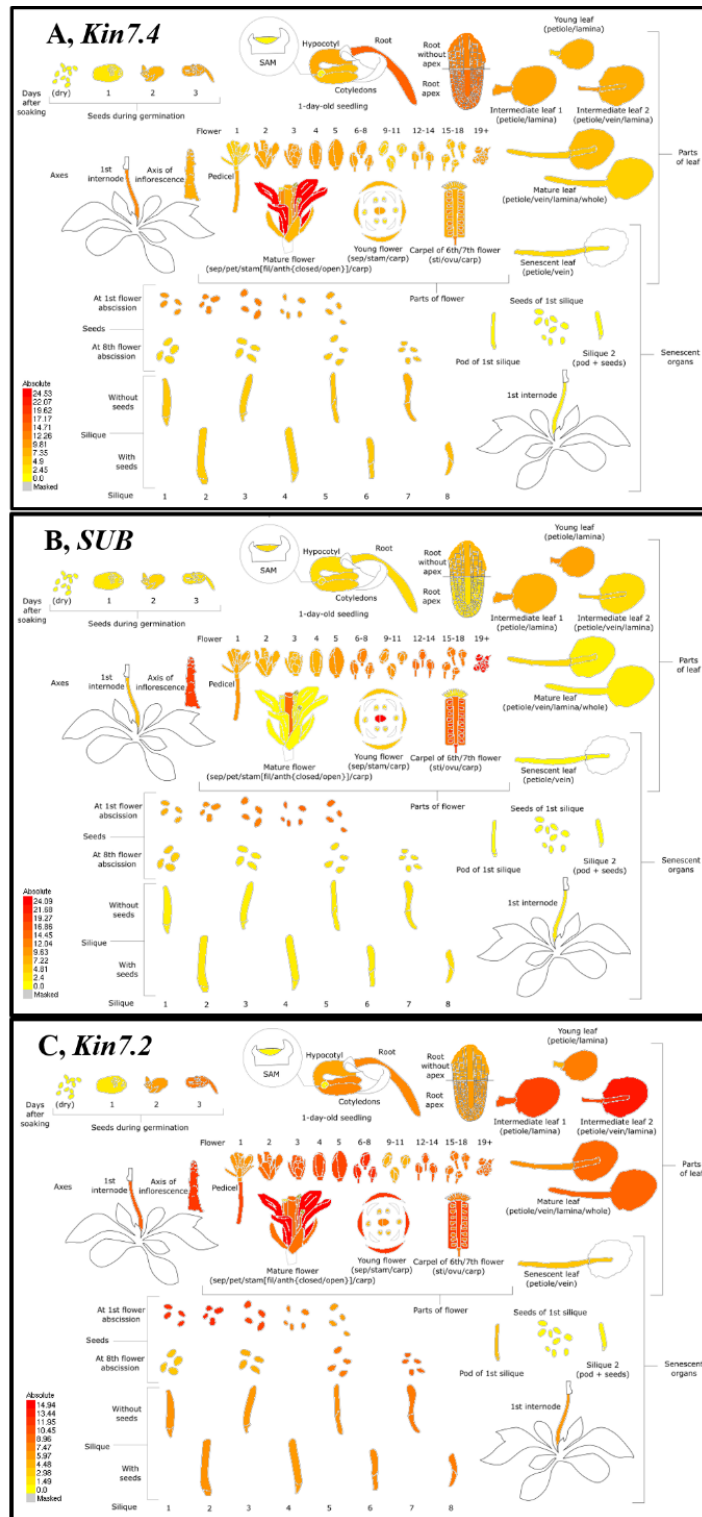
7 Supplementary Data



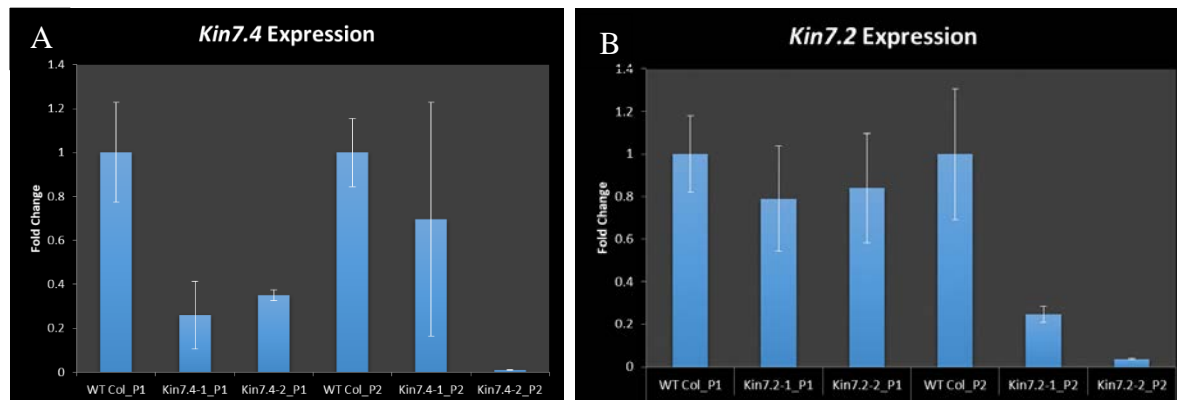
Supplementary figure 1. Phylogenetic analysis of KINESIN in Arabidopsis. Adapted from (Dagenbach and Endow, 2004; Moschou *et al.*, 2016)



Supplementary figure 2. Alignment of KIN7.4 and KIN7.2 protein sequences of Arabidopsis. Black highlighted indicate identity or high similarity. Lines show gaps. The alignment was performed in Geneious software using ClustalW algorithm with BLSM62 matrix.



Supplementary figure 3. Mean-normalized expression levels of *KIN7.4*, *KIN7.2*, and *SUB*. The expression levels of *KIN7.4* (A), *SUB* (B), and *KIN7.2* (C) according to AtGenExpress (Kilian et al. 2007) are shown. Both *KIN*s are expressed in all developmental stages as well as in all other tested conditions.



Supplementary figure 4. qRT-PCR analysis of *KIN7.4* and *KIN7.2* expression in t-DNA insertion lines. Gene expression levels of *KIN7.4* (A) and *KIN7.2* (B) by qPCR in t-DNA insertion line. The results from three biological replicates are shown.

Supplementary Table 1 TRAVA - transcriptome variation analysis.

Tissue	Absolute read counts		
	<i>SUB</i>	<i>KIN7.4</i>	<i>KIN7.2</i>
Carpels of the young flower	2334	1284	1136
Sepals of the young flower	697	1509	2601
Whole Inflorescence	2093	1390	1283
Inflorescence stage 9	1284	1113	1426
Inflorescence stage 9	1296	1030	1364
Inflorescence stage10	951	692	736
Inflorescence stage 11	1136	1366	1910
Inflorescence stage12	748	1583	1740
Inflorescence stage 12	951	1470	1722
Inflorescence stage13	759	1713	1749
Inflorescence stage 14	778	1459	1486
Inflorescence stage 15	851	849	1110
Internode	670	2100	1700
Whole mature leaf	216	873	1754
Inflorescence meristem at 16 days after germination	2016	1439	954
SAM at 7 days after germination	1639	925	664
Ovules stage 2i to 3iv	1825	1821	1199

Old Silique	322	1221	1548
Young silique	577	1925	2215
Seedling cotyledons	715	1679	1874
Seedling hypocotyl	398	1692	1095
Seedling meristem	980	451	280
Seedling root	392	2722	1231

Table 13 List of Primers**Genotyping primers**

No.	Primer name	Sequence
3727	RP_PRK53	TCCTCTTCAACACTCGCTCTC
3728	LP_PRK53	CTTTTTAGCAGCACGGTTTTG
3729	RP_BIR23	TCAACCAAGCTCGAGAGTAGC
3730	LP_BIR23	TCGTCAATCACGTTAATTGCTC
3731	RP_LRR10	ACTGTTGTTGAACTTGCCGTC
3732	LP_LRR10	TTGATTTTCGTGGTCCTCAC
3733	RP_BIR75	AACGAAAATTGGATTATCGCC
3734	LP_BIR75	TCGTCAATCACGTTAATTGCTC
3770	WAK2-LP_D05	CAAGCATGATAACCGAGAAGC
3771	WAK2-RP_D05	CCTTTTGGTACTTCTCCAGG
3772	TOR1-LP_39	CTCCATCTGTTTGTGAGCCTC
3773	TOR1-RP_39	AACGCACAAGCAAGTAGCTTG
3774	TOR1-RP_91	TAAGGCTGGTGTGTAAACGG
3775	TOR1-LP_91	ATCCATAGTCGAACATGCGTC
3776	SYT1-LP_08	AGGTCTCGCGATTTATTAGGG
3777	SYT1-RP_08	GCCTCCTGACAAGTATAGGGG
3778	S17-LP_18	TTTCGACCTGTGGAATGTTTC
3779	S17-RP_18	TCAGCAAAAGTGTGTCGTGAG
3780	L28e-LP_808	GAGTGAACGTTGGTGAGGTTG
3781	L28e-RP_808	CATTGGGACCATGTTGTAACC
3782	ATPIN8-LP_65	TGAAAGACATTTTGATGGCAT
3783	ATPIN8-RP_65	CCAAATCAAGCTTTGCAAGAC
3784	Porin-LP_01	TCGTTTCCGTCAGATTTATGC
3785	Porin-RP_01	TGCCAGATTCGGTGTATAGG
3786	CLT-LP_21	TGTTCTGCAAGTTCATGTTTCG
3787	CLT-RP_21	AGGTGGATGACCTGGAAGAAG
3788	CLT-LP_80	TGAGGTCAACCAAATTCTCATG
3789	CLT-RP_80	TGAAAAGAATTGGTCCAGACG
3790	CLT-LP_D10	TCCAGCCTGTTGATGTAATCC

3791	CLT-RP_D10	TCTGTGCGATAGTGAGGATCC
3792	PAP15-LP_D01	GACTCAGTGAGTGCCCTCAAGG
3793	PAP15-RP_D01	TGCTTGATATCCACTGGGTAATC
3794	60S-LP_33	TTGAGAAAATGTGCCAAATCC
3795	60S-RP_33	CAGACTTGAAATCTGTTGGGC
3796	L28e-L_337	CCTTTCCTTTCTCCATTTTGC
3797	L28e-RP_337	GTGGTTTCAGGTCTTGCAAAC
3798	Glyco-LP_685	CAGCTGAAATTTCTTTTCCCC
3799	Glyco-LP_856	TGTGACATGTCTTTCACCAGC
3800	Glyco-RP_685	GTTACGCAAGAGCTTACGAGC
3801	Glyco-RP_856	GTTACCACCGAAAAGAAGCC
3802	HD-LP_125	ATTTCTTCGAGCCTTGAGCTC
3803	HD-RP_125	CGACAAAACCCAAAATTCATG
3804	TP-LP_609	TCTTCAGTTGTTGGTTTTGGC
3805	TP-RP_609	TCTGCTGTTTATGATTTGGGG
3806	Gly-LP_255	CTCCTCGGTTTCCATATCCTC
3807	Gly-RP_255	CGATCTTCCACAAGAACCATG
3808	Bir-XmaF	TATCCCGGGATGATGATGGGTAGGTTAG
3809	Bir-XmaR	TATCCCGGGTCAACGAGCAACTATGAG
3810	LRR1-XmaF	TATCCCGGGATGAAGAACAAGACCAATTTAG
3811	LRR1-XmaR	ATACCCGGGTCAATCGGACAAAGGAC
3812	PRK2-XmaF	TATCCCGGGATGGAATCCAAATGTCTCATG
3813	PRK2-XmaR	ATACCCGGGTCATGACAAGTTAATTCCC
3814	Bir-ECD-XmaF	ATACCCGGGATGGATCAGGCCAACATAGATTGC
3815	BirECD-XmaR	TATCCCGGGAACAACTTTACCACGAGAG
3816	Bir-ICD-XmaF	TATCCCGGGATGTTCCGTAATTTGGGTGCTG
3817	LRR1-ECD-XmaF	TATCCCGGGATGGATCTAGAAGCTGATCGACG
3818	LRR1-ECD-XmaR	ATACCCGGGCAGATAAATTGTGCTTTTTC
3819	LRR1-ICD-XmaF	TATCCCGGGATGTGTCTCTGTAGAAAGAAG
3820	PRK2-ECD-XmaF	ATACCCGGGATGGTATCAGAGACCGAAACTCTC
3821	PRK2-ECD-XmaR	ATACCCGGGCTTTGATGATGTTTTCTTG
3822	PRK2-ICD-XmaF	TATCCCGGGATGTTTCTTATCCGAAGACGAAAG
3823	FAB-XmaF	TATCCCGGGATGAGTTCTGGTCTGAACGAAG
3824	FAB-XmaR	ATACCCGGGTTATGAATTGTTGAGCAAGTC
3874	AGL_LP09	TCAAGTGTCTTGAGCATGCTG
3875	AGL_RP09	TCCAAATACCATCAATTCTCCAG
3876	AGL_LP23	ATAACCTTTGTGCCTCGTGTC
3877	AGL_RP23	TCATAGAGCTTTCCACGGTTG
3878	AGO_LP36	AGAGAACGGGAAGAGTCAAG
3879	AGO_RP36	TTTCGTCAATTTGCGGGTAC
3880	AGO_LP57	AGGTGGCAATCAAGTTTGTTC
3881	AGO_RP57	AATTTTGCATGCCTACATTGG
3882	BoP2_LP67	GTTGTGAAGGCTTTGCTTGAG
3883	BoP2_RP67	ACACCCGATAAGACATTGCTG
3884	C2_LP30	ATCACACCCACTCCAACAAAC
3885	C2_RP30	TCCATTAGGAAGTCTTGTC
3886	C2_LP68	TGGTGAACCGAAGAGATTG
3887	C2_RP68	TCTTCGGTTTCTCAACGTTTG
3888	C2_LP73	ATCTGATGGACTCATGATCGG
3889	C2_RP73	AACTTGTGTTGTGCGCCTTTTG
3890	CIPK_LP02	AATGTGCGATCGTATGGTCCAC
3891	CIPK_RP02	TGTGCGATTAAACCTCCTTTG
3892	CIPK_LP40	TCACCTCCACGAACATACTCC

3893	CIPK_RP40	AATGTCGATCGTATGGTCCAC
3894	CIPK_LP46	TCACCTCCACGAACATACTCC
3895	CIPK_RP46	AATGTCGATCGTATGGTCCAC
3896	Dicer_LP10	TGGCGTTTCTGATACCAATTC
3897	Dicer_RP10	TAACAGGCGAAGCAGTCATTC
3898	Dicer_LP95	CTTCAAGAACATTGGCAAGC
3899	Dicer_RP95	CGTACTCGTAATTGGGACGAG
3900	Dof_LP05	TTTTTGGTGTGAAAGGGAGTG
3901	Dof_RP05	TCACACGTTTTGATGGCATAG
3902	Dof_LP536	ACGTGGACTGTTCTGTTTTCC
3903	Dof_RP536	TCTTGAAAGAAGAGCCACCAG
3904	EDA_LP9	TCCTCCCAATTAGACAGTCAATC
3905	EDA_RP9	CTCTTCGTCTTCGTCCAAGTG
3906	EDA_LP302	TTTTTGGTGGTCAGCTTTTCTC
3907	EDA_RP302	TGCGTGTTCTTGTGTGAGAAG
3908	FAT_LP01	GCTACTTGCCATTGTATGTC
3909	FAT_RP01	GATCTGATATACAGACAAGGAC
3910	FAT_LP219	ACGGTTAGATAACGCCCAAAC
3911	FAT_RP219	TGCTTATGGAGCTGAGGAGAG
3912	FAT_LP923	GATCCCGTCTTTAGCTTCGTC
3913	FAT_RP923	AGTTGTTGCCGACATGAGAAC
3914	Kin_LP86	TGCTCCAACAATGCAGTGTAC
3915	Kin_RP86	CAACGAGTGGTTCTCTTTTG
3916	Kin_LP88	TTGGTTCTACCCCTGTCACAG
3917	Kin_RP88	TCAACTTGCCAACAAGTACCC
3918	LRR_LP66	AGTTTGGGCGGAAATAAAAAC
3919	LRR_RP66	GTCACGAAGTGCATTAGAGC
3920	LRR_LP412	CCATGAAATAAAAGGGGCTTC
3921	LRR_RP412	GACTCGGAGATTGGTTTTTCC
3922	OBE_LP40	CCTGCAGGCTGCTTACAATAG
3923	OBE_RP40	TTGTCACCGAATTTTCAGGAC
3924	OBE_LP74	ATCTAGGAGCCGCTTTTTGAG
3925	OBE_RP74	TTGTCACCGAATTTTCAGGAC
3926	TRM_LP24	TCATCCTTAAATTGAGCACGG
3927	TRM_RP24	CTCGCAAATCACTTCTTCCTG
3928	UN_LP149	CTAGCATGTCCCTCGTCTCTG
3929	UN_RP149	ACCCGAGAGGATATGGTGATC
3930	UN_LP845	TCTCCTCGAGCTGGTGTTFAG
3931	UN_RP845	CAACTGTGCAAAAGCTTAGGC
3932	SUB_LP158	TTTGTTTGAGTGGACAGGGAC
3933	SUB_RP158	GATGTTGTTGTGGTTGCAGTG
3934	qky_LP123	GGAAGAAATGGGTCAGGACTC
3935	qky_RP123	TAGCCGTAGGCATTGTGTCTC
3944	FAT_FRT	CCTTGAAGTACCCAGCTTTC
3945	FAT_RRT	TATCGGCTCCATTCTTCGAG
4268	CHC1_LP13	TGGTGAAAGGAAATATGCAGC
4269	CHC1_LP52	TAATAAGGCGCAAGTGACCAG
4270	CHC1_RP13	TATATTGAAACGGAGGAAGCG
4271	CHC1_RP52	TTTATCCGAGCTGATGACACC
4272	CHC2_LP26	AAAAGTCATGACACTTCTCCATTC
4273	CHC2_RP26	AATTCGAGGAAACCGTTATGG
4274	Gene Trap_GT	ACCCGACCGGATCGTATCGGT
4385	Kin2_LP78	ACCGGAAGAGAGTTTTCTGCTC

4386	Kin2_RP78	TGATGTATGCACCCTCTTTCC
4387	Kin2_LP17	TTGCTAATGCATCATCGATTG
4388	Kin2_RP17	TTGGTTGAGGTTCCATGAGTC
4389	Sub-4_For	GGAGGGGCATTTACCTTCTTCC
4390	Sub-4_Rev	CCTCGGTGGTTGTTGCAGCGG
4391	Tor1-2_Rev	CAAGCACGGTAATGGTGGAAATC
4392	Tor1-2_For	CGTCGTTAGCGGTGGTTTTG
4393	Sub-4_For1	GTCCAATGATACTGCTTCAAAG
4394	Sub-4_Rev1	GAAGCCGAGGAATCGCCCAC
4395	Tor1-Taq1_F	GCATCCATGATTGCCTTGGAAGTACAGATTGGGTAACCTC
4396	Tor1-Taq1_R	CTTTAGATTACTAGAAAAATGTAGCTACCTTG
4681	CesA6_qRT-RP	GAACCCAGAGACTCGTATCA
4682	CesA6_qRT-LP	ACCCGGATTTGATCACCATA
4683	CesA3_qRT-RP	GCTTAGGCATGCAGTAAATGG
4684	CesA3_qRT-LP	GTCAGATTGGGGAATGGAGA
4685	CesA1_qRT-RP	CACATTCATTACACGCGACA
4686	CesA1_qRT-LP	GATCCGACATGAATCTGATGG
4687	ERECTA_RP55	TGTGTGTGAGAAATGGCTCTG
4688	ERECTA_LP55	TTCGAAATCGAAAACGGTATG
4689	ERECTA_RP10	GCAACGTTGCTGGAGATTAAG
4690	ERECTA_LP10	CCGGGTAATGAAGAGACATTG
4691	Wak4_RP-F08	TTAACCAATTGTTCCCTGCAG
4692	Wak4_LP-F08	ACTATCTCTTTGAGCGGCTCC
4693	Wak3_RP13	GCACAAGATGCAACCAAAAAC
4694	Wak3_LP13	TTGGAGTTTCTTGAAAAATC
4695	Wak5_RP65	TTATCGACGCAAGGTGATACC
4696	Wak5_LP65	AACCACAACAATCTTATGCAGC
4697	Wak5_RP81	TTATCGACGCAAGGTGATACC
4698	Wak5_LP81	AACCACAACAATCTTATGCAGC
4699	Wak1_LP75	GCTTCTTGGTCATTCTGCTTG
4700	Wak1_RP75	TTGTGCTGACAAGATGTGACC

qRT-PCR primers

No.	Primer name	Sequence
1	R1(at4g33380) LP	5'- TGAAGGAGAGGAAGAGCCTGAGGAA -3'
2	R1(at4g33380) RP	5'-CCCCATCTCACTGCAGCACCAC -3'
3	R2 At2g28390 LP	5'-AGATTGCAGGGTACGCCTTGAGG-3'
4	R2 At2g28390 RP	5'- ACACGCATTCCACCTTCCGCG -3'
5	R3 At5g46630 LP	5'- CCAAATGGAATTTCAAGGTGCCAATG -3'
6	R3 At5g46630 RP	5'- CAATGCGTACCTTGAGAAAACGAAC -3'
7	CCR1(At1G15950) LP	5'-GTTCTCTTTGCTGCTTTTCGAC-3'
8	CCR1(At1G15950) RP	5'-GCAAACCCCTGACCATGT-3'
9	CCR2(At1G80820) LP	5'-GTTCTCTTTGCTGCTTTTCGAC-3'
10	CCR2(At1G80820) RP	5'-GCAAACCCCTGACCATGT-3'
11	PDF1.2(AT5G44420) LP	5'- TCTTTGCTGCTTTTCGACGC-3'
12	PDF1.2(AT5G44420) RP	5'- TCTTGCATGCATTACTGTTTCCG-3'

13	<i>VSP1</i> (AT5G24780) LP	5'-GATATGGGACCGAGAACACAGC-3'
14	<i>VSP1</i> (AT5G24780) RP	5' TTCGTATAGATGCAAGGTCTCCG-3'
15	<i>FRK1</i> (At2g19190) LP	5'-ATCTTCGCTTGGAGCTTCTC-3'
16	<i>FRK1</i> (At2g19190) RP	5'-TGCAGCGCAAGGACTAGAG-3'
17	<i>CYP81F2</i> (At5g57220) LP	5'-AATGGAGAGAGCAACACAATG-3'
18	<i>CYP81F2</i> (At5g57220) RP	5'-ATACTGAGCATGAGCCCTTTG-3'
19	<i>RBOHD</i> (AT5G47910) LP	5'-CTGCTCCGTGCTTTTCAGAT-3'
20	<i>RBOHD</i> (AT5G47910) RP	5'-AATCCTTGTGGCTTCGTCAT-3'
21	<i>TCH4</i> (AT5G57560) LP	5'-GATCACTTGGGGTGATGGTC-3'
22	<i>TCH4</i> (AT5G57560) RP	5'-GGGACAAGCTTCATTTGCAT-3'
23	<i>TIP2;3</i> (AT5G47450) LP	5'-GAAGTTGGAAGTGTGGGAGACT-3'
24	<i>TIP2;3</i> (AT5G47450) RP	5'-GCTCCATCAGAGGTTAGTTTGG-3'
25	<i>CesA1</i> (At4g32410) LP	5'-GATCCGACATGAATCTGATGG-3'
26	<i>CesA1</i> (At4g32410) RP	5'-CACATTCATTACACGCGACA-3'
27	<i>CesA3</i> (At5g05170) LP	5'-GTCAGATTGGGGAATGGAGA-3'
28	<i>CesA3</i> (At5g05170) RP	5'-GCTTAGGCATGCAGTAAATGG-3'
29	<i>CesA6</i> (At5g64740) LP	5'-ACCCGGATTTGATCACCATA-3'
30	<i>CesA6</i> (At5g64740) RP	5'-GAACCCAGAGACTCGTATCA-3'
31	<i>CesA2</i> (At4G39350) LP	5'-CGCTAGAGAATGTCGACGAA-3'
32	<i>CesA2</i> (At4G39350) RP	5'-TAGGAATGCGAGTCCAGCTT-3'
33	<i>CesA5</i> (AT5G09870) LP	5'-CCGTAGATCCACCCAATCTC-3'
34	<i>CesA5</i> (AT5G09870) RP	5'-GAAAATTCATCGTCCCTGAGA-3'
35	<i>CesA9</i> (AT2G21770) LP	5'-CGTTACCGCAATGGACATAA-3'
36	<i>CesA9</i> (At2G21770) RP	5'-GTTCTCTTTGCTGCTTTTCGAC-3'
37	<i>SUB</i> (AT1G11130) LP	5'-GTTTGGATCTTTGACCTAGACGA-3'
38	<i>SUB</i> (AT1G11130) RP	5'-CAAGTTATTAATCGCCGAAACAT-3'
39	<i>SUBgRNA</i>	5' TAATAACTTGTATATCAACTT-3'
4610	qRT2_Kin2-Rev	CAACTCGTGAATGGACATGAA
4611	qRT2_Kin2-For	CTTTCATCTCTTGCATTCTTGC
4612	qRT1_Kin2-For	TCATATTGGTCTCCATGAGCA
4613	qRT1_Kin2-Rev	AGCTGGGGAAGAACATCGT
4614	qRT2_Kin4-Rev	GACGGAAACGCAAAGAGCCG
4615	qRT2_Kin4-For	CGCAAGCGAATGGAGACGC
4616	qRT1_Kin4-For	CCAAGAACAACACTACAGGAAAAGTGT
4617	qRT1_Kin4-Rev	CCAGATACCGCTTTATTGGAA
4620	qRT3_Kin4-Rev	CAGTTCTTAGAGACCTTTTCAACTGGTT
4621	qRT3_Kin4-For	GTCATTTCTGCTTATGTAAATCCTGTTC

Yeast two hybrid cloning primers

No.	Primer name	Sequence
4139	TOR1-R_XmaI	TAGCCCGGGTACTTGTGCGAACTGTTGG
4140	TOR1-F_NdeI	TACCATATGATGAGCACACCTACAACCTC

4152	TOR1-For2	CTTTCCAAAAGCTTTGCC
4153	TOR1-For3	GAGTTTTTCCAAAGACTAG
4154	TOR1-Rev1	GCTCATTCTCATATTGTTC
4155	WAK-TM_Nde1F	TATCATATGAAAATCTTCACTGAGAAAGG
4156	WAK-TM_Xma1R	CAGCCCCGGGTCAACGGCCAGCTTCAATGT
4157	WAK_ECD-Xma1R	ATCCCCGGGTCCATCTAAAGTATTCAGGC
4158	WAK_ECD-Nde1F	TAGCATATGCAACCTCGCAAGGAGTGCCAAAC
4226	Kin2_AD-SacR	CTTGAGCTCTCAAGACGGGAAGGCGAA
4227	Kin2_AD-Xmaf	ACTCCCCGGGATGGCTTCATCGTCGTCT
4228	Kin2_BD-NcoF	TGGCCATGGATGGCTTCATCGTCGTC
4229	Kin2_BD-XmaR	ATCCCCGGGTCAAGACGGGAAGGCG
4230	Kin4_AD-SacR	CTCGAGCTCTTAAGACGGAAACGCAAA
4231	Kin4_AD-XmaF	CCACCCGGGATGGCTTCATCCTCATCG
4232	Kin4_BD-NcoF	TGGCCATGGATGGCTTCATCCTCATC
4233	Kin4_BD-XmaR	ATCCCCGGGTAAAGACGGAAACGC
4264	Kin2_AD-Xmaf	ACTCCCCGGAATGGCTTCATCGTCGTCTAG
4265	Kin2_BD-NcoF	TGGCCATGGAAATGGCTTCATCGTCGTC
4266	Kin4_AD-XmaF	CCACCCGGGAATGGCTTCATCCTCATCG
4267	Kin4_BD-NcoF	TGGCCATGGAAATGGCTTCATCCTCATC
4429	WAK1_BD_ECD-NocF	TGGCCATGGAGCAACATCAACCTGGTG
4430	WAK1_BD_ECD-XamR	ATCCCCGGGAACCTTTACGCTTGCAG
4431	WAK1_BD_ICD-NocF	TGGCCATGGAGGTTGCCTGTATAACAACAG
4432	WAK1_BD_ICD-XamR	ATCCCCGGGTCAGCGGCCAGTTTCAATG
4433	WAK3_BD_ECD-NocF	TGGCCATGGAGCAACATCAACCTCGCG
4434	WAK3_BD_ECD-XmaF	ATCCCCGGGTTGCATGTTGTATAACAG
4435	WAK3_BD_ICD-NocF	TGGCCATGGATTGAGGAGCAGGGTTG
4436	WAK3_BD_ICD-XmaR	TCCCCGGGTCAGCGGCCAGTTTCAATG
4437	WAK4_BD_ECD-NocF	TGGCCATGGCAACCTTGCCTCGTTGCCCGG
4438	WAK4_BD_ECD-XmaR	ATCCCCGGGTCCATTCAACGTATTCAGG
4439	WAK4_BD_ICD-NocF	TGGCCATGGTAGAACATAAAAATGAAG
4440	WAK4_BD_ICD-XmaR	ATCCCCGGGTCAGCGCCTGCTTCAATG
4441	WAK5_BD_ECD-NocF	TGGCCATGGCGCAACCTCGCGATGATTG
4442	WAK5_BD_ECD-XmaR	ATCCCCGGGAGTACTTAGGCTCTTCTTTAG
4443	WAK5_BD_ICD-NocF	TGGCCATGGACAAAAAATGAGGCAC
4444	WAK5_BD_ICD-XmaR	ATCCCCGGGTCAGCGGCCAGTTTCAATG
4445	WK1_AD_ECD-XhoR	CAGCTCGAGAACTCTTTACGCTTGCAGC
4446	WK1_AD_ECD-XmaF	CCACCCGGGGCAACATCAACCTGGTGAG
4447	WK1_AD_ICD-XamF	CCACCCGGGAGTTGCCTGTATAACAACAG
4448	WK1_AD_ICD-XhoR	CAGCTCGAGTCAGCGGCCAGTTTCAATGTC
4449	WK3_AD_ECD-XhoR	CAGCTCGAGTTGCATGTTGTATAACAGATC
4450	WK3_AD_ECD-XmaF	CCACCCGGGACAACATCAACCTCGCG
4451	WK3_AD_ICD-XhoR	CAGCTCGAGTCAGCGGCCAGTTTCAATGTC
4452	WK3_AD_ICD-XmaF	CCACCCGGGTTGAGGAGCAGGGTTG

4453	WK4_AD_ECD-XhoR	CAGCTCGAGTCCATTCAACGTATTCAG
4454	WK4_AD_ECD-XmaF	CCACCCGGGAACCTTGCCTCGTTGCCCCG
4455	WK4_AD_ICD-XmaF	CCACCCGGGACTAGAACATAAAAATGAAG
4456	WK4_AD_ICD-XhoR	CAGCTCGAGTCAGCGGCCTGCTTCAATG
4457	WK5_AD_ECD-XhoR	CAGCTCGAGAGTACTTAGGCTCTTCTTTAG
4458	WK5_AD_ECD-XmaF	CCACCCGGGACCGCAACCTCGCGATG
4459	WK5_AD_ICD-XhoR	CAGCTCGAGTCAGCGGCCAGTTTCAATG
4460	WK5_AD_ICD-XmaF	CCACCCGGGACAAAAAATGAGGCACCG
4507	Kin4-For_Cla	GATCGATCGATGGCTTCATCCTCATCGAG
4508	Kin4-Rev_Nco	TTCCATGGTTAAGACGGAAACGCAAAGAG
4509	Tor1-For_Kpn1	CTGGTACCTGATGAGCACACCTACAACCTC
4510	Tor1-Rev_Kpn1	ATGGTACCTTACTTGTGCGAACTGTTGGAG
4511	Kin4A-AD-SacR	CTCGAGCTCGTTTTTCGTCATTCAAC
4512	Kin4A-BD-XmaR	TCCCCGGGGATGTTTTTCGTCATT
4513	Kin4B-AD-XmaF	CACCCGGGCATGCAATCAAGATTGG
4514	Kin4B-BD-NcoF	TGGCCATGGAAATGCAATCAAGATTG
4515	Kin4-For_Nco	GTACCATGGTATGGCTTCATCCTCATCG
4516	Kin4-Rev_Nco	ATTCCATGGTTAAGACGGAAACGCAAAGAG
4574	KATP_AD-XMAF	TTCCACCCGGGCATGGCTTCATCCTCATCG
4575	KATP_AD-XMAR	CCCACCCGGGATCCCGCTCAGAGCTAATAG
4576	KMotar_AD-XMAF	TCCACCCGGGCATGAGTATCTCCGTCACCG
4577	KMotar_AD-XMAR	CCCACCCGGGTATACTCTTTGCCCTGCTGG
4578	KSTALK_AD-XMAF	TCCACCCGGGCAATGTAGAAATATATGCTTC
4579	KSTALK_AD-XMAR	CCACCCGGGATGTGAGAGTTTGCGTCTC
4580	KZn_AD-XMAF	TCCACCCGGGAATGTGTAAGTATGTTTCG
4581	KZn_AD-XMAR	CCCACCCGGGTTAAGACGGAAACGCAAAG

Binary vector cloning primers

No.	Primer name	Sequence
4461	Kin4Pro_GGAF1	AACAGGTCTCAACCTTGCACCAAACACTCTCTAACTTTG
4462	Kin4Pro_GGAF2	AACAGGTCTCAGTCGCACCATCTCTGTCTACC
4463	Kin4Pro_GGAR1	AACAGGTCTCTTGTTCCTAACCTCGAAACTCGAGGGTC
4464	Kin4Pro_GGAR2	AACAGGTCTCGCGACCATTGAAGAGAGAAAG
4465	Kin4Ter_GGF1	AACAGGTCTCACTGCCAGTTGAAAAGGTAACCTTTCTAG
4466	Kin4Ter_GGF2	AACAGGTCTCGGACTCTAAGAACTGTGGGTG
4467	Kin4Ter_GGR1	AACAGGTCTCTTAGTCTTTGATCTTCTTCTTCTTCTC
4468	Kin4Ter_GGR2	AACAGGTCTCGAGTCCTGCATAATCATGCAAG
4537	gKIN4_For-SbfI	ATCGCCTGCAGGATGGCTTCATCCTC
4538	gKIN4_Rev-PmeI	AGATGTTTAAACTTAAGACGGAAACG
4543	N-EGFP_For-XmaI	TAACACCCGGGATGGTGAGCAAGGGC
4544	N-EGFP_Rev-SbfI	GCCATCCTGCAGGCGATCCAGAGCCG

4545	gKIN4_CRev-SbfI	GCGGCCCTGCAGGTTAAGACGGAAAC
4546	gKIN4_CFor-XmaI	TAACACCCGGGATGGCTTCATCCTC
4547	C-EGFP_For-SbfI	CTTAACCTGCAGGGCCGCTAGTGCG
4548	C-EGFP_Rev-PmeI	GAGATGTTTAAACCTTGTACAGCTCG
4549	gKIN4_For-SbfI	ATCGCCTGCAGGATGGCTTCATCCTCATC
4550	gKIN4_Rev-PmeI	AGATGTTTAAACTTAAGACGGAAACGCAAAGAGCC
4551	pKIN-XmaF	GTACCCGGGTGCACCAAACACTCTCTAAC
4552	pKIN-XmaR	CATCCCGGGCCACTAACCTCGAAACTCG
4553	tKIN-PmeF	TAAGTTTAAACCCAGTTGAAAAGGTAACC
4554	tKIN-PmeR	GATAGTTTAAACCTTTGATCTTCTTCTTC
4555	pCAMBIA3300_For	CGCCCTTCCCAACAGTTGC
4556	pCAMBIA3300_Rev	CACGCCCTTTTAAATATCC

8 Acknowledgements

I would like to thank Prof. Dr. Kay Schneitz for providing me the opportunity to work in his lab. I am particularly grateful to him for his excellent supervision, support, and motivation throughout the course of this thesis. He has been instrumental in improving my scientific presentation and writing skills.

I would like to thank past and present colleagues: Prasad, Janys, Sebastian, Jin, Xia, Athul, Athul, Rachele, Anne, Barbara, Regina and Katrin for the friendly atmosphere, scientific discussions and fun moments in lab.

Special thanks go to Susana, and our administrative secretary Beate Seeliger for helping me with the German language related issues and bureaucracy.

I would like to thank the bachelor and master students who worked with me. I would like to thank members of Lehrstuhl für Botanik and Lehrstuhl für Systembiologie der Pflanzen for their support.

Last but not least, I would like to thank my family and freinds for their support and constant encouragement through all these years.

